

The University of Maine

DigitalCommons@UMaine

Electronic Theses and Dissertations

Fogler Library

8-2022

Modeling Life History and Population Dynamics of American Lobster and Atlantic Sea Scallops in a Warming Gulf of Maine

Cameron T. Hodgdon

University of Maine, cameron.hodgdon@maine.edu

Follow this and additional works at: <https://digitalcommons.library.umaine.edu/etd>



Part of the [Marine Biology Commons](#)

Recommended Citation

Hodgdon, Cameron T., "Modeling Life History and Population Dynamics of American Lobster and Atlantic Sea Scallops in a Warming Gulf of Maine" (2022). *Electronic Theses and Dissertations*. 3658.
<https://digitalcommons.library.umaine.edu/etd/3658>

This Open-Access Thesis is brought to you for free and open access by DigitalCommons@UMaine. It has been accepted for inclusion in Electronic Theses and Dissertations by an authorized administrator of DigitalCommons@UMaine. For more information, please contact um.library.technical.services@maine.edu.

**MODELING LIFE HISTORY AND POPULATION DYNAMICS OF
AMERICAN LOBSTER AND ATLANTIC SEA SCALLOPS
IN A WARMING GULF OF MAINE**

By

Cameron Tyler Hodgdon

B.S. University of New England, 2017

A DISSERTATION

Submitted in Partial Fulfillment of the

Requirements for the Degree of

Doctor of Philosophy

(in Marine Biology)

The Graduate School

The University of Maine

August 2022

Advisory Committee:

Yong Chen, Professor, Stony Brook University, Co-Advisor

Walter Golet, Assistant Professor, School of Marine Sciences, Co-Advisor

Burton Shank, Research Fishery Biologist, Northeast Fisheries Science Center

James Sulikowski, Associate Director and Professor, Arizona State University

Andrew Thomas, Professor, School of Marine Sciences

David Hiebeler, Professor, Department of Mathematics and Statistics

© 2022 Cameron Hodgdon

**MODELING LIFE HISTORY AND POPULATION DYNAMICS OF
AMERICAN LOBSTER AND ATLANTIC SEA SCALLOPS
IN A WARMING GULF OF MAINE**

By Cameron Tyler Hodgdon

Dissertation Advisors: Dr. Yong Chen and Dr. Walter Golet

An Abstract of the Dissertation Presented
in Partial Fulfillment of the Requirements for the
Degree of Doctor of Philosophy
(in Marine Biology)
August 2022

Climate change is impacting many marine species distributions, life histories, and behaviors, as well as their associated fisheries and overall production. This is perhaps especially true for the Gulf of Maine (GOM). Here, warming rates are exceeding a vast majority of the world's oceans. This highly dynamic system supports myriad species, but is both economically recognized and culturally known for its Atlantic sea scallop (*Placopecten magellanicus*) and American lobster (*Homarus americanus*) fisheries. This dissertation examines the influence of regional climate change on these species in an effort to predict how these stocks and their fisheries may change in the future. For scallops, this was accomplished by examining and aging shells collected throughout the GOM to determine if spatial and temporal differences in growth patterns could be explained by regional thermal habitats and salinities. For lobster, a five-step process was developed. Firstly, I conducted a simulation study to evaluate the stock assessment model performance under possible changes in lobster molting probability, lobster molt increment size, and size-at-maturity as a result of changes in thermal habitat. Secondly, using two temperature covariates important for early survival and development, a stock-wide, thermally-explicit

Beverton-Holt stock-recruit relationship was estimated for the GOM. This relationship served as the basis of a framework to be used by management to test what levels of spawning biomass are necessary in the current year to achieve the desired levels of recruitment in the near future. Thirdly, a delta-generalized linear mixed model was used to predict lobster spatial density throughout the GOM. This spatial density informed a stock-wide abundance index which was used to replace the traditionally used design-based indices in the stock assessment model. Fourthly, a stock forecasting model was developed that could utilize the aforementioned stock-recruit relationship and consequences of ignoring this thermal influence on recruitment estimations were explored. Lastly, a bioclimate envelope model was used to determine relationships of multiple habitat covariates to lobster abundance from trawl survey data before using these relationships to map and forecast lobster habitat in the GOM.

DEDICATION

This work is dedicated to my mother, who showed me the importance of teaching and learning, and to my father, who sparked an early interest for my love of the ocean. I owe my professional and personal development to them both and this dissertation would not exist without their influences and limitless support. Thank you to all my friends and family who stood with me throughout this process.

ACKNOWLEDGEMENTS

Firstly, thank you Yong Chen. I would not be the researcher I am today without your guidance. You saw potential in me I didn't even know I had and always pushed me to do beyond what I thought was my best. I would also like to thank the rest of my committee members: Walt Golet, Burton Shank, Andy Thomas, David Hiebeler, and James Sulikowski. Your collaborations and expertise were invaluable during this process. Special thanks to James, who provided me with the foundation and knowledge to even be considered as a Chen Lab applicant.

Thank you all graduate and undergraduate members of the Chen Lab past and present. Thank you Kisei Tanaka and Mackenzie Mazur for answering my never-ending questions and unparalleled support and guidance. Thank you Nathan Willse, Noah Khalsa, Claire Ober, John Carlucci, Robyn Linner, Robert Boenish, Luoliang Xu, Ming Sun, Yunzhou Li, Shu Su, Hsiao-Yun Chang, Libin Dai, Mike Torre, Jamie Behan, Jay Kim, Stephanie Arsenault, Katrina Rokosz, Emily Fitting, and Patricia Woodruff for everything from professional discussions and collaborations to personal connections I hope never to lose.

I would like to additionally thank Dvora Hart and Toni Chute of NOAA Northeast Fisheries Science Center, Sam Truesdell of MA Marine Fisheries, Jeff Kipp of the Atlantic States Marine Fisheries Commission, Kevin Friedland of the National Marine Fisheries Service, Jocelyn Runnebaum of the Nature Conservancy of Maine, and Jie Cao of North Carolina State University. Thank you to the Maine Department of Marine Resources and NOAA Fisheries for sample and data collection. I would also like to thank the members of the Lobster Research Collaborative and the National Sea Grant Lobster Research Initiative. Thank you to the *Journal of Northwest Atlantic Fishery Science*, the *Canadian Journal of Fisheries and Aquatic Sciences*, and *ICES Journal of*

Marine Science for providing permission to use the published journal articles of Chapters 2, 5, and 7, respectively.

Financial support of this study was provided by the Maine Department of Marine Resources, NOAA Scallop RSA Program, National Marine Fisheries Service/Sea Grant Population and Ecosystem Dynamics Graduate Fellowship (Award #: NA20OAR4170464), and the NOAA Fisheries and the Environment (FATE) program via the Cooperative Institute for the North Atlantic Region (CINAR).

TABLE OF CONTENTS

DEDICATION	iii
ACKNOWLEDGEMENTS	iv
LIST OF TABLES	xii
LIST OF FIGURES	xv
CHAPTER 1: AN INTRODUCTION TO THE GULF OF MAINE AND ITS FISHERIES	1
1.1 Oceanography of the Gulf of Maine	1
1.2 The Atlantic Sea Scallop and it's Fishery in the Gulf of Maine	3
1.3 The American Lobster and it's Fishery in the Gulf of Maine	5
1.4 Objectives	8
CHAPTER 2: SPATIOTEMPORAL VARIABILITY IN ATLANTIC SEA SCALLOP (<i>PLACOPECTEN MAGELLANICUS</i>) GROWTH IN THE NORTHERN GULF OF MAINE	10
2.1 Abstract	10
2.2 Introduction	11
2.3 Methods	15
2.3.1 Study Area	15
2.3.2 Ageing & Growth Modelling	15
2.3.3 Modelling Environmental Effects	18
2.4 Results	22

2.4.1 Spatial Differences in Growth Parameters L_{∞} and K	22
2.4.2 Temporal Differences in Growth Parameters L_{∞} and K	23
2.4.3 Regression Model Selection	26
2.4.4 Results of Regression Analyses.....	33
2.5 Discussion	35
CHAPTER 3: IMPLICATIONS OF CLIMATE DRIVEN CHANGES ON GROWTH AND SIZE-AT-MATURITY FOR GULF OF MAINE LOBSTER STOCK ASSESSMENT	
3.1 Abstract	40
3.2 Introduction	40
3.3 Methods.....	44
3.3.1 Shifting Growth and Size at Maturity.....	44
3.3.2 Stock Assessment and Sensitivity Analyses.....	47
3.4 Results	52
3.5 Discussion	56
CHAPTER 4: DEVELOPING A FRAMEWORK TO CALCULATE DYNAMIC REFERENCE POINTS USING A THERMALLY EXPLICIT SPAWNING BIOMASS / RECRUITMENT RELATIONSHIP.....	
4.1 Abstract	61
4.2 Introduction	61
4.3 Methods.....	66

4.3.1 Spawning Biomass and Recruitment Levels	66
4.3.2 Determining an Appropriate SSB/R Relationship.....	66
4.3.3 Dynamic Reference Point Calculator	69
4.3.4 Environmental Forecasts and Subsequent Management Advice.....	70
4.4 Results	70
4.4.1 The SSB/R Relationship.....	70
4.4.2 Hindcasts and Forecasts from the Reference Point Calculator.....	71
4.5 Discussion	82
4.5.1 Lobster Recruitment Relationships	82
4.5.2 Forecasts from the Calculator.....	84
4.5.3 The Importance of Dynamic BRPs under Climate Change.....	85
 CHAPTER 5: A FRAMEWORK TO INCORPORATE ENVIRONMENTAL EFFECTS INTO STOCK ASSESSMENTS INFORMED BY FISHERY-INDEPENDENT SURVEYS: A CASE STUDY WITH AMERICAN LOBSTER (<i>HOMARUS AMERICANUS</i>).....	
5.1 Abstract	87
5.2 Introduction	87
5.3 Methods.....	91
5.3.1 Delta-generalized linear mixed model (delta-GLMM)	91
5.3.2 The Stock Assessment Model.....	93

5.3.3 Abundance Index Calculations and Assessment Model Configurations.....	95
5.3.4 Model Run Comparisons and BRPs	96
5.4 Results	102
5.5 Discussion	112
 CHAPTER 6: COMPARISON OF STOCHASTIC AND THERMALLY EXPLICIT RECRUITMENT PROJECTIONS FOR GULF OF MAINE AMERICAN LOBSTER	
6.1 Abstract	117
6.2 Introduction	117
6.3 Methods.....	119
6.3.1 The Stock Assessment Model.....	119
6.3.2 The Forecasting Model.....	120
6.3.3 Forecasting Model Specifications	121
6.3.4 Comparison of Forecasting Scenarios	123
6.3.5 Comparison to Stock Assessment.....	125
6.4 Results	125
6.5 Discussion	131
 CHAPTER 7: CONSEQUENCES OF MODEL ASSUMPTIONS WHEN PROJECTING HABITAT SUITABILITY: A CAUTION OF FORECASTING UNDER UNCERTAINTIES	
7.1 Abstract	135

7.2 Introduction	135
7.3 Methods	140
7.3.1 Base Case: The Bioclimate Model	140
7.3.2 Base Case: Input Data.....	142
7.3.3 What-If Scenarios	144
7.3.4 Bioclimate Model Comparative Diagnostics.....	148
7.4 Results	150
7.4.1 Suitability Indices	150
7.4.2 Historical and Forecasted HSI.....	151
7.5 Discussion	162
7.5.1 Choice of Extrapolation Data	164
7.5.2 The Importance of Spatial Scale.....	165
7.5.3 Inclusion and Exclusion Criteria	167
7.5.4 On Separating Life History Data	168
7.5.5 Conclusions	170
CHAPTER 8: CONCLUSIONS AND FUTURE DIRECTIONS	173
8.1 Maine’s Top Fisheries under Climate Change	173
8.1.1 Atlantic Sea Scallops: The Future of the Stock and the Future of Research.....	173
8.1.2 American Lobster: The Future of the Stock and the Future of Research.....	174
8.2 Concluding Statement	176

BIBLIOGRAPHY.....	177
APPENDIX A.....	195
APPENDIX B.....	226
APPENDIX C.....	228
APPENDIX D.....	231
APPENDIX E.....	233
BIOGRAPHY OF THE AUTHOR.....	247

LIST OF TABLES

Table 2.1. L_{∞} and K values for Gulf of Maine scallops compared to southern regions	23
Table 2.2. L_{∞} and K values for scallops across the Gulf of Maine	23
Table 2.3. L_{∞} and K values for scallops of different year classes in the Gulf of Maine	24
Table 2.4. Tukey's Post Hoc results for one-way ANOVA of L_{∞}	25
Table 2.5. Tukey's Post Hoc results for one-way ANOVA of K	25
Table 2.6. Correlation matrix of predictor variables used in Chapter 2	27
Table 2.7. VIFs of combinations predictor variables used in Chapter 2	27
Table 2.8. Root mean squared error of generalized additive models in Chapter 2	28
Table 2.9. Root mean squared error of boosted regression trees in Chapter 2	29
Table 2.10. Deviance explained of generalized additive models in Chapter 2	30
Table 2.11. Deviance explained of boosted regression trees in Chapter 2	31
Table 2.12. Akaike information criterion of generalized additive models in Chapter 2	32
Table 2.13. Akaike information criterion of boosted regression trees in Chapter 2	33
Table 2.14. Deviance explained and akaike information criterion of generalized additive models and boosted regression trees for analyses of Cobscook Bay scallops in Chapter 2	35
Table 3.1 List of all individual based lobster simulator scenarios in Chapter 3	51
Table 3.2 Settings and data used in the lobster stock assessment model in Chapter 3	52
Table 3.3 Biological reference points for each scenario in Chapter 3	56

Table 3.4 Terminal year stock status and abundance of all scenarios in Chapter 3	56
Table 4.1 Data input for generalized additive models in Chapter 4	79
Table 4.2 Variance inflation factor test results for Chapter 4.....	80
Table 4.3 Deviance explained and akaike information criterion from generalized additive models in Chapter 4	80
Table 4.4 Forecasted temperature values used in Chapter 4.....	81
Table 4.5 Acceptable ranges of spawning biomass that lead to management desired recruitment levels for lobster	81
Table 5.1 Description of all parameters used in equations 5.1 and 5.2	98
Table 5.2 All settings and data used in the delta-generalized additive model in Chapter 5	99
Table 5.3 All settings and data used in the lobster stock assessment model in Chapter 5	101
Table 5.4 All scenarios in Chapter 5.....	102
Table 5.5 Performance metrics for all generalized additive models used to predict bottom temperature in Chapter 5	109
Table 5.6 Mean coefficients of variation for all scenarios and surveys in Chapter 5.....	110
Table 5.7 Reference abundance for the optimal model in Chapter 5.....	111
Table 5.8 Reference exploitation rate for the optimal model in Chapter 5.....	112
Table 6.1 All test statistics comparing linear trends between scenarios in Chapter 6	129
Table 6.2 Slopes from all linear trends of all scenarios in Chapter 6	130

Table 6.3 All test statistics comparing linear trends between scenarios in Chapter 6 with trends from management-derived recruitment.....	130
Table 6.4 Slopes from all linear trends of all scenarios in Chapter 6 compared with slopes from management-derived recruitment.....	130
Table 7.1 The seven scenarios in Chapter 7	149
Table 7.2 Summary statistics of suitable habitat for the historical and future periods used in Chapter 7.....	160
Table 7.3 Root mean squared error for all scenarios and life history combinations in the historical period in Chapter 7.....	161
Table 7.4 Root mean squared error for all scenarios and life history combinations in the forecasted period in Chapter 7	162

LIST OF FIGURES

Figure 1.1. Bathymetric map of the Gulf of Maine and its currents	3
Figure 2.1. An Atlantic sea scallop with important features labeled	14
Figure 2.2. The northern Gulf of Maine with scallop management zones	14
Figure 2.3. Yearly bottom temperature of the Gulf of Maine 1997-2013	20
Figure 2.4. Average bottom temperature of the Gulf of Maine 1997-2013.....	21
Figure 2.5. Average bottom salinity of the Gulf of Maine 1997-2013.....	21
Figure 3.1 Growth and size-at-maturity shifts for lobster in the individual-based lobster simulator model in Chapter 3.....	51
Figure 3.2 Reference abundance between the base case and all scenarios tested in the global sensitivity analysis in Chapter 3	54
Figure 3.3 Global sensitivity analysis results from Chapter 3.....	55
Figure 4.1 NOAA Statistical areas of the Gulf of Maine/Georges' Bank	65
Figure 4.2 Partial dependence plots of the Beverton-Holt generalized additive model in Chapter 3.....	73
Figure 4.3 Three-dimensional surface plot of temperature and spawning biomass effects on recruitment in Chapter 3	74
Figure 4.4 Forecasts of acceptable ranges of spawning biomass that lead to management desired recruitment levels under a temperature change of $0.072^{\circ}\text{C}/\text{year}$	75

Figure 4.5 Forecasts of acceptable ranges of spawning biomass that lead to management desired recruitment levels under a temperature change of 0.242°C/year	76
Figure 4.6 Forecasts of recruitment per spawning biomass under a temperature change of 0.072°C/year	77
Figure 4.7 Forecasts of recruitment per spawning biomass under a temperature change of 0.242°C/year	78
Figure 5.1 NOAA statistical areas	91
Figure 5.2 Mohn’s rho values for all lobster stock assessment model runs in Chapter 5.....	105
Figure 5.3 Differences between objective function values for each scenario in Chapter 5 and the base case.....	106
Figure 5.4 Reference abundance 1984-2013 for the optimal model in Chapter 5.....	107
Figure 5.6 Reference exploitation rate 1984-2013 for the optimal model in Chapter 5.....	108
Figure 6.1 Lobster biomass estimates and linear trends produced by the forecasting model in Chapter 6.....	127
Figure 6.2 Lobster biomass estimates and linear trends produced by the forecasting model in Chapter 6 compared with recruitment estimates from management	128
Figure 7.1 Survey domain boundaries in the Gulf of Maine	139
Figure 7.2 Suitability indices from the base case run in Chapter 7	154
Figure 7.3 Suitability indices from the base case compared to all scenarios for adult female lobsters in the spring in Chapter 7	155

Figure 7.4 Suitability indices from the base case compared to all scenarios for adult female lobsters in the fall in Chapter 7	156
Figure 7.5 Change in spatial habitat suitability from the historical to future periods used in Chapter 7.....	157
Figure 7.6 Historical and future spatial habitat suitability changes between the base case and all scenarios in Chapter 7 for spring female adults	158
Figure 7.7 Historical and future spatial habitat suitability changes between the base case and all scenarios in Chapter 7 for fall female adults.....	159

CHAPTER 1: AN INTRODUCTION TO THE GULF OF MAINE AND ITS FISHERIES

1.1 Oceanography of the Gulf of Maine

Anthropogenic climate change has both directly and indirectly been altering the planet's natural abiotic and biotic equilibria (Beardall and Raven 2003; Perry et al. 2005; Hazen et al. 2013; Anderson et al. 2013). Of major concern is the warming in many areas of the oceans, which are causing shifts in many species distributions as they seek more preferable and tolerable environments (Perry et al. 2005; Hazen et al. 2012; Anderson et al. 2013; Schuetz et al. 2019). These cascading effects are causing local extirpations (Mantyka-pringle et al. 2011), novel predator-prey interactions (Stebbing et al. 2002), and changes to how mankind interacts with the sea (Engelhard et al. 2013; Rogers et al. 2019). This undeniably provides evidence for the strong connection between the abiotic environment and its biotic inhabitants. The fate of many species across the planet are inexplicably linked with climate change. An ecosystem of particular interest is that of the Gulf of Maine, where the warming rates here are higher than most anywhere else in the oceans (Mills et al. 2013; Pershing et al. 2015).

The Gulf of Maine region (hereafter referred to as the GOM) is the northernmost area of the US Northeast Continental Shelf, comprised of the Gulf of Maine proper and George's Bank (Figure 1.1) and is distinguished by its high value fisheries. Historically, this ecosystem was exploited by European settlers who found an abundance of Atlantic cod (*Gadus morhua*) and other groundfish (Roberts 2007). Today, it is renowned for its American lobster (*Homarus americanus*) and Atlantic sea scallop (*Placopecten magellanicus*) fisheries. The Gulf of Maine has been a remarkable fishing ground for many species over the years because of the oceanography of the system that allows for the proliferation of many shelled and benthic marine species.

The Gulf of Maine is a highly dynamic environment (Durbin et al. 2003; Wanamaker et al. 2008), but relatively cold compared to regions south of Cape Cod and Georges Bank (Figure 1.1). This region represents the southernmost extent of the Labrador Current, which brings cold Arctic waters into the Gulf of Maine at depth through the Northeast Channel between Georges Bank and Nova Scotia (Petrie & Drinkwater 1993; Durbin et al. 2003; Wanamaker et al. 2008) (Figure 1.1). This cool Labrador slope water moves into the Gulf of Maine at depth. The much warmer Gulf Stream brings warm water from the south and moves offshore in this region (Wanamaker et al. 2008; Mountain 2012) (Figure 1.1). Water input from the Gulf Stream is less than that supplied from the Labrador Current and this imbalance has historically kept Maine waters relatively cool (Wanamaker et al. 2008).

However, in recent history, the waters in this system have been warming at an alarming rate (Mills et al. 2013; Pershing et al. 2015), due in part by melting Arctic sea ice (Saba et al. 2016). This melting phenomenon is releasing a lot of fresh water into the Arctic Ocean. Normally, this Arctic water is what the Labrador Current brings to the Gulf of Maine. However, fresh water is less dense than salt water and this current is now redirected and not as much is entering the Gulf of Maine at depth (Saba et al. 2016). This decrease in cold water from the North has allowed an increase in warm waters to enter the Gulf of Maine through the Gulf Stream (Saba et al. 2016). The hydrogeography of the Gulf of Maine in this sense is what is now allowing for this region of the ocean to warm at such a high rate.

Naturally, there has been much effort in improving predictive capacity for this region. The strong connection of the New England culture and economy to the GOM and its fisheries are fueling this analysis. How will the Atlantic Sea Scallop and American lobster fisheries in the GOM be changed under increased global warming scenarios?

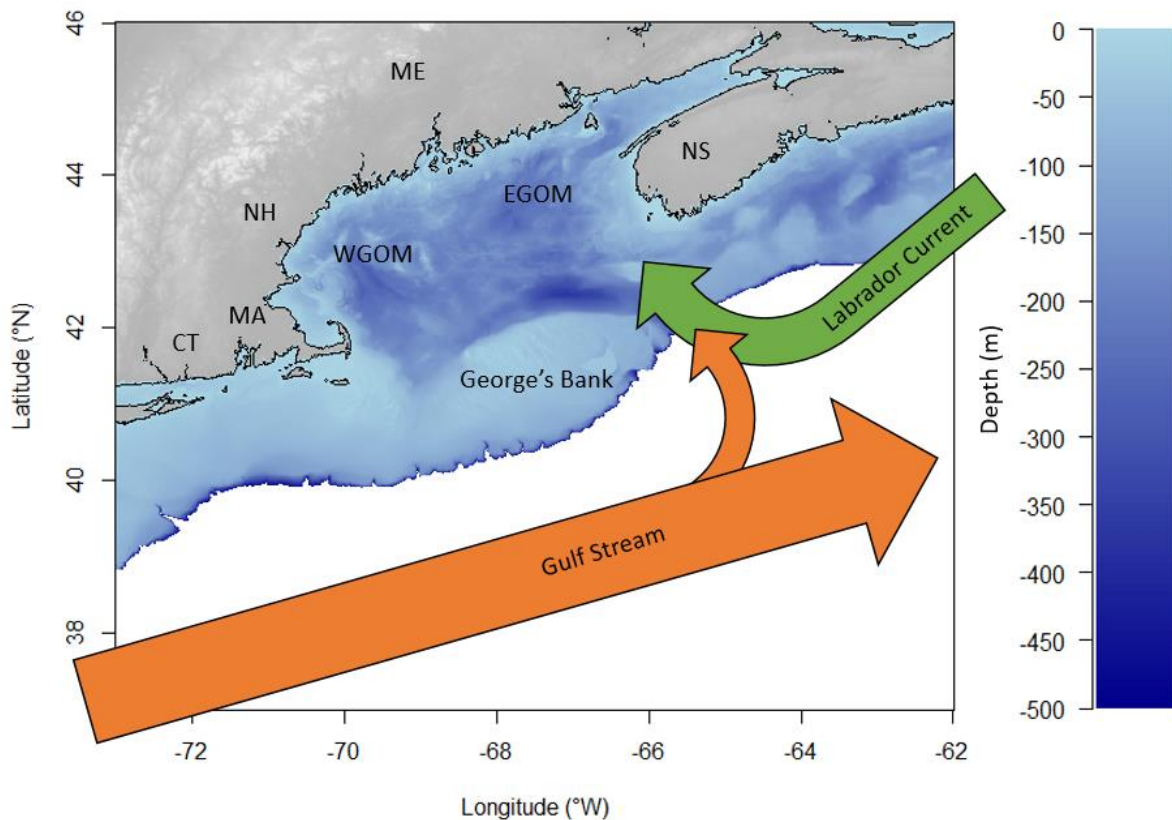


Figure 1.1. Bathymetric map of the Gulf of Maine showing depth in meters (m) and the supplying currents. The regions of the Gulf of Maine are the Western Gulf of Maine (WGOM), the Eastern Gulf of Maine (EGOM), and George's Bank. The Labrador Current brings cool Arctic waters to the Gulf of Maine at depth and the Gulf Stream brings warm waters from the south. The ratio of these two currents to the Gulf of Maine determines the temperature of the area. Also labeled are the states of Maine (ME), New Hampshire (NH), Massachusetts (MA), and Connecticut (CT), and the province of Nova Scotia (NS).

1.2 The Atlantic Sea Scallop and its Fishery in the Gulf of Maine

The Atlantic Sea Scallop (*Placopecten magellanicus*; ASC) is a bivalve mollusk; having a calcium carbonate exoskeleton comprised of two parts connected by an adductor muscle which forms its shell (Chapter 2: Figure 2.1). This shell is created through a process known as biomineralization, whereby the animal secretes mantle proteins that harness environmental ions,

namely calcium carbonate, to form the outermost layer of crystalized tissue (Marin and Luquet 2004; Hart and Chute 2009a; Hart and Chute 2009b). This process ensures the shell expands as the animal grows. Because of this specific growth process, the oldest material is closest to the hinge and the newest is at the outer edge of the shell. Because ASCs do not shed their hard parts as they grow like crustaceans, their shells can be used as a personalized life history transcribed in mineralized calcium carbonate (Hart and Chute 2009a; Hart and Chute 2009b) (see Chapter 2). This fact has allowed for extremely comprehensive analyses of ASC growth (Hart and Chute 2009a; Hart and Chute 2009b), which, in combination with extensive survey efforts, has led to exceptionally data-rich and well informed stock assessments for the animal and a well-managed fishery.

In the United States, ASCs are harvested using dredges from Cape Hatteras, North Carolina to Cobscook Bay, Maine (Hart and Chute 2004) and are prized for their large and tasty adductor muscles. Extensive and comprehensive management measures have ensured that ASCs across this range remain not overfished and have kept overfishing from occurring (NEFSC 2018). Moreover, catch of ASCs has more than doubled in the last decade over their range (NEFSC 2018). The Northern Gulf of Maine (NGOM) (Chapter 2: Figure 2.2), represents the northernmost extent of this range in the United States. Here, ASC management is segregated into two zones: state waters and federal waters.

In state waters, management is done through the Maine Department of Marine Resources (MEDMR). In federal waters, management is conducted by the New England Fishery Management Council (NEFMC). In federal waters, management relies on the use of the Scallop Area Management Simulator (SAMS) model, whose purpose is to calculate total allowable catches (TACs), based on the expected abundance and landings estimates (Hart 2010). The SAMS model

is an effective predictive tool for the scallop fishery. Since its implementation by the NEFMC in 1999, ASCs have not been overfished and landings have remained high (NEFSC 2018). There are limits to the SAMS model's predictive capacity in areas like the NGOM, due to lack of input information. The SAMS model has historically been limited in Maine's state waters because of the lack of information regarding growth rates of ASCs in this area.

ASCs in the NGOM are of course also subject to the rising temperatures of the region, which can affect their growth rates and overall life history (Côté et al. 1993). It is thus imperative to develop measures to infer how these animals and, by extension, this fishery will change in the future. The ASC fishery in the NGOM has a huge impact on the state, both economically and culturally as they have been fished for in this region for over a century and are second in value only to lobster (Schick & Feindel 2005).

1.3 The American Lobster and it's Fishery in the Gulf of Maine

The American lobster fishery on the North American East coast began over 150 years ago in the waters of the Cranberry Isles in Maine (Corson 2004). Fishermen began the practice of setting baited wooden traps on the seafloor and hauling them up regularly to collect what was inside (Corson 2004). The animals they targeted were American lobsters: *Homarus americanus*. This decapod crustacean has since become a staple of the GOM and a large part of the culture of the New England area.

Modern day lobster fishing has similarities to its early days. The fishermen (or lobstermen) each set hundreds of baited steel traps on the sea floor tied to floating buoys uniquely colored for the fisherman and haul them regularly to collect lobsters who have wandered into the traps to seek food and shelter (Corson 2004). Lobster as a food source has evolved to become a sought after delicacy in many areas creating an incredibly large fishery throughout the stock areas of the GOM

and Southern New England. This demand and subsequent fishing effort increase has caused lobstering to become the most lucrative single-species fishery in the United States with an annual estimated value of over half a billion dollars (MEDMR 2016; NMFS 2018).

Within the last few decades of this 150-year lobstering reign, there have been some large shifts in the fishery. What were once notable areas for lobster fishing have dwindled in output and areas not previously thought of as fishing grounds are now booming with these animals (ASMFC 2015). The entire fishery dynamic has had to subsequently shift: fisherman have had to change how they target these animals or quit altogether. This species is experiencing shifts in their habitats and typical life histories and the fishery is having to adapt to keep up (ASMFC 2015; Tanaka et al. 2018). A driving force behind these shifts is of course climate change.

Lobster biology and life history are directly impacted by temperature and other abiotic factors (Green et al. 2014; Madeira et al. 2012). This is because they are ectothermic crustaceans; meaning their internal body is not physiologically regulated, but rather driven by the outside environment (Madeira et al. 2012). This link means that lobsters as individuals and lobsters as a population have a strong connection with the warming GOM. Warming waters are affecting this species' growth (Staples et al. 2019), natural mortality (Mills et al. 2013), and reproduction (Goode et al. 2019; Tanaka et al. 2019). Climate driven changes on these life history parameters are predicted to have significant consequences for the size-structured stock assessment process (Audzijonyte et al. 2016) and thus many measures are being undertaken to mitigate these impacts (ASMFC 2020). It is imperative to transform the stock assessment and forecasting processes to incorporate these effects from temperature in many aspects of the lobster stock. To aid in this effort, appropriate modelling and forecasting of lobster habitat is also necessary.

As sea temperatures are rising in the GOM, historical locations of lobster abundance are shifting (ASMFC 2015). Much of the GOM is becoming more suitable for lobster (Tanaka & Chen 2016). However, as lobster habitat suitability in the GOM is increasing, lobster habitat suitability in Southern New England is decreasing (ASMFC 2015).

The southernmost extent of the American lobster stock is the lower tip of New Jersey. This area from New Jersey to Georges Bank is the Southern New England Stock of American lobster (Chapter 3: Figure 3.1). Southern New England was once renowned for its lobster landings in much the same way the GOM was. Landings by weight in metric tons of lobster was split relatively equally through the 1970s (NMFS 2018). However, there has been a large shift in landings as American lobster populations rise in the GOM and fall in Southern New England. Landings from 2010 to present have averaged approximately 500 to 1000 mt for Southern New England, but have risen substantially to 60,000 to 80,000 mt in the GOM (NMFS 2018). This decrease in Southern New England is thought to be due to in part to many years of low recruitment combined with a relatively low habitat suitability (ASMFC 2015). There is a combination of cultural fear and denial that this could or would ever happen to the GOM region. In order to appropriately and scientifically address the risk, there needs to be significant advancement in forecasting processes, both in terms of the lobster population and its habitat.

Lobster in the GOM is a cultural icon and a large contributor to the New England economy. However, climate change is affecting this species distribution, behavior, and life history. Many changes in the fishery have occurred over the past few decades, with many lobstermen having to give up their jobs and others experiencing higher paydays than ever. Fisherman and researchers alike expect more change in the future, but substantial research in stock assessment, forecasting, and habitat modelling processes are necessary to quantify it.

1.4 Objectives

Given the shifting thermal habitat of the GOM, there is a need to evaluate these changes on Atlantic Sea Scallops and American lobster. For scallops, a lack of growth information is limiting assessment effort in this region and so, in Chapter 2, a collection of shells from the GOM will be used to quantify spatiotemporal patterns in growth and link these patterns to the abiotics of the region. This will aid management and expand the modelling capacity of the SAMS to better estimate population dynamics and biomass estimates. For lobster, much of the stock assessment process is thermally static, violating the assumptions discussed in section 1.3 that this species' life history is heavily impacted by temperature. Thus, it is the goal of the following chapters to use these climate impacts to increase modelling capacity and reliability of the stock assessment, forecasting, and habitat modelling processes for GOM lobster.

Lobster growth is less understood compared to scallops and thus the same analysis cannot be adequately done. However, modelling capacity in the context of climate effects on growth can be and thus Chapter 3 details a sensitivity analysis of the stock assessment process to changes in growth and size-at-maturity that would come from increased warming scenarios. Chapter 4 takes this a step further by linking a novel spawning biomass/recruitment relationship to thermal habitat and using this tool as a way to inform management how to keep high levels of recruitment in the future, even under these increased warming scenarios. Chapter 5 uses a delta-generalized linear mixed effects model to estimate the effect of thermal habitat on survey abundance indices used in the stock assessment process and compares these to the traditionally used design-based indices. Chapter 6 uses the findings from the previous chapters to develop a forecasting model for American lobster that is thermally explicit and seasonal and shows how an environmentally explicit model is more reliable and accurate. Chapter 7 uses a bioclimate envelope model to map

and forecast lobster habitat and uses the results in a larger study to show the dangers of forecasting habitat in the absence of a high knowledge base of the species' life history a priori. Finally, Chapter 8 summarizes these findings and discusses how this information can be used to better assessment and forecasts of both species and additionally outlines the key next steps in the research process. This framework and the tools developed in this dissertation in whole and in part can be used to evaluate climate effects on other species life history and stock assessments.

**CHAPTER 2: SPATIOTEMPORAL VARIABILITY IN ATLANTIC SEA SCALLOP
(*PLACOPECTEN MAGELLANICUS*) GROWTH IN THE NORTHERN GULF OF
MAINE**

2.1 Abstract

Simulation-based assessment tools coupled with large-scale and consistent monitoring efforts contribute to the overall success of the Atlantic sea scallop (*Placopecten magellanicus*; ASC) fishery on the North American east coast. However, data from the Northern Gulf of Maine (NGOM) are usually excluded from the assessment because limited monitoring effort and an overall lack of information regarding the growth of ASCs in this region have led to large uncertainty of fine-scale dynamics. The objectives of this study are to determine if ASC growth varies spatially and/or temporally across the NGOM and if the variation in growth can be explained in part by variability in bottom temperature and bottom salinity. To achieve these objectives, ASC shells have been continually collected through a partnership between the University of Maine and Maine Department of Marine Resources since 2006. Individualistic ASC length-at-age curves are developed to evaluate small and large scale spatio-temporal variabilities. In comparison to ASC growth on Georges Bank and in Southern New England, it appears that ASCs in the NGOM are growing at a similar rate yet have the potential to grow to a larger size. No clear spatio-temporal trends in ASC growth are identified in the NGOM. However, our analysis reveals that bottom temperature and bottom salinity may be influencing inter-annual variabilities and contribute to growth rate differences seen between locations and years. This may imply changes in ASC growth in the future with increasing warming in the Gulf of Maine.

2.2 Introduction

The Atlantic sea scallop (*Placopecten magellanicus*; ASC) is a historically important commercial bivalve on the North American east coast. In the United States, ASCs are harvested from Cape Hatteras, North Carolina to Cobscook Bay, Maine (Hart & Chute 2004). ASC biomass (in metric tons of meat) has more than doubled in the last decade over their range (NEFSC 2018) and ASCs are not overfished and overfishing is not occurring (NEFSC 2018). This is due largely to extant and detailed approaches used to manage this fishery on a large-scale level. Techniques have been developed that allow for population-wide simulations under different fishing scenarios to determine catch limits per area for consecutive years (Rheuban et al. 2018; NEFSC 2018). However, areas like the Northern Gulf of Maine (NGOM) are usually excluded from these predictive models because of lack of information regarding the growth of ASCs in these regions. More southern areas such as Georges Bank (GBK) and the Mid-Atlantic Bight (MAB) are high-production fishing grounds for this species and so the bulk of knowledge concerning ASC growth rates has been from samples collected from these areas (Hart & Chute 2009a; Hart & Chute 2009b; Mann & Rudders 2019).

A scallop is a bivalve mollusk, having two hardened calcium carbonate structures connected by a hinge and a large adductor muscle (Figure 2.1). Unlike exoskeletal animals that shed their outer layers during a molt, scallops must expand their shell as they grow (Marin & Luquet 2004). Because of this, they must constantly be laying down new material. This new material (in the form of the aforementioned calcium carbonate) is set in place on the outer edges of shells, resulting in ring formation much like trees (Hart & Chute 2009a; Hart & Chute 2009b). This growth allows for simple calculation of length-at-age curves (a.k.a. growth curves). The rings are formed due to seasonal changes in growth rates; with shell formation being faster in the warmer months and slower in the colder months (Côté et al. 1993; Harris & Stokesbury 2006; Hart &

Chute 2009a; Hart & Chute 2009b), forming a single ring per year of growth. This is due to the direct effect that environmental variables (such as temperature and salinity) have on the metabolism of the animals (Côté et al. 1993). Many studies have demonstrated linkages between the rate of ASC growth and environmental conditions such as temperature, salinity, and depth (MacDonald & Thompson 1985a; MacDonald & Thompson 1985b; Thouzeau et al. 1991; Harris & Stokesbury 2006; Hart and Chute 2009a; Chute et al. 2012), yet few studies have looked at the spatiotemporal variation of these effects at finer spatial scales than large marine ecosystems (LMEs) such as GBK and the MAB.

Climate change is causing the NGOM ecosystem to warm at an accelerated rate compared with a majority of the world's oceans; with an average-per-year increasing temperature of 0.026°C (Pershing et al. 2015). Bottom temperature and bottom salinity fluctuate around yearly means as seasons change, but these yearly means for both variables are rising in the face of climate change (Pershing et al. 2015; Saba et al. 2016). This means that ASC growth has the potential to change as well. If it can be understood how these environmental variables affect ASC growth in the NGOM, it can be inferred if and how their growth will change into the future.

Understanding spatiotemporal variation in growth is important for the management of any marine resource, especially those in an environment experiencing rapid environmental changes (Maunder & Piner 2015). Mann & Rudders (2019) stated the importance of understanding age/length structures to inform the current assessment model for ASCs in GBK and the MAB, referring to using this information to enhance the current understanding of ASC recruitment and mortality. Assuming incorrect growth structures can lead to large effects on stock assessment outcomes and incorrect management advice (Maunder & Piner 2015). Little is known about the NGOM LME as it pertains to ASC growth, accentuating the increased likelihood of wrongly

assumed growth parameters. Most information about NGOM ASC growth comes from a singular study by Truesdell (2014), wherein growth is analyzed across different spatial zones in the NGOM. In short, Truesdell (2014) concluded that NGOM scallops grow to larger sizes, yet grow slower than scallops in GBK and the MAB. This study, however, only addresses spatial differences in growth and spatial effects of environmental variables.

The objectives of this study were to 1) Determine if ASC growth varies spatially and/or temporally across the four management zones in the NGOM (Figure 2.2) and 2) Determine if variation in ASC growth in these areas and across years can be explained in part by bottom temperature and bottom salinity. To achieve these objectives, von Bertalanffy growth parameters for multiple locations and age classes are determined using methods from Hart & Chute (2009a) and growth increment data is used in multiple regression analyses to determine relative influence of environmental factors bottom temperature and bottom salinity as well as spatial (latitude and longitude) and time-varying (year of growth) factors. This same process to determine spatiotemporal variation and influence of environmental factors can be applied to many bivalve species whose historical size-at-age is determinable from their shells or for fish species who have reliable otolith size to fish length relationships.

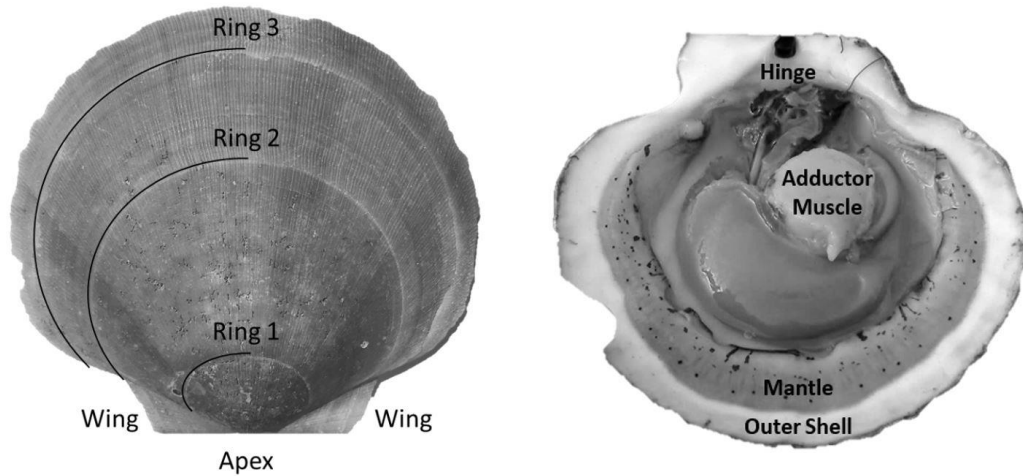


Figure 2.1. An ASC top shell (left) and bottom shell (right) with important features labelled. Growth rings are outlined for this three year old specimen.

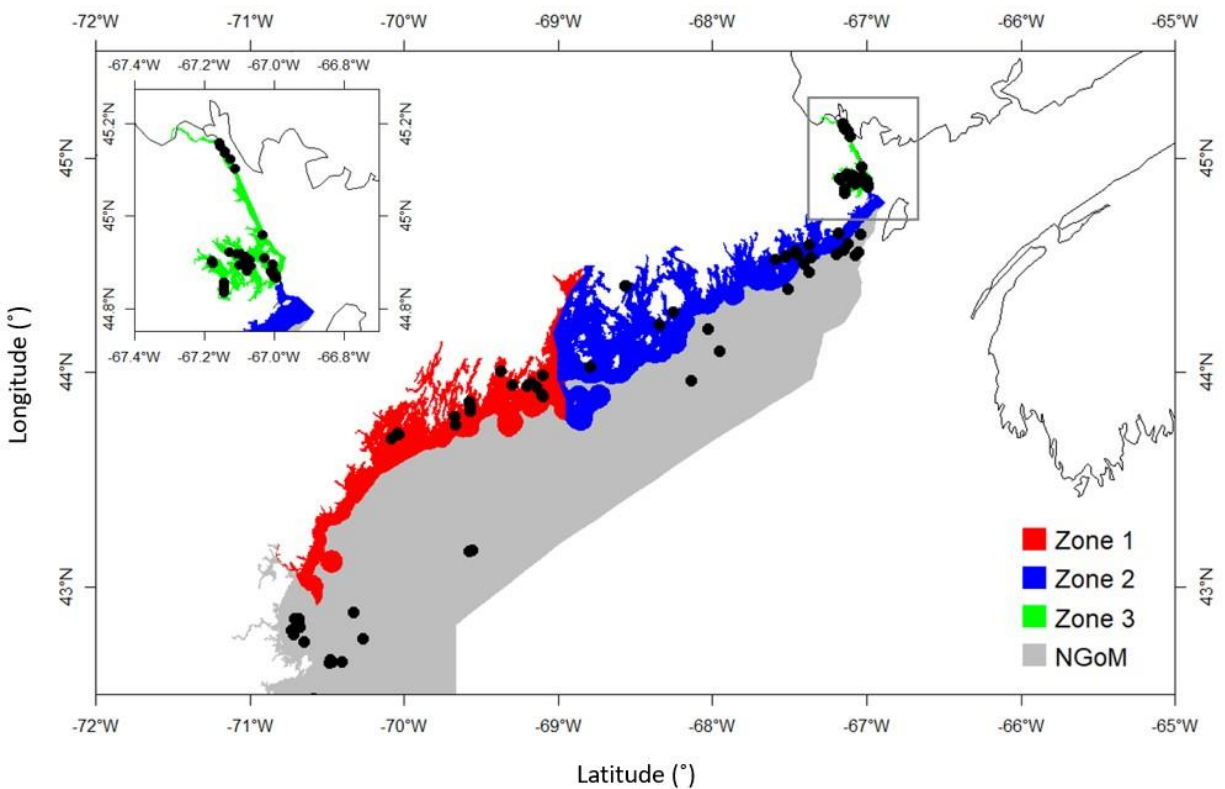


Figure 2.2. The Northern Gulf of Maine (management zone 4; grey) with management zones 1-3 colored red, blue, and green, respectively. Black dots represent locations where scallops were collected over the entire survey.

2.3 Methods

2.3.1 Study Area

The NGOM management area (Figure 2.2) is the most northern extent of the United States' ASC stock. This area is managed on smaller scales: namely inshore (<3 nautical miles (nm) from shore) and offshore (>3nm from shore). The inshore NGOM is split into three distinct management sections: Zone 1 (commonly referred to as the Western Gulf of Maine), Zone 2 (commonly referred to as the Eastern Gulf of Maine), and Zone 3 (Cobscook Bay; Figure 2.2), with each zone having slightly different management techniques, but the same management entity: the Maine Department of Marine Resources (MEDMR). The offshore NGOM (referred to here as management zone 4) is treated as a single large unit and is managed jointly at both state and federal levels (by MEDMR and the New England Fishery Management Council).

The NGOM is characterized as having fluctuating yearly temperatures and salinities, influenced by a combination of the warm and salty North-bound Gulf Stream and the colder, less salty South-bound Labrador Current (Durbin et al. 2003; Wanamaker et al. 2008). Additionally, year to year variations are also present in these variables due to changing ratios of incoming water masses due to climate change (Mills et al. 2013; Pershing et al. 2015), resulting in higher observed temperatures and salinities.

2.3.2 Ageing & Growth Modelling

A partnership between the University of Maine and the MEDMR has been responsible for collecting ASC shells from the study area since 2006 which are subsequently stored at the University of Maine until they are aged. Part of these shells were utilized for Truesdell's (2014) analyses, but the sample size has been greatly improved in recent years with additional samples being collected from broader areas in the NGOM.

Aging of shells followed methods from Hart and Chute (2009a). Each shell is measured from the apex (center of the hinge; Figure 2.1) to each consecutive ring, producing a number of data points for each scallop as there are visible rings. The number of rings, though, is not always indicative of absolute age, however. The first two years of growth of an ASC are not as predictable or uniform as from two years onward. Because of this, the one-year growth ring or the two-year growth ring may be the first visible ring. Agers are taught how to infer which year the first visible ring corresponds to based on typical shell size-at-age, as well as which rings are actual growth rings, and which are false rings caused by stress (additionally, each new person introduced to the project partakes in a trial period to make sure their ageing technique does not produce measurements statistically dissimilar from previous agers). The differences between these data points is what is known as incremental growth. Fabens (1965) has modified the von Bertalanffy growth function to model this particular type of growth data. The function is as follows:

$$L_{t+1} = \exp(-K) \times L_t + L_{\infty} \times (1 - \exp(-K)) \quad (2.1)$$

where L_t is the length at time t , L_{t+1} is the length at time $t+1$, L_{∞} is the theoretical asymptotic maximum size at which length approaches, and K is the Brody growth coefficient.

Following Hart & Chute (2009a), L_{∞} and K were found for each individual ASC via the Ford-Walford method, in which L_{∞} and K are found from a linear fit of all L_t and L_{t+1} pairs for each individual with at least 3 growth rings (the same cutoff used by Hart & Chute 2009a). Once L_{∞} and K values were found for each individual, population values for each Zone (1, 2, and 3) as well as for offshore waters were established. Additionally, the entire NGOM population was also split into year classes with sufficient sample sizes (1998-2010). These results could not be obtained

from a regression of all data points in each group due to the possibility of large bias (Hart & Chute 2009a). Nor could they be obtained simply from taking an average of all individual values for L_∞ and K for the same reason. Thus, following the methods outlined by Hart & Chute (2009a),

$$m_i = \exp(-K_i) \quad (2.2)$$

$$b_i = L_{\infty,i} \times (1 - m_i) \quad (2.3)$$

representing the slope and intercept of each individual's L_{t+1} vs L_t plot respectively, were obtained (with K_i and $L_{\infty,i}$ representing the K and L_∞ of individual i). Additionally, $m = \text{mean}(m_i)$ and $b = \text{mean}(b_i)$, representing the population slope and population intercept respectively, were calculated. Letting α_i and β_i represent the deviations of each m_i from m and each b_i from b , respectively, the equations for approximating population L_∞ and K values are as follows (Hart & Chute 2009a):

$$L_\infty \cong \frac{b}{1 - m} + \frac{1}{(1 - m)^2} \times \left(\frac{b \times \text{Var}(\alpha_i)}{1 - m} + \text{Cov}(\alpha_i, \beta_i) \right) \quad (2.4)$$

$$K \cong -\ln(m) + \frac{\text{Var}(\alpha_i)}{2 \times m^2} \quad (2.5)$$

with $\text{Var}(\alpha_i)$ and $\text{Cov}(\alpha_i, \beta_i)$, being the variance of α_i and covariance of α_i and β_i , respectively. Additionally, the standard errors (σ) of L_∞ and K were approximated as (Hart & Chute 2009a):

$$\sigma_{L_\infty} \cong L_\infty^2 \times \left(\frac{\sigma_b^2}{b^2} + \frac{\sigma_m^2}{(1-m)^2} + \frac{2 \times \sigma_b \times \sigma_m \times \rho}{b \times (1-m)} \right) \quad (2.6)$$

$$\sigma_k \cong \frac{\sigma_m}{m} \quad (2.7)$$

with σ_{L_∞} , σ_K , σ_b , and σ_m representing the standard errors of L_∞ , K , b , and m respectively. All calculations were completed using R software (version 3.4.1). All R scripts used in modelling and analyses can be made available upon request.

2.3.3 Modelling Environmental Effects

L_∞ and K cannot be associated with a particular year, only a location (they are constant throughout an individual scallop's life). Thus, these values cannot be matched to any time-dependent environmental covariates. Because of these limitations, a different response variable had to be chosen for regression testing. The variable chosen was the change in length from one ring to the next: the growth over the course of a time-step in millimeters: Δmm . Because ASCs are sedentary after their spat stage (before 1 year old), each Δmm can be associated with a location (latitude and longitude), a time (year of growth), and by extension, abiotic variables associated with those locations and averaged over that year. The variables used in this study were bottom temperature (Figures 2.3 and 2.4) and bottom salinity (Figure 2.5). Additionally, because Δmm varies widely between age classes, separate regression tests were conducted for each, allowing for any age-specific environmental interactions to be explored.

Bottom temperature and bottom salinity data were obtained from University of Massachusetts (UMass) Dartmouth School for Marine Science and Technology (SMAST)'s Finite

Volume Community Ocean Model (FVCOM). This geophysical model has been shown to have reliable performance in predicting bottom water parameters at fixed locations called stations, especially for well-stratified areas like the NGOM (Li et al. 2017). For each ASC, an average bottom temperature and salinity was obtained for each year of its growth. If the location of the tow was within ½ kilometer (km) of a FVCOM station, then the closest station was used to determine the abiotic conditions at the tow location. If no FVCOM station existed within ½ km radius, then the average of all FVCOM stations within a 1 km by 1 km grid centered on the tow location was used as a proxy.

Correlation coefficient calculation and variance inflation factor (VIF) tests were used to determine which combinations of predictor variables could be used together to have reliable regression output. Correlation coefficient values outside the range of (-0.5, 0.5) for a correlation coefficient meant those variables could not be used in the same test due to high collinearity. VIF values greater than 10 represent high multi-collinearity and do not allow for those variables to be used together in the same regression (O'brien 2007). These methods were used in tandem: correlation coefficients for all combinations of two factors were calculated and then VIF tests were conducted on all factor combinations used in regressions. This was done as to assume high robustness in factor selection for regression testing.

Three different types of regression testing were conducted on each combination of factors that passed the two-step process above: linear regression (LR), boosted regression trees (BRT), and generalized additive models (GAMs). Model selection was based on root mean squared error (RMSE) and Akaike information criterion (AIC). Additionally, in an effort to further explore patterns in temporal trends, an additional six regression tests were run for each age class with year of growth as the only predictor variable only for ASCs from Cobscook Bay. The intent of these

six models was to see if temporal trends could be more readily determinable if spatial differences were ignored.

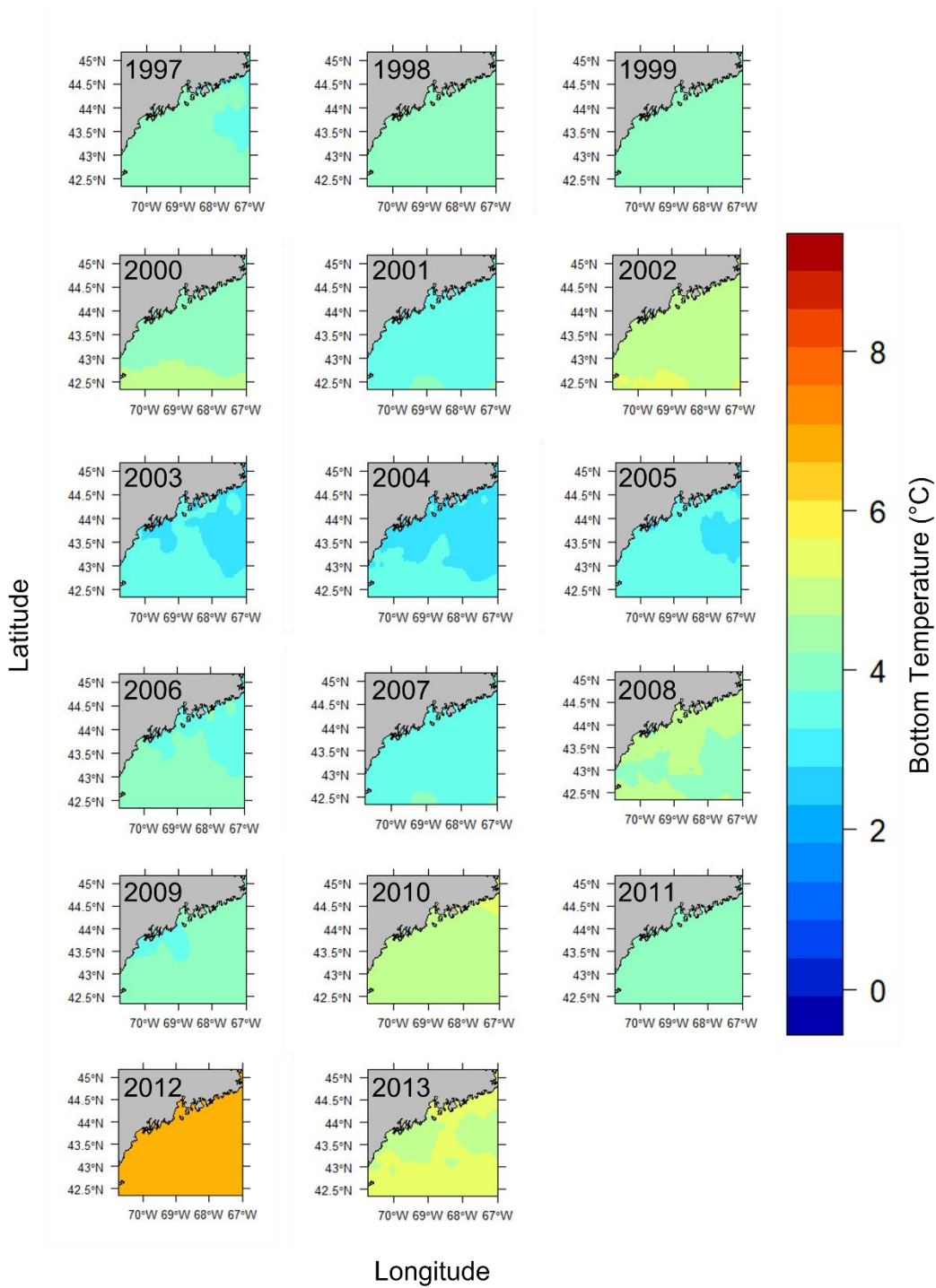


Figure 2.3. Average yearly bottom temperature over the study region 1997-2013. Temperature values are in degrees Celsius.

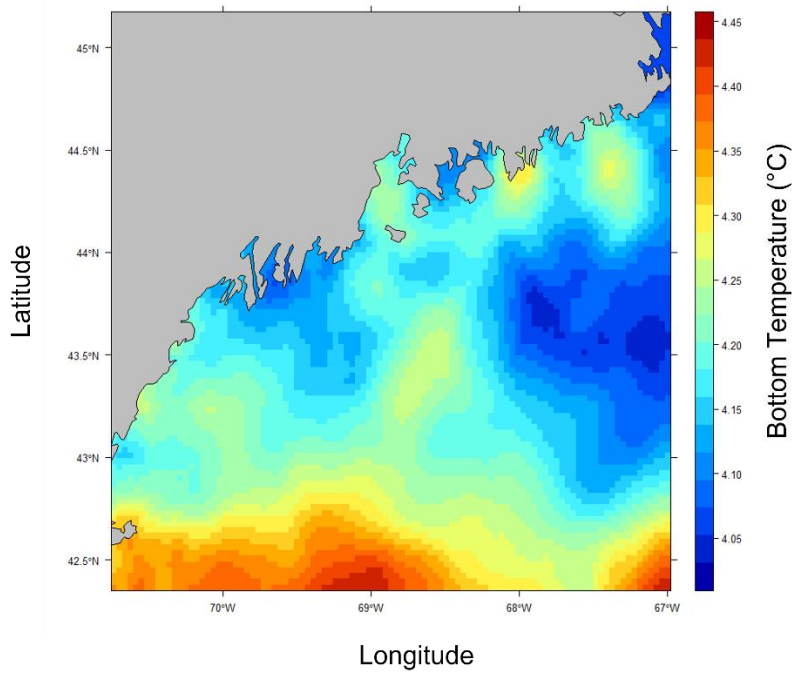


Figure 2.4. Average bottom temperature over the study region averaged across years 1997-2013. Temperature values are in degrees Celsius.

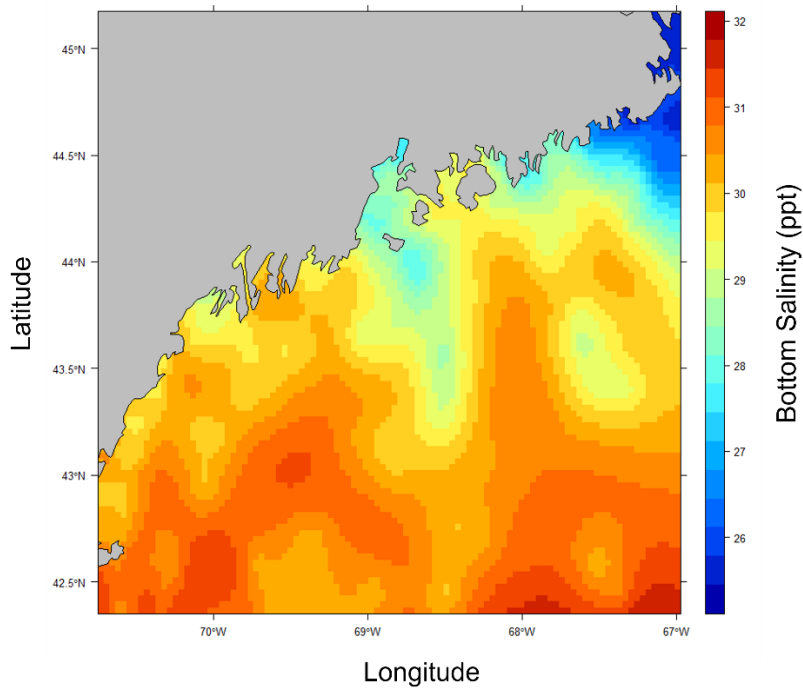


Figure 2.5. Average bottom salinity over the study region averaged across years 1997-2013. Salinity values are in parts per thousand.

2.4 Results

2.4.1 Spatial Differences in Growth Parameters L_{∞} and K

Final L_{∞} and K spatial values with associated standard errors are presented in Tables 2.1 and 2. L_{∞} was statistically different in the NGOM compared to Georges Bank (GBK) and the Mid-Atlantic Bight (MAB) (One-way Analysis of Variance (ANOVA) test: $F(2, 9030) = 654.54$, $p < 0.01$, Tukey's post hoc: all $p < 0.01$), with an apparent increasing trend in L_{∞} with increasing latitude (Table 2.1). K was statistically different in the NGOM compared to GBK and the MAB (One-way ANOVA test: $F(2, 9030) = 227.50$, $p < 0.01$, Tukey's post hoc: all $p < 0.01$), but no trend was apparent (Table 2.1). Data for GBK scallops and MAB scallops were obtained from Truesdell (2014) and Hart and Chute (2009a).

Within the NGOM, L_{∞} was statistically different in all 4 management zones (One-way ANOVA test: $F(3, 2643) = 146.02$, $p < 0.01$, Tukey's post hoc: all $p < 0.01$), with highest values in Zone 2 and lowest in Zone 3 (Table 2.2). K was statistically different across all three inshore zones, but Zone 4 was only statistically different from zones 1 and 3 (One-way ANOVA test: $F(3, 2643) = 67.89$, $p < 0.01$, Tukey's post hoc: $p < 0.01$ for zone pairings 1&2, 1&3, 1&offshore, 2&3, and 3&offshore, $p > 0.05$ for zone pairing 2&offshore), with highest values in Zone 3 and lowest values in Zone 2 (Table 2.2). ASCs in Zone 1 appear to have the potential to grow to larger sizes than those in Zone 2, yet at a slower rate (Table 2.2). Cobscook Bay scallops (Zone 3) grow very rapidly, but do not reach the large sizes they do in the rest of the NGOM. Additionally, offshore (Zone 4) ASCs tend to grow at similar rates to scallops in Zone 1.

Table 2.1. Mean L_{∞} and K values with associated standard errors (SE) and sample sizes (n) for the Northern Gulf of Maine (NGOM), Georges Bank (GBK), and the Mid-Atlantic Bight (MAB).

Area	L_{∞} (mm)		K(1/yr)		n
	Mean	SE	Mean	SE	
NGOM	154.05	0.58	0.45659	0.00384	2647
GBK	143.9	0.23	0.427	0.00172	4092
MAB	133.3	0.28	0.508	0.00271	2294

Table 2.2. Mean L_{∞} and K values with associated standard errors (SE) and sample sizes (n) for each of four management zones in the Northern Gulf of Maine.

Zone	L_{∞} (mm)		K(1/yr)		n
	Mean	SE	Mean	SE	
1	152.72	1.21	0.44656	0.00877	448
2	173.08	2.01	0.36869	0.00985	298
3	142.97	0.71	0.50646	0.00552	1262
1+2+3	150.3	0.63	0.47154	0.00437	2014
4	166.71	1.36	0.40203	0.00757	639
1+2+3+4	154.05	0.58	0.45659	0.00384	2647

2.4.2 Temporal Differences in Growth Parameters L_{∞} and K

Final L_{∞} and K temporal values with associated standard errors are presented in Table 2.3. L_{∞} was statistically different in most year classes than others, but with no discernable trend over the time series (One-way ANOVA test: $F(12, 647) = 742.18$, $p < 0.01$, Tukey's post hoc results presented in Table 2.4). K was statistically different in some year classes than others, but with no discernable trend over the time series (One-way ANOVA test: $F(12, 647) = 978.4075$, $p < 0.01$, Tukey's post hoc results presented in Table 2.5).

Table 2.3. Mean L_{∞} and K values with associated standard errors (SE) and sample sizes (n) for year classes of Atlantic sea scallops from 1998 to 2010.

Year Class	L_{∞} (mm)		K(1/yr)		n
	Mean	SE	Mean	SE	
2011	-	-	-	-	2
2010	135.73	2.47	0.61338	0.03821	50
2009	132.73	2.01	0.59659	0.03372	36
2008	149.09	3.68	0.345	0.02594	19
2007	179.43	9.00	0.35026	0.04863	14
2006	155.47	1.75	0.47155	0.0144	111
2005	157.76	2.27	0.38128	0.01262	128
2004	169.36	3.48	0.30349	0.01446	80
2003	155.37	2.54	0.34145	0.01804	59
2002	154.02	3.41	0.27901	0.01909	22
2001	150.17	3.84	0.37391	0.04103	11
2000	140.1	2.23	0.49285	0.02046	79
1999	153.38	3.95	0.36228	0.0204	34
1998	166.09	5.83	0.35855	0.04746	17
1997	-	-	-	-	3
All	154.05	0.58	0.45659	0.00384	2647

Table 2.4. Tukey’s Post Hoc test results for One-way ANOVA test of L_∞ in year classes 1998 through 2010 ($F(12, 647) = 742.18, p < 0.01$). p values are presented right of black boxes and a “*” left of black boxes denotes statistical significance with $\alpha = 0.05$.

	2010	2009	2008	2007	2006	2005	2004	2003	2002	2001	2000	1999	1998
2010		<0.01	<0.01	<0.01	<0.01	<0.01	<0.01	<0.01	<0.01	<0.01	<0.01	<0.01	<0.01
2009	*		<0.01	<0.01	<0.01	<0.01	<0.01	<0.01	<0.01	<0.01	<0.01	<0.01	<0.01
2008	*	*		<0.01	<0.01	<0.01	<0.01	<0.01	<0.01	1.00	<0.01	<0.01	<0.01
2007	*	*	*		<0.01	<0.01	<0.01	<0.01	<0.01	<0.01	<0.01	<0.01	<0.01
2006	*	*	*	*		<0.01	<0.01	1.00	0.69	<0.01	<0.01	0.03	<0.01
2005	*	*	*	*	*		<0.01	<0.01	<0.01	<0.01	<0.01	<0.01	<0.01
2004	*	*	*	*	*	*		<0.01	<0.01	<0.01	<0.01	<0.01	<0.01
2003	*	*	*	*	*	*	*		0.85	<0.01	<0.01	0.11	<0.01
2002	*	*	*	*	*	*	*	*		0.03	<0.01	1.00	<0.01
2001	*	*	*	*	*	*	*	*	*		<0.01	0.11	<0.01
2000	*	*	*	*	*	*	*	*	*	*		<0.01	<0.01
1999	*	*	*	*	*	*	*	*	*	*	*		<0.01
1998	*	*	*	*	*	*	*	*	*	*	*	*	

Table 2.5. Tukey’s Post Hoc test results for One-way ANOVA test of K in year classes 1998 through 2010 ($F(12, 647) = 978.41, p < 0.01$). p values are presented right of black boxes and a “*” left of black boxes denotes statistical significance with $\alpha = 0.05$.

	2010	2009	2008	2007	2006	2005	2004	2003	2002	2001	2000	1999	1998
2010		0.05	<0.01	<0.01	<0.01	<0.01	<0.01	<0.01	<0.01	<0.01	<0.01	<0.01	<0.01
2009	*		<0.01	<0.01	<0.01	<0.01	<0.01	<0.01	<0.01	<0.01	<0.01	<0.01	<0.01
2008	*	*		1.00	<0.01	<0.01	<0.01	1.00	<0.01	0.05	<0.01	0.29	0.86
2007	*	*	*		<0.01	<0.01	<0.01	0.99	<0.01	0.34	<0.01	0.91	1.00
2006	*	*	*	*		<0.01	<0.01	<0.01	<0.01	<0.01	<0.01	<0.01	<0.01
2005	*	*	*	*	*		<0.01	<0.01	<0.01	1.00	<0.01	<0.01	0.01
2004	*	*	*	*	*	*		<0.01	<0.01	<0.01	<0.01	<0.01	<0.01
2003	*	*	*	*	*	*	*		<0.01	<0.01	<0.01	<0.01	0.25
2002	*	*	*	*	*	*	*	*		<0.01	<0.01	<0.01	<0.01
2001	*	*	*	*	*	*	*	*	*		<0.01	0.96	0.88
2000	*	*	*	*	*	*	*	*	*	*		<0.01	<0.01
1999	*	*	*	*	*	*	*	*	*	*	*		1.00
1998	*	*	*	*	*	*	*	*	*	*	*	*	

2.4.3 Regression Model Selection

Correlation coefficients and VIF values (Tables 2.6 and 2.7, respectively) allowed for 14 unique combinations of predictor variables. LR could not capture the appropriate trends in the data available. Due to very poor fit, this regression type was rejected. BRT and GAM both well outperformed LR, with BRT usually having lower RMSE (Table 2.9) and AIC values (Table 2.13) when compared to GAM (Table 2.8 for RMSE and Table 2.12 for AIC). However, GAMs allowed for the additional testing of spatial interaction terms more efficiently. Due to a general agreement in trends between BRT and GAM output, results from both types of regression testing are presented. Conclusions are made from both types of models.

Nineteen BRTs were run for each of six ASC age classes (Tables 2.9, 2.11, and 2.13): totaling 114 regression outputs. Twenty-two GAMs were run for each of six age classes (Table 2.8, 2.10, and 2.12): totaling 132 regression outputs. This discrepancy again is the testing of spatial interactions on single variables. An additional six GAMs were used to explore temporal trends in Cobscook Bay (see section 2.3). Neither GAMs nor BRTs are inherently and universally better than the other and model performance and fit depends on the data set (Martínez-Rincón et al. 2012). This accentuates the importance of testing multiple methodologies for modelling different data sets.

Table 2.6. A correlation matrix of all predictor variables used in this study. Values denote the correlation coefficients of those predictor variable pairings. Any variable pair corresponding to a correlation coefficient outside the range of (-0.5, 0.5) were not used together in this study. Two pairings were outside this range: Latitude with Longitude and Latitude with Salinity. These combinations could not be used in the same regression analysis. Lat = Latitude, Lon = Longitude, Temp = Temperature, Sal = Salinity, Year = Year of Growth, Δ mm = change in scallop shell size from one year to the next: shown here only to determine the direction and strength of relationships with each predictor variable in regression testing.

	Year	Lat	Lon	Temp	Sal	Δ mm
Year	-	-0.16	-0.11	-0.24	0.12	-0.19
Lat	-0.16	-	0.95	0.19	-0.53	0.13
Lon	-0.11	0.95	-	0.13	-0.37	0.11
Temp	-0.24	0.19	0.13	-	-0.11	0.19
Sal	0.12	-0.53	-0.37	-0.11	-	-0.03
Δ mm	-0.19	0.13	0.11	0.19	-0.03	-

Table 2.7. Variance inflation factors (VIF) of fourteen different combinations (rows) of abiotic variables used in the generalized additive models. Blank cells represent the absence of that variable in the combination. No VIF test was done on single parameter models or models with location interaction terms.

	Abiotic Factors				
	Year of Growth	Latitude	Longitude	Temperature	Salinity
1	1.07	-	-	1.07	1.02
2	-	-	-	1.01	1.01
3	1.06	-	-	1.06	-
4	1.01	-	-	-	1.01
5	1.07	1.05	-	1.09	-
6	1.03	1.03	-	-	-
7	-	1.04	-	1.04	-
8	1.07	-	1.18	1.07	1.17
9	-	-	1.17	1.02	1.17
10	1.07	-	1.02	1.07	-
11	1.02	-	1.17	-	1.17
12	1.01	-	1.01	-	-
13	-	-	1.02	1.02	-
14	-	-	1.16	-	1.16

Table 2.8. Root-mean-squared-error (RMSE) values of different generalized additive models for combinations of abiotic variables and age class. Lat = Latitude, Lon = Longitude, Temp = Temperature, Sal = Salinity, Year = Year of Growth. Models surrounded with 'I()' are treated as a single interaction term.

	Age Class					
	0-2	2-3	3-4	4-5	5-6	6-7
Lat	9.30	8.28	5.80	4.89	4.38	3.69
Lon	9.21	8.16	5.75	4.92	4.32	3.52
Year/Temp/Sal	8.71	8.02	5.61	4.70	4.18	3.49
Temp/Sal	9.03	8.13	5.61	4.77	4.21	3.56
Year/Temp	9.10	8.25	5.69	4.94	4.30	3.67
Year/Sal	8.76	8.07	5.66	4.78	4.21	3.58
Year	9.18	8.39	5.77	5.00	4.31	3.80
Temp	9.58	8.46	5.69	5.04	4.42	3.85
Sal	9.23	8.19	5.80	4.88	4.23	3.64
Year/Temp/Lat	8.72	7.98	5.61	4.68	4.22	3.60
Year/Lat	8.77	8.10	5.69	4.76	4.29	3.62
Temp/Lat	9.13	8.14	5.61	4.74	4.35	3.65
Year/Temp/Sal/Lon	8.39	7.86	5.47	4.61	4.08	3.42
Temp/Sal/Lon	8.72	7.88	5.48	4.64	4.17	3.56
Year/Temp/Lon	8.66	7.93	5.57	4.75	4.21	3.47
Year/Sal/Lon	8.44	7.88	5.57	4.67	4.14	3.56
Year/Lon	8.64	7.99	5.69	4.76	4.27	3.49
Temp/Lon	9.06	7.99	5.57	4.76	4.25	3.50
Sal/Lon	8.92	7.98	5.64	4.73	4.18	3.49
I(Year/Lat/Lon)	8.44	7.76	5.53	4.73	4.34	3.40
I(Temp/Lat/Lon)	8.71	7.76	5.57	4.74	4.31	3.37
I(Sal/Lat/Lon)	8.71	7.69	5.55	4.69	4.11	3.40

Table 2.9. Root-mean-squared-error (RMSE) values of different boosted regression trees for combinations of abiotic variables and age class. Lat = Latitude, Lon = Longitude, Temp = Temperature, Sal = Salinity, Year = Year of Growth.

	Age Class					
	0-2	2-3	3-4	4-5	5-6	6-7
Lat	9.03	8.21	5.54	4.77	4.31	3.58
Lon	8.85	8.16	5.52	4.88	4.41	3.66
Year/Temp/Sal	8.74	7.96	5.50	4.72	4.30	3.68
Temp/Sal	8.95	7.99	5.52	4.71	4.26	3.69
Year/Temp	9.01	8.17	5.62	4.90	4.41	3.68
Year/Sal	8.85	8.05	5.59	4.75	4.31	3.63
Year	9.22	8.47	5.74	5.01	4.37	3.77
Temp	9.35	8.22	5.64	4.93	4.37	3.86
Sal	9.10	8.09	5.60	4.79	4.29	3.64
Year/Temp/Lat	8.65	8.06	5.45	4.67	4.34	3.63
Year/Lat	8.71	8.12	5.50	4.73	4.39	3.57
Temp/Lat	8.98	8.14	5.50	4.69	4.34	3.62
Year/Temp/Sal/Lon	8.48	7.81	5.38	4.58	4.30	3.62
Temp/Sal/Lon	8.65	7.87	5.40	4.59	4.25	3.57
Year/Temp/Lon	8.52	8.07	5.43	4.70	4.37	3.69
Year/Sal/Lon	8.52	7.84	5.41	4.65	4.23	3.59
Year/Lon	8.58	8.08	5.50	4.77	4.42	3.69
Temp/Lon	8.77	8.04	5.42	4.70	4.37	3.69
Sal/Lon	8.74	7.88	5.46	4.71	4.26	3.65

Table 2.10. Deviance explained (DE) of different generalized additive models for combinations of abiotic variables and age class. Lat = Latitude, Lon = Longitude, Temp = Temperature, Sal = Salinity, Year = Year of Growth. Models surrounded with 'I()' are treated as a single interaction term. Highest DE for each class are bolded.

	Age Class					
	0-2	2-3	3-4	4-5	5-6	6-7
Lat	9.18	7.70	2.90	14.90	4.16	12.23
Lon	10.82	10.38	4.53	13.86	6.62	20.00
Year/Temp/Sal	20.41	13.41	9.25	21.34	12.89	21.38
Temp/Sal	14.29	11.04	9.26	19.07	11.30	18.00
Year/Temp	13.12	8.36	6.72	13.05	7.72	13.01
Year/Sal	19.49	12.49	7.66	18.79	11.47	17.45
Year	11.46	5.26	3.86	10.99	7.11	6.95
Temp	3.62	3.64	6.61	9.59	2.20	4.18
Sal	10.57	9.78	3.05	15.35	10.73	14.58
Year/Temp/Lat	20.20	14.29	9.28	22.17	11.19	16.17
Year/Lat	19.25	11.80	6.79	19.32	8.09	15.38
Temp/Lat	12.43	10.97	9.19	20.10	5.55	14.10
Year/Temp/Sal/Lon	26.06	16.91	13.58	24.28	16.84	24.47
Temp/Sal/Lon	20.07	16.37	13.51	23.22	13.23	18.17
Year/Temp/Lon	21.17	15.48	10.58	19.74	11.42	22.05
Year/Sal/Lon	25.26	16.37	10.38	22.50	14.21	18.06
Year/Lon	21.55	14.03	6.70	19.28	8.84	21.22
Temp/Lon	13.78	14.14	10.54	19.46	9.69	20.78
Sal/Lon	16.51	14.42	8.41	20.32	12.89	21.41
I(Year/Lat/Lon)	25.16	19.08	11.89	20.55	5.77	25.26
I(Temp/Lat/Lon)	20.42	19.06	10.40	19.99	7.05	26.77
I(Sal/Lat/Lon)	20.30	20.35	11.08	21.57	15.64	25.32

Table 2.11. Deviance explained (DE) of different boosted regression trees for combinations of abiotic variables and age class. Lat = Latitude, Lon = Longitude, Temp = Temperature, Sal = Salinity, Year = Year of Growth. Highest DE for each are class are bolded.

	Age Class					
	0-2	2-3	3-4	4-5	5-6	6-7
Lat	23.09	23.80	17.03	24.05	4.44	18.19
Lon	23.50	23.06	17.82	23.68	5.85	22.67
Year/Temp/Sal	31.89	28.64	24.92	30.28	12.37	24.17
Temp/Sal	28.93	27.89	25.10	27.84	12.56	19.55
Year/Temp	23.88	20.56	19.14	24.53	9.99	8.20
Year/Sal	27.83	25.31	21.31	25.94	10.34	19.31
Year	11.80	4.65	3.93	11.28	7.24	10.22
Temp	20.16	19.69	19.50	24.00	3.09	8.90
Sal	23.46	24.09	20.49	24.03	10.17	16.70
Year/Temp/Lat	34.12	28.07	24.75	27.15	12.01	22.80
Year/Lat	30.77	25.10	20.30	27.44	6.67	19.45
Temp/Lat	29.70	28.00	24.55	27.80	7.56	16.33
Year/Temp/Sal/Lon	36.37	32.25	26.20	32.42	15.34	25.63
Temp/Sal/Lon	33.68	32.06	26.22	31.21	10.88	25.28
Year/Temp/Lon	33.96	28.62	23.02	30.29	11.60	24.79
Year/Sal/Lon	35.29	30.21	24.31	30.99	15.23	21.11
Year/Lon	30.61	24.69	19.98	26.45	9.62	19.72
Temp/Lon	30.22	28.69	23.97	30.21	6.20	23.30
Sal/Lon	31.40	29.53	25.01	31.92	15.40	23.25

Table 2.12. Akaike information criterion (AIC) of different generalized additive models for combinations of abiotic variables and age class. Lat = Latitude, Lon = Longitude, Temp = Temperature, Sal = Salinity, Year = Year of Growth. Models surrounded with 'I()' are treated as a single interaction term. Lowest AIC values for each age class are bolded.

	Age Class					
	0-2	2-3	3-4	4-5	5-6	6-7
Lat	14076	12748	10106	5234	2130	904
Lon	14040	12695	10079	5248	2130	893
Year/Temp/Sal	13850	12652	10017	5197	2111	891
Temp/Sal	13980	12690	10015	5208	2110	895
Year/Temp	14006	12752	10045	5271	2121	906
Year/Sal	13862	12669	10042	5213	2114	894
Year	14028	12795	10085	5278	2122	905
Temp	14191	12823	10045	5292	2136	913
Sal	14047	12707	10104	5234	2113	896
Year/Temp/Lat	13860	12649	10017	5189	2115	896
Year/Lat	13867	12684	10052	5204	2120	896
Temp/Lat	14024	12700	10017	5196	2128	905
Year/Temp/Sal/Lon	13730	12598	9958	5173	2108	890
Temp/Sal/Lon	13864	12605	9957	5179	2110	897
Year/Temp/Lon	13817	12624	9994	5204	2115	893
Year/Sal/Lon	13735	12605	10005	5188	2109	895
Year/Lon	13811	12638	10053	5207	2117	892
Temp/Lon	13992	12635	9993	5205	2128	894
Sal/Lon	13932	12629	10031	5197	2111	894
I(Year/Lat/Lon)	13736	12550	9979	5212	2130	895
I(Temp/Lat/Lon)	13858	12551	10006	5213	2128	894
I(Sal/Lat/Lon)	13860	12521	9995	5196	2120	896

Table 2.13. Akaike information criterion (AIC) of different boosted regression trees for combinations of abiotic variables and age class. Lat = Latitude, Lon = Longitude, Temp = Temperature, Sal = Salinity, Year = Year of Growth. Lowest AIC values for each age class are bolded.

	Age Class					
	0-2	2-3	3-4	4-5	5-6	6-7
Lat	8271	7272	5334	2659	1082	416
Lon	8261	7290	5318	2663	1077	407
Year/Temp/Sal	8041	7158	5179	2588	1054	408
Temp/Sal	8121	7175	5173	2616	1052	415
Year/Temp	8254	7349	5295	2655	1062	437
Year/Sal	8151	7238	5251	2639	1061	416
Year	8535	7676	5566	2794	1071	431
Temp	8343	7367	5285	2659	1087	433
Sal	8262	7265	5266	2659	1059	419
Year/Temp/Lat	7977	7172	5183	2627	1056	410
Year/Lat	8071	7243	5272	2621	1075	415
Temp/Lat	8100	7172	5185	2617	1072	422
Year/Temp/Sal/Lon	7912	7066	5154	2563	1044	406
Temp/Sal/Lon	7990	7070	5151	2577	1061	405
Year/Temp/Lon	7982	7158	5219	2588	1058	406
Year/Sal/Lon	7943	7118	5192	2580	1042	414
Year/Lon	8075	7253	5278	2633	1064	415
Temp/Lon	8086	7155	5197	2587	1077	407
Sal/Lon	8053	7134	5175	2566	1040	407

2.4.4 Results of Regression Analyses

Deviances explained (DE) and AICs for all 114 BRTs in this study are presented in Tables 2.11 and 2.13, respectively. Highest DEs and lowest AICs usually coincided with each other (most being associated with the BRT with predictor variables year of growth, temperature, salinity, and longitude), with the exception of age classes 3-4 and 5-6. Even so, differences were not substantial. DEs and AICs for all 132 GAMs in this study are presented in Tables 2.10 and 2.12, respectively. Highest DEs and lowest AICs usually coincided with each other (most being associated with the

GAM with predictor variables year of growth, temperature, salinity, and longitude), with the exception of age classes 2-3 and 6-7. Even so, differences were not substantial.

DEs for BRTs were usually higher than those for GAMs. All DEs for GAMs were seemingly low; no DE surpassing 27%. The same was true for BRTs, with no DE surpassing 37%. Bottom temperature and salinity, therefore, are only capable of explaining at most 37% of the variance in ASC growth in the NGOM. Salinity alone explained more of the deviance in both types of models than temperature alone for all age classes, meaning ASCs in the NGOM appear to be affected more by salinity than by temperature. Concerning only the GAMs, predictor variables that included an interaction with location (both latitude and longitude) highly outperformed their counterparts; the same variable without a location interaction. This means that both temperature and salinity may affect ASC growth non-linearly over space and influences may vary by location. No clear trend was found to exist as a function of age class. The results of the correlation coefficient matrix (Table 2.6) seem to reveal that Δ_{mm} has very weak positive relationships with each of the predictor variables except for year of growth and salinity, which both appear to be very weak negative relationships.

The six regression analyses using data only from Cobscook Bay ASCs revealed results very similar to results pooled from the entire NGOM (Table 2.14), with the exception of the BRT for age class 3-4, whose DE was considerably high. In general, ignoring any spatial differences, it appears that year of growth alone does not sufficiently describe trends seen in scallop growth over time. This corroborates findings from section 3.2. It is important to note that of these analyses, only the first three age classes provided reliable results (Table 2.14). This was due to the often low number of older individuals (>4 years) found in Cobscook Bay over the time series.

Table 2.14. Deviance explained (DE) and Akaike information criterion (AIC) for three generalized additive models (GAM) and three boosted regression trees (BRT) run using only year of growth as a predictor variable per age class for only the Cobscook Bay region. Low counts of Atlantic sea scallops older than 4 years in Cobscook Bay made results from age classes 4-5, 5-6, and 6-7 unreliable and are thus not presented. Lat = Latitude, Lon = Longitude, Temp = Temperature, Sal = Salinity, Year = Year of Growth.

	Age Class					
	0-2	2-3	3-4	4-5	5-6	6-7
BRT DE	10.83	4.96	14.34	-	-	-
BRT AIC	6504	5823	4431	-	-	-
GAM DE	15.12	5.18	4.77	-	-	-
GAM AIC	10767	10090	8391	-	-	-

2.5 Discussion

ASC in the NGOM appear to be growing to a larger size and growing at dissimilar rates when compared to populations in Georges Bank and the Mid-Atlantic Bight (Table 2.1; Truesdell 2014; Hart & Chute 2009a). A trend in growth coefficient L_{∞} seems to be occurring up the Atlantic coast, with ASCs of the Mid-Atlantic Bight having the lowest values and ASCs of the NGOM having the largest (Table 2.1). This is similar to findings from Truesdell (2014), which showed larger L_{∞} values for the NGOM region. Within the NGOM, ASC growth seems to vary spatially: varying between management zones (Table 2.2). This is again similar to findings by Truesdell (2014), but this study presents higher calculations of both L_{∞} and K for most regions. This could be due to the addition of new data since 2014 mostly concentrated inshore, where higher coefficients were observed.

This study expanded on work by Truesdell (2014), calculating growth coefficients for each year class. With low sample sizes questioning the reliability of some year classes, it doesn't appear that ASC growth parameters are changing in a predictable way. They do seem to be fluctuating and ANOVA tests revealed those fluctuations result in year classes that are statistically different

from one another. Due to the ever-changing location of MEDMR tow stations in this project over the time series coupled with the low sample size per year class in this analysis, this fluctuation and by extent the statistical differences may not be what would be observed with larger sample sizes over the same time series. However, when spatial data were ignored in the Cobscook Bay subsample regression tests (which also have the highest density of samples of any region in this study), there was no more considerable influence of year of growth when compared to the original analyses with spatially pooled data over years.

These differences in growth over time do not match the change in the abiotic parameters observed in this study. Given that the regression analyses revealed that these parameters do have influence on ASC growth in the NGOM, it could be that pooling all data spatially does not allow for observation of these influences. Given that many studies have shown strong links between growth and temperature and salinity (Thouzeau et al. 1991; Stewart & Arnold 1994; Hart & Chute 2004), these effects may occur at finer spatial scales than what was used in this study. This highlights the need for more samples in the future so that finer spatial resolutions than what was utilized in this study can be explored.

The regression tests revealed that ASCs in the NGOM appear to be influenced by both temperature and salinity when abiotic data are not observed as spatial averages over time. However, these influences are relatively weak considering the deviance explained values associated with the tests. This highlights an important constriction of this study: abiotic data were temporally averaged in order to be associated with an increment of ASC growth. Future studies should look at abiotic ranges, anomalies, normality of distribution, and the like to infer more fine-scale temporal influences of these variables. Knowing this as a limitation, it can be assumed that the influence of temperature and salinity on ASC growth in the NGOM would be at least as strong

as what was observed in this study, but has the potential to be stronger if abiotic data in a form other than yearly averages were utilized.

Additionally, when temperature and salinity were supplied with an interaction term of location, the DE rises substantially. This could mean that ASCs in different areas of the Gulf of Maine respond differently to similar abiotic variables. This is most likely because these variables are acting in this study as a proxy for other variables known to heavily influence ASC growth such as phytoplankton density (Macdonald & Thompson 1985a; Macdonald & Thompson 1985b; Macdonald et al. 1987). Phytoplankton represent ASC food supply and mollusk growth has been shown to be highly correlated with phytoplankton density (Pilditch & Grant 1999; Weiss et al. 2007). Phytoplankton density is a function of temperature, salinity, and other factors (Wagner et al. 2001; Friedland et al. 2015). The interaction term of location could be accounting for some of these other location-sensitive variables in the NGOM. This could also hinder the ability to determine direct abiotic-growth relationships if most influence is acting through a different force and these highly complex abiotic-growth relationships acting through proxy would be difficult for regression models to calculate. This accentuates the assumption that abiotic-growth influences were underestimated in this study. However, this study was aware of this connection when selecting the original model parameters. Given that the Gulf of Maine is changing rapidly in the face of climate change (Pershing et al. 2015), it was important to determine any direct relationships that ASC growth had to the abiotics directly affected by this change: temperature and salinity. This is why no model selection process took place based on AIC. This study was not meant to create a model for ASC growth, but to use multiple models to tease apart relationships.

Even though abiotic-growth relationships were relatively weak in this study, they were still present. These relationships have the potential to be affected in the coming years by climate

change. Warming rates for the NGOM are suggested between 0.02°C and 0.07°C per year (Pershing et al. 2015) for sea-surface temperature, with bottom temperature experiencing this same trend (Pershing et al. 2015; Saba et al. 2016). Average yearly bottom temperature mean for all sample locations in this study area in recent years (2012-2016) averaged around 7.60°C . These values are below optimal growth temperatures of 10.0°C to 15.0°C for ASC (Thouzeau et al. 1991; Hart & Chute 2004), and well below the maximum temperature threshold of 21.0°C (Hart & Chute 2004). Bottom salinity is also expected to rise for the NGOM under climate change (Saba et al. 2016). Average yearly bottom salinity mean for all sample locations in this study area in recent years (2012-2016) averaged around 31.9‰. These values are below optimal growth salinity of full strength seawater: $\sim 35\text{‰}$ (Stewart & Arnold 1994; Hart & Chute 2004). With temperature and salinity in the NGOM both rising, and because of the relationships teased apart in this study, as well as support from previous research on optimal growth conditions (Thouzeau et al. 1991; Stewart & Arnold 1994; Hart & Chute 2004), there is potential for ASCs to grow faster and/or larger. However, this conclusion is strictly based on direct and uniform relationships. Most studies focused on determining abiotic influence to ASC growth usually linking fluctuations directly to something like metabolic activity (Pilditch & Grant, 1999) and are done so in the lab. If conclusions from these studies state high influence of variables like temperature and salinity to growth, this may not be that accurate in a natural setting where these variables are acting both directly and through proxy. Because these variables are most likely acting both directly on ASC metabolism and indirectly through things such as food availability and can vary spatiotemporally, it can be difficult to infer the magnitude of the change in ASC growth given large changes in temperature and salinity.

Other ASC stock characteristics like abundance are more easily calculable from abiotic data through use of habitat suitability indices (HSIs). Torre et al. (2018) suggests that inshore habitats will become more suitable for ASCs in the NGOM as temperature and salinity rise. With suitable habitat predicted to rise and with a potential for increased growth, the NGOM may be able to support a higher intensity fishery in the future.

There is need for more research concerning ASC life history and climate change to better understand their dynamics in the inshore NGOM. This study has shown the impact of abiotic variables on ASC growth to be weak yet present in this region. As suggested in other studies, biotic variables such as phytoplankton density, are posited to be more influential to ASC growth with abiotic variables influencing ASC growth directly and through this proxy of food availability. Future research should consider biotic variables as well as geospatial variables such as depth in an effort to better understand the NGOM ASC population dynamics.

CHAPTER 3: IMPLICATIONS OF CLIMATE DRIVEN CHANGES ON GROWTH AND SIZE-AT-MATURITY FOR GULF OF MAINE LOBSTER STOCK ASSESSMENT

3.1 Abstract

Crustaceans are socioeconomically and ecologically crucial globally. However, as ectotherms, anthropogenic climate change threatens to significantly alter key life history characteristics such as size-at-maturity and growth. Size-structured stock assessments are commonly utilized for assessing crustacean fisheries because of difficulty in aging crustaceans, but climate-induced changes in maturation and growth can greatly influence the performance of these models. We couple an individual-based model and size-structured stock assessment model for American lobster (*Homarus americanus*) to conduct a novel sensitivity analysis altering maturity and growth-related input parameters using bottom-up (parameters shifted independently) and top-down (parameters shifted jointly as influenced by climate change) approaches. The objective of this research is to demonstrate the importance of evaluating the sensitivity of the size-structured stock assessment model for lobster to climate influenced shifts in maturation and growth-related inputs. We found the lobster stock assessment model to be resilient of relatively extreme shifts in biological input parameters. We then discuss the need to expand sensitivity analyses for size-structured stock assessments of crustaceans to evaluate the influence of climate-driven shifts on life history input parameters for time-varying life history traits in stock assessment modelling and for research on quantifying the relationship of lobster life history parameters with the environment.

3.2 Introduction

Anthropogenic climate change is transforming many marine ecosystems through warming waters, ocean acidification, freshening, and deoxygenation (Brander 2010; Doney et al. 2012;

Gattuso et al. 2018; Doney et al. 2020). Perturbations to the abiotic environment, in particular to temperature, are especially influential on marine ectotherms because they do not physiologically regulate their body temperature, rather, it is driven by the environment (Madeira et al. 2012). As a consequence, temperature directly influences individual and population level biological processes of crustaceans such as metabolism, recruitment, reproduction, growth, size-at-maturity (SAM), and natural mortality (Madeira et al. 2012), which have significant implications for assessment and management of crustacean fisheries (Audzijonyte et al. 2016). Typically, data-rich crustacean stock assessments utilize size-structured models (Punt et al. 2013), the outputs of which can be influenced by environmentally driven variability in size-related life history parameters, such as growth and SAM. Thus, it is important to quantify how climate driven shifts in key life history parameters will influence crustacean stocks and manifest in assessment models for guiding future management decisions.

As ectotherms, crustacean's biology, especially growth, is directly influenced by temperature (Green et al. 2014; Madeira et al. 2012). A plethora of crab and lobster species have shown similar responses to rising temperature including increasing growth rates, decreasing intermolt duration, and smaller SAM (Green et al. 2014). American lobster (*Homarus americanus*) represent an ecologically and socioeconomically vital crustacean species in the Northwestern Atlantic Ocean (Le Bris et al. 2018), and lobster biology is directly influenced by temperature. Lobster, like many crustaceans, grow through a series of molts, also known as ecdysis. During ecdysis, the old carapace is replaced with a new, larger one (Comeau & Savoie 2001). Molting typically occurs annually in adult lobsters, although it can happen more than once, or be skipped entirely depending on the size, age, and maturity of the individual (Aiken and Waddy 1976; Aiken 1977; Comeau & Savoie 2001). While individual lobster physiology is known to influence growth

processes, temperature is also a primary abiotic driver of growth changes in lobster. Research has demonstrated that warming waters have considerable impacts on lobster life history, especially in relation to growth and SAM (Aiken 1977; Le Bris et al. 2017). Rising temperatures have been shown to increase molting frequency and decrease molting increment: the length a lobster grows in a given molting event (Aiken 1977). Additionally, several studies have found that warmer temperatures contribute to a reduced SAM for American lobster (Little and Watson, 2003; Little & Watson 2005; Le Bris et al. 2017; Waller et al. 2021). Indeed, climate driven changes in these life history parameters can likely impact the size-structured stock assessment currently utilized for American lobster management (ASMFC 2020).

Understanding the impact climate driven shifts in life history input parameters for stock assessment models will have on assessment outputs is critical for guiding future fisheries management and model development. Recent research found that incorporating temperature driven recruitment improved the performance of a size-structured stock assessment model for American lobster (Tanaka et al. 2019). When simulating the impacts of pooling multiple populations of southern rock lobster (*Jasus edwardsii*) with varying growth rates, the performance of a size-structured stock assessment model was not reduced (Punt 2003), suggesting that accounting for different growth rates of assessed populations may not be consequential for estimating reference points. If pooling population data of lobsters had reduced model performance, it may have indicated a need to further consider the importance of variable growth in future assessments of the population. In contrast, research suggests that failing to account for the plasticity of growth in fisheries stock assessment models can lead to deviations of more than 30% in outputs, critically altering the calculation of reference points (Lorenzen 2016). Indeed, depending on the species biology and stock assessment model design, changes in growth will have inconsistent impacts on

model outputs. Typically, sensitivity analyses can evaluate whether uncertainties in model assumptions, input data sources, and biological parameters have an impact on reference points or other model outputs (Maunder & Punt 2013; Maunder & Piner 2015). However, these analyses usually only consider adjustments to inputs on their own, rather than in combination (Lehuta et al. 2010; Saltelli et al. 2019), and seldom test whether models are sensitive to inputs which are based on life history and developed outside of the assessment model, such as growth transition matrices. Given the potential for dissimilar consequences of changing life history on stock assessment model outputs, and yet unrealized shifts in crustacean growth in the future, it is important to evaluate the sensitivity of size-structured stock assessment models on a case-by-case basis.

Here, we conducted a novel sensitivity analysis of a length-structured stock assessment model for American lobster using an individual-based simulation model to evaluate the sensitivity of the stock assessment model to shifts in growth related life history input parameters. We conducted a series of sensitivity analyses by shifting molting probability, molt increment probability, and SAM. These analyses used classical bottom-up methodologies where each parameter was shifted independently, but also used a top-down approach where parameters were jointly shifted under the driving mechanism of climate change. These were both conducted so as to understand at what point changes of these input parameters will result in a significant change in reference points estimated using the length structured stock assessment model, relative to a historical baseline. Our overarching goal for this study is to determine what degree of impact climate change has upon the reliability and robustness of lobster stock assessment model output.

3.3 Methods

3.3.1 Shifting Growth and Size at Maturity

Seasonal growth matrices in this study were calculated from an individual-based lobster simulator model (IBLS) first developed by Chen et al. (2005) and later expanded by Chang (2015) and Mazur et al. (2018). This model simulates individual lobsters from recruitment to mortality by sending each lobster through random Bernoulli trials representative of life history and fishery parameters derived from prior field research and modelling (Chen et al. 2005; Chang 2015; Mazur et al. 2018). This seasonal probabilistic model is used to simulate lobster fishery dynamics to capture complex fishery dependent and independent processes (Chen et al. 2005; Zhang et al. 2011) and has historically been used to test the performance of the American lobster stock assessment model (Chen et al. 2005). The model creates individual lobster records over a given time series with information including sex, size bin, carapace length, maturity, and mortality allowing for calculation of population abundance, spawning stock biomass, and landings (Mazur et al. 2018). A full explanation of this model can be found in Mazur et al. (2018).

The IBLS can be used to create seasonal growth matrices by simulating lobsters with total absence of fishery dependent and independent mortality as well as recruitment. This effectively means that the abundance of lobsters remains constant over the simulated time series, but the biomass changes exclusively because of data input for growth of the animals. At each step, a lobster is in 1 size bin (35 size bins from 53 mm to 223+ mm). The simulation should be run long enough so that every lobster should end up in the final size bin at the end of the time series. Every growth instance for every lobster for a given season over the entire time series is marked in a matrix of ‘size bin before molting event’ on the X axis and ‘size bin after molting event’ on the Y axis and scaled so the sum of each row is effectively 1. This creates a probabilistic growth matrix

where each row is a function of size change for a given lobster of that size class. This process is done 4 times: once for each season (January-March: Winter; April-June: Spring; July-September: Summer; and October-December: Fall).

Growth input to the IBLS is a combination of 2 independent factors: molting probability and probability for different molt increments. Molting probability is the probability of a lobster molting in a particular time step dependent on the carapace length, maturation status of the individual, and how many seasons it has gone without molting (Figure 3.1). Molt increment probability is the probability of a lobster growing a certain size (1 to 20 millimeters (mm) in 1 mm bins) due to a molting event and is dependent on the carapace length of the individual (Figure 3.1). The input data for the base case of these parameters came from ASMFC (2015).

Under climate change, lobsters are expected to molt more frequently, but grow less per molt (ASMFC 2015). To simulate these effects on overall growth, both molting probability (P_M) and molt increment probability (P_{MI}) were manipulated in the IBLS. Molting probability was increased by shifting left in relation to years since prior molt (Figure 3.1) and described by the following equations:

$$P_M = \frac{yas + b}{k_{CL}} \quad (3.1)$$

$$yas = \begin{cases} 1, \dots, k_{CL} & \text{if immature} \\ 2, \dots, k_{CL} & \text{if mature} \end{cases} \quad (3.2)$$

$$k_{CL} = 1 + e^{-8.08127 + (0.076535 \times CL)} \quad (3.3)$$

where P_M is molting probability, yas is time spent (in units of the timestep of the model; in this case: seasons) at current size of an individual lobster, k_{CL} is the longest time a lobster of carapace length CL (mm) could feasibly go before molting (NEFSC 1996; ASMFC 2000), and b is the

shifting parameter. Thus, $b=1$ would represent a shift of 1 season, increasing the overall probability of molting in comparison to the unshifted probability.

Average size increase per molt was lowered by shifting molt increment probability left in relation to the size increase per molt (Figure 3.1) described by the equations below:

$$P_{MI} = N(\overline{\Delta L_L} - b, \sigma^2) \quad (3.4)$$

$$\overline{\Delta L_L} = \begin{cases} 1.2236 + 0.1294 * L & \text{and } \textit{for } L < 95 \textit{ and } s = \textit{Male} \\ 1.2236 + 0.1294 * 95 & \text{and } \textit{for } L \geq 95 \textit{ and } s = \textit{Male} \\ 1.2288 + 0.1285 * L & \text{and } \textit{for } L < 82 \textit{ and } s = \textit{Female} \\ 1.2288 + 0.1285 * 82 & \text{and } \textit{for } L \geq 82 \textit{ and } s = \textit{Female} \end{cases} \quad (3.5)$$

where P_{MI} is the probability of molting an increment length, N is the normal distribution truncated by upper and lower boundary probabilities of 0.975 and 0.025, respectively, with σ being equal to 2.1 (ASMFC 2006), $\overline{\Delta L_L}$ is the change in length (mm) given current length L (mm) and sex s , and b is the shifting parameter. Thus, $b=1$ would represent a shift of 1 mm, decreasing the overall size increment change during a given molt.

To maintain some biological realism, shifts of molting probability and molt increment probability were paired and the corresponding growth matrices reflect possible impacts from climate change. Two paired shifts were conducted in this study and will be referred to throughout as G1 and G2. G1 was a leftward shift of molting probability by 1 year and molt increment probability by 1 size bin; $b = 1$ (Figure 3.1). G2 was a leftward shift of molting probability by 2 seasons and molt increment probability by 2 size bins; $b = 2$ (Figure 3.1).

Probabilistic SAM (P_{SAM}) in the IBLS is calculated from the below equation:

$$P_{SAM} = \frac{1}{1 + e^{-0.3 \times (CL - L_{50})}} \quad (3.6)$$

where P_{SAM} is the probability of maturity of an individual lobster of a given carapace length CL (mm) and L_{50} is the predefined carapace length (mm) that corresponds to 50% maturity. L_{50} was set to 90.81 mm for the base case (ASMFC 2015). Given that lobster SAM is expected to decrease 2.8 mm per 1°C rise in bottom temperature (Le Bris et al. 2017) and given current projections of bottom temperature for the Gulf of Maine rising 2°C by 2050 and 4°C by 2100 (IPCC 2019), L_{50} values of 85.21 mm and 79.61 mm were additionally tested in this study.

The IBLS generated a total of 7 sets (4 in each set corresponding to seasons) of growth matrices in this study (Table 3.1). The first set (referred to throughout as the base case) was calculated from the original (unshifted) molt probability and molt increment probability paired with the original L_{50} value of 90.81 mm. Sets 2-5 were calculated from shifts of either growth (G1 or G2) or L_{50} (85.21 or 79.61), and sets 6-7 were calculated from paired shifts of both growth and L_{50} (G1 and 85.21 or G2 and 79.21). Tests 2-5 were conducted to observe effects from specific parameters, whereas tests 6-7 were meant to be more biologically realistic and expected given the predicted relationships between climate change and these parameters.

3.3.2 Stock Assessment and Sensitivity Analyses

The University of Maine Lobster Stock Assessment Model (UMM) was initially developed by Chen et al. (2005) and expanded in ASMFC (2015) and Tanaka et al. (2019). It is a seasonal, sex-specific, length-structured assessment model for American lobster in the Gulf of Maine, Georges Bank, and Southern New England. It was designed with input from the Atlantic States

Marine Fisheries Commission (ASMFC) with the intent of being used for future lobster stock assessments. The population dynamics equation of the UMM is:

$$N_{t,s} = N_{t,s-1} \times G_s \times e^{-F_{t,s} + M_s} + R_{t,s} \quad (3.7)$$

where $N_{t,s}$ is a vector of the number of lobster in each size bin in year t and season m , G is the seasonal growth transition matrix, F is the seasonal fishing mortality, M is the seasonal natural mortality, and R is recruitment abundance to each size bin (Chen et al. 2005). A list of all data input to the UMM consistent across scenarios can be found in Table 3.2. For a more detailed description of this model, see Chen et al. (2005) and Tanaka et al. (2019) or by contacting the Chen Lab at the University of Maine.

The base case of the UMM saw the original growth matrices and SAM of 90.81 mm used as input data (section 3.3.1). Growth transition matrices and SAM data from the other six IBLS scenarios (section 3.3.1) were individually input to the UMM for a total of 7 scenarios (all growth matrices used can be found in the supplementary material). For each scenario, biological reference points (BRPs) were calculated for output reference abundance using the methods outlined by ASMFC (2015): the target was calculated as the 75th percentile of reference abundance over the time series and the threshold was calculated as the 25th percentile of reference abundance over the time series (ASMFC 2015). It is important to note that the reference time series for these calculations used by the ASMFC is 1982 to 2003, but this study used a reference period of 1984-2003 due to data input limitations. These BRPs allowed for determination of historical fishery status over time, which is simply the reference abundance of a given year in relation to the predefined BRPs (below the 25th percentile; between the 25th and 75th percentile; above the 75th percentile). Using these reference points, terminal year stock status was compared between all

UMM runs in this study. However, all sensitivity analyses in this study were based on historical fishery statuses over the entire time series compared between each UMM scenario and the base case.

IBLS scenarios 6 and 7 (section 3.3.1) were designed to represent small and large future climate effects, respectively. These effects on growth and SAM are plausible given future climate projections (IPCC 2019), but it is unknown if these changes are large enough to affect stock assessment output on a level that would shift management practices away from what they would be under the base case. To this end, a sensitivity analysis was to be conducted if results from the UMM using IBLS scenarios 6 and 7 showed significant differences in trends over time from the base case. Differences were simply if stock status differed in consecutive years between the given scenario and the base case.

This analysis would add IBLS scenarios representative of smaller and smaller incremental shifts in growth and SAM to determine the level of sensitivity (breaking point) and use those new growth matrices and SAMs in the UMM. For example, if historical fishery statuses from the UMM using IBLS scenario 6 had no differences in relation to the base case but UMM scenarios using IBLS scenario 7 did, then the breaking point of sensitivity would lie somewhere between these 2 shifts. The next step was to estimate growth matrices and a SAM for a shift representative of halfway between these 2 shifts. For molting probability, this was the average probability of both G1 and G2 for each season since last molt. For molt increment probability, this was the average probability of both G1 and G2 for each size increase in mm. For SAM, it was simply the average of 85.21 mm and 79.61 mm. BRPs and historical fishery statuses were then calculated for these new UMM scenarios. Retrospective patterns were also evaluated and results from these tests can be found in the supplementary material (Figures S3.1-S3.11). To further determine the breaking

point, these new UMM scenarios took the place in the above methods of either UMM scenarios that used IBLS scenario 6 or UMM scenarios that used IBLS scenario 7 (depending on whether the results of these new scenarios were significantly different from the base case), and the above process was repeated. This process continued until a breaking point within 1/16th of a shift was found.

Two more sensitivity analyses took place focused on the effects of changing growth independent of SAM and changing SAM independent of growth. These followed the same methods as above, but for UMM scenarios that used IBLS scenarios 2-3 and UMM scenarios that used IBLS scenarios 4-5, respectively. The above 3 analyses can help determine the sensitivity of the UMM to growth, SAM, and the combination of growth and SAM, all of which can assist in determining the necessity of research dedicated to direct linkages of climate change to these life history parameters for use in lobster stock assessment.

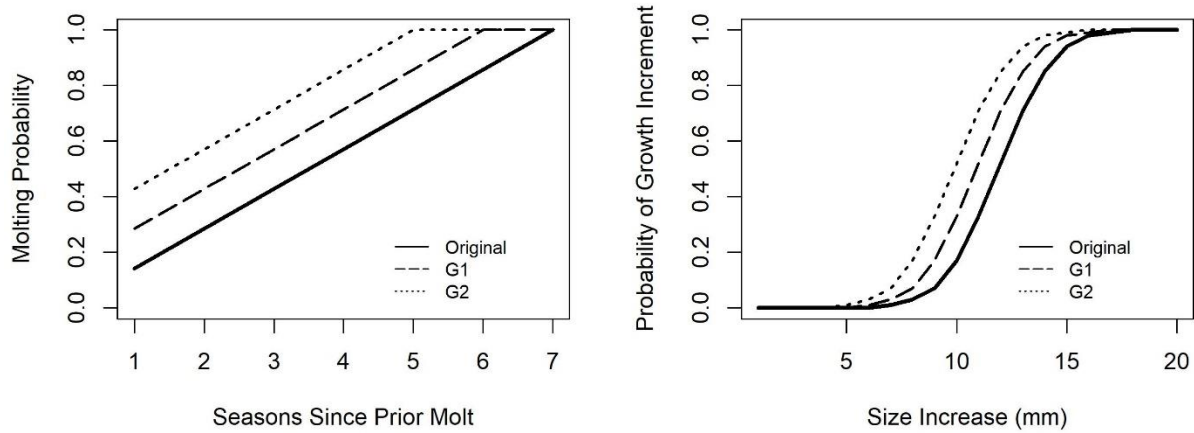


Figure 3.1. Molting probability in the summer vs seasons passed with no molting (left) and cumulative molt increment probability vs size increase in millimeters (mm) (right) of a 130 mm carapace length lobster. Presented are lines for the probabilities in the base case (“Original”) as well as those that correspond to G1 (Dashed) and G2 (Dotted).

Table 3.1. Individual based lobster simulator scenarios present in this study marked by the paired growth dynamic (Growth) and value of L_{50} that correspond to each scenario.

IBLS Scenario	1	2	3	4	5	6	7
Growth	Original	G1	G2	Original	Original	G1	G2
L_{50} (mm)	90.81	90.81	90.81	85.21	79.61	85.21	79.61

Table 3.2. Settings and data that were consistent across scenarios in the UMM. Acronyms correspond to the Maine Department of Marine Resources (MEDMR), Massachusetts Division of Marine Fisheries (MADMF), New Hampshire Fish and Game Department (NHFGD), and NOAA Northeast Fisheries Science Center (NEFSC).

Time Series	1984 through 2013
Seasons	4 (Each 3 month time blocks - same as IBLS)
Number of sexes	1 (Data averaged across male and female)
Size range	53 to 223 mm carapace length
Size bin length	5 mm
Initial conditions	First year size composition from survey data
Recruitment size	53 to 73 mm
SSB/R relationship	None
Number of commercial fleets	1
Commercial fleet selectivity at size	Double logistic
Survey data	MEDMR Ventless Trap Survey 2006-2012 Spring MEDMR/NHFGD Inshore Bottom Trawl Survey 2001-2013 Fall MEDMR/NHFGD Inshore Bottom Trawl Survey 2000-2013 Spring MADMF Bottom Trawl Survey 1984-2013 Fall MADMF Bottom Trawl Survey 1984-2013 Spring NEFSC Bottom Trawl Survey 1984-2013 Fall NEFSC Bottom Trawl Survey 1984-2013
Survey selectivity at size	Double logistic
Fishing mortality rate	Instantaneous
Natural mortality rate	0.15 year ⁻¹

3.4 Results

Target and threshold BRPs for the 7 UMM scenarios can be found in Table 3.3 and all accompanying reference abundance plots showcasing historical fishery statuses as compared to the base case can be found in Figure 3.2. Terminal year stock statuses did not change across any of the 7 UMM runs in this study (Table 3.4). Most alterations in historical reference abundance

from the base-case appeared to be magnitudinal: consistent overestimations of abundance per year, but similar temporal trends, with slight alterations causing some discrepancies in historical fishery statuses. Instances of consecutive years differing from the base case are much more relevant to discussion as these are indicative of larger trends-based differences and not simply 1-year lags that seem to be the reason behind solitary differing years. These consecutive difference years appeared in only 1 UMM scenario: scenario 7. This scenario used a growth shift of G2 and a SAM of 79.61 (the large climate effect scenario).

Given that a SAM change of over 10 mm in CL did not appear to cause consecutive year differences in reference abundance independent of a change in growth, a sensitivity analysis was not conducted for this variable. Likewise, changes in growth independent of SAM did not appear to cause consecutive year differences. Thus, a sensitivity analysis was not conducted for growth independent of SAM.

In the biologically realistic scenarios (UMM scenarios using data from IBLS scenarios 6 and 7), the combination of G1 and SAM of 85.21 mm had no consecutive year differences in historical fishery status when compared to the base case. However, the combination of G2 and SAM of 79.61 mm had consecutive year differences compared to the base case. Thus, the breaking points of sensitivity existed somewhere between a small-climate-effects scenario (G1 and SAM of 85.21 mm) and a large-climate-effect scenario (G2 and SAM of 79.61 mm). Results from this sensitivity analysis done for these biologically realistic scenarios can be found in Figure 3.3. The final breaking point was between a growth shift of 1.4375 and 1.5000 and SAM values of 82.41 mm and 82.76 mm.

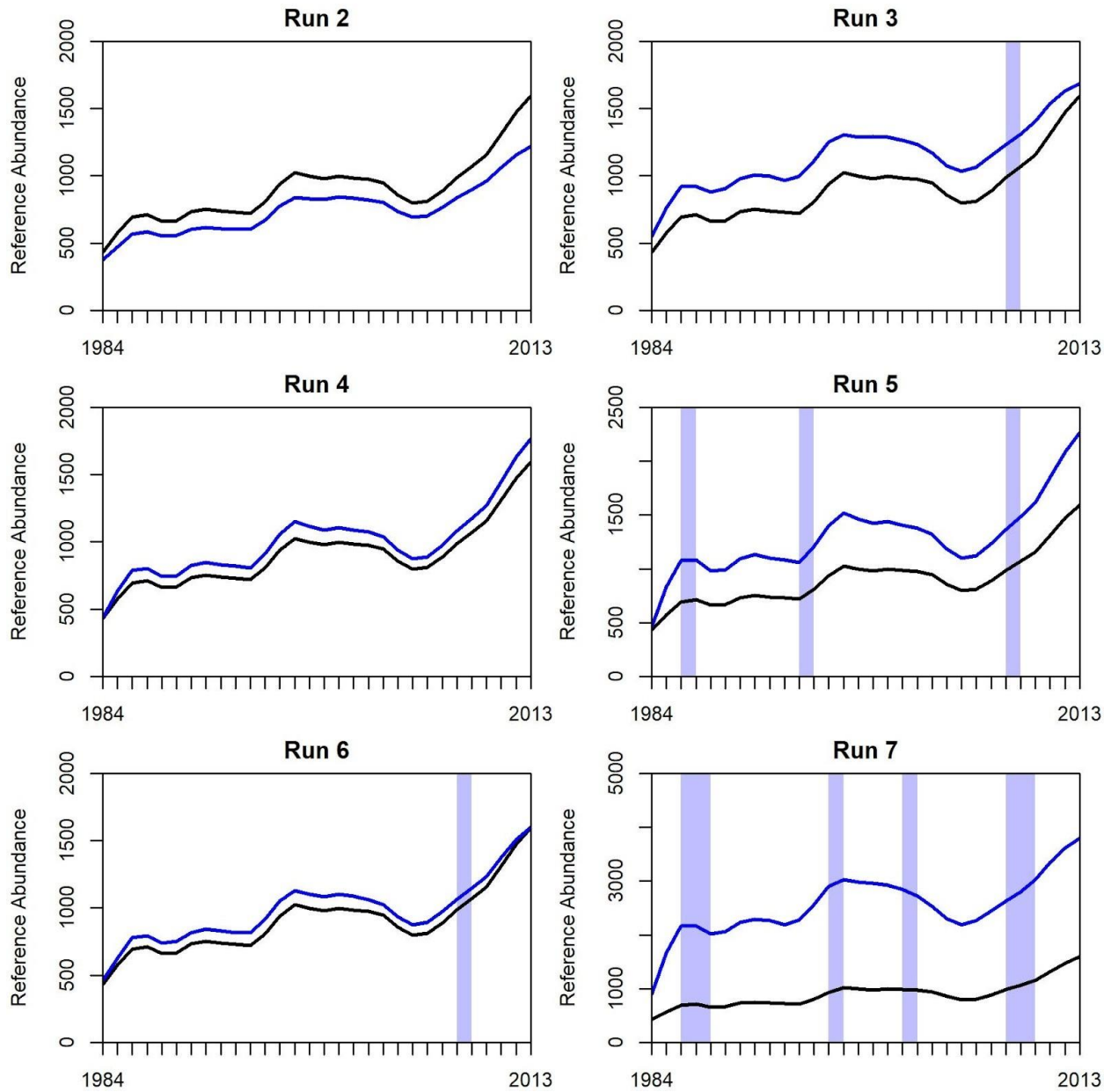


Figure 3.2. Estimated reference abundance (in millions of individuals) 1984-2013 for University of Maine Model scenarios corresponding to those in Tables 3.1 and 3.3 (blue trend lines) compared to the base case (black trend lines). Shaded regions indicate years where the historical fishery status (as calculated from BRPs in Table 3.3) is different from that of the base case for the same year. Note the differences in vertical axes ranges between plots.

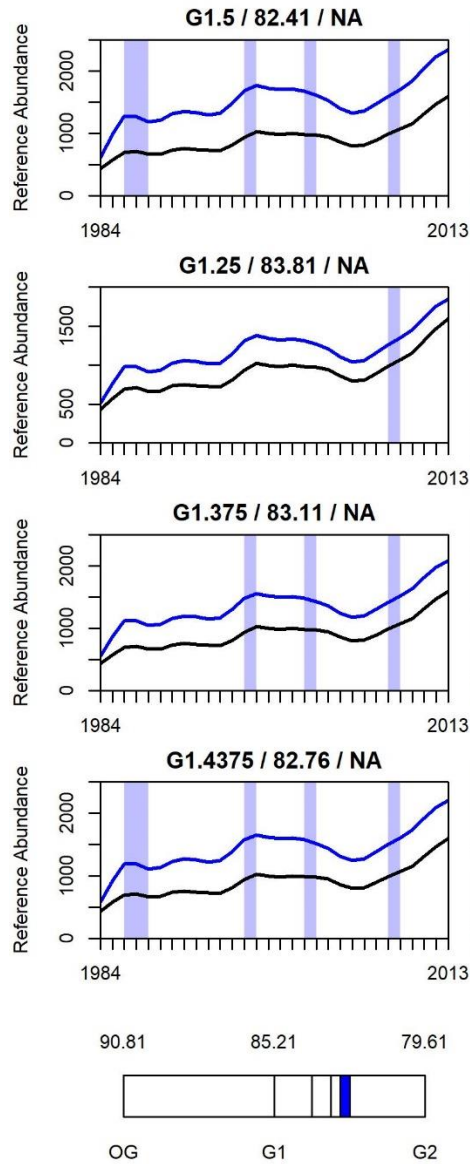


Figure 3.3. Estimated reference abundance (in millions of individuals) 1984-2013 for University of Maine Model scenarios in the growth sensitivity analysis (blue trend lines). Each row represents a consecutive scenario in the sensitivity analysis based on the scenario in the previous row. Shifts are represented as a proportion between a full shift of 1 and a full shift of 2 for both growth and SAM. All scenarios were compared to the base case (black trend lines). Shaded regions indicate years where the historical fishery status (as calculated from BRPs in Table 3.3) is different from that of the base case for the same year. Below is a diagram of the location of the breaking point of sensitivity within 1/16 of a shift (blue bar) in relation to the base case data. Here, unmarked vertical lines represent the above tests of partial shifts in the same column. Note the differences in vertical axes ranges between plots.

Table 3.3. Target and threshold biological reference points (in millions of individuals) for all UMM scenarios. Each column represents a UMM scenario that utilized growth transition matrices and SAM produced by the corresponding IBLS scenario (Table 3.1).

BRP	UMM Scenario						
	1	2	3	4	5	6	7
Target	976.0	823.1	1256.3	1078.1	1403.6	1067.0	2857.5
Threshold	707.8	579.6	919.6	801.2	1074.9	788.9	2170.5

Table 3.4. Terminal year stock abundance (in millions of individuals) and stock status for all UMM scenarios. Stock status is presented in relation to the biological reference points in Table 3.3. Each column represents a UMM scenario that utilized growth transition matrices and SAM produced by the corresponding IBLS scenario (Table 3.1).

Terminal Year	UMM Scenario						
	1	2	3	4	5	6	7
Abundance	1594.5	1217.9	1687.7	1769.5	2265.5	1599.5	3792.7
Stock Status	>Target	>Target	>Target	>Target	>Target	>Target	>Target

3.5 Discussion

Traditional sensitivity analyses are bottom-up: they are designed to determine how model output changes when specific parameters are altered (Booshehrian et al. 2012; Salciccioli et al. 2016). This practice is very common in stock assessment procedures to determine model stability and quantify uncertainty (Rosenberg & Restrepo 1994; Hilborn 2001; Salciccioli et al. 2016). UMM scenarios in this study that used IBLS scenarios 1-5 were an example of this classic type of analysis. UMM scenarios in this study that used IBLS scenarios 6-7, however, represent a top-

down approach to sensitivity analysis. Here, a larger model-free mechanism controlled how multiple variables changed together and would affect model results. This type of approach tries to answer the question of how sensitive the model is to this larger mechanism, in this case: climate change. Climate change will affect molting probability, molt increment probability, and SAM of lobster together. Thus, this type of analysis is important to determine these cumulative effects on model output, succeeding where traditional sensitivity analyses fail. This type of analysis is sometimes referred to as a global sensitivity analysis and is very rarely used in fisheries stock assessment (Lehuta et al. 2010; Saltelli et al. 2019; García 2020). We agree with Saltelli et al. (2019), that a lack of this methodology throughout the fields of environmental science and biology is concerning. We further postulate that both a bottom-up and top-down approach may be beneficial and increasingly imperative in a changing world to ensure that the stock assessment model is stable under ensemble changes brought by larger mechanisms.

Sensitivity of the UMM to growth and SAM are relatively and biologically low. SAM values associated with breaking points in the biologically realistic scenarios are not expected to reach such low levels for at least 50 years (LeBris et al. 2017; IPCC 2019). The relationship of lobster growth to temperature and climate change are well-known (Aiken 1977; Le Bris et al. 2017), but strict predictions cannot be so easily extrapolated and may be less appropriate (Punt et al. 2014). This, coupled with the fact that most information on these parameters found in laboratory settings may not be directly applicable to wild scenarios (Jury & Watson 2013) means that forecasting lobster growth and SAM is incredibly challenging. This highlights an advantage of our modelling framework in that strict relationships of tested parameters to the larger mechanism (e.g., climate change or temperature change) are not necessary. The framework does not determine

future changes to modelling efforts, but rather highlights the limitations of the stock assessment under climate change.

For the UMM, terminal year stock status estimates, which are most relevant to lobster management, did not change over all scenarios in the current study, indicating the robustness of the UMM to changes in these life history parameters. However, the combination of shifts to growth and SAM did show differences in hindcasted fishery statuses. Consequently, scenarios tested in this study may not alter input data enough to produce different results for current management, but given that historical deviations were present, caution should be given to the assumptions of low sensitivity. Deviations of historical stock statuses were mostly magnitudinal, representing overestimations of lobster abundance throughout the time series, but having very similar temporal trends. This is due to the use of relative BRPs calculated for each scenario as opposed to static values over all scenarios. Lobster management, like much of fisheries management in general, is more concerned with trends (ASMFC 2015) instead of absolute values. This implies that large growth and SAM shifts can alter model results, but would not have severely impacted historical management. As expected, these UMM scenarios had worse fits than the base case (see supplementary material). This is most likely due to the model approximating biologically unrealistic freely estimated parameters in an attempt to fit to the data while also using the growth and SAM data provided (Slezak et al. 2010). These differences in fit are not relatively high, even for the largest shifts in this study, but work on other models should be aware of this phenomenon. Caution should be used by management when using this approach and careful attention should be paid to the freely estimated parameters of the model.

It is important to note the combined effects of growth and SAM shifts. The largest alteration in comparison to the base case was when the largest effects from growth and SAM were combined.

However, smaller shifts seem to indicate that combined effects may not be strictly additive and future work should focus on the complex relationship of growth, SAM, and temperature, especially as it pertains to the lobster stock assessment model. Quantifying the relationships between these parameters and thermal habitat is a research priority (ASMFC 2015), but another priority is to develop modelling capacity to handle temporally dynamic life history parameters. If climate change affects key life history characteristics, then traditional stock assessment methodologies that use static values for variables such as growth, SAM, and others may be misinformed (Correa et al. 2021). Temporally dynamic life histories in stock assessment may require quantifying relationships with the environment, but would ultimately increase accuracy in model results and precision of forecasts. Another avenue for future research would be the application of a management strategy evaluation (MSE) within the current framework. This addition would see the IBLS used as an operating model so that results from the UMM could have a “true” population to compare with.

Ultimately, knowing the breaking points does not aid in management if there is a lack of knowledge on the life history parameters tested a priori, specifically concerning the relationship with each of them to thermal habitat and hypotheses as to the predicted scale of future change. Foremost, there is a critical need to quantify the relationship these lobster life history parameters have with a changing climate, a concern that management shares (ASMFC 2015). This is because a comparison of predicted changes to the model’s breaking points aids in determining research necessity. If the breaking points are higher than the predicted changes, then changes under climate change may not significantly impact assessments if the life history parameters (e.g., growth and SAM) are not updated. If the breaking points are lower than the predicted changes, then there is the possibility that modelling efforts with old parameters may not yield accurate results anymore

if the parameters are not updated and future research should be targeted at understanding those parameters.

Lobster, and by extension, crustacean, physiology and life history are directly linked to the environment and most often are consequences of thermal habitat (Madeira et al. 2012). As climate change alters thermal habitat of crustaceans, stock assessment methodologies that rely on these life history characteristics have the potential for their input data to be out-of-date. This can be mitigated with persistent monitoring efforts and scientific research. However, many crustacean fisheries, even in well-funded areas, have limited resources for these cost-intensive research efforts. The framework proposed in this paper has the potential to mitigate research loads by prioritizing those input parameters that the specific stock assessment model is most sensitive to under the top-down mechanism of climate change. A complete analysis of dependent and independent effects from all variables together under this framework has the potential to aid in management practices, advance crustacean stock assessment, and steer future research projects.

CHAPTER 4: DEVELOPING A FRAMEWORK TO CALCULATE DYNAMIC REFERENCE POINTS USING A THERMALLY EXPLICIT SPAWNING BIOMASS / RECRUITMENT RELATIONSHIP

4.1 Abstract

Management of marine species often relies on biological reference points (BRPs): threshold and target indicators that trigger management actions. These BRPs are usually based on the biology of the species and rarely consider environmental effects. Under climate change, this is problematic as many biological/physiological relationships are assumed temporally static. This spurious assumption can lead to inaccurate management practices. To combat this problem, recent research highlights the importance of developing temporally dynamic BRPs. This paper sees the development of a dynamic BRP calculator to inform management of levels of spawning biomass necessary to sustain the desired future levels of recruitment given forecasted climate scenarios. We test this calculator on American lobster of the Gulf of Maine and Georges' Bank. Results for lobster indicate a temperature-driven, but complex, spawning biomass/recruitment relationship. Increased warming scenarios appear to yield overall higher recruitment per spawning biomass and dynamic BRPs calculated under these scenarios reveal that smaller population levels can sustain management-desired recruitment levels. This study highlights the importance of developing dynamic BRPs for fisheries management in a changing environment.

4.2 Introduction

Many data-rich stock assessments rely on some assumed spawning stock biomass (SSB)/recruitment (R) relationship (Ricker 1954; Cury et al. 2014). This relationship is both the most important and the most difficult in fisheries stock assessments (Hilborn & Walters 1992). The concept is simple: there must exist a connection between the breeding group of a population

and the abundance of their offspring (Ricker 1954; Beverton & Holt 1957; Hilborn & Walters 1992; Cury et al. 2014). With an assumed connection, R should be estimable if the SSB is known. Realistically, there are exogenous barriers that both complicate the relationship and inhibit discovery (Fogarty 1993; Cardinale & Arrhenius 2000).

Recently, there have been large developments towards the incorporation of environmental covariates in these types of relationships (Tang 1985; Subbey et al. 2014). As climate change is continuing to alter environments, these changing variables are likely to result in temporally dynamic SSB/ R relationships. These complex associations can be difficult to design, interpret, and utilize in traditional stock assessment frameworks (Myers 1998; Subbey et al. 2014) and their reliability is often in question due to potentially spurious correlations (Chen & Irvine 2001). Nevertheless, directional change on these relationships brought about by climate change is continually necessitating incorporations (Subbey et al. 2014).

Conventional management of marine species requires biological reference points (BRPs) which are usually used to define what managers would like to achieve and avoid in fisheries management (Sissenwine & Shepard 1987; Mace 1993). These BRPs can be fishing mortality-associated and/or abundance/biomass-associated targets for the management and thresholds that, when reached, trigger management action (Mace 1993; Berger 2019). BRPs are traditionally determined only by fish biology and usually assumed environmentally independent. As the environment changes, in particular unidirectional, these static thresholds are having to be continuously re-estimated and thus there is often substantial ambiguity in estimations (Mace 1993; Gabriel & Mace 1999; Fogarty & Gendron 2003). To combat this issue, recent research has been working towards establishing dynamic BRPs: BRPs whose components are inherently affected by the environment and are thus temporally dynamic (Berger 2019; O'Leary et al. 2020). As an

example: if a threshold BRP for fishing pressure is set to a level that would cause the stock to decline to 40% of its maximum spawning potential (F40%MSP), a dynamic BRP framework would temporally alter this value based on environment-fishing mortality relationships (i.e., a relationship between temperature and catchability). A static BRP framework would estimate a fixed value for F40%MSP, not considering exogenous variability and therefore decreasing reliability and confidence (Fogarty 1993; Subbey et al. 2014) in a changing environment. It is the goal of this research framework to develop a dynamic BRP calculator that utilizes an environmentally explicit Spawning Stock Biomass (SSB) and Recruitment (R) relationship with a wide applicability across taxa and assessments. The framework is initialized and tested on American lobster (*Homarus americanus*) in the Gulf of Maine/Georges Bank (GOM/GBK) stock area (Figure 4.1).

A reliable SSB/R relationship for American lobster in the GOM/GBK would allow for better R estimations and more dependable forecasts for stock dynamics. However, there are currently two issues constraining implementation of a SSB/R relationship in lobster stock assessments (ASMFC 2020). Previous research concluded that a SSB/R relationship for American lobster may be spatially explicit (Xue et al. 2008; Chang et al. 2015), constraining estimation in stock assessment models that perform on large spatial scales. This spatially-dependent relationship may be linked to temperatures of the region, especially those effects on larvae and juveniles (Ennis 1986; Annis 2005). Realistically, most or all SSB/R relationships in nature are spatially varying, but many stock assessment models lack the capacity to consider these effects directly (Cadrin & Secor 2009).

An additional problem for lobster is that there may be a disconnection between biological R (newborn lobster larvae) and model R (lobsters that have grown into the smallest size classes

used in the assessment model; lobsters that have the potential to reach the fishery's minimum legal size in just one molting event) (Wahle 2003, ASMFC 2020), the latter of which is the input data necessary for stock assessment purposes for the species (ASMFC 2020). Any functional SSB/R relationship for GOM/GBK lobster must establish a connection between SSB and model R. Many outside forces act on lobster as they grow from biological R to model R. These include biological forces such as predation (Hanson 2009) and environmental forces such as temperature (Ennis 1986; Annis 2005). The lag between biological R and model R is also not well defined, meaning model R of a given year has potential to have come from spawning events from multiple years in the past: lobsters of a certain size are not all of a certain age (Wahle et al. 1996; Chang et al. 2011; ASMFC 2020). This disconnection is often found in crustacean stock assessments as many of the models are length-based due to a general difficulty in aging many crustaceans (Chen et al. 2005; Chang et al. 2011; Punt et al. 2013). From this point on, unless directly specified, all mention of R in this study is model R.

Knowing these problems for American lobster in the GOM/GBK stock area, it is the intention of this research framework to design a dynamic BRP calculator that can be used reliably in length-based stock assessments without deconstruction of the inherent spatially-lacking methodologies. For lobster, this starts with determining a stock-wide SSB/R relationship using multiple generalized additive models (GAMs) to estimate effects of stock-wide SSB and thermal habitat on R estimations. The subsequent calculator uses this relationship to provide management advice concerning current SSB levels so that desired R levels can be achieved in the future. The generality of the framework at every stage is kept high to achieve applicability across many taxa and assessments.

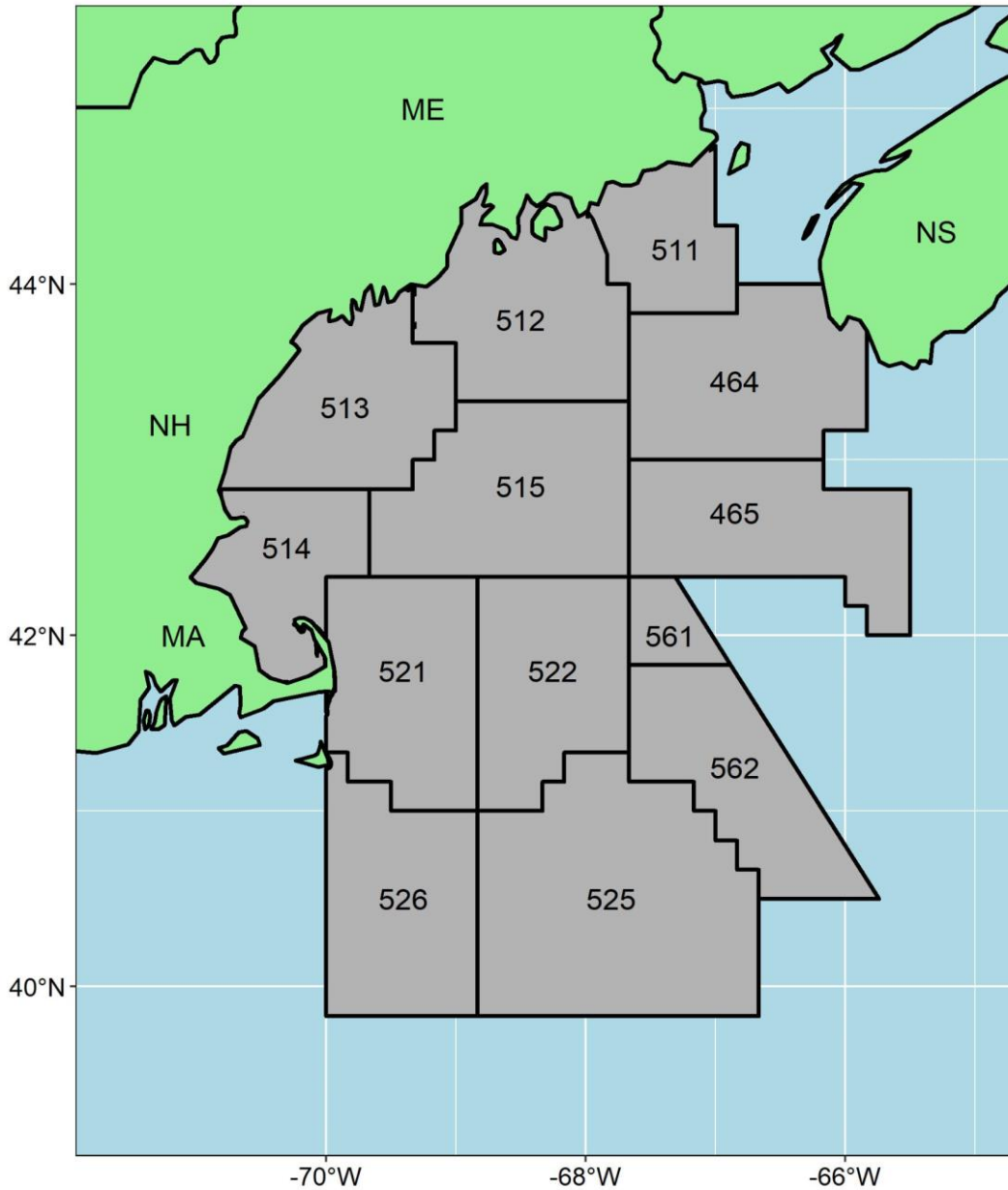


Figure 4.1. National Oceanic and Atmospheric Administration (NOAA) statistical areas that represent the Gulf of Maine/Georges Bank American lobster stock area. Statistical areas in grey have their number designation displayed. Additionally, the states of Maine (ME), New Hampshire (NH), and Massachusetts (MA) along with the province of Nova Scotia (NS) are shown.

4.3 Methods

4.3.1 Spawning Biomass and Recruitment Levels

Spawning stock biomass (SSB) in metric tons and recruitment (R) in millions of individuals are both output from a seasonal, length structured assessment model for American lobster in the GOM/GBK stock area known as the University of Maine Lobster Stock Assessment Model (UMM). The UMM was developed and coded by Chen et al. (2005) in ADMB and was subsequently modified by Cao et al. (2017a; 2017b) and Tanaka et al. (2019). For additional details on the model, see Chen et al. (2005), ASMFC (2015), and Tanaka et al. (2019) or contact the Chen Lab at Stony Brook University.

Among other UMM outputs, SSB and R are calculated by the model per year over the time series 1984 through 2013. These values of SSB and R were chosen to be used in this study to increase applicability, ensuring this framework can be used with model-generated data.

4.3.2 Determining an Appropriate SSB/R Relationship

American lobster model R takes three to five years to reach these sizes from their larvae stages (McCay et al. 2003; Whale & Fogarty 2006; Mazur 2020). Thus, R values for each year “X” were paired with an average SSB value calculated as the average SSB from years “X-5” to “X-3”. Two bottom temperature parameters were initially tested for inclusion in this relationship.

The first was LM, which represented the bottom temperature (°C) during the months of October through December (again, averaged from years “X-5” to “X-3” for each R), representing the first seasonal period after lobster settlement in the GOM/GBK area (Wahle et al. 2010). LM was meant to capture the thermal environment of early stage juvenile lobsters: a crucial developmental period that is temperature dependent (Barrett et al. 2016; ASFMC 2020) and that

has the highest mortality rate across post-settlement life stages (James-Pirri & Cobb 2000). Bottom temperature data was collected from the University of Massachusetts Dartmouth's School of Marine Science and Technology's Finite Volume Community Ocean Model (FVCOM) (Chen et al. 2006a), shown to be effective at predicting and mapping bottom temperature parameters in areas like the GOM/GBK (Li et al. 2017). These bottom temperature data were rasterized into uniform grids using bivariate splines and subset to specific depth gradients. In the case of LM, this depth gradient was less than 50 meters, which represented appropriate depths of lobster settlement (ASMFC 2020; Goode et al. 2019). This data was subset again to specific NOAA statistical areas representing the GOM/GBK lobster stock area (Figure 4.1) before a spatial mean (LM) was calculated for data October through December.

The second parameter used was DM, representing the mean temperature over the period from biological R to model R. Because model R was assumed to come from three separate biological recruitment events in this study, the true mean calculated represented the temperature years "X-5" to "X", "X-4" to "X", and "X-3" to "X". FVCOM data in this case were rasterized and subset to a depth gradient of less than 480 meters, representing depths where lobsters of these sizes can be found (Holthuis 1991; Tshundy 2003) before again being subset to the GOM/GBK stock area.

Next, variance inflation factor (VIF) tests were conducted on the data to evaluate whether all three variables (SSB and the two environmental variables; LM and DM) could be used together as explanatory variables in the same model. All combinations that maximized the amount of variables to be used while also producing VIF values less than three (Zuur et al. 2009), were tested and compared.

Any combinations of explanatory variables tested were done using an environmentally explicit Ricker or Beverton-Holt equation deconstructed into a generalized additive model (GAM). The environmentally explicit Ricker stock-recruitment (top) and Beverton-Holt stock-recruitment (bottom) equations are:

$$R = \alpha \cdot SSB \cdot e^{-\beta \cdot SSB + \delta_1 T_1 + \delta_2 T_2 + \dots} \quad (4.1)$$

$$R = \frac{\alpha \cdot SSB}{(1 + \beta \cdot SSB)} \cdot e^{\delta_1 T_1 + \delta_2 T_2 + \dots} \quad (4.2)$$

where R is recruitment, SSB is spawning stock biomass, T is an environmental parameter, and α , β , and δ are coefficients (Subbey et al. 2014). Each of these deconstructed into GAM equations are:

$$\ln\left(\frac{R}{SSB}\right) \sim SSB + T_1 + T_2 + \dots \quad (4.3)$$

$$\ln\left(\frac{R}{SSB}\right) \sim -\ln\left(\frac{1}{1 + SSB}\right) + T_1 + T_2 + \dots \quad (4.4)$$

where \ln is the natural log; Ricker is above and Beverton-Holt is below. Each of these GAMs were run with each combination of environmental explanatory variables allowed by the VIF tests above. If a variable was not significant in the model, it was removed and the respective GAM was modelled without it. The model with the highest deviance explained and lowest Akaike Information Criterion (AIC) between Ricker and Beverton-Holt and between combinations of explanatory variables was chosen as the best representative model.

4.3.3 Dynamic Reference Point Calculator

The dynamic reference point calculator was built in the *R* environment and requires three objects as inputs. The first is the object of class “*gam*”, “*glm*”, or “*lm*” that represents the thermally explicit SSB/R relationship. The second object is of class “*data.frame*” where rows represent years and there are columns for SSB, R, and any environmental variables used in the analysis. If using this model to hindcast, then the entire data frame should be filled with observed values. If forecasting, the SSB and R columns will be present, but empty for any future years. Any environmental parameters must be forecasted a priori (see section 4.3.4). The third object is a value that represents an R-based reference point. This reference point is interpreted as “desired future levels of recruitment”. For this study, this was set at the 75th percentile of R from 1984-2013.

The calculator then utilizes the “*predict()*” function in the base *R* environment to estimate R levels over the entire observed time-series range of SSB values (*n* values ranging from the lowest to highest observed values of SSB) for every row of environmental data representing a year. Every predicted R value has the user-chosen R-based reference point subtracted from it and those final values (*n* values per year) are positive if the value of SSB paired with that year’s associated environmental data yields R levels higher than the chosen reference point and are negative if it yields R levels lower than the chosen reference point. Plots of this data are created per year over the range of SSB. Lastly, values of SSB that yield the R-based reference point exactly are found by calculating the root linear interpolants from the plots described above. These are used to compute the final ranges of SSB given the environmental parameters that will yield at least the desired recruitment levels. Additionally, plots of recruitment per spawning stock biomass (R/SSB in individuals per metric ton) over the range of SSB are generated for each forecasted year.

4.3.4 Environmental Forecasts and Subsequent Management Advice

To hindcast 1989 through 2013, the SSB and R values from section 3.1 were paired with FVCOM values from section 3.2. These values allowed for the yearly calculation of appropriate SSB levels to ensure the desired R levels. The usefulness of hindcasting the data is only to see how well the model performed (i.e. how well the predicted ranges match observed patterns) and has little management applicability.

To forecast 2014 through 2018, temperature data must be forecast a priori. Kleisner et al. (2017) estimates an average yearly increase of GOM/GBK bottom temperature of $0.072^{\circ}\text{C}/\text{year}$ over the next 80 years. This rate was used in initial analyses. Pershing et al. (2015) estimated a warming rate of GOM/GBK surface waters at $0.2420^{\circ}\text{C}/\text{year}$. This rate was used to represent an extreme warming scenario for GOM/GBK bottom temperature. Both rates of changes were used to create two separate forecasts bookending a range of future change. Thus, any mean temperature data 2014 on were calculated as the mean plus the yearly rate of change multiplied by the number of years into the future.

4.4 Results

4.4.1 The SSB/R Relationship

Yearly SSB and R data from the UMM were paired with LM and DM generated from FVCOM data (Table 4.1), and were all able to be used in the same GAMs due to their VIF results (Table 4.2). All three explanatory variables (SSB, LM, and DM) were significant in the Beverton-Holt GAM, but only SSB and DM were significant in the Ricker. A second Ricker model was run (hereby referred to as the lesser Ricker) that only considered SSB and DM. Thus, three total GAMs were run in this study: one for all variables in the Beverton-Holt, one for all variables in the Ricker,

and one with only SSB and DM in the Ricker. Deviance explained (DE) and AIC values for all models can be found in Table 4.3.

Beverton-Holt had a lower AIC and a higher DE than both Ricker models (Table 4.3), indicating it was better suited for modelling the American lobster SSB/R relationship in the GOM/GBK region. Partial dependence plots for SSB, LM, and DM using the Beverton-Holt GAM are shown in Figure 4.2. Note that the partial dependence plot for SSB is $\ln(1/(1+SSB))$ as is denoted by equation 4.4. At too high and too low SSB values, the effect is negative towards R, but positive at moderate ranges of SSB. LM has a positive effect at lower temperatures and a negative effect at higher temperatures, while DM has a positive effect at low and high temperatures and a negative effect at moderate temperatures. Figure 4.3 shows the combined effect of all three variables on R using a surface plot of interpolated observed values. At low values of LM, a wide range of SSB and DM can lead to desired R levels, but as LM increases, both DM and SSB must also increase to provide those levels of R.

4.4.2 Hindcasts and Forecasts from the Reference Point Calculator

Hindcasted ranges of SSB 1984-2013 that yield desired R levels can be found in the supplementary material (Figure S4.2). The lower-bound and upper-bound yearly rates of change yielded values for LM and DM 2014-2018 (Table 4.4). These two sets allowed for two separate forecasts of SSB ranges to be made (Figures 4.4 and 4.5; Table 4.5). Each plot represents a year where the x axis is a range of SSB in mt and the y axis is the difference between the calculated R (over the range of SSB) and the user-chosen R-based reference point (75th percentile of R 1984-2013; calculated as 557 million individuals), called R difference. Any range of SSB that yields a positive R difference value means that SSB in that range will yield at least the desired R levels. From a management viewpoint, SSB would have to be within ranges that yield positive R

difference values across years “X-5” to “X-3” in order to have R levels at least as high as those desired in year “X”. As an example: concerning the plot for 2018 in Figure 4.5, at a future rate of bottom temperature change of 0.242°C/year, management must keep SSB levels 2013-2015 on average to be higher than 67790.9 mt in order to achieve desired recruitment levels in 2018.

A higher rate on bottom temperature change actually provided larger ranges of acceptable SSB to yield the desired R, perhaps due to the positive effects of higher temperatures of DM. A rate this large may also be more realistic than the lower bound rate used, as surprisingly this rate occasionally had no acceptable ranges of SSB. This relationship between R and bottom temperature was additionally seen in the R/SSB over SSB plots (Figures 4.6 and 4.7), where the extreme scenario had comparatively higher R/SSB values across the range. These R/SSB plots per forecasted year all seem to display the same basic relationship, but are changed due to changes in forecasted temperature parameters. R/SSB values at low SSB are relatively high then drop before rising to a relative maximum at moderate ranges of SSB and then seemingly leveling off at high SSB values.

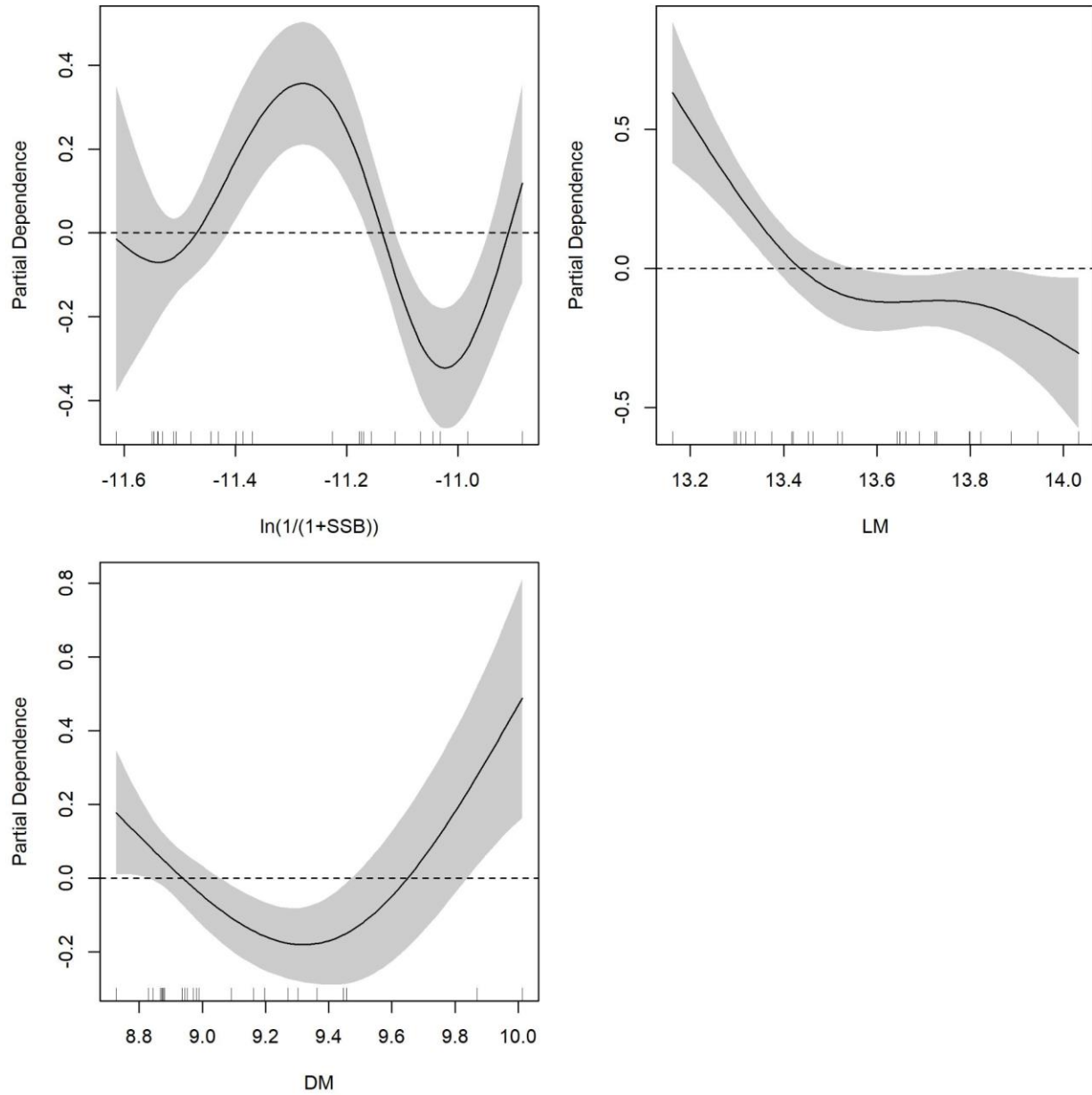


Figure 4.2. Partial dependence plots of the Beverton-Holt GAM for $\ln(1/(1+SSB))$ (top left), LM in °C (top right), and DM in °C (bottom left). Dotted line represents the line of no effect. Dashed bars on the x axes denote the values of the input data to the GAM.

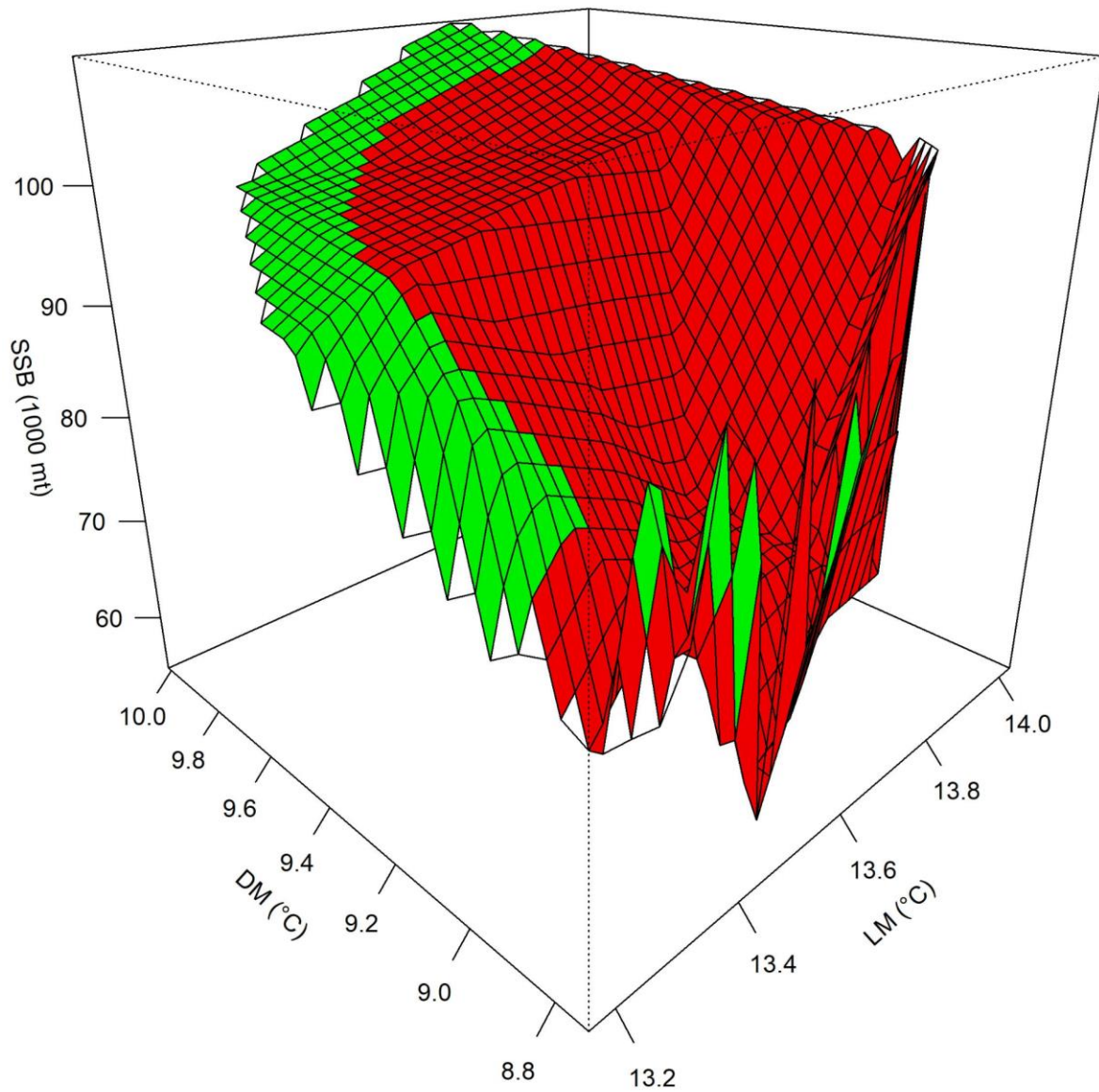


Figure 4.3. Surface plot of the combined effects of spawning stock biomass (SSB), LM, and DM on recruitment (R). Red represents areas where the combined effects from SSB, LM, and DM yield R values lower than the reference point (75th percentile of R 1984-2013; calculated as 557 million individuals) and green represents areas where the combined effects from SSB, LM, and DM yield R values higher than the reference point. For additional angles, see the supplementary material (Figure S4.1). All plots generated in R (version 3.5.3) with package “akima” by interpolating observed values of variables.

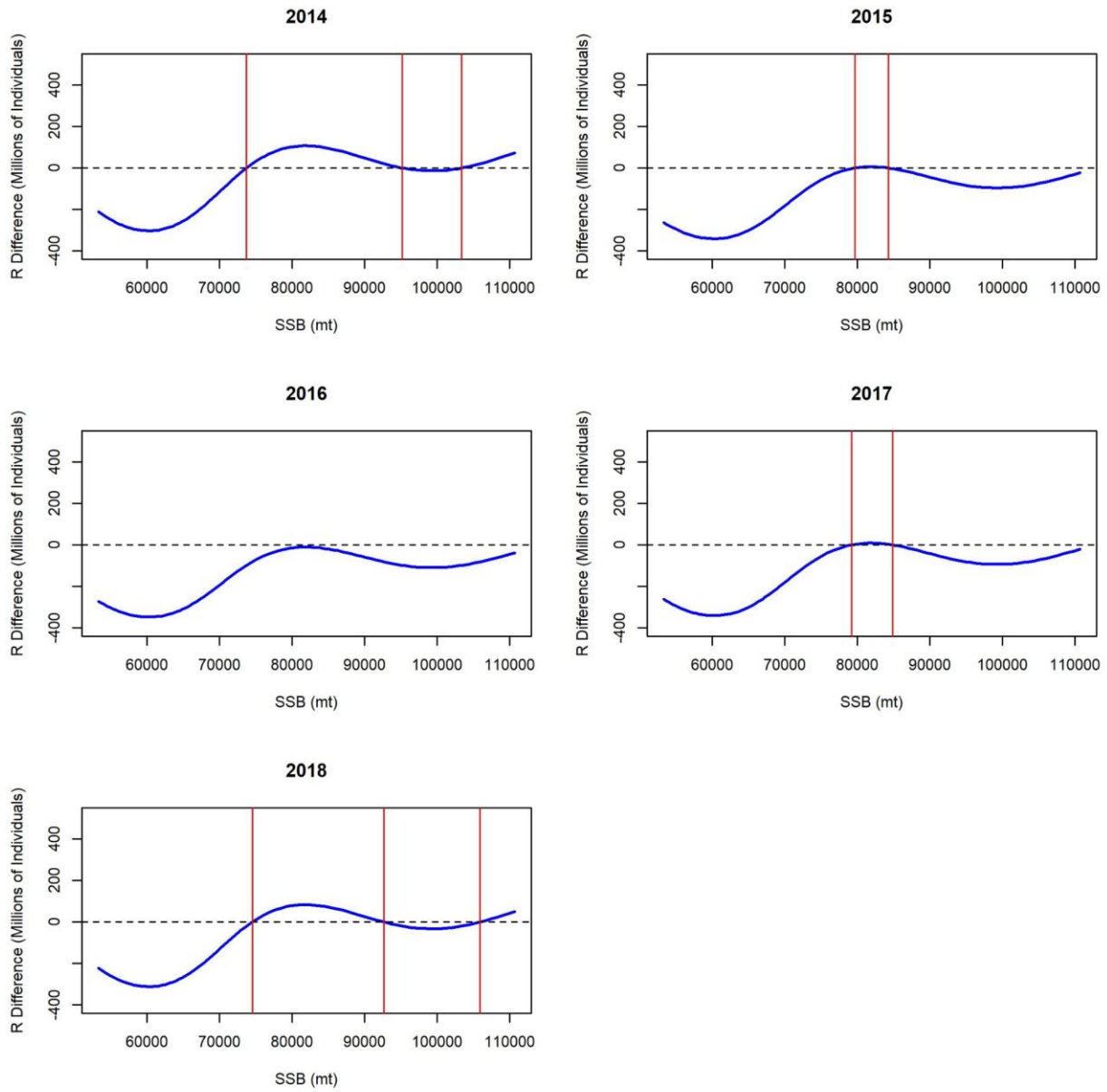


Figure 4.4. Forecasts 2014-2018 of acceptable ranges of spawning stock biomass (SSB) in mt of years “X-5” through “X-3” that yield the desired recruitment (R) levels of the given year. R difference represents the difference between the calculated recruitment at a given value of SSB at the associated LM and DM and the chosen R-based reference point; in this case, the 75th percentile of R 1984-2013. Locations where the blue line is above the dotted R difference = 0 line represent acceptable SSB ranges. Red lines represent where the blue line crosses the R difference = 0 line. Numeric ranges can be found in Table 4.5. All results presented use LM and DM values calculated using a rate of bottom temperature change of 0.072°C/year.

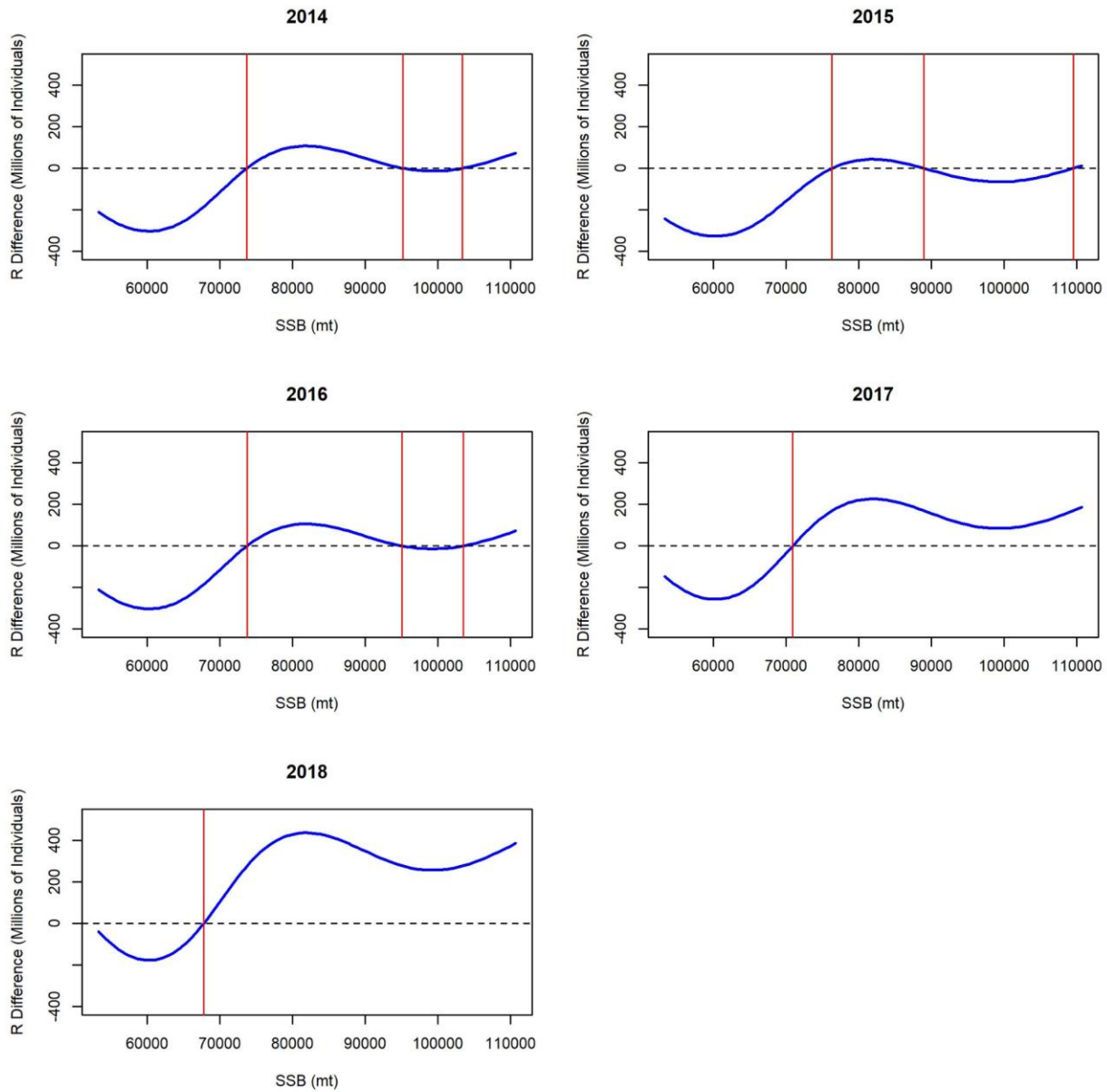


Figure 4.5. Forecasts 2014-2018 of acceptable ranges of spawning stock biomass (SSB) in mt of years “X-5” through “X-3” that yield the desired recruitment (R) levels of the given year. R difference represents the difference between the calculated recruitment at a given value of SSB at the associated LM and DM and the chosen R-based reference point; in this case, the 75th percentile of R 1984-2013. Locations where the blue line is above the dotted R difference = 0 line represent acceptable SSB ranges. Red lines represent where the blue line crosses the R difference = 0 line. Numeric ranges can be found in Table 4.5. All results presented use LM and DM values calculated using a rate of bottom temperature change of 0.242°C/year.

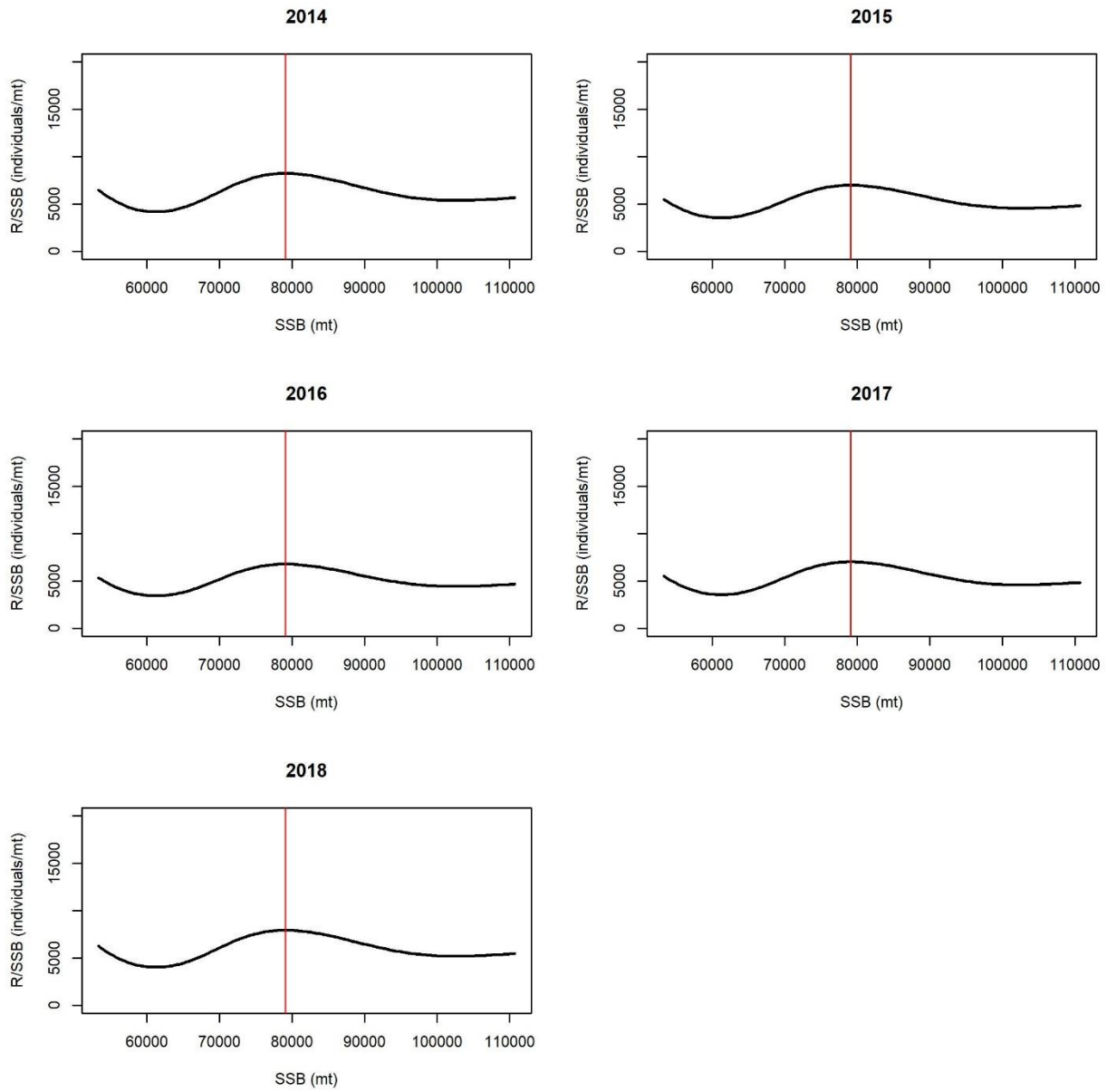


Figure 4.6. Forecasts 2014-2018 of recruitment per spawning stock biomass (R/SSB) in individuals per metric ton (mt) over the historically observed range of spawning stock biomass (SSB) in mt. LM and DM values change per forecasted year as described in section 4.3.4. Red lines represent the SSB size that yields the maximum R/SSB. All results presented use LM and DM values calculated using a rate of bottom temperature change of $0.072^{\circ}\text{C}/\text{year}$.

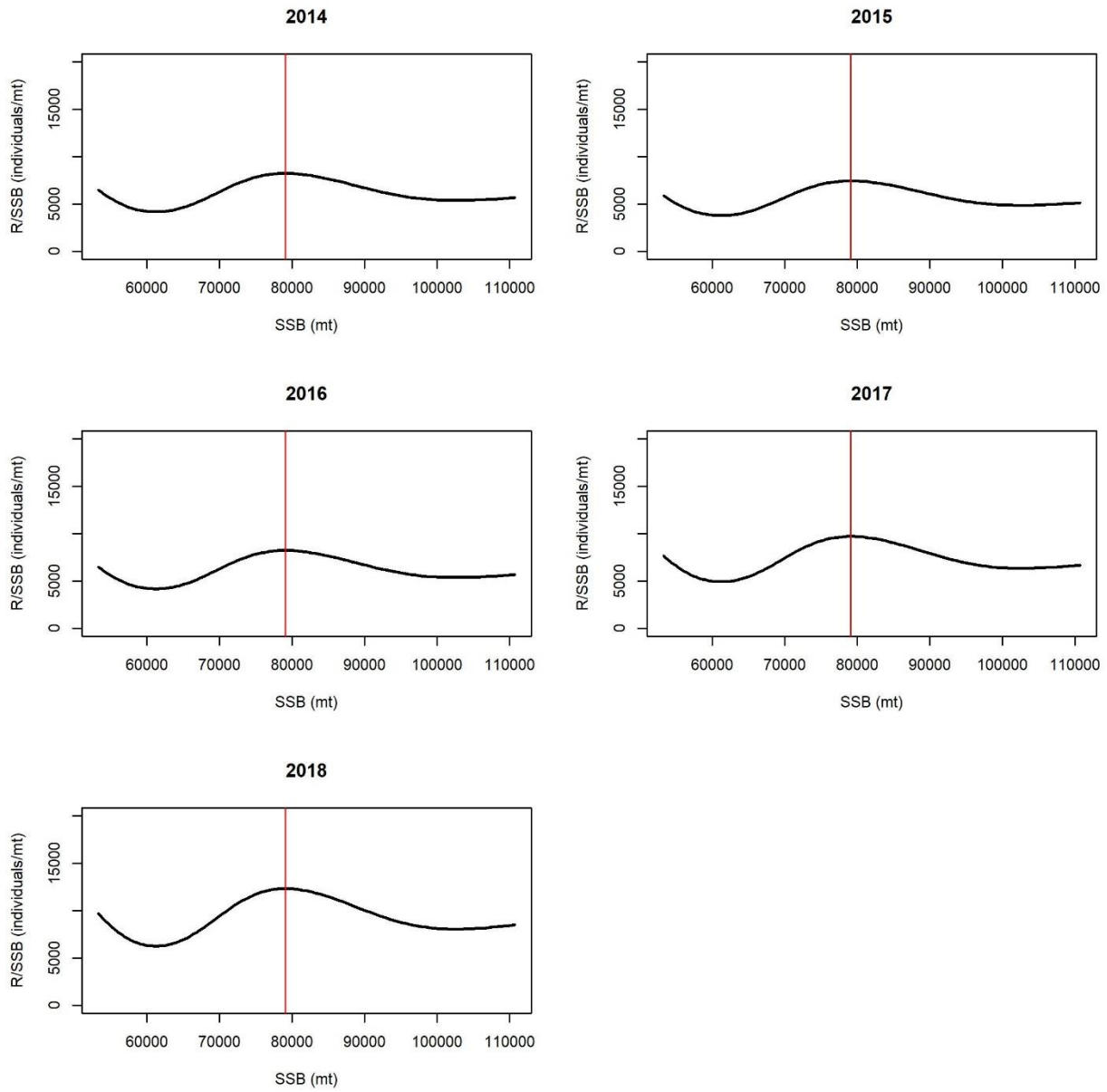


Figure 4.7. Forecasts 2014-2018 of recruitment per spawning stock biomass (R/SSB) in individuals per metric ton (mt) over the historically observed range of spawning stock biomass (SSB) in mt. LM and DM values change per forecasted year as described in section 4.3.4. Red lines represent the SSB size that yields the maximum R/SSB. All results presented use LM and DM values calculated using a rate of bottom temperature change of 0.242°C/year.

Table 4.1. Data input for relationship determination using generalized additive models. Year, recruitment of that year in millions of individuals (R), lagged spawning stock biomass in metric tons (SSB), Gulf of Maine/Georges Bank bottom temperature during the fall spawning event at depths less than 50m in °C (LM), and Gulf of Maine/Georges Bank bottom temperature during the developmental period from biological R to fisheries R at depths less than 480m °C (DM). For additional explanation of parameters, see section 4.3.2.

Year	R	SSB	LM	DM
1989	325.254	53317.233	13.515	8.829
1990	265.591	58825.867	13.375	8.871
1991	277.569	61781.833	13.319	8.989
1992	306.346	62612.333	13.339	8.952
1993	247.488	64029.633	13.662	8.874
1994	316.432	67033.967	13.800	8.867
1995	345.555	71200.133	13.691	8.936
1996	474.357	71518.967	13.420	8.880
1997	367.745	69954.367	13.464	8.972
1998	376.302	70943.333	13.725	8.981
1999	475.807	75016.433	13.643	9.162
2000	363.715	86670.433	13.525	9.271
2001	467.347	96763.667	13.308	9.364
2002	425.552	102677.000	13.798	9.457
2003	338.156	103445.000	13.888	9.303
2004	337.804	101827.000	14.032	9.092
2005	405.071	103789.667	13.945	8.945
2006	447.832	102742.000	13.822	8.877
2007	557.609	99421.867	13.649	8.727
2008	556.596	93349.000	13.453	8.843
2009	605.486	89233.100	13.417	8.952
2010	791.289	88130.933	13.298	9.197

Table 4.1. Continued.

2011	854.597	92140.700	13.162	9.447
2012	889.501	99846.267	13.294	9.870
2013	858.238	110701.233	13.729	10.013

Table 4.2. Variance inflation factor values for spawning stock biomass (SSB), Gulf of Maine/Georges Bank bottom temperature during the fall spawning event at depths less than 50m (LM), and Gulf of Maine/Georges Bank bottom temperature during the developmental period from biological R to fisheries R at depths less than 480m (DM). For additional explanation of parameters, see section 4.3.2.

Parameter	VIF Value
SSB	1.825
LM	1.299
DM	1.645

Table 4.3. Deviance explained (DE) and Akaike Information Criterion (AIC) of the Ricker GAM with all explanatory variables, the lesser Ricker with only SSB and DM explanatory variables, and the Beverton-Holt GAM with all explanatory variables.

Model	DE	AIC
Ricker	82.2	-13.418
Lesser Ricker	69.3	-5.311
Beverton-Holt	91.6	-29.724

Table 4.4. Forecasted Gulf of Maine/Georges Bank bottom temperature (°C) during the fall spawning event at depths less than 50m (LM), and Gulf of Maine/Georges Bank bottom temperature during the developmental period from biological R to fisheries R at depths less than 480m (DM) 2014-2018 under two regimes of minimum (0.072°C/year) and maximum (0.242°C/year) rates of change.

Year	0.072°C/year		0.242°C/year	
	LM	DM	LM	DM
2014	14.125	10.013	14.125	10.013
2015	14.433	10.119	14.433	10.162
2016	14.472	10.127	14.472	10.255
2017	14.448	10.133	14.505	10.388
2018	14.344	10.143	14.515	10.553

Table 4.5. Acceptable ranges of spawning stock biomass in metric tons during years “X-5” to “X-3” to produce at least the desired R levels of year “X” (column 1). Ranges are presented for both future rates of bottom temperature change: 0.072°C/year and 0.242°C/year. Exact range limits were calculated using root linear interpolants. Data are presented as “(lower limit of acceptable range, upper limit of acceptable range)” or “(lower limit of acceptable range +)” if there exists no upper limit in the observed historical range of SSB. Multiple ranges can exist for a given year and rate of change.

Year	0.072°C/year	0.242°C/year
2014	(73724.0, 95189.8), (103391.8+)	(73750.0, 95189.8), (103391.8+)
2015	(79670.7, 84271.1)	(76310.4, 88969.5), (109520.6+)
2016	-	(73750.0, 95078.8), (103502.3+)
2017	(79185.5, 84870.8)	(70924.6+)
2018	(74507.5, 92653.7), (105928+)	(67790.9+)

4.5 Discussion

4.5.1 Lobster Recruitment Relationships

When the SSB is low, the relative R/SSB is high and there seems to be little sign of depensation or an Allee effect. However, the population is still too small to produce the management-desired levels of R . This phenomenon may be due in part to a single pre-1990 data point during a year of low SSB, but high R . Realistically, this lack of data points for lobster during low SSB events may hinder our ability to estimate biological realism in this range. As SSB increases, so does the R/SSB to a relative maximum: the most efficient for the species in terms of reproduction potential and the most effective population size to maximize fisheries catch. However, contrary to a traditional Beverton-Holt relationship (Beverton & Holt 1957), this effect becomes negative again at even higher values of SSB, seemingly indicating some sort of density-dependence effect common with a Ricker SSB/ R model (i.e., compensation) (Ricker 1954). Given that the Beverton-Holt model was selected as the more realistic of the two tested relationships coupled with the possible presence of positive effects on R at the highest SSB values (Figure 4.2), the relationship is seemingly more complex than either a traditional Ricker or Beverton-Holt model. The changing amplitudes from the partial dependence plot of SSB on R (Figure 4.2) may be consequences of effects from unconsidered variables. Additionally, this also seems to show that environmental effects are the primary drivers of this relationship and that R may vary largely at similar SSB values if the environment is variable.

The relationships of the two thermal habitat variables on R appear to be more simplistic (Figure 4.2). For LM, low temperatures during early post-settlement give way to larger fisheries R . This could be a proxy for a predator-prey relationship, where colder temperatures limit predatory fish-feeding by lowering their systematic need for nutrition and decreasing their overall

swim speed and intent to forage (Stoner 2004). The decreased predation during this highly vulnerable stage of lobster development (James-Pirri & Cobb 2000), may allow for larger cohorts.

For DM, the relationship may be similar to LM. At lower temperatures, limited predator feeding may promote larger R. As temperature increases, predation will increase and R will decrease. However, at very high temperatures, the effect on R becomes positive again. Where the first part of this relationship was predator-driven, the latter part may be metabolism driven. Lobster molting frequency is a function of environmental temperature (Aiken 1977) and growth rate is positively correlated with temperature (Green et al. 2014; Madeira et al. 2012). At these very high temperatures during development from biological R to fisheries R, lobsters may be growing so rapidly that their vulnerability to early life-stage predators is limited compared to lobsters that grow more slowly.

These relationships of course have uncertainty associated with them. The GOM/GBK large marine ecosystem has seen considerable regime shifts in recent decades (Friedland & Hare 2007; ASMFC 2020). With limited data over thirty years, it can be difficult to capture effects from these ecosystem-wide shifts. Additionally, there most likely exists spatial effects across the ecosystem influencing trends in these patterns. The resulting relationships discussed here are likely a combination of our definitions coupled with more complicated ecosystem and spatial effects. Lastly, bottom temperature has been shown to have effects on mature lobsters (i.e. SSB), not just juveniles (Tanaka & Chen 2016; Mazur et al. 2020; Hodgdon et al. 2021). These relationships were not apparent with the specific temperature variables used in this study (Table 4.2), indicating a potential for ontogenetic thermal effects on the species.

4.5.2 Forecasts from the Calculator

Using bottom temperature rate of change data from Kleisner et al. (2017), acceptable ranges of SSB that lead to desired R levels are limited compared to extreme warming scenarios from Pershing et al. (2015). This is most likely due to the trend in SSB, R, and temperature over time. All three of these variables are estimated at higher values today than 20 years ago (ASMFC 2020) and temperature in the GOM/GBK is predicted to keep rising (Pershing et al. 2015; Saba et al. 2016). These trends seem to indicate that (at least for the recent future) R has greater odds of being at acceptable levels with higher warming rates. This is in agreement with LeBris et al. (2017), who cites increasing temperatures driving recruitment for GOM/GBK lobster as a driving factor of the region's recent increase in landings. Between the two projections, the extreme scenario seems to yield comparatively higher R/SSB ratios, indicating that increasing temperatures will continue to increase R in the region, even if SSB does not change.

These forecasts do reveal a high sensitivity based on environmental projections. This sensitivity is most likely a result of the SSB/R relationship for lobster being very environmentally-driven. This may serve as a caution to using this calculator with species whose SSB/R relationships are environmentally driven: forecasts and subsequent management advice will be very dependent on the climate projections used. Hilborn and Walters (1992) and Chen and Irvine (2001) forewarn the use of environmental covariates in SSB/R relationships in general for this very reason- stating that these relationships have inherently low predictive capacity. However, this problem does not seem to be directly applicable to the dynamic BRP calculator, because its product is not, by definition, a forecast. The dynamic BRP calculator uses forecasted environmental data (generated a priori) to determine suitable ranges of SSB necessary to produce desired levels of future R.

Management need only keep current SSB levels within these ranges to effectively produce this future R.

4.5.3 The Importance of Dynamic BRPs under Climate Change

Climate change continues to alter marine ecosystems and many species' thermal habitats (Perry et al. 2005; Anderson et al. 2013). Marine populations are changing, but many stock assessments do not currently consider environmental effects (Haltuch et al. 2009; Skern-Mauritzen et al. 2016), leading to false assumptions surrounding the fluid nature of stocks (Haltuch et al. 2009; Vert-pre et al. 2013). Fixed assumptions of population dynamics may be hindering discovery of true/natural relationships. This study indicates that American lobster in the GOM/GBK has a SSB/R relationship that is heavily affected by thermal habitat: a response only apparent because of the rising temperatures of the region. Management of marine species must now consider these environmental effects and thus BRPs often need to be adapted. These dynamic BRPs can strengthen many management frameworks by accounting for environmental variability (Berger 2019; O'Leary et al. 2020) and their importance is ever-growing under climate change, especially for those species whose SSB/R relationships are impacted by the environment.

The dynamic BRP calculator and associated framework presented here was built with the intention of being a post hoc analysis for stock assessments having a wide applicability over taxa. The framework can be used to establish both Ricker and Beverton-Holt SSB/R models that incorporate an unlimited number of environmental covariates and any amount of lag time between SSB and fisheries R. The calculator can be used solely with model-generated data and can be used to examine multiple R-based reference points. There is potential for improvement upon this model as there are four inherent issues: 1) forecasts are limited to historically observed ranges of SSB, 2) reliable results can only be achieved with an extensive knowledge of the species' life history, 3)

forecasts may be heavily dependent on the environmental data used, and 4) it is difficult to ascertain overfitting in the relationship. Future research and development of this framework should combat these issues. Regardless, in its current state, this calculator has revealed interesting information about American lobster in the GOM/GBK region and has significant potential for use in developing dynamic BRPs for many stock assessments.

**CHAPTER 5: A FRAMEWORK TO INCORPORATE ENVIRONMENTAL EFFECTS
INTO STOCK ASSESSMENTS INFORMED BY FISHERY-INDEPENDENT SURVEYS:
A CASE STUDY WITH AMERICAN LOBSTER (*HOMARUS AMERICANUS*)**

5.1 Abstract

Stock assessments for a majority of the world's fisheries often do not explicitly consider the effects of environmental conditions on target species, which can raise model uncertainty and potentially reduce forecasting quality. Model-based abundance indices were developed using a delta generalized linear mixed model that incorporates environmental variability for use in stock assessment to understand how the incorporation of environmental variability impacts our understanding of population dynamics. For this study, multiple model-based abundance indices were developed to test the incorporation of environmental covariates in a length-structured assessment of the American lobster stock in the Gulf of Maine/Georges Bank on the possible improvement of stock assessment quality. Comparisons reveal that modelled indices with environmental covariates appear to be more precise than traditional indices, but model performance metrics and hindcasted fishery statuses revealed that these improvements to indices may not necessarily mean an improved assessment. Model-based abundance indices are not intrinsically better than design-based indices and should be tested for each species individually.

5.2 Introduction

Climate change has been shown to affect many commercially important marine species' distributions, life histories, and overall production (Perry et al. 2005; Hazen et al. 2012; Anderson et al. 2013; FAO 2016; IPCC 2019). However, the effects of environmental change are often absent in stock assessments for many species (Haltuch et al. 2009; Skern-Mauritzen et al. 2016). This discount of change has the potential to incorrectly inform fisheries managers due to biological

reference point (BRP) calculations under false assumptions of population equilibria (Haltuch et al. 2009; Vert-pre et al. 2013). As the global climate continues to change, the need to estimate these effects and determine if consideration of them is necessary in stock assessment frameworks becomes progressively more apparent to both researchers and fisheries managers (Hollowed et al. 2009; Maunder & Piner 2015).

Many stock assessment frameworks heavily rely on fishery-independent data (i.e. survey catch rates), which can act as indices for target species abundance (Richards & Schnute 1986; Chen et al. 2004; Maunder et al. 2006). These indices are meant to represent fluctuations in the target species' population over both space and time. However, there exist uncertainties surrounding these data. Surveys may not accurately capture changes in abundance due to environmental drivers that affect both the distribution of the target species and the catchability of the survey itself (Maunder et al. 2006; Conn 2010; Shelton et al. 2014). Species density is rarely spatially homogeneous, but would be expected to gradually change over space due to habitat preferences caused in part by environmental parameters. Attempts to account for these environmental effects in design-based indices can result in high variability and may not represent true population density (Shelton et al. 2014; Thorson 2019).

If environmental effects could be accounted for in calculation of abundance indices, then there exists a potential to improve their overall reliability (Thorson 2019). Additionally, if this process took place outside an existing stock assessment, then only model input data would need to be changed and no assessment reconfiguration would be necessary for implementation of the new modelled indices. In developing a framework to accomplish this, a spatiotemporal delta-generalized linear mixed model (delta-GLMM) initially designed by Thorson et al. (2015) was applied (using the *VAST* package in R; Thorson and Barnett 2017; Thorson 2019). This framework,

hereafter referred to as the delta-GLMM, incorporates environmental covariates for both species density and survey catchability in abundance index calculations outside of an existing stock assessment model. This framework can therefore be used with any stock assessment that uses abundance indices. This study evaluates the implications of accounting for environmental variability in survey abundance indices for use in stock assessments using the Gulf of Maine (GOM)-Georges Bank (GBK) American lobster (*Homarus americanus*) fishery as a case study for how to account for variability in catch rates due to environmental conditions.

The lobster fishery in the GOM/GBK (Figure 5.1) large marine ecosystem (LME) has a rich cultural and economic history. It is a year-round trap fishery, with the bulk of effort in the summer and fall seasons when the population is in shallow, near-shore waters. It currently represents the United States' most valuable single species fishery, with recent average yearly worth estimated at around half a billion US dollars (MEDMR 2016; NMFS 2018). However, this species' distribution and physiology has been shown to be affected by changing environmental conditions (ASMFC 2015; Boudreau et al. 2015). Changes in both recruitment and adult lobster population size and dynamics have been linked to changes in rising temperatures and suitable habitat (Mills et al. 2013; Boudreau et al. 2015; Tanaka et al. 2019). Warming trends have directly caused changes in migrational timing and molting events, increases in natural mortality, and increases in fisheries recruitment numbers (Mills et al. 2013; Boudreau et al. 2015; Staples et al. 2019; Tanaka et al. 2019). Additionally, lobster mobility, and by extension catchability, could potentially be linked to bottom temperatures as well with increasing temperatures meaning a higher catchability (Zhao et al. 2019). These effects could also be attributed to water column depth as American lobsters perform yearly migrations in the summertime to shallower waters where they are more active; feeding and spawning (Ennis 1973; Uzmann et al. 1977). Current stock assessment

methodology for this species does not consider environmental effects such as thermal habitat or depth (ASMFC 2015), but the Atlantic States Marine Fisheries Commission (ASMFC) recognizes this as a future priority (ASMFC 2015).

This study aims to determine if consideration of dynamic bottom temperatures and water column depth improves estimation of abundance indices for the lobster stock in the GOM/GBK LME. To accomplish this, retrospective patterns and model fit will be compared between runs of a length-based assessment model for lobster using traditional design-based abundance indices and model-based abundance indices created with environmental covariates bottom temperature and depth. Additionally, calculations of biological reference points (BRPs) for each run will determine if hindcasted fishery status differs between assessment model runs.

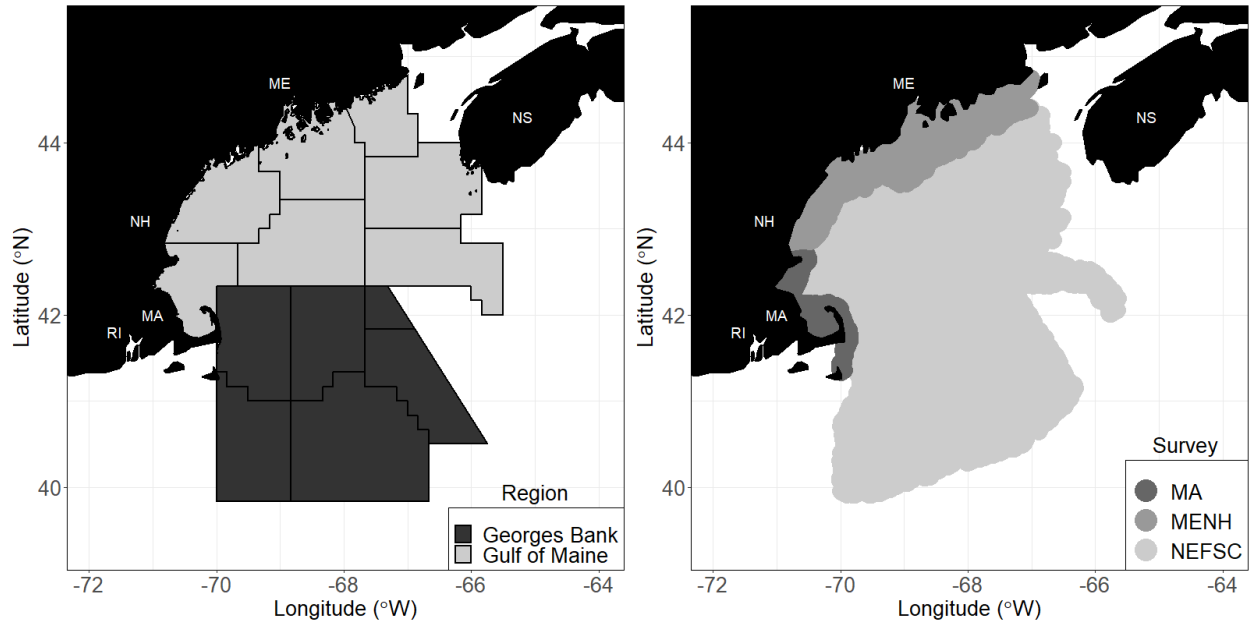


Figure 5.1. Right: NOAA Statistical Areas (outlined in black) that comprise the stock management boundaries of American lobster of the GOM/GBK LME. Left: Survey boundaries across years and seasons for the MEDMR/NHFGD Inshore Bottom Trawl Survey 2001-2013 (MENH), the MADMF Bottom Trawl Survey 1984-2013 (MA), and the NEFSC Bottom Trawl Survey 1984-2013 (NEFSC). Also labelled are the states of Maine (ME), New Hampshire (NH), Massachusetts (MA), and Rhode Island (RI), and the Canadian province of Nova Scotia (NS). Maps generated in R using package *ggplot2*. Shapefile for statistical areas provided by the NEFSC. See bibliography for all data sources.

5.3 Methods

5.3.1 Delta-generalized linear mixed model (delta-GLMM)

The delta-GLMM applied in this study (R *VAST* package version 3.2.2; Thorson and Barnett 2017; Thorson 2019) uses catch data from a single given survey with optional environmental covariates for density and/or catchability to derive modelled abundance indices.

The delta-GLMM designates a user defined number n_s knot locations throughout a pre-defined bounded spatial area. Knots do not represent surveyed locations in the spatial area, although the density of knots throughout the spatial area is indicative of the density of survey

locations. The model then estimates population density at each knot in a multi-step process, with survey data being fit for presence-absence of the target species and then again for estimating the catch given that the target species is present (supplemental material; Thorson et al. 2015; Thorson 2019). Both of these linear predictors are estimated with spatial random effects, spatio-temporal random effects, seasonal species density (or habitat) covariates, and catchability covariates (Thorson et al. 2015; Thorson 2019). Random effects are spatially smoothed using a stochastic partial differential equation approximation to a Matérn correlation function assumed to be both isotropic and two-dimensional (Thorson 2019). Predicted density at knot s in year t , $d(s, t)$, can be calculated from transformed linear predictors, $p_1(i)$ and $p_2(i)$ used for estimating encounter probability and positive catch rates, respectively (supplemental material), and dropping catchability effects. This process is formulated as:

$$\begin{aligned}
d(s, t) = & \text{logit}^{-1}[\beta_1(t_i) + \sum_{f=1}^{n_{\omega 1}} L_{\omega 1}(f)\omega_1(s_i, f) + \sum_{f=1}^{n_{\varepsilon 1}} L_{\varepsilon 1}(f)\varepsilon_1(s_i, f, t_i) \\
& + \sum_{p=1}^{n_p} \gamma_1(t_i, p)X(s_i, t_i, p)] \times \exp[\beta_2(t_i) + \sum_{f=1}^{n_{\omega 2}} L_{\omega 2}(f)2(s_i, f) \\
& + \sum_{f=1}^{n_{\varepsilon 2}} L_{\varepsilon 2}(f)\varepsilon_2(s_i, f, t_i) + \sum_{p=1}^{n_p} \gamma_2(t_i, p)X(s_i, t_i, p)]
\end{aligned} \tag{5.1}$$

where all parameters are listed and described in Table 5.1. Additionally, an index of abundance for year t , I_t , can be calculated by integrating over space (knots):

$$I_t = \sum_{s=1}^{n_s} d(s, t) \quad (5.2)$$

Lastly, coefficients of variation for each I_t , CV , were calculated as:

$$CV = SE/N \quad (5.3)$$

where SE is the standard error of I_t and N is the total number of survey instances in year t . For more detailed information concerning equations/calculations within the delta-GLMM, see Thorson et al. (2015) and Thorson (2019). A Table of all settings for the framework used in this study can be found in Table 5.2.

5.3.2 The Stock Assessment Model

The Lobster Stock Assessment model (UMM) is a seasonal integrated length-structured assessment model for lobster in the GOM/GBK LME. It was initially developed and coded with ADMB (Chen et al. 2005; ASMFC 2015). The program codes were later modified by Cao et al. (2017a; 2017b) and Tanaka et al. (2019). Due to the inability to appropriately and reliably age wild-caught lobster and thus lack of knowledge on age-length relationships (Wahle et al. 1996; Chang et al. 2011; ASMFC 2015), a length-based assessment model was deemed more appropriate than an age-based assessment model (Chen et al. 2005): a practice common with many crustacean species (Chang et al. 2011; Punt et al. 2013). The population dynamics equation this model employs is:

$$N_{t,m} = N_{t,m-1} \times e^{-F_{t,m} + M} \times G_{m-1} + R_{t,m} \quad (5.4)$$

where $N_{t,m}$ is a vector of the number of lobster in each of the pre-specified size bins in year t and season m , F is seasonal fishing mortality, M is seasonal natural mortality, G is the seasonal growth transition matrix (estimated a priori from an individual-based model; Mazur et al. 2018), and R is the recruitment to each size bin (Chen et al. 2005). In the UMM, G and M are pre-specified and R and F are estimated. G is averaged across both sexes: a practice commonly and historically done with the UMM (Tanaka et al. 2019). M is expected to be the same for both sexes and so no average is taken (ASMFC 2015). Additionally, spawning stock biomass (SSB) can be estimated using proportion female and proportion mature per-size-bin vectors. A detailed explanation of this model can be found in Chen et al. (2005), ASMFC (2015), and Tanaka et al. (2019). All model settings used for this study can be found in Table 5.3. For additional details on the UMM, contact the Chen Lab at the University of Maine.

The surveys used in the UMM are the Maine Department of Marine Resources' (MEDMR) Ventless Trap Survey, the Maine/New Hampshire Inshore Bottom Trawl Survey conducted in a partnership between the MEDMR and the New Hampshire Fish and Game Department (NHFGD), the Massachusetts Division of Marine Fisheries' (MADMF) Inshore Bottom Trawl Survey, and the Northeast Fisheries Science Center's (NEFSC) Bottom Trawl Survey. Each of the last three surveys are split into a fall and a spring survey, for a total of seven surveys. Spring and fall periods are different across the surveys but are confined to the six month blocks January-June and July-December. A list of the spatial coverages of these surveys can be found in Figure 5.1 and their temporal coverages can be found in Table 5.3. Citations for all data used in this study are available in the bibliography.

There is an abundance index associated with each of the seven surveys for each year. This abundance index is a calculation of survey catch rate over the spatial area for the survey in that

year and season and is meant to be a proxy for population biomass. Traditionally, this survey catch rate was calculated as the number of individuals caught over 53 mm carapace length divided by the number of unique survey instances.

5.3.3 Abundance Index Calculations and Assessment Model Configurations

For this study, the delta-GLMM was run on each of six surveys individually. The six surveys were the spring and fall MEDMR/NHFGD Inshore Bottom Trawl Surveys, the spring and fall MADMF Inshore Bottom Trawl Surveys, and the spring and fall NEFSC Bottom Trawl Surveys.

Each of the above surveys collects bottom temperature data. Using sea surface temperature (SST) data from the National Oceanic and Atmospheric Administration's (NOAA) Advanced Very High Resolution Radiometer (AVHRR) (Reynolds et al. 2007; Banzon et al. 2016) alongside the survey data, generalized additive models (GAMs) were used to estimate the relationship between predictor variables latitude, longitude, month, depth, and surface temperature and the response variable bottom temperature. This allowed for predicted bottom temperature values based on the surface temperature and how this relationship changed over space and across seasons. This relationship was calculated for each survey area and was used to predict bottom temperature at each knot and survey location in the bounded spatial area of the survey. As a density covariate, bottom temperature was calculated over six-month time blocks to match survey time blocks and to maintain consistency (above). As a catchability covariate, bottom temperature was calculated per month to match with survey month. This was done to address potential seasonal changes in catchability which may not be derived from point measurements taken from the surveys. Depth was treated as a static variable, with identical values year to year at each knot and survey location. Descriptions of how each variable was used in the delta-GLMM can be found in Table 5.2.

There were nine delta-GLMM runs per survey, each with different combinations of density and catchability covariates (Table 5.2). The same covariate was not used in the delta-GLMM as both a density and as a catchability covariate so as to avoid model inflation due to multicollinearity and reduction in power. Additionally, bottom temperature and depth in this framework were tested for multicollinearity using a traditional variance inflation factor (VIF) test.

Stock-wide abundance from each survey in each year was assembled and used to replace the design-based survey catch rate data in the UMM, totaling nine UMM model runs plus the original run with the design-based abundance indices (Table 5.4). The CVs historically used in the UMM with the design-based indices was a single value representing an average across all seven surveys: 0.25. This value represented the mean SE/N across all surveys across all years with equal weighting given to each of the surveys, regardless of their temporal coverages. In an effort to properly compare UMM model runs and directly compare CV data, mean CVs from the delta-GLMM for each of the six surveys (Table 5.3) were averaged with the MEDMR Ventless Trap Survey 2006-2012 CV: 0.019. This totaled nine new mean CVs, one for each new UMM run.

5.3.4 Model Run Comparisons and BRPs

Retrospective patterns and objective function values (OFVs) were used to compare and evaluate UMM model outputs. Mohn's Rho values were calculated from seven-year peels (2006-2013) for *SSB* in metric tons, *R* in millions of individuals, and *F*:

$$\rho_v = \frac{\sum_{q=1}^Q \frac{E_q - F_q}{F_q}}{Q} \quad (5)$$

where ρ_v is Mohn's Rho of variable v (SSB , R , or F), Q is the number of peels (seven), E_q is the terminal variable value when the UMM is run for years 1984 through 2013- q , and F_q is the variable value in year 2013- q when the UMM is run for years 1984 through 2013. Calculations were completed with package *icesAdvice* (version 1.4-2) in R. Lower Mohn's Rho values represent lower retrospective bias, lower systematic inconsistency, and an overall more reliable calculation (Mohn 1999; Deroba 2014; Hurtado-Ferro et al. 2014). To capture the overall retrospective bias, absolute Mohn's Rho values for SSB , R , and F of a single UMM run were summed. This value allowed for direct comparisons of total retrospective bias between the ten UMM runs (Table 5.4). OFVs were calculated as summed negative log likelihoods of (1) predicted length compositions from fishery-independent surveys, (2) predicted abundance from fishery-independent surveys, (3) predicted length compositions from commercial fleet catch, (4) predicted total commercial fleet catch, and (5) predicted recruitment. Lower OFVs represent models with a better fit and lower residuals. The model with the lowest overall retrospective bias and lowest OFV were chosen as the optimal model(s).

BRPs were then calculated for each optimal model and the design-based model. BRPs for the GOM/GBK American lobster stock are calculated as the seventy-fifth and twenty-fifth percentiles of reference abundance and exploitation rate from 1982-2003 (ASMFC 2015). For reference abundance, the seventy-fifth percentile acts as the target and the twenty-fifth percentile acts as the threshold. For exploitation rate, this is reversed. BRPs in this study were calculated much the same way, except the reference period was shortened to 1984-2003 due to UMM data input limitations. Using these BRPs, hindcasted fishery statuses were compared.

Table 5.1. A description of the parameters used in equations 5.1 and 5.2. Parameter definitions are from Thorson et al. 2019. For more information, see Thorson et al. (2015) and Thorson (2019).

Parameter	Description
$\beta_1(t_i)$	Intercept for first linear predictor in time interval t
$\beta_2(t_i)$	Intercept for second linear predictor in time interval t
$L_{\omega_1}(f)$	Loadings matrix for spatial covariation for first linear predictor for factor f
$L_{\omega_2}(f)$	Loadings matrix for spatial covariation for second linear predictor for factor f
$L_{\varepsilon_1}(f)$	Loadings matrix for spatio-temporal covariation for first linear predictor for factor f
$L_{\varepsilon_2}(f)$	Loadings matrix for spatio-temporal covariation for second linear predictor for factor f
$\gamma_1(t_i, p)$	Impact of habitat covariate p on first linear predictor in year t
$\gamma_2(t_i, p)$	Impact of habitat covariate p on second linear predictor in year t
$\omega_1(s_i, f)$	Spatial factors for first linear predictor for knot s and factor f
$\omega_2(s_i, f)$	Spatial factors for second linear predictor for knot s and factor f
$\varepsilon_1(s_i, f, t_i)$	Spatio-temporal factors for first linear predictor for knot s , factor f , and year t
$\varepsilon_2(s_i, f, t_i)$	Spatio-temporal factors for second linear predictor for knot s , factor f , and year t
n_{ω_1}	Number of spatial factors for first linear predictor
n_{ω_2}	Number of spatial factors for second linear predictor
n_{ε_1}	Number of spatio-temporal factors for first linear predictor
n_{ε_2}	Number of spatio-temporal factors for second linear predictor
$X(s_i, t_i, p)$	Covariate value for habitat covariate p in knot s and year t
n_p	Number of habitat covariates

Table 5.1 Continued.

f	Factor number
p	Habitat covariate number
t_i	Time interval number (year) associated with observation i
s_i	Spatial location number (knot) associated with observation i
i	Observation number (survey instance)
$d(s, t)$	Predicted density for knot s in year t
I_t	Index of abundance for year t
n_s	Number of knots

Table 5.2. Settings and data used in the delta-GLMM for each run. All settings except ‘Density Covariates’, ‘Catchability Covariates’, and ‘Surveys’ were kept constant throughout the runs. All combinations of four different ‘Density Covariates’, four different ‘Catchability Covariates’, and six different ‘Surveys’ meant ninety-six delta-GLMM runs. For a list of each component's properties, see the documentation for the R VAST package version 3.2.2 or Thorson (2019).

Density Covariates	None.
	Average bottom temperature of a six-month period: January through June for all “Spring” surveys and July through December for all “Fall” surveys.
	Depth at knot.
	Average bottom temperature of a six-month period: January through June for all “Spring” surveys and July through December for all “Fall” surveys and depth at knot.

Table 5.2 Continued.

Catchability Covariates	None.
	Average bottom temperature of a 30 day period centered on the survey instance.
	Depth at each survey location.
	Average bottom temperature of a 30 day period centered on the survey instance and depth at survey location.
Surveys	Spring MEDMR/NHFGD Inshore Bottom Trawl Survey
	Fall MEDMR/NHFGD Inshore Bottom Trawl Survey
	Spring MADMF Inshore Bottom Trawl Survey
	Fall MADMF Inshore Bottom Trawl Survey
	Spring NEFSC Bottom Trawl Survey
	Fall NEFSC Bottom Trawl Survey
Number of Knots	100
Method	Mesh
Grid Size	25km
FieldConfig	$\Omega_1 = 1$; $\epsilon_1 = 1$; $\Omega_2 = 1$; $\epsilon_2 = 1$
RhoConfig	$\beta_1 = 0$; $\beta_2 = 0$; $\epsilon_1 = 0$; $\epsilon_2 = 0$
OverdispersionConfig	$\eta_1 = 0$; $\eta_2 = 0$
Bounded spatial areas	Varied by survey.

Table 5.3. Settings and data used in the UMM for each run. For more information, see Cao et al. (2017a; 2017b) and Tanaka et al. (2019).

Years	1984 through 2013
Seasons	4 (Each 3 month time blocks)
Number of sexes	1 (Averaged across male and female)
Size range	53 mm to 223 mm carapace length
Size bins	5 mm (For a total of 34 bins)
Initial conditions	First year size composition assumed from survey data
Recruitment size	53 mm to 73 mm
SSB/R relationship	None
Growth	Prespecified seasonal growth transition matrices averaged across both sexes; Supplement
Number of commercial fleets	1
Commercial fleet selectivity at size	Double logistic averaged across both sexes
Survey data*	MEDMR Ventless Trap Survey 2006-2012 Spring MEDMR/NHFGD Inshore Bottom Trawl Survey 2001-2013 Fall MEDMR/NHFGD Inshore Bottom Trawl Survey 2000-2013 Spring MADMF Bottom Trawl Survey 1984-2013 Fall MADMF Bottom Trawl Survey 1984-2013 Spring NEFSC Bottom Trawl Survey 1984-2013 Fall NEFSC Bottom Trawl Survey 1984-2013
Survey selectivity at size	Double logistic averaged across both sexes
Fishing mortality rate	Instantaneous rates averaged across both sexes

Table 5.3 Continued.

Natural mortality rate	0.15 year ⁻¹ across all size groups, seasons, and sexes
------------------------	--

* Survey indices changed across runs according to Table 5.4.

Table 5.4. The ten UMM model runs in this study outlining which covariates were used in each run. Covariates were calculated as described in Table 5.2.

Run #	Type of Indices	Habitat Covariates	Catchability Covariates
1	Design-based	None	None
2	Model-based	None	None
3		None	Temperature
4		None	Depth
5		None	Temperature and Depth
6		Temperature	None
7		Temperature	Depth
8		Depth	None
9		Depth	Temperature
10		Temperature and Depth	None

5.4 Results

Results from the six GAMs used to predict bottom temperature values for the six surveys used in the delta-GLMM are displayed in Table 5.5. A VIF value of 1.99 between bottom

temperature and depth revealed relatively low correlation and thus all nine originally proposed combinations of predictor variables (Table 5.5) could be reliably tested. CVs calculated for all UMM model runs are presented in Table 5.6. All nine model-based CVs were substantially lower than the design-based CV of 0.25, showing an overall decreased dispersion when using modeled indices. The lowest model-based CV was 0.02 for Run #s 2, 6, 7, 8, and 10. The highest model-based CV was 0.06 for Run # 5.

Retrospective patterns are summarized in Figure 5.2. Mohn's Rhos for *SSB* and *R* improved across all nine model runs, whereas Mohn's Rho for *F* was worse across all nine runs. Overall, two of nine model runs showed improved cumulative retrospective patterns over the design-based. It also appears that temperature as a density covariate produces smaller retrospective patterns over temperature as a catchability covariate and that the reverse is true for depth. Model fits are summarized in Figure 5.3. OFV remained the lowest in the stock assessment when using the traditional design-based indices. All other OFVs were between nine and forty-two percent larger. However, of the model-based OFVs, the addition of covariates over model-based with no covariates yielded significantly improved results: the smallest OFV being for run #5 (temperature and depth as catchability covariates).

Using absolute Mohn's Rho summed across *SSB*, *R*, and *F* as the indicator to choose an optimal model, the model that utilized depth as a catchability covariate performed best, showing an overall improvement of retrospective patterns by 12.6% (0.709 compared to 0.620; Figure 5.2). Using OFV as the indicator to choose an optimal model, the design-based model outperformed all model-based ones. Therefore, only one optimal model was chosen to compare hindcasted fishery status to the design-based: the model that utilized depth alone as a catchability covariate. It is

important to note that the optimal model for retrospective patterns had an OFV that was 20.4% larger than the design-based OFV (81,614.6 compared to 67,777.7; Figure 5.3)

Hindcasted reference abundance and BRPs for both the optimal model and design-based model are displayed in Figure 5.4 and Table 5.7). Twenty-fifth percentiles for reference abundance were calculated for the optimal and design-based models to be 198.392 million individuals and 160.347 million individuals, respectively. Seventy-fifth percentiles for reference abundance were calculated for the optimal and design-based models to be 260.149 million individuals and 250.865 million individuals, respectively. For the design based model, the fishery was below the threshold 1984-1986 and 1988-1989, between the threshold and the target 1987, 1990-1998, and 2004-2006, and above the target 1999-2003 and 2007-2013 (Figure 5.4). For the optimal model, the fishery was below the threshold 1984, 1987-1989, 2002, and 2004-2006, between the threshold and the target 1985-1986, 1990, 1993-1994, 1998-2001, 2003, and 2007-2008, and above the target 1991-1992, 1995-1997, and 2009-2013 (Figure 5.4). Thus, the design-based and optimal models only agreed in 40% of the years.

Hindcasted reference exploitation rates and BRPs for both the optimal model and design-based model are displayed in Figure 5.5 and Table 5.8. Twenty-fifth percentiles for reference exploitation rates were calculated for the optimal and design-based models to be 0.190 and 0.190, respectively. Seventy-fifth percentiles for reference exploitation rates were calculated for the optimal and design-based models to be 0.321 and 0.213, respectively. For the design based model, exploitation rate was above the threshold 1984, 1991, 1994, 2000, 2002, and 2004-2013, between the threshold and the target 1985, 1988-1990, 1995-1997, 1999, and 2003, and below the target 1986-1987, 1992-1993, 1998, and 2001 (Figure 5.5). For the optimal model, exploitation rate was above the threshold 1988, 1990-1991, 1993, 1997, and 2013, between the threshold and the target

1984-1987, 1989, 1992, 1994-1996, 2000, 2006, and 2012, and below the target 1998-1999, 2001-2005, and 2007-2011 (Figure 5.5). Thus, the design-based and optimal models only agreed in 27% of the years.

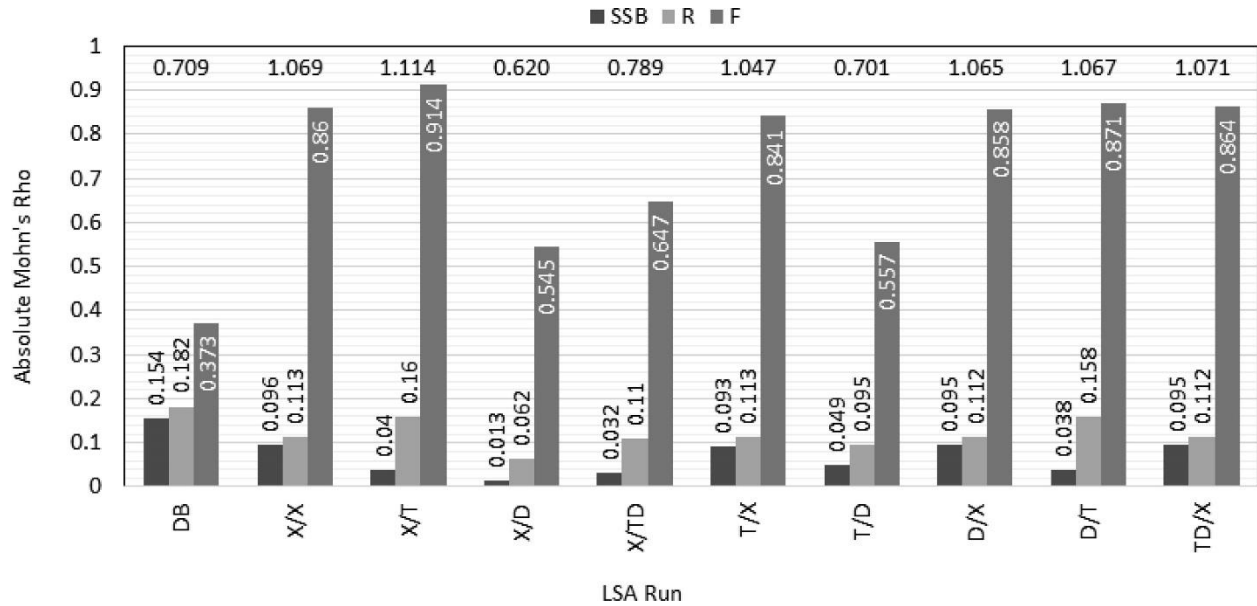


Figure 5.2. Absolute Mohn's Rho values for each UMM run for *SSB*, *R*, and *F*. Mohn's Rho values displayed on top or inside of their respective boxes. Absolute summed Mohn's Rho values for each run are at the top of each column. The X axis denotes each UMM run as either 'DB' (Design-based) or as 'A/B', where 'A' represents the density covariates used in index calculation and 'B' represents the catchability covariates used. 'X' = None, 'T' = Bottom Temperature, 'D' = Depth, 'TD' = Temperature and Depth.

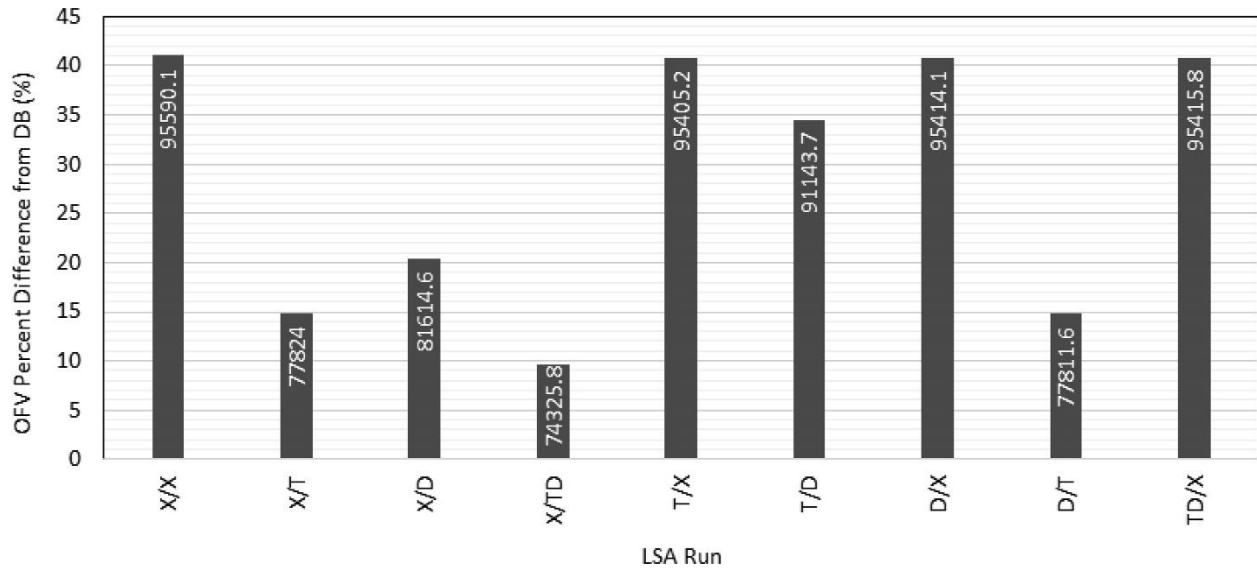


Figure 5.3. Differences between OFVs for each UMM run with model-based indices from OFVs of the UMM run with design-based indices. The design-based OFV was 67777.7. OFVs for each model-based run are displayed inside their respective bars. The X axis denotes each UMM run as ‘A/B’, where ‘A’ represents the density covariates used in index calculation and ‘B’ represents the catchability covariates used. ‘X’ = None, ‘T’ = Bottom Temperature, ‘D’ = Depth, ‘TD’ = Temperature and Depth. Order of indices left to right represent highest to lowest differences. All OFVs from UMM runs using model-based indices were higher than those using the design-based, making the design-based the optimal model using OFV as the indicator.

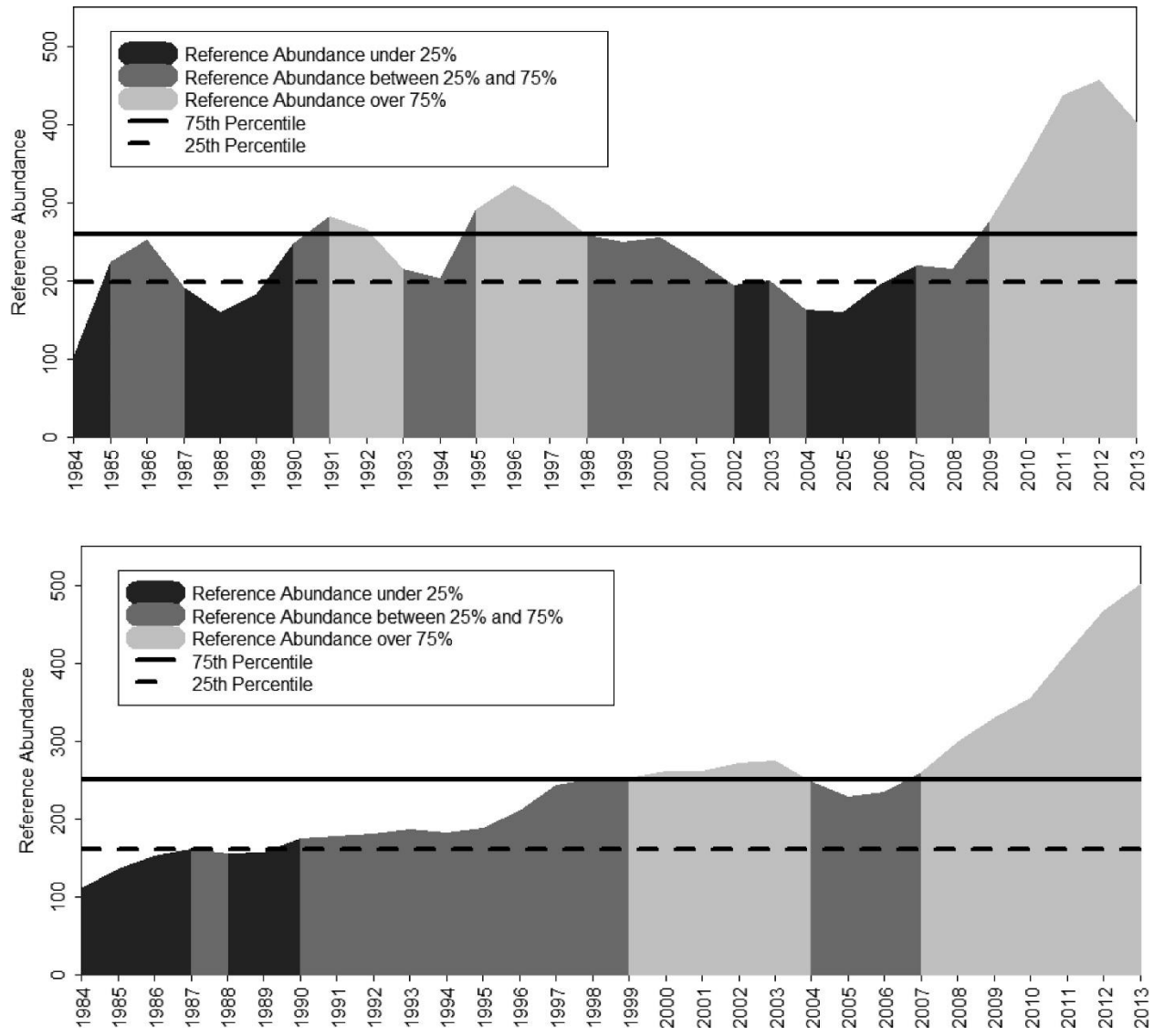


Figure 5.4. Reference abundance 1984-2013 for the optimal model (above) and design-based model (below). BRPs are calculated separately for each model. Numbers are in millions of individuals.

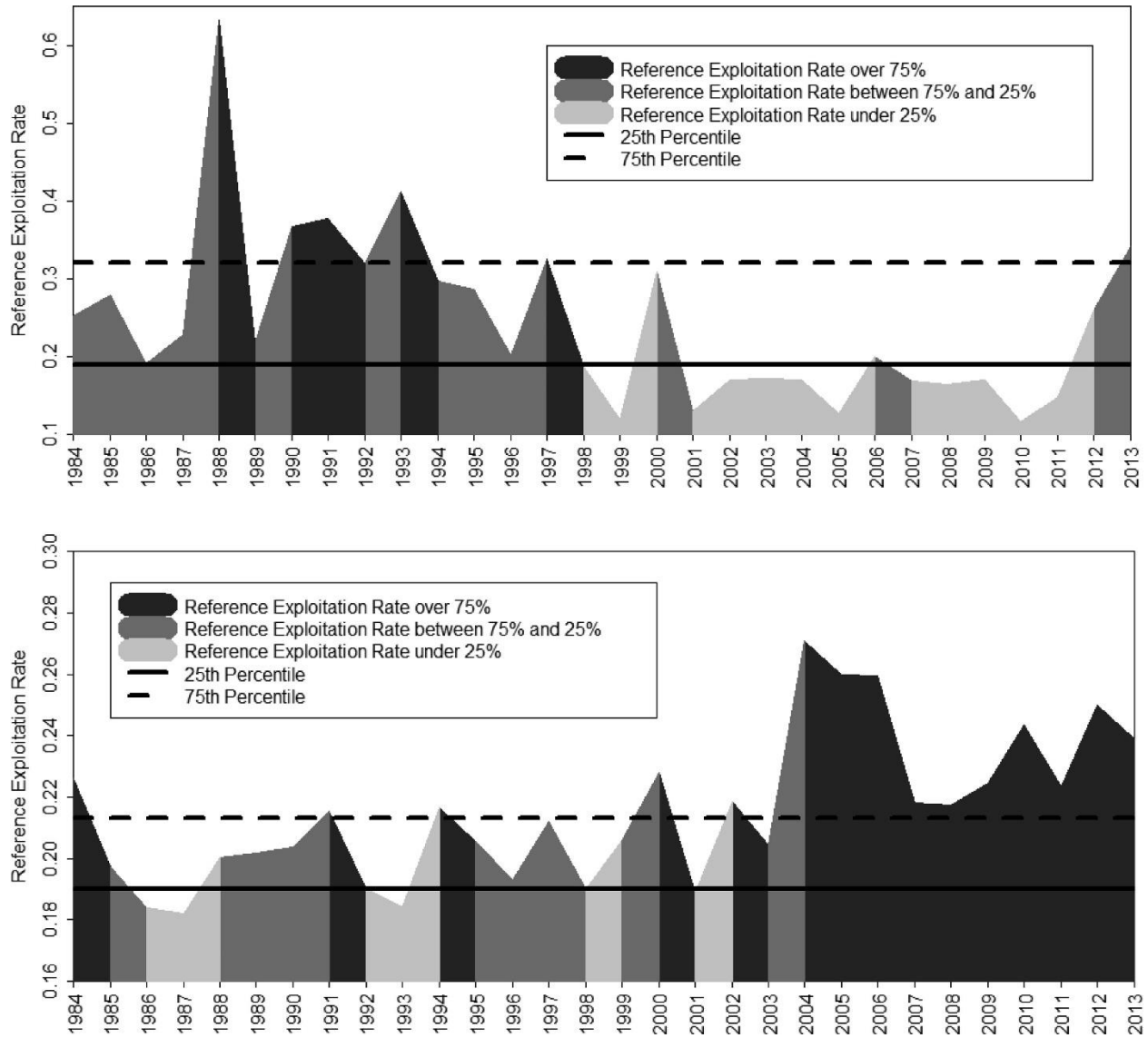


Figure 5.5. Reference exploitation rate 1984-2013 for the optimal model (above) and design-based model (below).

BRPs are calculated separately for each model.

Table 5.5. Deviance explained (DE), root mean squared error (RMSE), and data range (Range) of the six generalized additive models used to predict bottom temperature from sea surface temperature, latitude, longitude, depth, and month for each of the six surveys: MEDMR/NHFGD Inshore Bottom Trawl Spring Survey (MENHSP), MEDMR/NHFGD Inshore Bottom Trawl Fall Survey (MENHFL), MADMF Bottom Trawl Spring Survey (MASP), MADMF Bottom Trawl Fall Survey (MAFL), the NEFSC Bottom Trawl Spring Survey (NEFSCSP), and the NEFSC Bottom Trawl Fall Survey (NEFSCFL).

	MENHSP	MENHFL	MASP	MAFL	NEFSCSP	NEFSCFL
DE (%)	77.8	77.1	84.6	87.5	75.5	81.3
RMSE (°C)	0.60	0.80	1.19	1.74	1.21	2.00
Range (°C)	9.40	9.20	17.20	19.00	15.47	21.27

Table 5.6. Mean coefficients of variation (CVs) values for each of the six surveys averaged across years from delta-GLMM output. Run # designates the combination of covariates used in the delta-GLMM (see Table 5.4). SPMENH = Spring MEDMR/NHFGD Inshore Bottom Trawl Survey 2001-2013, FLMENH = Fall MEDMR/NHFGD Inshore Bottom Trawl Survey 2000-2013, SPMA = Spring MADMF Bottom Trawl Survey 1984-2013, FLMA = Fall MADMF Bottom Trawl Survey 1984-2013, SPNEFSC = Spring NEFSC Bottom Trawl Survey 1984-2013, and FLNEFSC = Fall NEFSC Bottom Trawl Survey 1984-2013. UMM CV is the mean CV value used in the UMM run that is calculated as the average of all six survey CVs and the CV of the MEDMR Ventless Trap Survey 2006-2012: 0.019.

Run #	Survey						UMM CV
	SPMENH	FLMENH	SPMA	FLMA	SPNEFSC	FLNEFSC	
1	0.322*	0.266*	0.275*	0.330*	0.259*	0.274*	0.25*
2	0.009	0.013	0.021	0.035	0.013	0.014	0.02
3	0.040	0.075	0.033	0.064	0.018	0.024	0.04
4	0.098	0.016	0.024	0.033	0.014	0.014	0.03
5	0.083	0.092	0.072	0.125	0.020	0.025	0.06
6	0.009	0.013	0.021	0.035	0.013	0.014	0.02
7	0.011	0.016	0.025	0.033	0.015	0.015	0.02
8	0.009	0.013	0.021	0.035	0.013	0.014	0.02
9	0.040	0.074	0.035	0.066	0.018	0.024	0.04
10	0.009	0.013	0.021	0.035	0.013	0.014	0.02

*design-based CV values

Table 5.7. Reference abundance per year 1984-2013 for the optimal model and design-based model. Numbers are in millions of individuals.

Year	Optimal Model Reference Abundance	Design-based Model Reference Abundance
1984	101.665	105.158
1985	223.258	128.635
1986	252.132	146.381
1987	191.163	154.289
1988	159.179	147.811
1989	182.158	151.702
1990	248.393	171.712
1991	281.559	176.182
1992	265.169	180.269
1993	214.218	185.529
1994	202.525	179.969
1995	290.751	186.378
1996	322.812	210.048
1997	295.882	244.946
1998	258.476	253.434
1999	249.385	253.756
2000	255.233	261.687
2001	226.173	265.435
2002	194.663	274.046
2003	199.635	276.414
2004	163.176	247.395
2005	159.827	227.777
2006	193.893	234.428
2007	219.967	263.925
2008	214.323	305.328
2009	276.191	335.388
2010	352.746	366.041
2011	437.106	435.538
2012	456.487	499.419
2013	403.016	543.324

Table 5.8. Reference exploitation rate per year 1984-2013 for the optimal model and design-based model.

Year	Optimal Model Reference Exploitation Rate	Design-based Model Reference Exploitation Rate
1984	0.252	0.226
1985	0.279	0.197
1986	0.191	0.184
1987	0.229	0.182
1988	0.634	0.200
1989	0.218	0.202
1990	0.367	0.204
1991	0.378	0.216
1992	0.320	0.190
1993	0.412	0.184
1994	0.298	0.217
1995	0.287	0.205
1996	0.201	0.193
1997	0.325	0.212
1998	0.186	0.190
1999	0.119	0.206
2000	0.308	0.228
2001	0.130	0.189
2002	0.170	0.218
2003	0.171	0.204
2004	0.170	0.271
2005	0.127	0.260
2006	0.200	0.260
2007	0.169	0.218
2008	0.164	0.217
2009	0.170	0.225
2010	0.116	0.244
2011	0.147	0.223
2012	0.259	0.250
2013	0.341	0.239

5.5 Discussion

The modelled abundance indices all showed much lower CVs than the traditional indices. This accentuates the variance reduction property of the geostatistical delta-GLMM; modelled indices tend to be more reliable and precise compared to design-based indices when the population's spatial distribution is variable (Shelton et al. 2014; Thorson et al. 2015). However, these indices provided relatively small improvements to retrospective bias and moderate

worsening of model fit for the American lobster assessment model. This could be due to survey design and coverage of the population, which may be sufficient enough as to capture the variability caused by environmental covariates that this study was explicitly estimating (Yu et al. 2013; Thorson et al. 2015).

The retrospective patterns for SSB , R , and F showed the most improvement when depth alone was used in the delta-GLMM as a catchability covariate. The second best model (which still had better retrospective patterns compared to the design-based) used temperature as a density covariate and depth as a catchability covariate. Temperature has been shown to be an important indicator of lobster habitat in the GOM (Boudreau et al. 2015; Tanaka et al. 2019), which would account for its effect on population density. Lobsters migrate inshore during the summer months to spawn and feed and migrate offshore in the winter months to deeper waters (Uzmann et al. 1977). Lobsters feed less in the winter months when they are in deeper water (Ennis 1973), and are thus less prompted to seek out food, having an overall lower mobility and are generally more sheltered (McLeese & Wilder 1958; Ennis, G. 1973; Tremblay & Smith 2002): this could be why depth has an effect on lobster catchability.

It is important to note that even though incorporation of these variables improves retrospective patterns in the stock assessment, this is at the cost of decreased model fit. The disagreement between retrospective patterns and OFVs could point to robust survey designs that accurately capture changes in population density when spatiotemporal changes in catchability are accounted for. The American lobster stock in the GOM/GBK LME is unique compared to most other marine stocks. They are privileged with near-full spatial coverage of multiple fishery-independent surveys over a long time series (Chen et al. 2006b). These high-intensity sampling efforts seem capable of accurately tracking population changes over space and time independent

of explicit consideration of environmental effects. The strength of geostatistical models such as the delta-GLMM comes from their ability to extrapolate into low sampled areas and times using statistical assumptions of population densities and often using environmental covariates (Thorson et al. 2015). This ability appears fruitless with a well-surveyed species like American lobster, whose fine-scale population densities appear to be well-documented already from surveys that encompass both their inshore and offshore ranges (Chen et al. 2006b).

This study cannot conclude that the implementation of abundance indices that incorporate environmental covariates is necessary for the GOM/GBK American lobster stock assessment, even though the indices themselves appear to be made more precise by the process. It is assumed that the consideration of environmental covariates means an improvement over current methodology, especially considering the variance reduction of the delta-GLMM. However, this study concludes that more precise modelled abundance indices may not necessarily improve stock assessment if the survey(s) that inform the assessment are robust enough to capture changes caused by the covariates. Additionally, this appears to highlight that model-based abundance indices are not a preferable substitute over improvements to survey methodology.

The overall general trends of hindcasted reference abundance between the optimal and design-based model were similar, but the yearly variability in the optimal model was greater, causing the disagreements of fishery status in many of the years (Figure 5.4). Peculiarly, hindcasted exploitation rates between the optimal and design-based models were significantly different (Figure 5.5). This is also reflected in the higher Mohn's Rho value for F in the optimal model (Figure 5.2). These results highlight the need to conceptualize hindcasted "what-if" scenarios when comparing modelled products. If these new indices had historically always been

used in place of the design-based indices, there would have been drastically different changes in management of the fishery.

A similar approach should be followed for any target species or any stock assessment that utilizes fishery-independent abundance indices as assessment input. This framework has the potential to improve current abundance indices while incorporating environmental covariates and would mean little to no impact on current stock assessment model design. Environmentally informed abundance indices have been shown to improve current interpretations of survey catch rates in abundance index calculation in other studies (Hampton et al. 1998; Wilberg et al. 2009), but there exists a lack of explicit incorporation of these indices in stock assessments (Haltuch et al. 2009; Skern-Mauritzen et al. 2016).

As climate change affects global fisheries more and more, the need to determine its effects on populations becomes ever more crucial concerning assessment purposes (Hollowed et al. 2009; Maunder & Piner 2015). Environmental covariates can be utilized in stock assessments in areas other than abundance index calculation. For example, environmental covariates can be used in calculation of *SSB/R* relationships in both Ricker and Beverton-Holt models (Planque & Frédou 1999; Subbey et al. 2014), as well as for recruitment calculations directly (Tanaka et al. 2019). Time-variant growth as a function of environmental covariates has also been utilized (Holsman et al. 2016). The need to determine the necessity of these relationships in stock assessment models is not negated if results from the discussed framework prove the way they did for lobster. The results from the lobster case study could show a robust survey methodology (well-designed and well-monitored) that remains capable of accurately capturing population changes; not null relationships between lobster with temperature and depth. This is an important distinction.

The case study presented here with American lobster has demonstrated that well-surveyed species may not benefit from using geostatistical models like the delta-GLMM to track abundance, but actually may produce a hindrance and overall less reliable assessment model output. This conclusion will not be universal. Model-based abundance indices are not intrinsically better than design-based indices and should be tested for each species individually. Accepting modelled indices without appropriate testing/simulations is highly cautioned against. The necessity for modelled indices will shift with different species and different fisheries depending on whether these dynamics are already captured by other parameters and/or data in the assessment model indirectly. In order to appropriately determine this, a procedure similar to the framework outlined in this paper must be completed. This framework is one of many alternatives and remains relatively easy to employ in most species' assessment frameworks.

CHAPTER 6: COMPARISON OF STOCHASTIC AND THERMALLY EXPLICIT RECRUITMENT PROJECTIONS FOR GULF OF MAINE AMERICAN LOBSTER

6.1 Abstract

Whether to include environmental covariates in recruitment estimations has been debated for some time. Recent research suggests that life history strategy may be a deciding factor in determining species-specific requirements. American lobster (*Homarus americanus*) are an opportunistic species, having a relatively short pre-recruit survival window. Thus, thermal habitat has substantial and established effects on early development and mortality. To test whether inclusion of these effects in recruitment estimations leads to significant differences in stock forecasts, this study sees the novel implementation of a forecasting model for Gulf of Maine (GOM) lobster that can project future recruitment and subsequent total biomass under both stochastic and environmentally-explicit recruitment scenarios. Results indicate substantial differences in recruitment estimations, with rising thermal habitat fueling a temporally compounding effect that, if ignored, may lead to spurious stock assumptions and erroneous management measures. In contrast, when results are compared to the most recent lobster stock assessment, temperature alone as a covariate may overestimate recruitments. This study highlights the importance of testing the inclusion of environmental covariates in recruitment estimations and predictions.

6.2 Introduction

The need for environmentally explicit effects in the stock assessment process has been questioned and challenged for a long time (Xu et al. 2017). Foremost, a reliable process to determine effective relationships of environment to life history is often incredibly challenging, requiring large data sets (Plagányi et al. 2019). Even so, the possibility of spurious conclusions of

environmental impacts is often imminent (Haltuch et al. 2019), and the omission of these relationships has been argued for concerning species with typically gadoid life histories (Basson 1999, Haltuch et al. 2019). In those gadoid case studies, there was often no substantial impact to management when recruitment was environmentally informed in the stock assessment process (Basson 1999). However, in species with non-gadoid life histories (like many demersal fish and crustaceans), the incorporation of these covariates to inform life history, especially recruitment processes, has had clear benefits (Xu et al. 2017, Haltuch et al. 2019). Recruitment predictions for yellowtail flounder were shown to have improved with the addition of environmental covariates (Xu et al. 2017), and Haltuch et al. (2019) argues that life history processes are a deciding factor concerning whether or not inclusion of environmental effects on recruitment processes in stock assessment and forecasting is necessary.

Haltuch et al. (2019) postulates that species having opportunistic life history strategies and thus having relatively short pre-recruit survival windows, have better defined pressure of environmental covariates, like temperature, on recruitment processes. The incorporation of this force on early life histories usually can lead to better informed and more accurate recruitment predictions and stock forecasts (Haltuch et al. 2019). In extreme cases, lack of these environmental responses on recruitment processes can lead to overfishing and stock collapse (Tommasi et al. 2016). It is thus imperative to test these effects on a case-by-case basis (Haltuch et al. 2019).

American lobster (*Homarus americanus*) of the Gulf of Maine (GOM) have a life history strategy conducive of a small pre-recruit survival window associated with high mortality (James-Pirri & Cobb 2000), and are thus are a principal case study to test inclusion of environmental covariates on recruitment predictions. Warming waters have been directly linked with American lobster movements (Mills et al. 2013), growth (Staples et al. 2019), size-at-maturity (Aiken 1977;

Le Bris et al. 2017), mortality (Mills et al. 2013), and recruitment (Goode et al. 2019; Tanaka et al. 2019). Notwithstanding, lobster stock assessment has only recently begun to incorporate environmental effects in modelling (ASMFC 2020), but does not use temperature as a covariate to inform recruitment projections (ASMFC 2020).

Herein, we compare estimated biomass trends produced by a forecasting model for American lobster of the GOM with and without thermally informed recruitment dynamics to show the implicit risks of omission of key environmental influences in the forecasting process. Additionally, this represents the implementation of a novel stock forecasting model for American lobster in the GOM.

6.3 Methods

6.3.1 The Stock Assessment Model

The University of Maine Lobster Stock Assessment Model (UMM) is a seasonal, integrated, length-structured assessment model developed by Chen et al. (2005) and modified by ASMFC (2015). This model is used in the American lobster (*Homarus americanus*) stock assessment in the Northeast U.S.A. by the Atlantic States Marine Fisheries Commission (ASMFC 2015, 2020). The version used here was further modified by Tanaka et al. (2019). The UMM's internal population dynamics equation is:

$$N_{Y,S} = N_{Y,S-1} \times G_{Y,S} \times e^{-F_{Y,S} + M_{Y,S}} + R_{Y,S} \quad (6.1)$$

where $N_{Y,S}$ is a vector of lobster in each of 35 size bins in year Y and season S , G is the seasonal growth transition matrix, F is the seasonal fishing mortality value, M is the seasonal natural mortality value, and R is a vector of recruitment abundance to each size bin (Chen et al. 2005). There are a total of four seasons in the model: winter (January – March; $S = 1$), spring (April –

June; $S = 2$), summer (July – September; $S = 3$), and fall (October – December; $S = 4$). For more details of the model, see Chen et al. (2005), ASMFC (2015, 2020), Tanaka et al. (2019), or contact the Chen Lab at Stony Brook University. This model fits to input fishery-dependent and fishery-independent data to produce estimates of abundance/biomass over the time series 1984-2013 in each of four seasons and overall size bins (53 millimeters to 223 millimeters in 5 millimeter increments) as well as commercial spawning biomass, fishery selectivity, and fishing mortality.

6.3.2 The Forecasting Model

A lobster forecasting model was developed to work in tandem with the stock assessment model in section 6.2.1. This model uses terminal year abundance values from the UMM to iteratively produce seasonal abundance and recruitment estimates. The forecasting model's population dynamics equation follows that of the stock assessment model (equation 6.1). Here, $N_{Y,S}$ is estimated using a terminal value of the abundance vector from the UMM ($N_{Y,S-1}$). $G_{Y,S}$ is replaced with $G_{Y,S-4}$ and $M_{Y,S}$ is replaced with $M_{Y,S-4}$ from the UMM. Growth and maturity change over seasons, but not years and so these replacements ensure seasonal values of G and M match in the UMM and in the forecasts. In the forecasting model, $F_{Y,S}$ is calculated as:

$$F_{Y,S} = f_{Y,S} \times C \quad (6.2)$$

where C represents a vector of commercial selectivity across each of the lobster size bins estimated from the UMM and $f_{Y,S}$ is a user-defined value of seasonal fishing mortality that is constant across years. Recall that $F_{Y,S}$ is a vector of values over size bins, but $f_{Y,S}$ is a single point value. $R_{Y,S}$ can be estimated one of two ways in the model. Option one is a seasonal-based stochastic approximation around a mean and option two is a covariate-dependent prediction based on an environmentally dependent spawning biomass/recruitment relationship. In the model, $N_{Y,S}$ is

estimated 100 times before a final average is taken and a seasonal biomass in metric tons (mt) over the time series ($B_{Y,S}$) is calculated as:

$$B_{Y,S} = \sum \gamma N_{Y,S}^{\theta} \quad (6.3)$$

where γ and θ are coefficients of the traditional length-weight relationship taken from the UMM. In this study, $\gamma = -6.98$ and $\theta = 2.96$ (ASMFC 2015; 2020).

6.3.3 Forecasting Model Specifications

The UMM was run with the same model specifications as in Hodgdon et al. (2020) from 1984 through 2013. UMM settings can be found in the supplementary material (Table S6.1). The UMM was only run once and the same terminal year data for $N_{Y,S-1}$, $G_{Y,S-4}$, and $M_{Y,S-4}$ was used in both forecasting model scenarios. For each scenario, the forecast model was run for a total of 20 time steps, representing a total of five years each with four seasons from winter 2014 to fall 2018. In both forecasting model scenarios, $f_{Y,S}$ in equation 6.2 was kept constant as terminal year output from the UMM. That is, each of the four seasons iteratively kept the same value of $f_{Y,S}$ throughout the forecast in all runs of the model. This meant that any potential future effects from shifting fishing mortality would not affect results. Thus, the only difference in forecasting model starting values and the sole proprietor of any potential differences in output was the calculation of recruitment.

In scenario 1, $R_{Y,S}$ was randomly selected about a mean representative of the terminal five years of recruitment from the UMM:

$$R_{Y,S} = D(m(R_{T-4:T}), \sigma^2) \times P \quad (6.4)$$

$$P = \begin{cases} 0.000 & \text{for } S = 1 \\ 0.000 & \text{for } S = 2 \\ 0.667 & \text{for } S = 3 \\ 0.333 & \text{for } S = 4 \end{cases} \quad (6.5)$$

where D is the normal distribution truncated by upper and lower boundary probabilities of 0.975 and 0.025, respectively, with $\sigma^2 = 0.25$, $m(R_{T-4:T})$ is the mean recruitment of four years before the terminal year in the UMM ($T-4$) to the terminal year in the UMM (T), representing a mean of the final five years of recruitment calculation from the UMM, and P is the proportion of the yearly recruitment R_Y of each season S , with values changing across the four seasons as shown in equation 6.5.

In scenario 2, a thermally explicit spawning biomass/recruitment relationship for American lobster was described in Hodgdon et al. (*Submitted*). Hodgdon et al. (*Submitted*) determined a 3-5 year lagged relationship of spawning biomass to recruitment using two environmental covariates: the bottom temperature ($^{\circ}\text{C}$) during the season immediately following lobster biological recruitment (LM) and the bottom temperature ($^{\circ}\text{C}$) over the period from biological recruitment to fisheries recruitment (DM). These parameters were meant to capture effects of thermal habitat on early stage mortality and developmental mortality, respectively (Hodgdon et al. *Submitted*). These covariates (LM and DM) were used on an environmentally explicit Beverton-Holt equation to link spawning biomass and recruitment:

$$R_Y = \frac{\alpha \cdot SSB_{m(Y-3:Y-5)}}{(1 + \beta \cdot SSB_{m(Y-3:Y-5)})} \cdot e^{\delta_1 LM_{m(Y-3:Y-5)} + \delta_2 DM_{m(Y-3:Y-5)}} \quad (6.6)$$

where R_Y is recruitment of year Y (sum of all S), $SSB_{m(Y-3:Y-5)}$ is the spawning stock biomass averaged from years $Y-3$ to $Y-5$ (representing a lagged relationship of 3 to 5 years), and α , β , δ_1 , and δ_2 are coefficients (Subbey et al. 2014; Hodgdon et al. *Submitted*). Following the methods of

Hodgdon et al. (*Submitted*), this relationship was deconstructed into a generalized additive model (GAM) following the form:

$$\ln\left(\frac{R_Y}{SSB_{m(Y-3:Y-5)}}\right) \sim -\ln\left(\frac{1}{1 + SSB_{m(Y-3:Y-5)}}\right) + LM_{m(Y-3:Y-5)} + DM_{m(Y-3:Y-5)} \quad (6.7)$$

where \ln is the natural log.

To utilize this relationship in the forecasting model, LM and DM were calculated from environmental data taken from University of Massachusetts Dartmouth School for Marine Science and Technology's Finite Volume Community Ocean Model (FVCOM) (Chen et al. 2006a) and SSB values were taken from UMM output. The GAM was constructed in R and the *predict* function in the base R environment was used to iteratively estimate recruitment in the forecasting model.

6.3.4 Comparison of Forecasting Scenarios

Scenarios 1 and 2 seasonal biomass predictions $B_{Y,S}$ were compared using a d -bar analysis and a slope comparison analysis to determine differences in values and trends, respectively. For the d -bar analysis, the test statistic T_d was calculated as:

$$T_d = \frac{m(B_{1,Y,S} - B_{2,Y,S})}{sd(B_{1,Y,S} - B_{2,Y,S})/\sqrt{YS - 1}} \quad (6.8)$$

where $m(B_{1,Y,S} - B_{2,Y,S})$ is the mean of the paired differences between scenario 1 and 2 over all seasons S in all years Y (all consecutive time steps), $sd(B_{1,Y,S} - B_{2,Y,S})$ is the standard deviation of the paired differences between scenario 1 and scenario 2 over all seasons S in all years Y , and YS represents the number of total time steps in the forecast from winter 2014 to fall 2018 ($YS = 20$).

This test statistic was compared to the critical value $T_{d,Crit}(\alpha = 0.05; df = 19)$ and a p -value was calculated to determine significance.

For the linear slope comparison, the test statistic T_L was calculated as:

$$T_L = \frac{MB_{Y,S,1} - MB_{Y,S,2}}{\sqrt{SB_{Y,S,1}^2 - SB_{Y,S,2}^2}} \quad (6.9)$$

$$SB = \frac{se(B_{Y,S})}{sd(B_{Y,S})\sqrt{YS - 1}} \quad (6.10)$$

where $MB_{Y,S,1} - MB_{Y,S,2}$ is the difference in slopes of the seasonal biomass predictions between scenarios 1 and 2, $se(B_{Y,S})$ is the standard error of the predicted B values over the forecasted time series, $sd(B_{Y,S})$ is the standard deviation of the predicted B values over the forecasted time series, and YS represents the number of total time steps in the forecast from winter 2014 to fall 2018 ($YS = 20$). This test statistic was compared to the critical value $T_{L,Crit}(\alpha = 0.05; df = 36)$ and a p -value was calculated to determine significance.

Additionally, if the slope comparison determined significant differences between the scenarios, a subsequent analysis would be run called a shrinking-window slope analysis, which would determine if there was a compounding effect of changing slope over time. This analysis would follow the same procedure as in equations 6.9 and 6.10, but for forecasted years 1 through 4, 1 through 3, and 1 through 2. Changes in significance (p -values) in each would determine any compounding effects. Retrospective prediction patterns, like this shrinking-window slope analysis are strongly encouraged in comparison of environmentally informed forecasts (Xu et al. 2017).

6.3.5 Comparison to Stock Assessment

Recruitment data generated for both scenarios in the forecasting framework will be for years 2014-2018. The most recent lobster stock assessment model (ASMFC 2020) has model-generated recruitment data for this period. Therefore, a slope comparison analysis similar to what was outlined in section 6.2.4 will be used to compare recruitment time series between scenarios to the recruitment time series from ASMFC (2020). Here, absolute values matter less, as it is known the relative magnitude between the two model versions (ASMFC 2020 and Tanaka et al. 2019) differ. Trends, however, should be similar. The recruitment data from ASMFC (2020), even though they are model-generated, can be thought of “true” data and hence this comparison will allow for both a quantification of forecasting model accuracy and a way to determine which of scenarios 1 and 2 are more biologically realistic.

6.4 Results

American lobster (*Homarus americanus*) total biomass B values near the start of the forecasted time series were seemingly similar between scenarios, but became more spread over time. This difference is statistically significant as shown in Table 6.1, where $T_{d,Crit} < T_d$ and $p < \alpha = 0.05$. These differences appear to come from differences across years, whereas general population biomass patterns within a year, were very similar between scenarios.

Both scenarios in the forecasting model produced similar seasonal patterns over the time series 2014-2018 (Figure 6.1). In the winter and spring seasons, there is no recruitment and no growth. Thus, during this time, the only forces acting on the population are fishing and natural mortality. Hence, during this time, population levels fall. In the summer and fall seasons, there are molting events and recruitment events, both adding to the biomass of the population. However, natural mortality still persists and fishing mortality actually rises during the height of the fishing

year. The amount of mortality is seemingly overcome by growth and recruitment, as during the winter and fall months, the population biomass rises.

The trend over years for scenario 1 steadily declined at an average slope of $MB_1 = -2917.18$ mt/S, whereas the trend over years for scenario 2 steadily rose at an average slope of $MB_2 = 7498.59$ mt/S (Table 6.2). This difference in trends was also statistically significant, as evident in Table 6.1, where $T_{L,Crit} < T_L$ and $p < \alpha = 0.05$. The shrinking-window slope comparison retrospective analysis (Table 6.2; Figure 6.1) revealed that longer time series of forecasts led to total biomass B estimations that were higher in scenario 2 (Table 6.1). This is evident as the values of $T_L - T_{L,Crit}$ became larger and p -values became smaller as additional years were added to the forecast. There was constant significant differences in slopes, however, across all forecasted time series between scenarios. This indicates that the omission of temperature effects on recruitment consistently leads to an underestimation of total lobster biomass B , but that there also exists temporal amplification effects, where longer time series compound this difference, most likely due to the positive relationship lobster recruitment has with rising temperatures (Hodgdon et al. *Submitted*).

The recruitment predictions generated for both scenarios by the forecasting model were significantly different from those generated by ASMFC (2020) (Table 6.3). When slopes for scenarios 1 and 2 were rescaled to match the range of ASMFC (2020), scenario 1 had a smaller rescaled slope, whereas scenario 2 had a larger rescaled slope (Table 6.4). Recruitment data from ASMFC (2020) had more year-to-year variation in the recruitment pattern; noise generated from complex real-world patterns affecting recruitment beyond temperature (Figure 6.2). This may indicate that the addition of temperature in recruitment predictions increases the overall recruitment trend, but that factors other than temperature lower this trend and produce more variation, leading to the recruitment pattern seen in ASMFC (2020) (Figure 6.2).

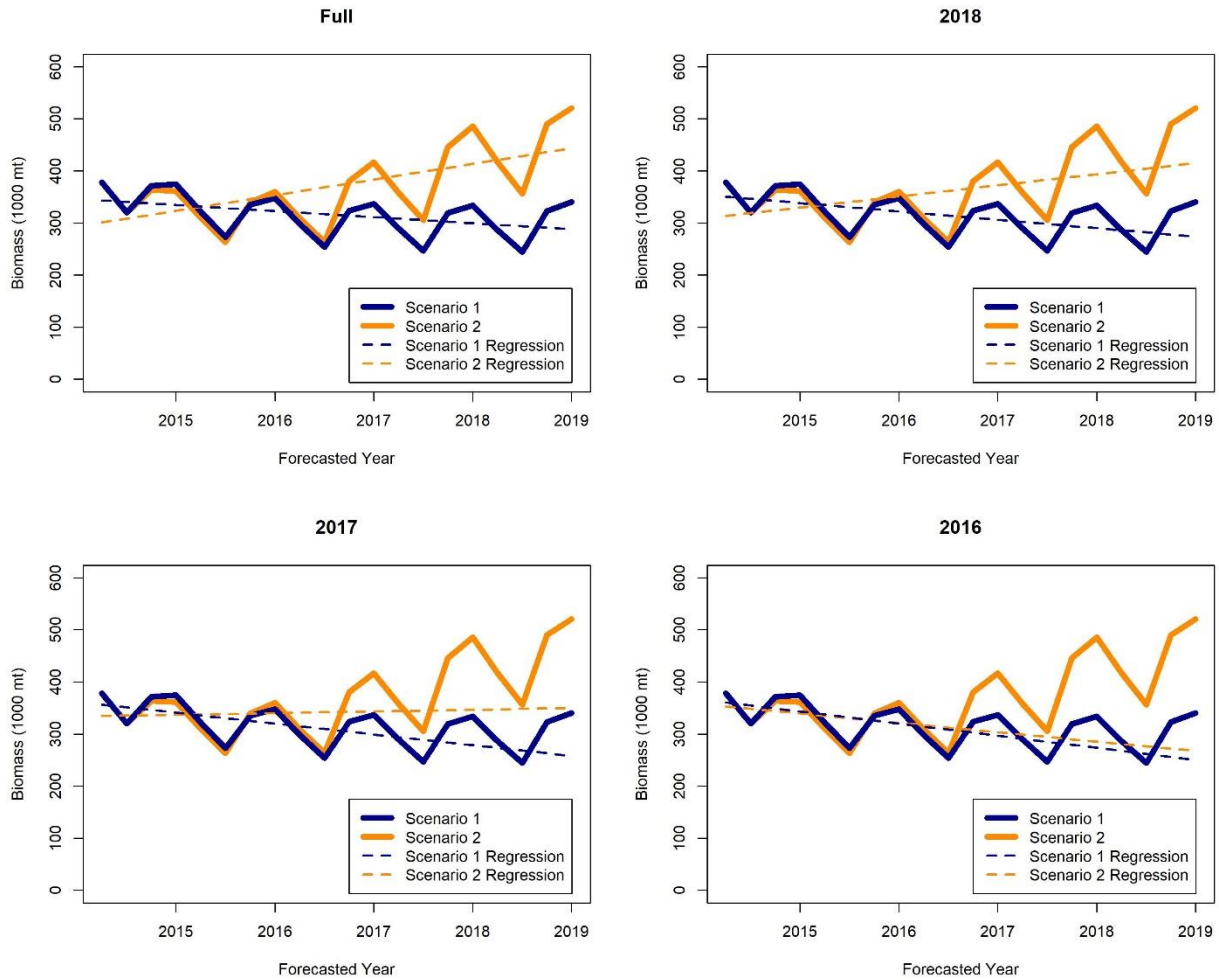


Figure 6.1. Predicted total lobster biomass B estimates in 1000 metric tons (mt) from the forecasting model produced under scenario 1 (orange) and scenario 2 (blue). Seasonal estimates for each scenario (solid lines) are consistent between all four plots, but linear regressions for each scenario (dotted lines) vary according to the shrinking-window slope analysis. Each plot title denotes the terminal year of the forecast that was used to produce the accompanying linear regression lines. For more information, see section 6.2.4 or Table 6.2. Tick marks of year denote the start of that year.

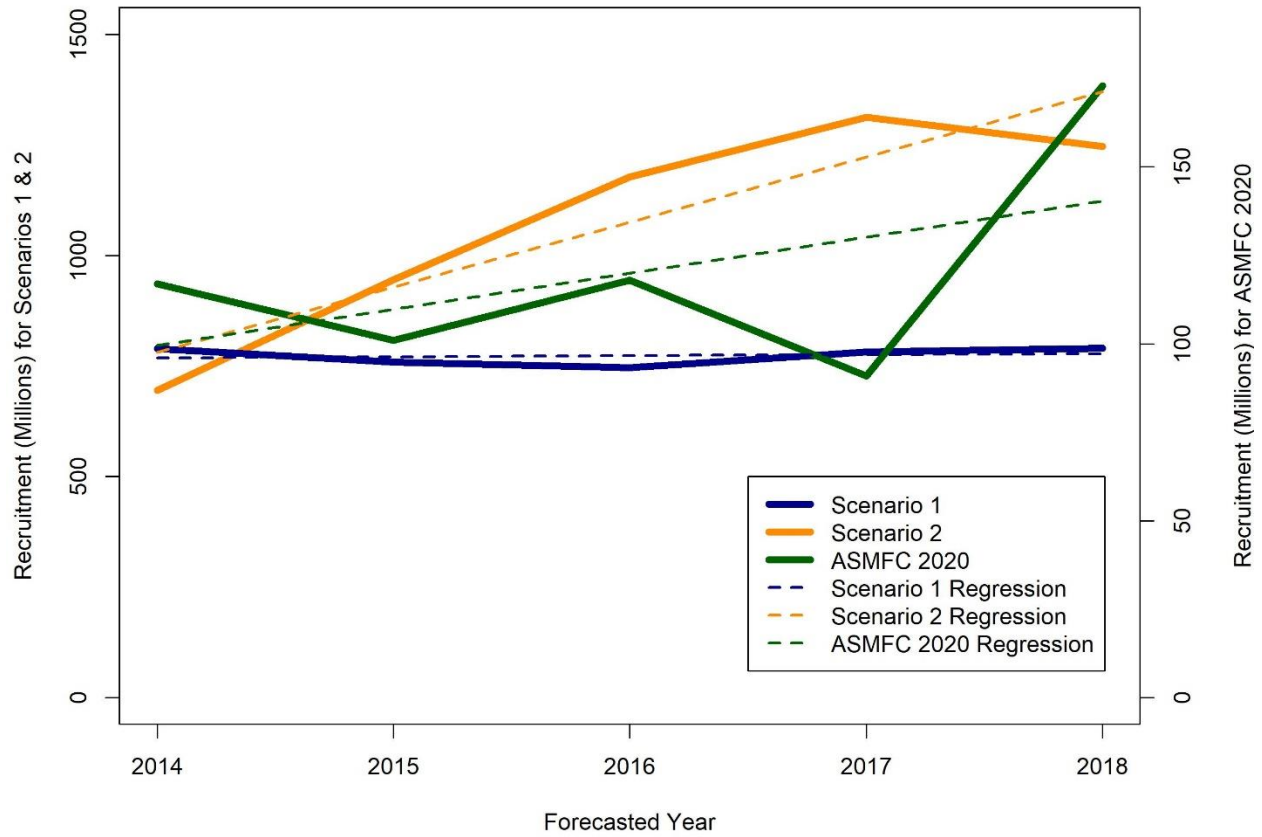


Figure 6.2. Predicted lobster recruitment (millions) from the forecasting model produced under scenario 1 (orange) and scenario 2 (blue) and for the recruitment time series generated in ASMFC (2020) (green). Yearly values are solid lines and linear regressions are dotted lines. Note the different axes for the scenarios (left) and ASMFC (2020) (right).

Table 6.1. Test statistics from the d -bar analysis and slope comparisons. The d -bar analysis was done to compare calculated biomass B values over the time series between scenarios 1 and 2. The slope comparisons were done to compare linear slopes MB between scenarios 1 and 2. Slope Comparison Full was an analysis comparing the slopes between scenarios 1 and 2 of a linear regression of biomass B over all seasons in all years of the forecast for a total of 20 data points. Slope Comparison 2018 did the same, but only for the first four years of the forecast (16 data points). Slope Comparison 2017 did the same, but only for the first three years of the forecast (12 data points). Slope Comparison 2016 did the same, but only for the first two years of the forecast (8 data points). In the d -bar and all Slope Comparison analyses, the critical values ($T_{d,Crit}$ and $T_{L,Crit}$ for the d -bar analysis and slope comparison, respectively) were smaller than the test statistics (T_d and T_L for the d -bar analysis and slope comparison, respectively), meaning that the values and trends between scenarios were statistically different. Significance levels are shown below using approximations of p -values. When terminal years were removed from the forecast in the consecutive slope comparison analyses, the significance lowered as the difference between $T_{L,Crit}$ and T_L became smaller and smaller and the p -value became higher and higher.

Test	Test Statistic	Value	Statistical Significance
d -bar	T_d	3.891	Yes
	$T_{d,Crit}$	2.861	
	p -value	0.001	
Slope Comparison Full	T_L	35.939	Yes
	$T_{L,Crit}$	2.028	
	p -value	< 0.001	
Slope Comparison 2018	T_L	29.816	Yes
	$T_{L,Crit}$	2.048	
	p -value	< 0.001	
Slope Comparison 2017	T_L	13.644	Yes
	$T_{L,Crit}$	2.086	
	p -value	< 0.001	
Slope Comparison 2016	T_L	2.211	Yes
	$T_{L,Crit}$	2.179	
	p -value	0.047	

Table 6.2. Slopes MB in 1000 metric tons of biomass B per season s for both scenarios. “Full” are the slopes of a linear regression of biomass B over all seasons in all years of the forecast for a total of 20 data points. “To 2018” is the same, but only for the first four years of the forecast (16 data points). “To 2017” is the same, but only for the first three years of the forecast (12 data points). “To 2016” is the same, but only for the first two years of the forecast (8 data points).

Forecasted Time Series	Scenario 1	Scenario 2
Full	-2.92	7.49
To 2018	-4.03	5.33
To 2017	-5.18	0.80
To 2016	-5.78	-4.50

Table 6.3. Test statistics from the slope comparison analyses between each of scenario 1 and 2 with the recruitment data from ASMFC (2020). In both slope comparison analyses, the critical values ($T_{L,Crit}$) were smaller than the test statistics (T_L), meaning that the trends between each scenario and ASMFC (2020) were statistically different. Significance levels are shown below using approximations of p -values.

Test	Test Statistic	Value	Statistical Significance
Scenario 1 to ASMFC 2020	T_L	9.146	Yes
	$T_{L,Crit}$	2.447	
	p -value	< 0.000	
Scenario 2 to ASMFC 2020	T_L	223.352	Yes
	$T_{L,Crit}$	2.447	
	p -value	< 0.000	

Table 6.4. Slopes (millions/year) and rescaled slopes of forecasted recruitment from scenarios 1 and 2 compared to the slope of recruitment from ASMFC (2020).

Scenario	Slope	Rescaled Slope
Scenario 1	2.500	0.547
Scenario 2	147.100	19.397
ASMFC 2020	10.200	

6.5 Discussion

Including temperature effects in the American lobster (*Homarus americanus*) stock recruitment process does significantly change forecasted biomass estimations. These differences seem to be the result of a temporally compounding effect that continuously underestimates recruitment predictions in an environmentally-independent scenario. These relative improvements seem to support Haltuch et al. (2019): lobster have a well-defined environmental pressure on early life stage development and mortality (Wahle & Steneck 1991, James-Pirri & Cobb 2000) and thus recruitment estimations appear to more heavily rely on environmental covariates. These results are also in accordance with results from Tanaka et al. (2019), which shows that environmentally-explicit recruitment estimations in the lobster stock assessment model were higher than those without environmental impacts. Seasonally, trends between scenarios were similar, but the addition of temperature in the forecasting model seemed to off-balance the mortality/recruitment relation.

In the environmentally-independent scenario (scenario 1), the combination of fishing and natural mortality over the year outweighs the amount of recruitment in the summer and fall months and so the trend of biomass over years slowly declines. However, the opposite effect is seen when thermal habitat is considered in the recruitment estimations. Here, the recruitment sizes are large enough to outweigh the loss due to fishing and natural mortality and so the population steadily rises over time. Additionally, from the shrinking window slope analysis, it is seen that the trend early in the time series was downward, but became positive over time. This is most likely due to the rising temperatures over years in the model, increasing recruitment estimations each year in consecutive forecasted years. Atypically to many case studies (Brunel & Boucher 2007), climate change appears to benefit the GOM lobster stock by increasing recruitment sizes.

This peculiar relationship is not unique to this study. Other studies of GOM lobster have shown similar conclusions that rising temperatures may lead to overall higher recruitment sizes and a larger range of suitable habitat (Goode et al. 2019, Tanaka et al. 2019). Hence, the lack of environmental covariates on recruitment estimations may not lead to overfishing (Tommasi et al. 2016), but rather may be the more cautious approach for GOM lobster. Yet, the cautious approach is not always the superior approach concerning fisheries management (Walters 1998). One of the most managerially crucial findings of this study is the temporally compounding effect. In iterative estimations of recruitment, the rising temperatures of the GOM seem to further divide recruitment and total biomass estimations from the environmentally-independent scenario perpetually. The longer the time series of the forecast, the more dangerous it becomes to accept results from the environmentally-independent model. Over enough time, those estimations become less meaningful and increasingly spurious. In this study, the environmentally-independent forecasts are more conservative. However, this does not mean they are more accurate.

Perhaps the most confounding result of the study is that both scenarios were significantly different from the recruitment estimated by the latest lobster stock assessment (ASMFC 2020). The trend of recruitment 2014-2018 from ASMFC (2020) showed an increasing trend over time with a lot of noise. Both scenarios in this study had less noise, but differed in their relation to these “true” recruitment estimates, with scenario 1 having a smaller relative slope, and scenario 2 having a larger relative slope. The noise in the ASMFC (2020) recruitment data alludes to more complex environmental relationships than what was used for forecasting in this study. Spatiotemporal fluctuations in predator-prey interactions, changing abiotics such as salinity at depth, and of course shifting fishing pressures will all impact the lobster stock (ASMFC 2015, 2020, Boudreau et al. 2015, Hodgdon et al. 2020), but these effects were not accounted for in this study. Perhaps then, it

is reasonable to suggest that the combined effects from these covariates would have a negative impact on recruitment estimates than just temperature alone because just this solitary variable seemed to overestimate recruitment. Evidently, there are many variables impacting fisheries recruitment estimations for GOM lobster (Chang et al. 2010, Goode et al. 2019, Tanaka et al. 2019, Hodgdon et al. 2021). Accounting for none of these will yield relatively static stochastic estimations (scenario 1) which under-predict “true” recruitment values. However, due to the net positive effect of rising temperatures on recruitment estimations for lobster, including temperature alone as a predictive covariate (scenario 2) may overestimate recruitment values. This study therefore cannot conclude which scenario is more appropriate for management use, only that the most realistic forecasts for lobster recruitment lie somewhere between the two scenarios tested.

Additional future research should target spatial relationships and the inclusion of additional covariates in estimations. Spawning biomass/recruitment estimations for lobster have been proposed to be spatially explicit (Xue et al. 2008, Chang et al. 2015), but the relationship used in this study is stock-wide so as to be incorporated into the stock assessment process (which is itself not spatially explicit). Regardless, spatially explicit forecasted recruitment estimations have the potential to improve prediction capacity and reveal more detailed spatiotemporal trends in the temperature-recruitment process. As previously stated, additional variables other than thermal habitat may affect recruitment estimations for GOM lobster. A framework that includes other environmental effects on both recruitment estimations and other aspects of the stock assessment and forecasting processes in combination with more complex spatiotemporal relationships have the potential to greatly enhance lobster assessment in the GOM.

Inclusion of environmental covariates in recruitment estimations for GOM lobster revealed significant differences in forecasted stock estimations, but inclusion may overestimate true

recruitment patterns whereas exclusion may under-estimate true recruitment patterns. This conclusion highlights the need for further research on lobster-environment relationships. Furthermore, there is a significant need to test inclusion of environmental covariates on many individual species recruitment estimations (Haltuch et al. 2019), but it may be more difficult. American lobster are a well-studied, well-surveyed, relatively data-rich species (Chen et al. 2006b, ASMFC 2015, Hodgdon et al. 2020), meaning that determination of environmental covariates in the recruitment estimation process may be more challenging for other species with less data (Plaganyi et al. 2019). However, given the ever-changing world these species live in, there is a serious urgency to test inclusions on a case-by-case basis (Haltuch et al. 2019).

CHAPTER 7: CONSEQUENCES OF MODEL ASSUMPTIONS WHEN PROJECTING HABITAT SUITABILITY: A CAUTION OF FORECASTING UNDER UNCERTAINTIES

7.1 Abstract

Climate change is continuing to influence spatial shifts of many marine species by causing changes to their respective habitats. Habitat suitability as a function of changing environmental parameters is a common method of mapping these changes in habitat over time. The types of models used for this process (e.g. bioclimate models) can be used for projecting habitat if appropriate forecasted environmental data are used. However, the input data for this process must be carefully selected as less reliable results can incite mis-management. Thus, a knowledge of the organism and its environment must be known a priori. This paper demonstrates that these assumptions about a species' life history and the environment are critical when applying certain types of bioclimate models that utilize habitat suitability indices. Inappropriate assumptions can lead to model results that are not representative of environmental and biological realities. Using American lobster (*Homarus americanus*) of the Gulf of Maine as a case study, it is shown that the choice of extrapolation data, spatial scale, environmental parameters, and appropriate subsetting of the population based on life history are all key factors in determining appropriate biological realism necessary for robust bioclimate model results.

7.2 Introduction

With the continuing pressure of global climate change, many species have adapted by shifting their distributions to new habitats that provide conditions within tolerable limits behaviorally and physiologically (Perry et al. 2005; Hazen et al. 2012; Anderson et al. 2013; Shuetz et al. 2018). This adaptation has caused cascading effects like altering predator and prey

interactions (Stebbing et al. 2002), causing local extirpation due to habitat reduction (Mantyka-pringle et al. 2011) and modifying fisheries and dependent communities (Engelhard et al. 2013; Rogers et al. 2019). The pace of climate change is not expected to abate in either the world ocean (Hayhoe et al. 2017) or in the context of the US Northeast Continental shelf (Saba et al. 2016), the study system of this analysis. Therefore, it is instructive for both current and future management planning to examine the predicted changes in habitat associated with ecologically and economically important species.

A commonly used method for projecting species habitat is a bioclimate envelope model, known variously as a bioclimate model, habitat suitability index (HSI) model, or simply habitat model (Mbogga et al. 2010; Watling et al. 2013; Tanaka and Chen 2016; Xue et al. 2017). There is still much variability in these models, but this study focuses on the type of model used in Tanaka and Chen (2015; 2016) that relies on relationships of target species abundance to environmental and biological variables to calculate what are known as suitability indices (SIs). SIs represent ranges of suitability of a specific habitat condition (e.g., temperature) on a scale of zero (unsuitable) to one (optimally suitable) (McMahon 1983; Xue et al. 2017). HSIs can be estimated from an average of SIs of the environmental and biological variables considered (McMahon 1983; Xue et al. 2017). Like SIs, HSIs vary over both space and time with changing conditions and are on a scale of zero to one. However, HSIs differ from SIs in that they represent the total suitability of a given habitat (McMahon 1983; Franklin 2010). Using environmental data at the appropriate temporal and spatial resolution, changes of HSI over both space and time can be estimated (Tanaka & Chen 2016). This creates a bioclimate envelope or a distribution of suitable habitat for a given species (Cheung et al. 2009; Tanaka & Chen 2016). With predictable relationships over time and space between target species and environmental/biological conditions, bioclimate envelopes in the

future can be predicted from forecasted conditions (Lawler et al. 2009), which can be used to infer changes in species distributions.

Within this modeling framework there are many assumptions about environmental and biological conditions, predictors, and life history of the target species that must be considered (Roloff & Kernohan 1999; Luoto et al. 2005; Huntley et al. 2010; Xue et al. 2017; Shuetz et al. 2018). These considerations take the form of deciding the type of environmental data used, determining the necessary environmental covariates, appropriate spatial/temporal coverage, and whether results are applicable to the entire population or only specific age/length subsets. These decisions and assumptions should be made so as to be most representative of the natural setting: a biological and environmental reality that is assumed true by the researcher a priori. This is important as there are issues with model fitting that can lead to overly optimistic characterizations of model performance (i.e. model uncertainties). Unrealistic assumptions can often lead to what appear to be reliable and robust predictions, but are not representative of the natural setting (Kuparinen et al. 2012). Sacrificing biological realism for model performance can undermine forecasting accuracy and predictive capacity (Luoto et al. 2005), potentially leading to inappropriate management actions. This study focuses on how changes in these assumptions can influence habitat modelling and forecasting.

The Gulf of Maine region (GOM; Figure 7.1), comprised of the Gulf of Maine and Georges Bank, has a highly dynamic marine climate characterized by annually fluctuating environmental conditions (Durbin et al. 2003; Wanamaker et al. 2008) with significantly increasing trends in bottom temperature and salinity in the last few decades (Mills et al. 2013; Pershing et al. 2015; Saba et al. 2016). The GOM also represents a hotspot of climate change with one representation of temperature change suggesting it is among the most rapidly warming ecosystems globally

(Pershing et al. 2015). Another key feature of the GOM is its eastern and western dynamics, which give way to differential localized oceanographic conditions (Mountain & Manning 1994; Townsend et al. 2014).

This dynamic ecosystem is an essential habitat of the American lobster (*Homarus americanus*), supporting the most valuable single-species fishery in the United States (NMFS 2018). This species is an ectothermic and eurythermic benthic crustacean native to coastal Canada and the United States in the North Atlantic Ocean (Spees et al. 2002). Even with its eurythermic physiology, climate change is partly responsible for the large decline of this species in Southern New England (SNE), severely depleting a once great fishery (Howell 2012; ASMFC 2015). With increasing temperatures in the GOM, the specter of change to the lobster population looms large for both fishers and the regional economy. There is recent evidence of change for the GOM lobster population in response to environmental conditions including effects on their seasonal movement timing (Mills et al. 2013), molting events (Staples et al. 2019), natural mortality (Mills et al. 2013), recruitment (Goode et al. 2019; Tanaka et al. 2019), and suitable habitat availability (Tanaka and Chen 2016; Goode et al. 2019; Friedland et al. 2020; Mazur et al. 2020).

In this study, relationships between lobster survey catch and environmental conditions were used to estimate and forecast lobster habitat suitability using a bioclimate model under a future warming schema. Furthermore, this study employs the use of “what-if” scenarios in an attempt to determine how changes in assumptions concerning 1) the type of environmental data, 2) key environmental covariates, 3) spatial coverage, and 4) subsets of the input data based on life history can influence bioclimate modelling and forecasting and by extension, management.

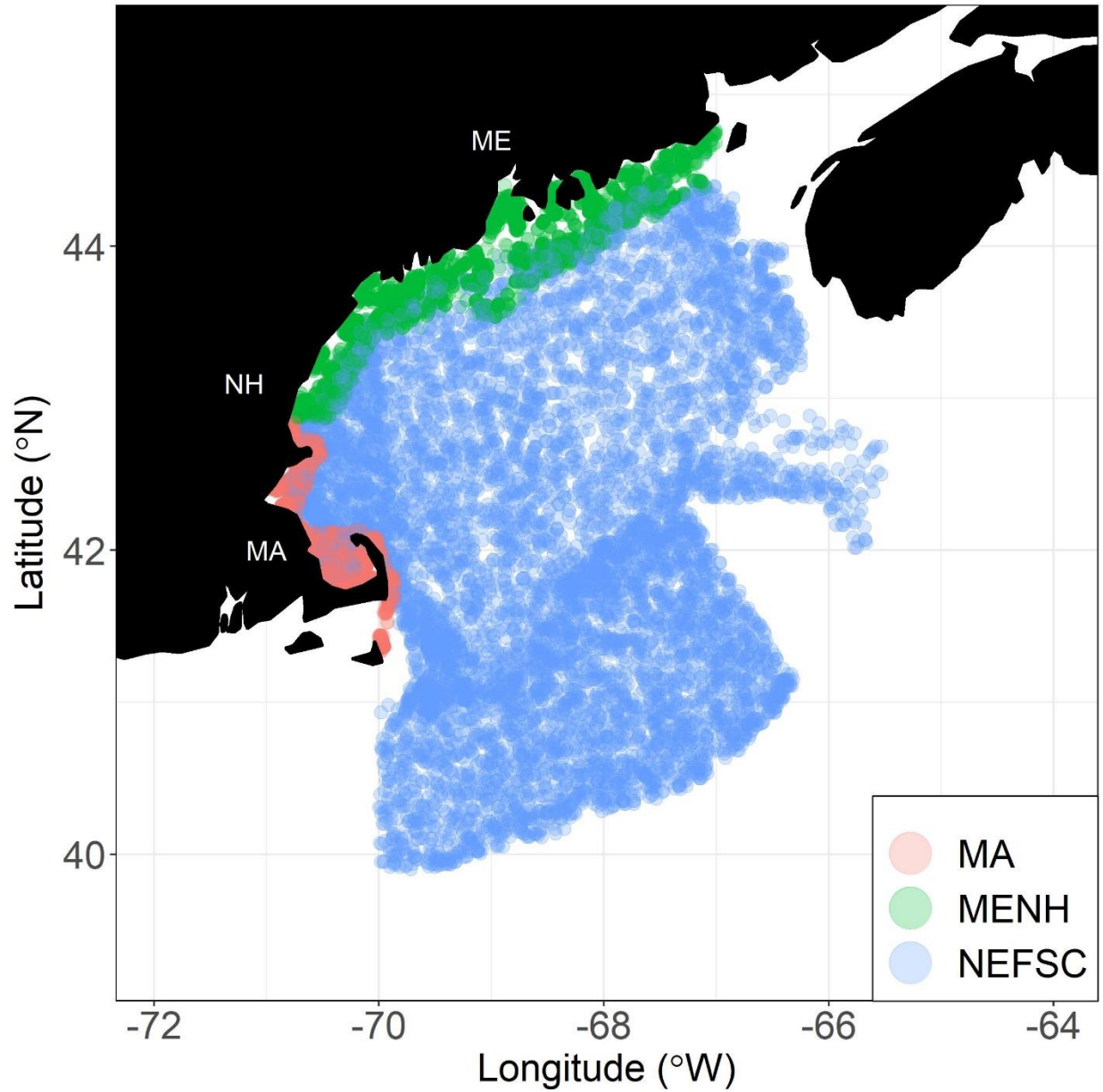


Figure 7.1. The Gulf of Maine with trawl survey stations of the Massachusetts Division of Marine Fisheries' Inshore Bottom Trawl Survey (MA), the Maine Department of Marine Resources and New Hampshire Fish and Game Department's Inshore Bottom Trawl Survey (MENH), and the NOAA Northeast Fisheries Science Center's Bottom Trawl Survey (NEFSC).

7.3 Methods

7.3.1 Base Case: The Bioclimate Model

The bioclimate model used in this study was developed by Tanaka and Chen (2015; 2016). It can determine spatially explicit changes in habitat suitability over time from regional environmental conditions using relationships between lobster survey catch and environmental variables and extrapolating onto grids with environmental data independent of those used in determining the relationships.

American lobster habitat preferences change with season, size, and sex (Chang et al. 2010; Tanaka et al. 2016). Size and sex-specific lobster catch data were obtained from the Maine Department of Marine Resources and New Hampshire Fish and Game Department's Inshore Bottom Trawl Survey (MEDMR/NHFGD 2000-2006), the Massachusetts Division of Marine Fisheries' Inshore Bottom Trawl Survey (MADMF 1978-2016), and NOAA's Northeast Fisheries Science Center's Bottom Trawl Survey (NEFSC 1978-2016). While these surveys cover much of the habitat for lobster in the GOM, it is important to note that there is not complete coverage. These data are not in the public domain, but interested parties may contact the Chen Lab at the University of Maine or the respective agencies for inquiries concerning data availability. Each of these three surveys has a distinct spring (April-June) and fall (September-October) component. The spatial coverages of these surveys used can be seen in Figure 7.1. The MADMF 1978-2016 and NEFSC 1978-2016 surveys cover more southern regions as well, but only trawl locations in the GOM lobster stock area were used for subsequent analyses. Standardized survey catch data (i.e., survey abundance index) were separated by sex (male and female), season (spring and fall), and life stage (adult and juvenile). Lobsters 60 millimeters (mm) carapace length and larger were treated as

adults and all lobsters smaller than 60 mm were treated as juveniles. This length represents the minimum size-at-maturity (ASMFC 2015; 2020).

Environmental data were obtained from the University of Massachusetts Dartmouth School for Marine Science and Technology's Finite Volume Community Ocean Model (FVCOM) (Chen et al. 2006a; data publically available from <http://fvcom.smast.umassd.edu/fvcom/>). This geophysical model has been proven effective at estimating fine-scale environmental parameters for the GOM (Li et al. 2017). Bottom temperature and bottom salinity values were matched to each trawl location and time, referred to as a station. This was done so as to maximize the data used as some surveys did not record environmental data. These, along with temporally stationary parameters depth, latitude, and longitude, were each used to determine SIs for lobster in the GOM. Bottom temperature, bottom salinity, and depth represent significant influencers of lobster habitat and have been used in previous studies to map lobster HSI (Tanaka & Chen 2016). Latitude and longitude were used as proxies to potentially capture spatial effects from parameters not directly considered in this study.

First, a catch-per-unit-effort (*CPUE*) value, treated as a nominal abundance index, was calculated for each combination of sex and life stage in a sampling instance:

$$CPUE = \frac{Count}{Width \times Length} \quad (7.1)$$

where *Count* is the number of lobsters caught, *Width* is the width of the trawl in meters, and *Length* is the distance trawled in meters. This process standardizes the index to units of “lobsters caught per square meter” and allows for direct comparisons between and within surveys.

Each of the five environmental variables were delineated into twenty classes (*k*) across the range present throughout the data using Fisher's natural breaks classification method (Tanaka et

al. 2015). SIs for each class k of environmental variable i for each combination of sex, season, and life stage were calculated as follows:

$$SI_{i,k} = \frac{CPUE_{i,k} - CPUE_{i,min}}{CPUE_{i,max} - CPUE_{i,min}} \quad (7.2)$$

where $CPUE_{i,k}$ is the average $CPUE$ across all trawl stations within class k of habitat variable i , $CPUE_{i,min}$ is the minimum average $CPUE$ value across all twenty classes of habitat variable i , and $CPUE_{i,max}$ is the maximum average $CPUE$ value across all twenty classes of habitat variable i . Generalized additive models (GAMs) were used to reduce bin-associated noise and create more realistic SI relationships. For each SI_i , a GAM was run with a single predictor variable (k), representing factorized bins. These GAMs were then used to predict SI values (GSI_i) for each bin k . Finally, HSI values were calculated using an arithmetic mean:

$$HSI = \sum_{i=1}^n GSI_i \quad (7.3)$$

where n is the total number of GSI_i s. Equal weights were applied to the GSI_i s to follow the methodology in Tanaka and Chen (2015; 2016) and thus assumptions of equal importance across variables were made.

7.3.2 Base Case: Input Data

Bottom temperature and bottom salinity anomalies for the GOM were obtained from the ensemble projection framework known as the Coupled Model Intercomparison Project 5 (CMIP5), data from which is publicly available through NOAA's Climate Change Web Portal (available from <https://psl.noaa.gov/ipcc/ocn/>). CMIP5 is an ensemble of many different climate forecasting models which together create climate projections used in the Intergovernmental Panel on Climate Change's 5th Assessment (IPCC 2019). CMIP5 anomalies are represented as changes in bottom

temperature and salinity in the future (2050-2099) in reference to the historical climate (1956-2005).

Historical fine-scale GOM bottom temperature and bottom salinity fields for spring (April-June) and fall (September-October) were obtained from FVCOM at points called stations. Values for each parameter for each station were temporally averaged from 1978-2005 to create the historical reference period used in this study. The upper bound of this reference period coincides with the upper bound of CMIP5 while the lower bound is representative of the earliest year of available FVCOM data. Depth, latitude, and longitude at each station were also obtained.

The anomalies were then used to estimate future bottom temperature and salinity fields through a downscaling process known as the delta method: a commonly used and robust statistical approach (Hare et al. 2012; Tanaka et al. 2020) shown to reduce bias in these types of estimations (Navarro-Racines et al. 2020). The anomaly fields were not as fine-scale as FVCOM data (anomaly fields are $1.0^{\circ} \times 1.0^{\circ}$), and so the anomalies were spatially interpolated using thin-plate splines to a grid size of $0.01^{\circ} \times 0.01^{\circ}$. Interpolated anomalies were then applied to the 1978-2005 FVCOM fields to calculate bottom temperature and salinity for both spring and fall for the period 2072-2099. These reference periods allowed for equivalent forecast lengths between CMIP5 and this study while also maximizing the amount of FVCOM data used. This process was done for Representative Concentration Pathway (RCP) 8.5, representing a “business-as-usual” future carbon emissions scenario.

This process yielded two fields of environmental variables: one for the historical reference period 1978-2005 and one for the future reference period 2072-2099 under RCP 8.5. Depth, latitude, and longitude were held constant throughout both fields; they were assumed not to change with warming effects over time. Lobster HSI values for each sex, season, and life stage were then

calculated for each field. This was done by employing equation 7.3 at each grid point in both fields, where SI values were determined from the environmental parameter values at that grid point. To reiterate, relationships of lobster abundance to each environmental covariate are determined from surveys in section 7.3.1 and SI values are predicted for each grid point using these relationships and the given values of those covariates associated with the grid points. Each HSI field was mapped using ordinary Kriging and average HSI, percent HSI > 0.20, percent HSI > 0.50, and percent HSI > 0.80 were calculated. These bounds represent habitat that is “Fair”, “Good”, and “Excellent”, respectively (McMahon 1983; Tanaka et al. 2019).

7.3.3 What-If Scenarios

A what-if scenario in the context of this study was an experimental simulation of the bioclimate model in which one aspect of the input data is altered from the base case (see sections 7.3.1 and 7.3.2). Thus, all changes made were to the calculation of SIs and extrapolation grids, not to our forecasting methodologies. The intent of these scenarios was to determine changes in model output and to infer larger possible effects on fisheries management. There were seven what-if scenarios tested in this study. A quick reference guide to the scenarios is shown in Table 7.1.

- *Scenario 1: Model-Generated vs. Interpolated Environmental Data.*

Model-generated environmental data are often used in HSI models, but interpolated data preserve the observational nature of sampled environmental data. This becomes increasingly important if models that produce environmental data are less than accurate. The interpolated environmental data in this study were based on a procedure described in Friedland et al. (2019; 2020). In this procedure, a kriged interpolation of annual data was combined with climatological data to estimate complete bottom temperature and bottom salinity fields, preserving the observational nature of the data. Most of the samples were

collected in the spring (February- April) and fall (September-November) with conductivity/temperature/depth (CTD) instruments. The spatial resolution of the data was 0.01 degrees. Interpolated bottom temperature and salinity took the place of FVCOM data as the extrapolation grid and were used as the historical reference period upon which CMIP5 data were used to estimate future climatologies. Due to observational data limitations, the historical reference period was shortened from 1978-2005 to 1992-2005 and subsequent future reference periods were shortened to match (2028-2055 to 2042-2055; 2072-2099 to 2086-2099). SIs in this scenario were calculated not from FVCOM data, but from observed values collected on the surveys at the time of the trawl instance. Thus, observational or interpolated data replaced modelled data throughout the process.

- *Scenario 2: Full vs. Partial Spatial Coverage of Survey Data.*

Fisheries stocks can occupy multiple locations, environments, and habitats, making spatial scale an important factor for calculating species-environment relationships (Roloff & Kernohan 1999; Barry & Elith 2006; Gaillard et al. 2010). In the base case, the three bottom trawl surveys were used in unison: data from all three surveys were used to estimate SIs. In this scenario, surveys were split into inshore surveys (MEDMR/NHFGD 2000-2006 and MADMF 1978-2016) and the offshore survey (NEFSC 1978-2016). Inshore and offshore surveys were used to estimate separate SIs and those SIs were then extrapolated to the entire stock area (e.g. inshore SIs were used to map HSIs both inshore and offshore). The intent of this scenario was to test whether the full range of environmental relationships is sufficiently captured with less spatial coverage and to examine the consequences of applying potentially localized relationships to a larger stock area.

- *Scenario 3: Stock-wide vs Species-wide Suitability Indices.*

The base case of this study is for the GOM, which represents a unit stock area for American lobster (ASMFC 2015). In the US, American lobster are effectively considered two stocks in assessment and management: the GOM and SNE, which extends as far south as North Carolina. These two stocks are treated separately in the American lobster stock assessment due to various apparent differences in population dynamics (ASMFC 2015), yet they remain of the same species. This scenario calculated SIs for the species range in the US, but then applied those SIs to calculate HSIs for the GOM stock. To accomplish this, four additional bottom trawl surveys were utilized: the Rhode Island Department of Environmental Management's Coastal Trawl Survey (RIDEM 1981-2016), the Connecticut Department of Energy and Environmental Protection's Long Island Sound Trawl Survey (CTDEEP 1984-2016), the New Jersey Department of Environmental Protection's Trawl Survey (NJDEP 1988-2016), and the Virginia Institute of Marine Science Northeast Area Monitoring and Assessment Program (NEAMAP 2007-2016). Following the methods in section 7.3.1, these surveys were standardized to be appropriately used and compared to the three surveys in the base case. Additionally, all trawl stations of MADMF 1978-2016 and NEFSC 1978-2016 were utilized; not just those that appeared in the GOM stock area, as was done in the base case (see sections 7.3.1 and 7.3.2). The intent of this scenario was to examine the consequences of applying species-wide habitat preferences to a subset of the population.

- *Scenario 4: Inclusion vs. Exclusion of Important Components of Habitat.*

One of the most common mistakes in habitat modelling is the exclusion of parameters that may be important in determining habitat suitability for a given species simply due to limited knowledge and understanding of the natural processes (Schuetz et al.

2018). For lobster, it is well known that temperature is a driving factor in determining habitat suitability (Tanaka and Chen 2016; Goode et al. 2019; Friedland et al. 2020; Mazur et al. 2020). For this scenario, temperature was removed from all stages of the analysis and only bottom salinity, depth, latitude, and longitude were used to estimate HSIs. This addresses the consequences of removing a variable whose importance is already well established to infer how HSI estimation and forecasting changes while missing key predictors.

- *Scenario 5: Seasonal vs. Annual Suitability Relationships.*

Species' environmental preferences can change throughout a year with seasonal differences in diet, sexual activity, or other behaviors (Crance 1986; Mäki-Petäys et al. 1997), and this has even been shown to be true for lobster (Chang et al. 2010; Tanaka et al. 2016). In this scenario, this assumption was ignored: SIs were determined per combinations of sex and life stage, but not per season. Subsequently, grids of environmental variables used for extrapolation of HSIs were annual as well. SI data only exist April-June (spring) and September-October (fall) and thus it would be inappropriate to use a true annual extrapolation grid of environmental parameters. Instead, the grids used were an average of the environmental parameters in the spring and fall periods.

- *Scenario 6: Separate vs. Combined Sexes.*

Species' environmental preferences can shift with sex if there is a high degree of sex-specific specialization (Van Toor et al. 2011). Previous studies have shown differences in sex-specific distributions for lobster (Chang et al. 2010), potentially in relation to habitat selection due to suitable spawning grounds (Jury et al. 1994). In this scenario, males and females were not treated separately in the framework. Males and females were combined

into a single *CPUE* and so SIs were only calculated for separate life stages for each season. The intent of this change was to evaluate model effects when sex related preferences in habitat are not considered.

- *Scenario 7: Separate vs. Combined Life Stages.*

Many marine species such as lobster show differential habitat preferences related to life stage and overall size (Pratchet et al. 2008; Chang et al. 2010). For lobster, this is due in part to shifts in seasonal movement patterns in relation to functional maturity (Chang et al. 2010). In this scenario, adults and juveniles were combined into a single life stage and so SIs were only calculated for separate sexes for each season. The intent of this change was to evaluate model effects when life stage related preferences in habitat are not considered.

7.3.4 Bioclimate Model Comparative Diagnostics

Typical cross-validation procedures cannot be done using this type of model as there are no actual “observed” HSI values to calculate error metrics. Thus, an application of a relative difference was conducted wherein each combination of season, sex, and life stage of lobster in each what-if scenario and period was compared to the base-case for the same combination of season, sex, and life stage during the same period and a single value was calculated representing the difference across all grid points. In what-if scenarios where season, sex, or life stage were combined, results would be compared to two base cases of split data (e.g. combined seasons in scenario 5 were compared to base case results for spring and base case results for fall). Under this method, it is assumed that the base case results are the most “correct” compared to the other scenarios. Given that American lobster is one of the most heavily studied and surveyed fisheries

on the planet (Chen et al. 2006b; ASMFC 2015; Hodgdon et al. 2020), confidence in this assumption was relatively high. A spatially average difference metric was calculated as follows:

$$RMSE_S = \sqrt{\frac{\sum_{p=1}^G (HSI_{S,p} - HSI_{BC,p})^2}{G}} \quad (7.4)$$

where $RMSE_S$ is the root mean squared error of what-if scenario S (for a specific combination of season, sex, life stage, and period), $HSI_{S,p}$ is the HSI value for what-if scenario S at grid point p (for the same combination of season, sex, life stage, and period), $HSI_{BC,p}$ is the HSI value for the base case at grid point p (for the same combination of season, sex, life stage, and period), and G is the total number of grid points. Here, larger $RMSE$ values represent larger deviations of HSI of a given scenario to the base case.

Table 7.1. A list of all seven scenarios and how each one was altered from the base case. Note scenario 2 has two components. GOM: Gulf of Maine; SNE: Southern New England.

Scenario	Alterations from the Base Case
1	Observed (kriged) environmental data used instead of modelled (FVCOM) environmental data
2	Inshore surveys used to create SIs and extrapolate to entire GOM
	Offshore surveys used to create SIs and extrapolate to entire GOM
3	Additional surveys from SNE used to create SIs
4	Removed bottom temperature from analysis
5	Did not separate results by season
6	Did not separate results by sex
7	Did not separate results by life stage

7.4 Results

7.4.1 Suitability Indices

There were large differences in SIs between seasons and nearly negligible differences between sexes and life stages with most environmental variables for the base case (Figure 7.2). Due to these results, many SI curves (and subsequent HSI maps) were nearly identical. Thus, only spring and fall adult female SI curves are presented in the text and all other combinations of sex and life stage can be found in the supplementary material. Adult females were chosen to depict simply because this group most closely represents the spawning stock biomass of lobsters in the GOM and is thus a managerially important subgroup (ASMFC 2015; 2020).

Results from the base case suggest that lobsters prefer warmer waters in the fall as compared to the spring (Figure 7.2). This same relationship was present throughout all subsequent scenarios, except scenario 5 where seasons were combined (Figures 7.3-7.4). There were small differences between scenarios in the ranges of temperature used to create the suitability indices as well as some minor differences concerning smoothness of fit and location of peaks (Figures 7.3-7.4).

In the base case, lobsters also appeared to prefer saltier waters in the fall as compared to the spring (Figure 7.2). This relationship, however, may be affected by what appears to be a group of data points representing high catches of lobster at very high salinity levels causing a potentially unnatural spike in suitability at unreasonably high levels. This tie-up was present throughout most subsequent scenarios except when using offshore indices in scenario 2 and when using species-wide indices in scenario 3 (Figures 7.3-7.4). Throughout the scenarios, salinity SI was the most affected and had drastic changes in scenarios 1, 2, 3, and 5 when compared to the base case (Figures 7.3-7.4).

Concerning the base case again, lobsters preferred deeper waters in the fall as compared to the spring (Figure 7.2). In all scenarios, lobsters prefer waters shallower than 300 m, with their most suitable depths shifting from zero to about 150 m depending on the scenario and the season.

Latitude SIs in the base case and across the scenarios seem to be a reflection of the fact that more lobsters are caught in the inshore/northern GOM than the offshore/southern GOM (and by extension SNE), with the greatest SI values being in the northern reaches of latitude (Figures 7.2-7.4). Longitude SIs, however, seem to change with seasons and across scenarios more drastically than latitude does (Figures 7.2-7.4). The western areas appear to have higher SIs overall except when only the inshore areas are considered or when areas from SNE are considered (Figures 7.3-7.4). This highlights that there appears to be a large-scale lobster abundance dynamic over the species range, but also a small-scale dynamic, smaller than the GOM stock area.

7.4.2 Historical and Forecasted HSI

The anomalies for bottom temperature and bottom salinity from CMIP5 under RCP 8.5 together with depth and location data allowed for forecasted HSI for each combination of season, sex, and life stage from the historical reference period. HSI coverage statistics, representing the change over time of the spatial coverage of different levels of suitable habitat, are presented in Table 7.2 for the base case and spatial maps of these changes from the historical to the future period are given in Figure 7.5 for the base case. Spatial maps for all “what-if” scenarios are presented as differences to the spatial map of the base case to clearly portray where the scenario under and overestimates HSI (Figures 7.6-7.7). Following minimal differences in SI curves between sexes and life stages, there were trivial differences in the spatial maps. Thus, following the outline in section 7.4.1, spatial maps for spring and fall female adults are presented in the text

(Figures 7.6-7.7) and all other combinations of sex and life stage are presented in the supplementary material.

Considering the base case, inshore habitat (and Georges Bank to some extent) appeared more preferential than offshore habitat, with the highest HSI values found in the inshore eastern GOM (Figures 7.6-7.7). Additionally, spring had higher HSIs than the fall for all combinations of sex and life stage for both the historical reference period and the future scenario. Differences between sexes and between life stages appeared negligible: mimicking the relationships seen in the base case SI curves (Figure 7.2).

The trends discussed previously remained largely constant from the base case through the remaining scenarios, with each scenario causing small intuitive changes in HSI based on variables considered. Additionally, *RMSE* values varied between all combinations of season, sex, and life stage as well as across all scenarios for GOM lobster in hindcasts (Table 7.3) and forecasts (Table 7.4). Only significant deviations from the base case for each scenario will be discussed to focus on the most important outcomes.

Scenario 1 had strikingly similar spatial dynamics to the base case during the historical period, but forecasted changes appeared more spatially homogeneous. The spatially homogenous forecasts yielded *RMSE* values that were largest through all scenarios except for juvenile males in the spring (Table 7.4), displaying a stark contrast in projections between envelopes that utilize modelled and observed environmental data. Scenario 2 inshore/offshore dynamics were not apparent, but there existed a stronger presence of an east-west dynamic when compared to the base case. *RMSE* values remained quite different as well when using inshore data to predict offshore (Tables 7.3 and 7.4). However, using offshore data to predict inshore yielded values closer to the base case: a phenomenon most likely due to the larger spatial coverage of the offshore versus

inshore surveys. The presence of more southern areas in scenario 3 seemed to cause an overestimation of habitat suitability in the GOM in comparison to the base case. *RMSE* values for this scenario displayed a seasonal dynamic (Tables 7.3 and 7.4), where this scenario was closer to realism in the spring than the fall. This may be due to closer resemblance of temperatures for the GOM and the southern Atlantic in the fall as opposed to the spring when GOM waters are colder. Not accounting for temperature underestimated GOM HSI in scenario 4, yet *RMSE* values remained relatively small across all seasons, sexes, and life stages. Ignoring season yielded somewhat “average” dynamics between fall and spring data, but *RMSE* values for scenario 5 show that this apparent averaging of the seasons may actually more closely resemble fall than spring. Ignoring sex and life stage appeared to have little effect and both scenarios (6 and 7) closely resembled the base case. Each of these had the lowest *RMSE* values as well; significantly lower than others in this study.

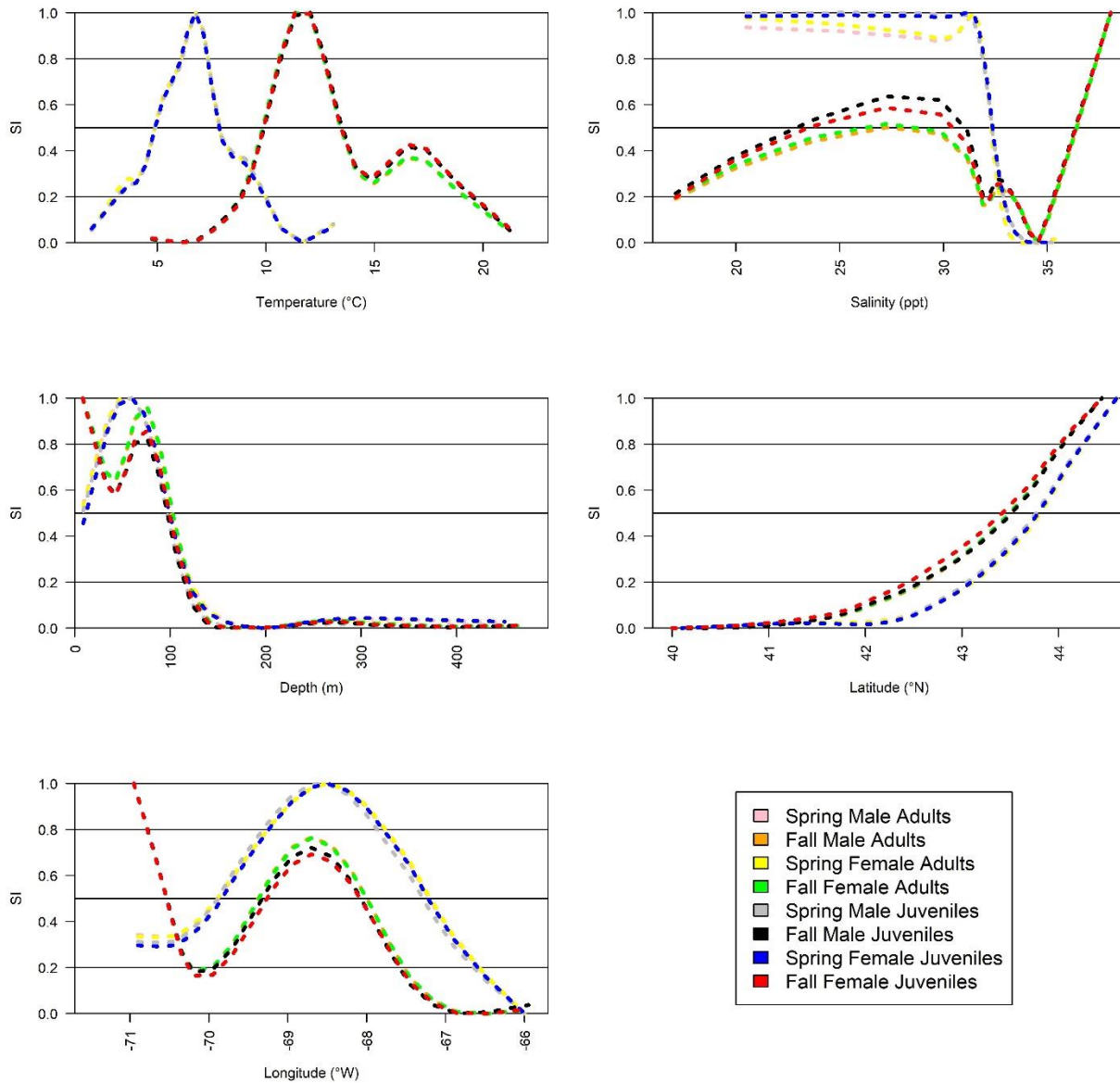


Figure 7.2. SIs of bottom temperature in degrees Celsius (top left), bottom salinity in parts per thousand (top right), depth in meters (middle left), latitude (middle right), and longitude (bottom left) to lobster of each combination of season, sex, and life stage. Also marked are SIs of 0.2, 0.5, and 0.8, representing values that are “Fair”, “Good”, and “Excellent”, respectively. Note that some lines are behind others; these “groups” seem to be for each season. Results are from the base case.

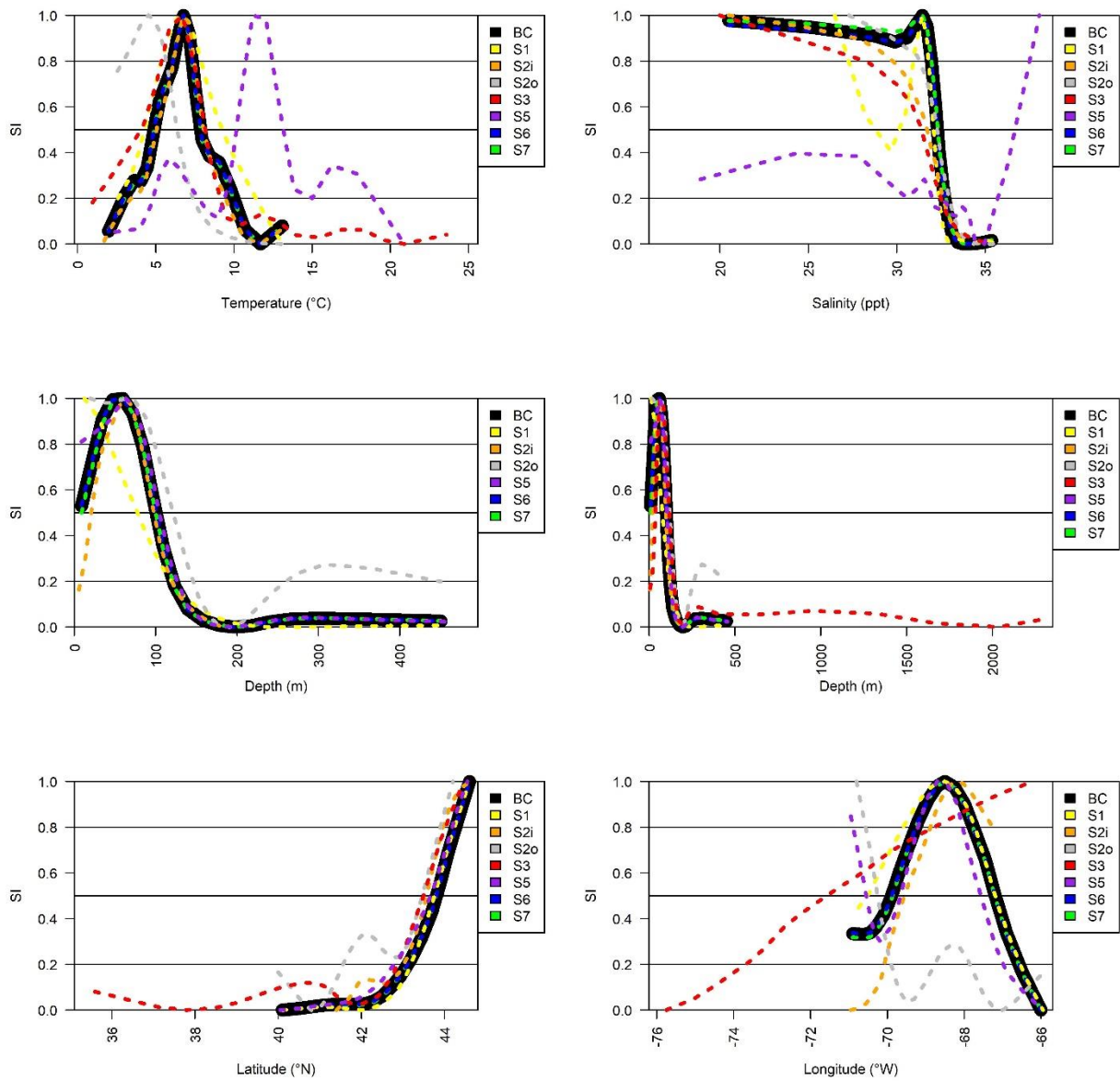


Figure 7.3. SIs for the base case and each scenario of bottom temperature in degrees Celsius (top left), bottom salinity in parts per thousand (top right), depth in meters with scenario 3 included (right) and without (right), latitude (middle right), and longitude (bottom left) to female adult lobsters in the spring. Note that scenario 4 SI curves are not presented as they are identical to the base case; only missing the temperature component. The base case is denoted as “BC”, and scenarios are listed as scenario 1 (S1), scenario 2 for inshore indices (S2i), scenario 2 for offshore indices (S2o), scenario 3 (S3), scenario 5 (S5), scenario 6 (S6), and scenario 7 (S7). Also marked are SIs of 0.2, 0.5, and 0.8, representing values that are “Fair”, “Good”, and “Excellent”, respectively.

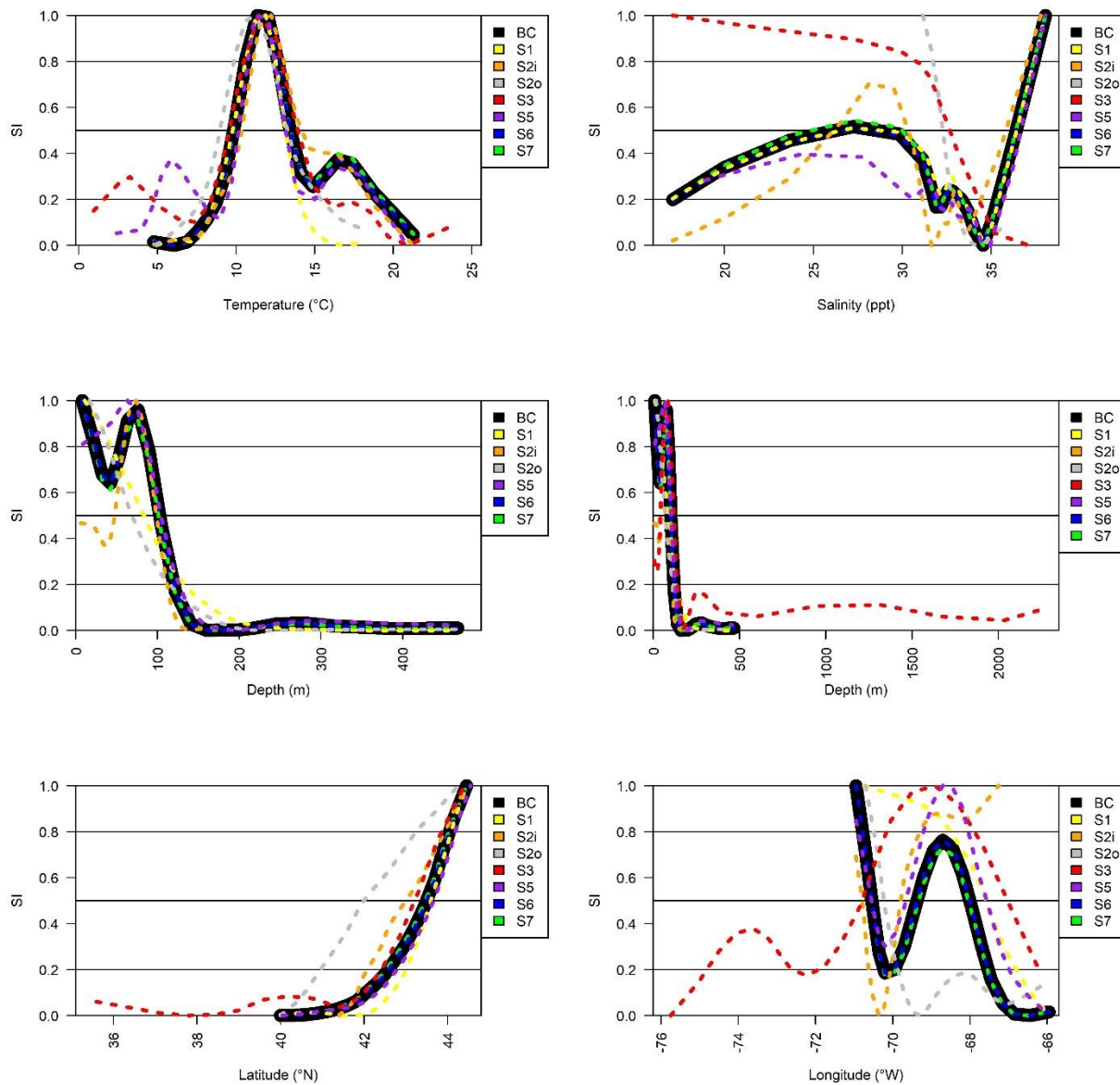
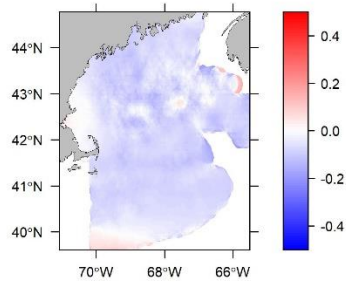
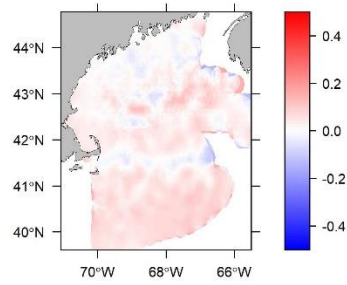


Figure 7.4. SIs for the base case and each scenario of bottom temperature in degrees Celsius (top left), bottom salinity in parts per thousand (top right), depth in meters with scenario 3 included (right) and without (left), latitude (bottom left), and longitude (bottom right) to female adult lobsters in the fall. Note that scenario 4 SI curves are not presented as they are identical to the base case; only missing the temperature component. The base case is denoted as “BC”, and scenarios are listed as scenario 1 (S1), scenario 2 for inshore indices (S2i), scenario 2 for offshore indices (S2o), scenario 3 (S3), scenario 5 (S5), scenario 6 (S6), and scenario 7 (S7). Also marked are SIs of 0.2, 0.5, and 0.8, representing values that are “Fair”, “Good”, and “Excellent”, respectively.

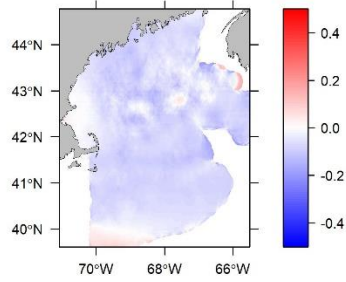
Sp Ma Ad Change in HSI = -0.046



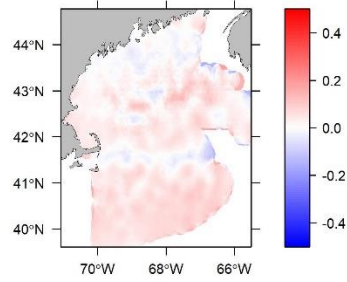
Fa Ma Ad Change in HSI = 0.042



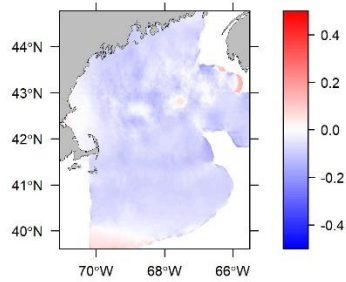
Sp Fe Ad Change in HSI = -0.046



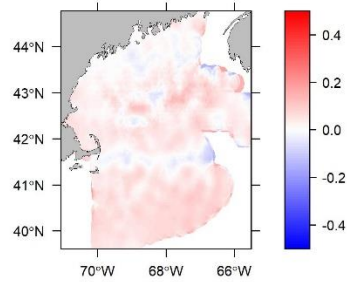
Fa Fe Ad Change in HSI = 0.043



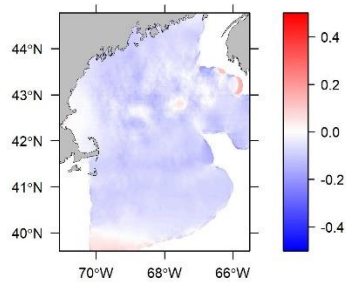
Sp Ma Ju Change in HSI = -0.046



Fa Ma Ju Change in HSI = 0.045



Sp Fe Ju Change in HSI = -0.048



Fa Fe Ju Change in HSI = 0.045

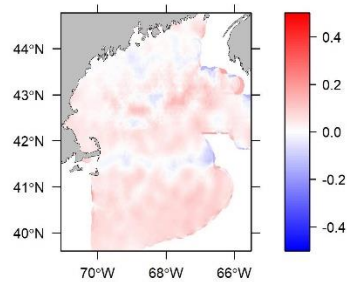


Figure 7.5. Change in spatial HSI from the historical reference period (1978 - 2005) to the future period (2072 - 2099) under RCP 8.5 for every combination of season, sex, and life stage. Season is indicated as spring (Sp) or fall (Fa); sex is indicated as male (Ma) or female (Fe); life stage is indicated as adult (Ad) or juvenile (Ju). Results are from the base case.

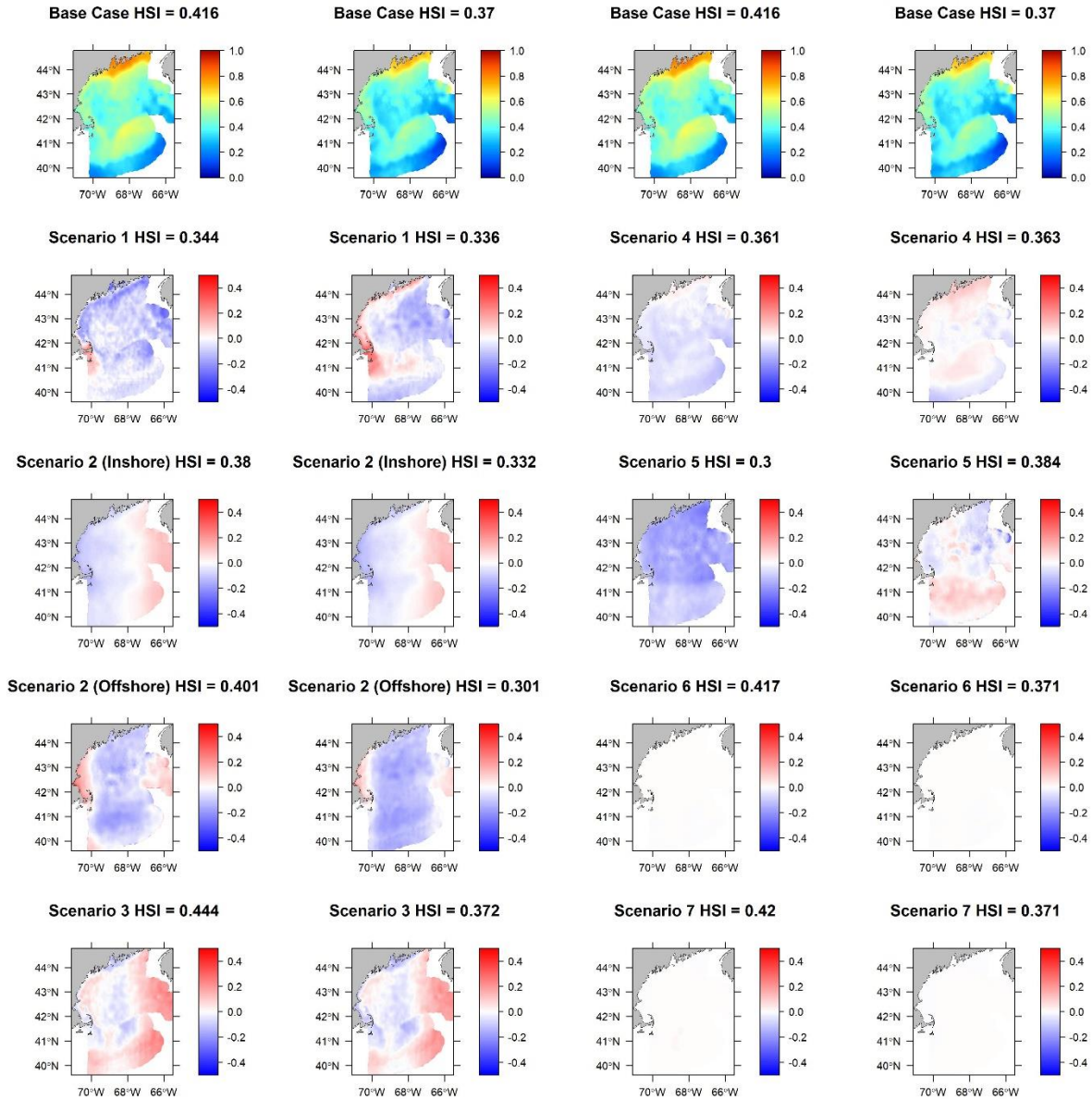


Figure 7.6. Spatial HSI from the base case (Row 1) for the historical period (Columns 1 and 3) and the future period (Columns 2 and 4) as well as spatial differences for each of the seven scenarios (Rows 2 through 5) to their respective base case maps in row 1 (Note that the base case maps in columns 1 and 3 are the same and those in columns 2 and 4 are the same). Blue represents areas in a given scenario that were predicted to have a lower HSI than the base case did. Red represents areas in a given scenario that were predicted to have a higher HSI than the base case did. The darker the respective shade, the greater the difference from the base case. Above each map is the scenario name and the average spatial HSI for that period and scenario. Results are for spring female adults. Note scenario 5 is combined seasons, scenario 6 is combined sexes, and scenario 7 is combined life stages.

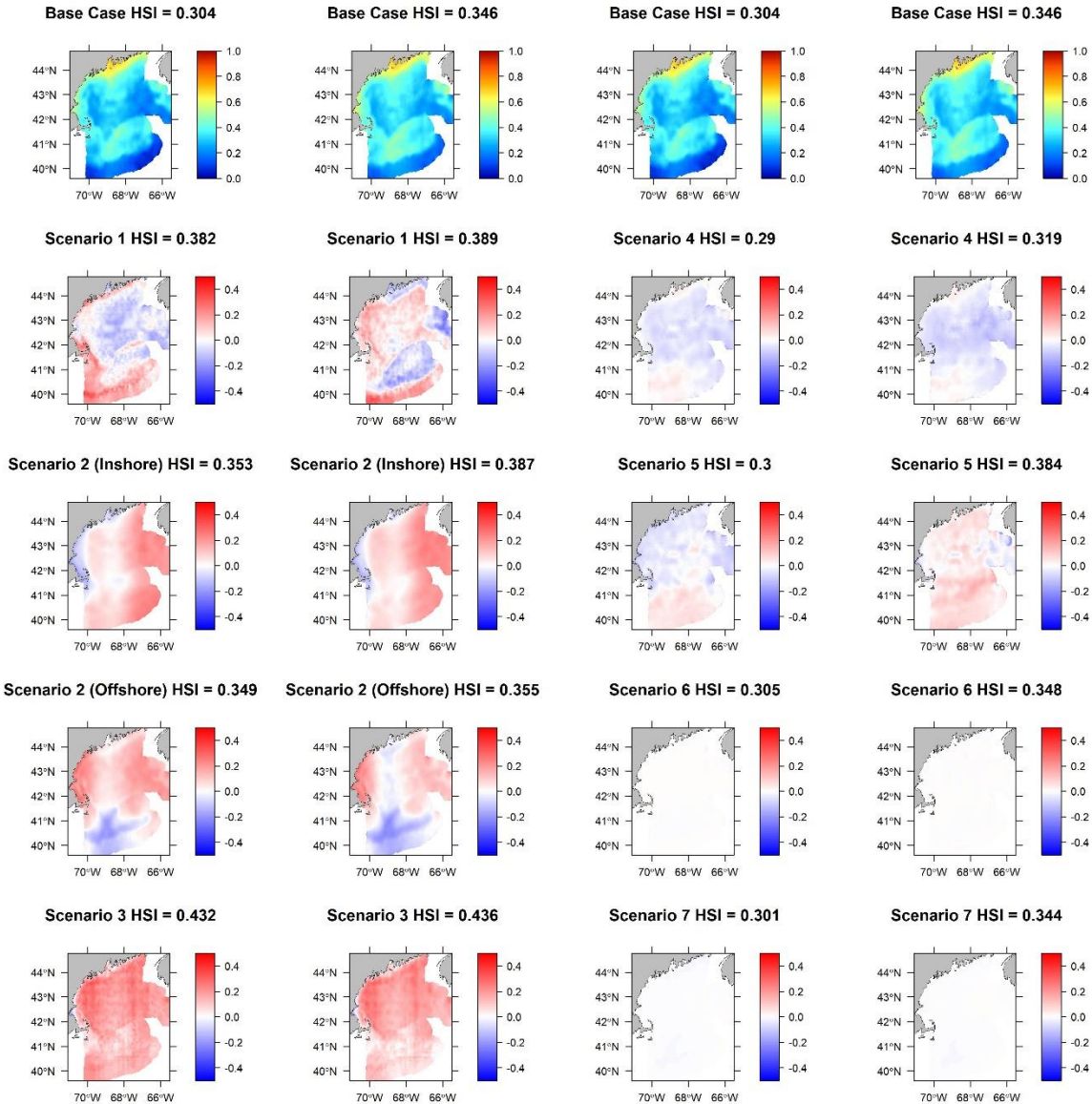


Figure 7.7. Spatial HSI from the base case (Row 1) for the historical period (Columns 1 and 3) and the future period (Columns 2 and 4) as well as spatial differences for each of the seven scenarios (Rows 2 through 5) to their respective base case maps in row 1 (Note that the base case maps in columns 1 and 3 are the same and those in columns 2 and 4 are the same). Blue represents areas in a given scenario that were predicted to have a lower HSI than the base case did. Red represents areas in a given scenario that were predicted to have a higher HSI than the base case did. The darker the respective shade, the greater the difference from the base case. Above each map is the scenario name and the average spatial HSI for that period and scenario. Results are for fall female adults. Note scenario 5 is combined seasons, scenario 6 is combined sexes, and scenario 7 is combined life stages.

Table 7.2. Summary statistics of suitable habitat for American lobster in the Gulf of Maine for two time periods: 1978-2005 (Historical) and 2072-2099 under RCP 8.5 (Forecasted). Statistics presented are HSI spatial averages, and percent spatial coverages of HSI more than 0.20 (Fair), 0.50 (Good), and 0.80 (Excellent) for each combination of season, sex, and life stage. Season is indicated as spring (Sp) or fall (Fa); sex is indicated as male (Ma) or female (Fe); life stage is indicated as adult (Ad) or juvenile (Ju). Results are from the base case.

Period	Historical				Forecasted			
	Average	Fair	Good	Excellent	Average	Fair	Good	Excellent
SpMaAd	0.462	97.499	34.232	1.717	0.401	94.213	16.381	0.000
FaMaAd	0.340	84.306	13.536	0.000	0.372	92.545	14.517	0.000
SpFeAd	0.459	97.499	33.399	1.030	0.398	94.164	15.204	0.000
FaFeAd	0.340	84.306	13.291	0.000	0.371	92.594	14.664	0.000
SpMaJu	0.453	97.057	31.976	0.834	0.395	93.624	14.321	0.000
FaMaJu	0.333	83.816	12.898	0.000	0.367	92.251	14.370	0.000
SpFeJu	0.456	97.303	31.829	0.490	0.395	94.164	13.977	0.000
FaFeJu	0.331	83.816	12.800	0.000	0.366	92.104	14.321	0.000

Table 7.3. Root-mean-squared-error (RMSE) values for each combination of season, sex, and life stage used in each of the seven scenarios in comparison to the base case for the hindcasted period. Season is indicated as spring (Sp) or fall (Fa); sex is indicated as male (Ma) or female (Fe); life stage is indicated as adult (Ad) or juvenile (Ju). Scenario 2 has two components: inshore indices extrapolated to the GOM (2i) and offshore indices extrapolated to the GOM (2o).

	Scenario							
	1	2i	2o	3	4	5	6	7
SpMaAd	0.112	0.081	0.143	0.083	0.081	0.142	0.002	0.006
FaMaAd	0.168	0.132	0.140	0.154	0.072	0.093	0.001	0.005
SpFeAd	0.111	0.082	0.145	0.082	0.081	0.141	0.002	0.006
FaFeAd	0.169	0.131	0.140	0.155	0.070	0.092	0.008	0.005
SpMaJu	0.109	0.075	0.148	0.084	0.082	0.140	0.005	0.011
FaMaJu	0.168	0.132	0.137	0.164	0.069	0.091	0.003	0.012
SpFeJu	0.111	0.077	0.142	0.081	0.081	0.143	0.005	0.009
FaFeJu	0.171	0.133	0.136	0.166	0.069	0.095	0.003	0.008

Table 7.4. Root-mean-squared-error (RMSE) values for each combination of season, sex, and life stage used in each of the seven scenarios in comparison to the base case for the forecasted period. Season is indicated as spring (Sp) or fall (Fa); sex is indicated as male (Ma) or female (Fe); life stage is indicated as adult (Ad) or juvenile (Ju). Scenario 2 has two components: inshore indices extrapolated to the GOM (2i) and offshore indices extrapolated to the GOM (2o).

	Scenario							
	1	2i	2o	3	4	5	6	7
SpMaAd	0.138	0.088	0.126	0.085	0.067	0.116	0.002	0.006
FaMaAd	0.142	0.116	0.139	0.126	0.081	0.109	0.001	0.005
SpFeAd	0.140	0.088	0.127	0.083	0.066	0.115	0.002	0.005
FaFeAd	0.142	0.115	0.139	0.126	0.079	0.110	0.011	0.005
SpMaJu	0.138	0.081	0.141	0.082	0.066	0.116	0.004	0.010
FaMaJu	0.142	0.118	0.132	0.135	0.079	0.112	0.003	0.014
SpFeJu	0.142	0.083	0.117	0.079	0.066	0.118	0.005	0.009
FaFeJu	0.142	0.118	0.137	0.136	0.079	0.114	0.003	0.008

7.5 Discussion

Input data used in this type of HSI modelling shapes the inherent biological and population assumptions that govern model predictions: the input data chosen is a consequence of the researcher’s assumptions (Roloff & Kernohan 1999). This study further asserts that in these types of situations, biological realism must be determined a priori by the researcher as there is a lack of reliable metrics to determine this from bioclimate model results. It is shown here that alterations to this assumed realism as was done in the “what-if” scenarios have potential to severely impact model output and thus negatively impact fisheries management decisions. Direct comparisons to explain this point can only be done with a stock or population that is well described with associated data and a large knowledgebase explaining its function. These features made American lobster in

the GOM an ideal testbed for the scenarios evaluated in this research framework, especially those that were known to be biologically unrealistic prior to testing.

The American lobster fishery in the GOM is expected to change due to shifting environmental conditions. Historically, the bulk of fishing effort has been concentrated in the summer and fall months (Boenish & Chen 2018), targeting the lobster when they are in shallower waters. This may be expected to shift later into the fall as spring HSI decreases and fall HSI increases. This is due to lobsters' propensity to behaviorally thermoregulate by following suitable thermal habitats inshore in the spring and offshore in the fall (Aiken & Waddy 1986; Crossin et al. 1998). Initially, the downward trends over time for HSI in the spring seemed to be consistent with upwards trends in the fall in this study. However, the spring forecasts show a loss of the best environments for lobster over time (complete loss of "excellent" habitat and halving of "good" habitat), whereas the fall is simply gaining new areas of "fair" habitat. Thus, overall suitability in the GOM is expected to decline out to 2099. This, coupled with the fact that areas with the most suitable habitat historically seem to be the areas most affected by a changing environment, illustrates a scenario similar to what happened to the lobster population and fishery in SNE where climate change has partially led to low recruitment and subsequent fishery collapse (Howell 2012; ASMFC 2015). Climate change is predicted to negatively alter the suitability of habitat for lobster in the GOM and this poses a threat to the future of the fishery in this region. It is important to note that these predictions are under a "business-as-usual" future carbon emissions scenario and that any efforts to ameliorate climate change compared to the RCP 8.5 scenario will likely to some degree mitigate these effects on GOM lobster habitat.

These conclusions, again, were drawn from the base case. Some of the scenarios conducted agreed with these results and others were drastically different. As outlined in the methods, the set

of input data and parameters chosen for the base case all had biological backing and supporting evidence from previous studies. The seven “what-if” scenarios conducted represented deviations from how this bioclimate model has historically been run (Tanaka & Chen 2015; 2016) and the results have led to four separate discussions, each of which is detailed below:

7.5.1 Choice of Extrapolation Data

When using kriged data, patterns in HSI seemed to vary spatially in magnitude in comparison to the base case. Kriged data show overall a decreased HSI and less drastic changes to lobster HSI in shallower waters, but more pronounced changes in deeper waters into the future. The same patterns of spring decreases and fall increases through time were still apparent, but the overall magnitudes of HSI do differ between the use of modelled and kriged data. These differences could have come from the decreased data point density set used to fuel scenario 1 (see section 7.3.3), and which subsequently could have impacted the *RMSE* values calculated for the scenario. Regardless, there does not seem to be a clear answer as to whether the use of modelled or kriged data is better in terms of being more biologically realistic.

For American lobster, environmental preferences in the lab are not always observed in the field (Jury & Watson 2013). This, coupled with the strong similarities in SIs between the two scenarios, complicates the process of determining appropriate biological and environmental realism. Kriged data, like those used in this study and Friedland et al. (2019; 2020), preserve the observational nature of the data. This is a property that is arguably more environmentally realistic than modelled data, which by nature has uncertainties in its estimation processes, especially for deep-water variables (Li et al. 2017; Friedland et al. 2020). The increased spatial homogenizing of the forecasts using this data urges future studies to further explore the relationship of environmental data and habitat forecasts. Furthermore, different data sets of the same

environmental variables have been shown to have large impacts on the end results when modelling habitat, but the exact reasons for these discrepancies are not well known (Peterson & Nakazawa 2008). Regardless, the choice of extrapolation data affects overall bioclimate results and must be carefully considered when modelling and forecasting HSI.

7.5.2 The Importance of Spatial Scale

Scenarios 2 and 3 both seemed to verify the claim that spatial scale is important. Looking at the SIs together from these scenarios and the base case, it seemed as though lobster preferences for temperature remained relatively constant, whereas preferences for salinity, depth, latitude, and longitude changed largely when calculated for the entire Northwest Atlantic and the GOM, as well as inshore and offshore areas. This is likely due to a combination of many things. For example: different surveys cover different areas with different ranges of environmental parameters and so lobsters captured in a given survey are assumed to only be subject to those ranges the survey operates in. This was easily seen in the differences in SIs of depth between the inshore and offshore GOM: the deepest station in the inshore surveys was at ~200 m whereas the offshore surveys reach over 500 m.

Different stocks of lobster may have physiologically and behaviorally different preferences for certain parameters due to divergences over time from little migration and interbreeding (ASMFC 2015; Tanaka & Chen 2015; 2016), and it appears that these divergent groups may have disparate population structures and environmental preferences (Stanley et al. 2018). The Atlantic States Marine Fisheries Commission (ASMFC) treats the GOM and SNE stocks separately in assessments due to this fact, and associated stock-localized recruitment (ASMFC 2015). Hence, it may be precarious to assume species-wide conformity to environmental parameter preferences.

Doing so with lobster seemed to drastically overestimate the suitability of GOM habitat because so much data from the less suitable SNE were used in calculation of SIs.

Within the GOM, calculating SIs for inshore or offshore areas and extrapolating into ranges of environmental conditions not present in the spatial subset causes some large problems with over and underestimation of HSI. The bioclimate model cannot predict relationships outside the ranges of parameters it is given and so often assumes false correlations extending beyond the limits of the variables when extrapolating HSI. This highlights the need for appropriate survey coverage and data collection that encompasses the niches of the species (MacLeod 2010) and cautions against extrapolating relationships into low or unsampled areas, especially if the environmental conditions of the region are different (Conn et al. 2015). Lobster dynamics in inshore and offshore waters appear different, evident by their seasonal migrations (Aiken & Waddy 1986; Crossin et al. 1998). The SI curves determined for the inshore and offshore GOM are not biologically unrealistic, it is only their extrapolations that are inappropriate. The respective SI curves should only be applied to the spatial area from which the data used to generate them was collected. Otherwise, this could introduce severe biases (Conn et al. 2015).

Salinity SI in the offshore GOM seemed more biologically reasonable than for the inshore GOM, presenting a more understandable and smooth curve over the range. This was most likely due to the nature of the data and few instances of survey effort at those large salinity values. Those instances, however, could have had large catches of lobster, skewing the SI relationship. This problem is discussed in Xue et al. (2017), where survey instances of large catch can skew overall SIs when modelling habitat. Xue et al. (2017) shows that use of a logged response variable (lobster abundance) can mitigate the effects of instances like this on overall relationships. It is important to note that this effect of logging the response variable is a change to model structure. All scenarios

in this study were for changes in input data or model assumptions while holding model structure constant. Model structure, which can also affect uncertainty, additionally needs to be appropriately determined (Wiens et al. 2009; Xue et al. 2017), but remained outside the scope of this study.

7.5.3 Inclusion and Exclusion Criteria

It can be difficult to determine whether a parameter warrants inclusion as a covariate of HSI calculations using this type of bioclimate modelling, as post hoc analyses of model fitting metrics are not appropriate (Kuparinen et al. 2012). Temperature has been shown in this study and others to be an important factor of lobster habitat (Tanaka & Chen 2016; Goode et al. 2019; Friedland et al. 2020; Mazur et al. 2020). When removed in scenario 4, the forecasts of HSI showed similar trends, but to a lesser degree in the spring and similar magnitude for the fall. Perhaps salinity is a more important factor in the fall and temperature is a more important factor in the spring for GOM lobster. Regardless, this underestimates the effects of climate change on lobster habitat and provides a forecast that understates the importance of preparing for change. Relatively low *RMSE* values hinted at possible collinearity of the variables used: latitude, longitude, and season may capture most of temperature's effects on lobster abundance. However, the model itself is less mechanistic without temperature. Temperature will be altered under climate change, but variables of latitude, longitude, and season are static parameters. Temporally dynamic and mechanistic variables such as temperature are important for forecasting HSI and a management framework that neglects effects from these types of covariates may not be prepared for changes in population dynamics and spatial domain that arise. Mechanistic components of habitat will likely lead to more biologically realistic forecasts of HSI.

The problem of determining the appropriate environmental parameters for HSI calculations is a common one (Schuetz et al. 2018). Most often, a starting list of potentially important covariates

is derived from a combination of researcher intuition of the target species and ecosystem as well as simply what data are available to model (Shuetz et al. 2018). This highlights the importance of understanding the life history of the target organism a priori. In this stage of bioclimate modelling, there is no substitute for a good knowledge base of the stock. Narrowing down this starting list of variables to appropriately use may potentially be done through use of a boosted regression tree to determine partial dependence of covariates or a similar weighting scheme to determine the relative importance of environmental variables. This would allow for narrowing down important variables through testing rather than risk missing what might potentially be an important habitat factor.

7.5.4 On Separating Life History Data

Compared to the previous discussions on data input assumptions, the discussion of when and when not to separate life history data is more explicit and direct. Previous literature has shown differences in the suitability of lobster habitat between seasons (Chang et al. 2010; Tanaka et al. 2016), sexes (Chang et al. 2010; Jury et al. 1994), and life stages (Chang et al. 2010). Previous bioclimate studies for American lobster have thus split HSI calculations accordingly (Tanaka & Chen 2015; 2016) and the base case in this study followed suit.

Season had a large effect on lobster HSI in the base case. Ignoring the effects of season, as was done in scenario 5, proved to be very dangerous to management of the fishery. The base case clearly showed seasonal changes in habitat preference: a claim backed by much previous literature (Chang et al. 2010). When this shifting preference was ignored, it appeared that the overall suitability of the GOM for lobster rose over time with climate change: ignoring exceedingly important seasonality in environmental relationships. This is because what is preferential for lobsters in the spring is not always preferred in the fall and vice versa. Fall and spring trawl survey

data were used together to estimate false SIs. This one false assumption could lead to spurious confidence about the state of GOM lobster.

This seasonal effect on lobster habitat is not something that could have been determined post hoc from a singular conglomerate analysis. This study asserts it is biologically unrealistic to assume non-seasonality in this case because of previous literature on the topic (Chang et al. 2010; Tanaka et al. 2016). This is a clear situation where researcher misunderstanding can lead to model mischaracterization and a false definition of biological realism. Expanding upon conclusions from May (2004), a clear understanding of model assumptions a priori is necessary as the model does not know more about the natural system than the researcher does. When it comes to this problem of separating life history data, simulations as was done in this study can help to infer what separations are appropriate. Comparing results from scenario 5 to the base case, it can clearly be seen that season has an effect on lobster HSI. The same was not necessarily true for sex and life stage.

Results from scenarios 6 and 7 appear strikingly similar to each other and the base case, seemingly indicating that separation of GOM lobster into sexes and life stages is not necessary for modelling HSI. For life stage, this could simply be due to the size of lobsters caught in the trawl surveys, with relatively few lobsters under 50 mm carapace length. These juvenile lobsters are old enough and large enough to behave like adults, following similar migration patterns (Lawton & Lavalli 1995), just not of the minimum size at maturity necessary to classify them as adults (ASMFC 2015). Differences in habitat preference between sexes has been documented for the GOM, but it has been shown that these differences are small when compared to the effects of both lobster size and season (Chang et al. 2010). Additionally, differences in habitat preference between sexes is more observed in laboratory studies, but shown to be less present in the field (Jury &

Watson 2013). Splitting up lobster data by sex and life stage in this sense may not be necessary, but should be tested in the future when new and updated data are used. This essentially means that whether or not certain subgroups should be split may be a cause of the informing surveys and their selectivities. Regardless, the same concept should be applied to other species and stocks: when determining how to separate life history data, simple bioclimate model simulations can be run to determine necessity. Those simulations, however, of course need to be constituted by the researcher a priori: again necessitating a need of understanding biological realism. Future research should determine what specific levels of differential effects from seasonality, sexes, life stages, and other life history qualities enhance the need to subset when bioclimate modelling and what levels are too low to influence results. This information would greatly aid in statistical bioclimate modelling, but may also vary by species, making it difficult to generalize.

7.5.5 Conclusions

The results from this study have shown that less accurate assumptions can lead to HSI forecasts that appear reliable, but may not be biologically realistic. Biological realism when calculating HSIs is not something that can be determined by the bioclimate model in most cases: it must be determined a priori. In scenarios where certain data were missing or not sequestered appropriately, there were dangers associated with interpreting model output such as overestimation of HSI or misleading HSI spatial dynamics. Nevertheless, forecasting HSI under biological and population dynamics uncertainties is highly cautioned against. However, this study acknowledges that in many cases, vague biological realism is accepted by the researcher due to limitations of data and increased model simplicity is a direct result of that. It may be necessary to perform bioclimate calculations with limited data, but this does not change the necessity of understanding biological realism a priori to aid in interpreting results with appropriate levels of caution.

Additionally, if too many uncertainties exist in the knowledgebase of the target population, it may be possible to infer some degree of biological realism from other similar species with more data (Araújo & Peterson 2012).

This methodology from Tanaka and Chen (2015; 2016) is a specific type of statistical bioclimate modelling, but there are many methods that can be used (Heikkinen et al. 2006). Key limitations of this model are the inability to determine collinearity between the factors used and the inability to directly perform typical cross-validation procedures. Other types of bioclimate modelling such as generalized additive modelling (Araújo et al. 2004) or locally-weighted regression methods modelling (Hill et al. 2002), may not have these issues. For example, locally weighted regression techniques would likely be more adept at extrapolating into unsampled regions (Beerling et al. 1995; Heikkinen et al. 2006), and may have alleviated deviations from the base case seen in scenario 2 of this study. Tanaka and Chen's (2015; 2016) model was chosen for this study for its ability to model and map the HSI metric and to compare results to prior studies on lobster. Additionally, this model's relative simplicity compared to other models allows it to be widely applicable to almost all pelagic and benthic species alike. Ultimately, there are different methods for estimating bioclimate envelopes and choice of modelling approach has potential to influence habitat predictions (Heikkinen et al. 2006) and thus must be carefully selected. For a more comprehensive overview of this topic, see Heikkinen et al. (2006).

GOM lobster is a very well-studied, well surveyed, and data-rich species (Chen et al. 2006b; ASMFC 2015; Hodgdon et al. 2020). In this sense, it is different from many other economically important species across the oceans. This inherent knowledge of GOM lobster dynamics and life history provided insight into the appropriate model assumptions and input data. For species with a lack of biological knowledge or data availability, it can be more treacherous to

calculate and forecast HSIs. Biological realism would be harder to interpret and understand, potentially leading to inherently less than accurate information about the target species habitat and misleading interpretations of forecasts. Data input and their inherent assumptions when forecasting HSI should be as biologically realistic as possible.

CHAPTER 8: CONCLUSIONS AND FUTURE DIRECTIONS

8.1 Maine's Top Fisheries under Climate Change

Climate change is most often seen as a force that negatively affects many species' distributions, life histories, behaviors, and production (Perry et al. 2005; Hazen et al. 2012; Anderson et al. 2013; FAO 2016; IPCC 2019). In the Gulf of Maine (GOM), climate change is causing warming effects exceeding the rates of most of the world's oceans (Pershing et al. 2015). The negative effects of this on the GOM ecosystem should not be underplayed. However, as can be seen from the preceding studies of Atlantic sea scallops (*Placopecten magellanicus*; ASC) and American lobster (*Homarus americanus*), there are some positive effects for these GOM species and their fisheries.

8.1.1 Atlantic Sea Scallops: The Future of the Stock and the Future of Research

Until recently, areas of the Northern GOM were not considered in runs of the scallop area management simulator (SAMS) model and were therefore not included in calculations of overfishing limits (OFL) or acceptable biological catches (ABC). However, through a combination of quantification of growth in the region and continued survey efforts expanding the dataset of samples, 2021 marked the first year that an area from the Northern GOM was included in the OFL and ABC calculations (NEFSC SSC 2021). This highlights not only the increasing knowledgebase of the species in this region, but also the growing significance and importance of the northern extent of this stock.

ASCs in the region have been shown to grow to larger sizes than their more southern counterparts; a trend at least somewhat attributable to the regional climatology. If these trends continue, there may be expansion potential for the fishery in this region. This speculation, however, can only be appropriately assessed through rigorous future research techniques. The

research on ASCs in this region outlined in Chapter 2 seems to suggest a more complex spatiotemporal relationship between the growth patterns of these animals the regional climate. Further research looking at how these relationships vary over space and time is necessary as well as other factors influencing ASC growth, namely phytoplankton density. Forecasts of these factors using these relationships can help to infer the future of ASC growth and by extent, the stock and the fishery.

8.1.2 American Lobster: The Future of the Stock and the Future of Research

American lobster in Southern New England have experienced significant population declines and subsequent declines in fishing effort and landings (ASMFC 2015). These diminishing trends have been linked in part to climate change of the region, where warming waters may have contributed to recruitment collapses and an overall northward migration of the stock to cooler waters (ASMFC 2015). Much research, including that in Chapters 3 through 7, have been aimed at determining whether this same trend will happen in the GOM.

Habitat for lobster in this region will experience declines in suitability due to rising temperatures and salinities, but the area will not become unsuitable. Much of the same spatial trends in suitability will still be apparent in the next 80 years in this region, perhaps indicating relatively small shifts in lobster distributions in the GOM during this time. However, habitat suitability is not a direct measure of species distribution. There are many other factors that could influence lobster distributions in the GOM beyond environmental suitability. As the climate warms, many species besides lobster are shifting their distributions. For example, black sea bass, a dominant predator of lobster in southern New England, have been moving up the Atlantic coast and have recently been found more consistently in areas of the GOM (McMahan et al. 2020). The influx of regionally novel predator species may drive future lobster distributions beyond those

assumed from the bioclimate model results. Further research is needed on biotic factors driving lobster distributions, such as predator influx and disease prevalence.

The relationships between lobster spawning biomass and recruitment points towards a future of large recruitment events due to rising temperatures. The thermally mediated recruitment estimations in Chapter 6 hint at this optimistic point of view. However, there will be novel factors influencing lobster distributions, life histories, and behaviors in the near and far futures. Epizootic shell disease (ESD), a bacterial infection that degrades the shell and limits lobster survival and reproduction (Glenn & Pugh 2006), may have higher prevalence and infection rates in warmer waters (Glenn & Pugh 2006). This would have led to a higher pervasiveness of ESD in southern New England than in the GOM, but with the possibility of increasing prevalence in GOM as the waters warm. Future research should further quantify infections of diseases such as ESD on the population and how these infections and severity may relate to regional climatologies.

Juxtaposing the negative effects of rising predator and disease influences, lobsters will most likely continue to molt more frequently, grow less per molting event, and reach size-at-maturity (SAM) at smaller and smaller sizes as the GOM warms (ASMFC 2015; Le Bris et al. 2017). The current fishery minimal legal size regulations are based on the knowledge that female lobsters should experience at least one recruitment event before reaching the legal size, thus contributing to the population before being caught. As SAM decreases, this would increase this probability, perhaps leading to overall more recruitment. However, smaller lobsters produce fewer eggs per reproduction event and spawn less frequently than larger individuals (Waddy & Aiken 1991), and this may not be enough to counteract the aforementioned negative effects.

As can be ascertained, there is a lot of uncertainty about the future of GOM lobster, with some facts indicating positive effects, and others pointing towards negative effects. This highlights

the rising importance of quantifying relationships of lobster life history to other biotic and abiotic factors so that more accurate predictions about this region can be made. On top of this, agencies like the ASMFC and the DMR are tasked with managing this species under these uncertainties. Analyses like those conducted in Chapters 4 and 5 are therefore essential in determining strengths and weaknesses of current model usage as well as where to best aim future field studies to more accurately inform these stock assessments.

The research in Chapters 3 through 7 accentuates an optimistic point of view concerning the future of the lobster stock. Threats that impacted southern New England may still be far into the future before there are large consequences for the GOM. Habitat will decrease, albeit relatively slowly over time, recruitment events may increase in magnitude with warming waters, and changes to life history will most likely not affect modelling capacity for some time. These conclusions are concurrently idealistic for the fate of the GOM lobster stock, but can only be substantiated with future research on factors not considered thus far and direct quantifications of uncertainty.

8.2 Concluding Statement

In conclusion, the results of this research framework are encouraging concerning the future of ASC and lobster stocks and management in the GOM ecosystem. Climate change will continue to impact the GOM and it is imperative to continue research efforts into assessing the future of these and other GOM stocks and fisheries. The models developed and outlined in this dissertation are not species-specific and can be used with other stocks and fisheries in the GOM and elsewhere. The methods outlined here have growing relevance as environments continue to warm and the world's fisheries are consequently impacted.

BIBLIOGRAPHY

- Aiken, D. E. 1977. Molting and growth in decapod crustaceans with particular reference to the lobster *Homarus americanus* (No. 7; pp. 41–73). CSIRO, Australia.
- Aiken, D. E., and Waddy, S. L. 1976. Controlling growth and reproduction in the American lobster. Proceedings of the Annual Meeting - *World Mariculture Society*. 7(1–4): 415–430.
- Aiken, D. and Waddy, S. 1986. Environmental influence on recruitment of the American lobster, *Homarus americanus*: a perspective. *Canadian Journal of Fisheries and Aquatic Sciences*. 43: 2258–2270.
- Anderson, J., Gurarie, E., Bracis, C., Burke B., and Laidre, K. 2013. Modelling climate change impacts on phenology and population dynamics of migratory marine species. *Ecological Modelling*. 264: 83–97.
- Annis, E. R. 2005. Temperature effects on the vertical distribution of lobster postlarvae (*Homarus americanus*). *Limnology and Oceanography*. 50(6): 1972–1982.
- Araújo, M. B., Cabeza, M., Thuiller, W., Hannah, L., and Williams, P. H. 2004. Would climate change drive species out of reserves? An assessment of existing reserve-selection methods. *Global Change Biology*. 10: 1618–1626.
- Araújo, M. B. and Peterson, A. T. 2012. Uses and misuses of bioclimatic envelope modeling. *Ecology*. 93: 1527–1539.
- Atlantic States Marine Fisheries Commission (ASMFC). 2006. *American Lobster Benchmark Stock Assessment and Peer Review Report*. American Lobster Stock Assessment Subcommittee. Boston, Massachusetts. 364 pages.
- Atlantic States Marine Fisheries Commission (ASMFC) American Lobster Stock Assessment Review Panel. 2015. *Atlantic States Marine Fisheries Commission: American Lobster Stock Assessment Peer Review Report*. Woods Hole, Massachusetts. 493 pages.
- Atlantic States Marine Fisheries Commission (ASMFC). 2020. *American Lobster Benchmark Stock Assessment and Peer Review Report*. American Lobster Stock Assessment Review Panel. 558 pages.
- Audzijonyte, A., Fulton, E., Haddon, M., Helidoniotis, F., Hobday, A. J., Kuparinen, A., Morrongiello, J., Smith, A. D., Upston, J., and Waples, R. S. 2016. Trends and management implications of human-influenced life-history changes in marine ectotherms. *Fish and Fisheries*, 17(4), 1005–1028. <https://doi.org/10.1111/faf.12156>
- Banzon, V., Smith, T. M., Chin, T. M., Liu, C., and Hankins, W., 2016. A long-term record of blended satellite and in situ sea-surface temperature for climate monitoring, modeling and environmental studies. *Earth System Science Data*. 8: 165–176.
- Barret, L., Miron, G., Ouellet, P., and Tremblay, R. 2016. Settlement behavior of American lobster (*Homarus americanus*): effect of female origin and developmental temperature. *Fisheries Oceanography*. 26(1): 69–82.

- Barry, S. and Elith, J. 2006. Error and uncertainty in habitat models. *Journal of Applied Ecology*. 43(3): 413-423.
- Basson, M. 1999. The importance of environmental factors in the design of management procedures. *ICES Journal of Marine Science* 56(6): 933–942.
- Beardall, J. and Raven, J. A. 2004. The potential effects of global climate change on microalgal photosynthesis, growth and ecology. *Phycologia*. 43(1): 26-40.
- Beerling, D. J., Huntley, B., and Bailey, J.P. 1995. Climate and the distribution of *Fallopia japonica*: use of an introduced species to test the predictive capacity of response surfaces. *Journal of Vegetation Science*. 6: 269–282.
- Berger, A. M. 2019. Character of temporal variability in stock productivity influences the utility of dynamic reference points. *Fisheries Research*. 217: 185-197.
- Beverton R. J. H. and Holt S. J. 1957. On the dynamics of exploited fish populations. *Fishery Investigation Series II, Vol. XIX*. UK. 533 pages.
- Boenish, R. and Chen, Y. 2018. Spatiotemporal dynamics of effective fishing effort in the American lobster (*Homarus americanus*) fishery along the coast of Maine, USA. *Fisheries Research*. 199: 231-241.
- Booshehrian, M., Möller, T., Peterman, R. M., and Munzner, T. 2012. Vismon: Facilitating Analysis of Trade-Offs, Uncertainty, and Sensitivity. *In Fisheries Management Decision Making. Computer Graphics Forum*. 31(3.3):1235-1244. <https://doi.org/10.1111/j.1467-8659.2012.03116.x>
- Boudreau, S., Anderson, S., and Worm, B. 2015. Top-down and bottom-up forces interact at thermal range extremes on American lobster. *Journal of Animal Ecology*. 84(3): 840-850.
- Brander, K. 2010. Impacts of climate change on fisheries. *Journal of Marine Systems*. 79(3–4): 389–402.
- Brunel, T. and Boucher, J. 2007. Long-term trends in fish recruitment in the north-east Atlantic related to climate change. *Fisheries Oceanography* 16: 336-349.
- Cadrin, S. X. and Secor, D. H. 2009. Accounting for Spatial Population Structure in Stock Assessment: Past, Present, and Future. *In The Future of Fisheries Science in North America*. Edited by Beamish, R.J. and Rothschild, B.J. Springer Science and Business Media, Berlin, Germany. 405-426.
- Cao, J., Chen, Y., and Richards, R. 2017a. Improving assessment of *Pandalus* stocks using a seasonal, size-structured assessment model with environmental variables. Part I: Model description and application. *Canadian Journal of Fisheries and Aquatic Sciences*. 74(3): 349-362.
- Cao, J., Chen, Y., and Richards, R. 2017b. Improving assessment of *Pandalus* stocks using a seasonal, size-structured assessment model with environmental variables. Part II: Model evaluation and simulation. *Canadian Journal of Fisheries and Aquatic Sciences*. 74(3): 363-376.

- Cardinale, M. and Arrhenius, F. 2000. The relationship between stock and recruitment: are the assumptions valid? *Marine Ecology Progress Series*. 196: 305-309.
- Chang, J. H., Chen, Y., Holland, D., and Grabowski, J. 2010. Estimating spatial distribution of American lobster *Homarus americanus* using habitat variables. *Marine Ecology Progress Series* 420: 145-156.
- Chang, Y. J., Sun, C. L., Chen, Y., and Yeh, S. Z. 2011. Modelling the growth of crustacean species. *Reviews in Fish Biology and Fisheries*. 22(1): 157-187.
- Chang, J. H. 2015. Population dynamics of American lobster: environmental, ecological, and economic perspectives. *Ph.D. diss.*, University of Maine, Orono, Maine.
- Chang, J.H., Chen, Y., Halteman, W., and Wilson, C. 2015. Roles of spatial scale in quantifying stock–recruitment relationships for American lobsters in the inshore Gulf of Maine. *Canadian Journal of Fisheries and Aquatic Sciences* 73(6): 885-909.
- Chen, D. G. and Irvine, J. R. 2001. A semiparametric model to examine stock–recruitment relationships incorporating environmental data. *Canadian Journal of Fisheries and Aquatic Sciences*. 58: 1178-1186.
- Chen, J., Thompson, M., and Wu, C. 2004. Estimation of fish abundance indices based on scientific research trawl surveys. *Biometrics*. 60(1): 116-123.
- Chen, Y., Kanaiwa, M., and Wilson, C. 2005. Developing and evaluating a size-structured stock assessment model for the American lobster, *Homarus americanus*, fishery. *New Zealand Journal of Marine and Freshwater Research*. 39:645-660. <https://doi.org/10.1080/00288330.2005.9517342>
- Chen, C., Beardsley, R., and Cowles, G. 2006a. An unstructured-grid, finite-volume coastal ocean model (FVCOM) system. *Oceanography*. 19: 78-89.
- Chen, Y., Sherman, S., Wilson, C., Sowles, J., and Kanaiwa, M. 2006b. A comparison of two fishery-independent survey programs used to define the population structure of American lobster (*Homarus americanus*) in the Gulf of Maine. *Fishery Bulletin*. 104(2): 247-255.
- Cheung, W., Lam, V., Sarmiento, J., Kearney, K., Watson, R., and Pauly, D. 2009. Projecting global marine biodiversity impacts under climate change scenarios. *Fish and Fisheries*. 10: 235-251.
- Chute, T., Wainright, S., and Hart, D. 2012. Timing of shell ring formation and patterns of shell growth in the sea scallop *Placopecten magellanicus* based on stable oxygen isotopes. *Journal of Shellfish Research*. 31: 649-662.
- Comeau, M. and Savoie, F. 2001. Growth increment and molt frequency of the American lobster (*Homarus americanus*) in the Southwestern Gulf of St. Lawrence. *Journal of Crustacean Biology*. 21(4):923–936. JSTOR.
- Conn, P. 2010. Hierarchical analysis of multiple noisy abundance indices. *Canadian Journal of Fisheries and Aquatic Sciences*. 67(1): 108-120.

- Conn, P. Johnson, D., and Boveng, P. 2015. On Extrapolating Past the Range of Observed Data When Making Statistical Predictions in Ecology. PLoS ONE. 10(10): e0141416.
- Connecticut Department of Energy and Environmental Protection (CTDEEP). 1984-2016. Long Island Sound Trawl Survey. Raw Data.
- Correa, G.M., McGilliard, C.R., Ciannelli, L., and Fuentz, C. 2021. Spatial and temporal variability in somatic growth in fisheries stock assessment models: evaluating the consequences of misspecification. ICES Journal of Marine Science. 78(5):1900-1908.
- Corson, T. 2004. The Secret Life of Lobsters (Book). Harper Perennial; Later Printing Edition. 320 pages.
- Côté, J., Himmelman, J., Claereboudt, M., and Bonardelli, J. 1993. Influence of density and depth on growth of juvenile sea scallops (*Placopecten magellanicus*) in suspended culture. Canadian Journal of Fisheries and Aquatic Sciences. 50: 1857-1869.
- Crance, J. 1986. Habitat suitability index models: And Instream flow suitability curves: Shortnose sturgeon. Fort Collins, CO: National Ecology Center – Fish and Wildlife Service – U.S. Department of the Interior. 31 pages.
- Crossin, G., Al-Youb, S., Jury, S., Howell, W., and Watson, W. III. 1998. Behavioral Thermoregulation in the American lobster *Homarus americanus*. The Journal of Experimental Biology. 201: 365–374.
- Cury, P. M., Fromentin, J., Figuet, S., and Bonhommeau, S. 2014. Resolving Hjort's Dilemma: How Is Recruitment Related to Spawning Stock Biomass in Marine Fish? Oceanography. 27(4): 42-47.
- Deroba, J. 2014. Evaluating the consequences of adjusting fish stock assessment estimates of biomass for retrospective patterns using Mohn's Rho. North American Journal of Fisheries Management. 34: 380-390.
- Doney, S. C., Ruckelshaus, M., Emmett Duffy, J., Barry, J. P., Chan, F., English, C. A., Galindo, H. M., Grebmeier, J. M., Hollowed, A. B., Knowlton, N., Polovina, J., Rabalais, N. N., Sydeman, W. J., and Talley, L. D. 2012. Climate change impacts on marine ecosystems. Annual Review of Marine Science. 4(1):11–37. <https://doi.org/10.1146/annurev-marine-041911-111611>
- Doney, S. C., Busch, D. S., Cooley, S. R., and Kroeker, K. J. 2020. The impacts of ocean acidification on marine ecosystems and reliant human communities. Annual Review of Environment and Resources. 45:83–112.
- Durbin, E., Campbell, R., Casas, M., Ohman, M., Niehoff, B., Runge, J., and Wagner, M. 2003. Interannual variation in phytoplankton blooms and zooplankton productivity and abundance in the Gulf of Maine during winter. *Marine Ecology Progress Series*. 254: 81-100.
- Eckel, F., Allen, M., and Sittel, M. 2012. Estimation of Ambiguity in Ensemble Forecasts. Weather and Forecasting. 27: 50–69.

- Engelhard G., Righton D., and Pinnegar J. 2013. Climate change and fishing: a century of shifting distribution in North Sea cod. *Global Change Biology*, 20: 2473–2483.
- Ennis, G. P. 1986. Stock definition, recruitment variability, and larval recruitment processes in the American lobster, *Homarus americanus*: a review. *Canadian Journal of Fisheries and Aquatic Sciences*. 43(11): 2072-2084.
- Fabens, A. 1965. Properties and fitting of the von Bertalanffy growth curve. *Growth*. 29: 265-289.
- Food and Agriculture Organization of the United Nations (FAO) Fisheries and Aquaculture Circular. 2016. Climate Change Implications for Fisheries and Aquaculture. Summary of the findings of the Intergovernmental Panel on Climate Change Fifth Assessment Report. 54 pages.
- Fogarty, M. J. 1993. Recruitment in randomly varying environments. *ICES Journal of Marine Science*. 50: 247-260.
- Fogarty, M. J. and Gendron, L. 2004. Biological reference points for American lobster (*Homarus americanus*) populations: limits to exploitation and the precautionary approach. *Canadian Journal of Fisheries and Aquatic Sciences*. 61: 1392-1403.
- Franklin, J. 2010. Mapping Species Distributions: Spatial Inference and Prediction. University Press, Cambridge, UK. 340 pages.
- Friedland, K. D. and Hare, J. A. 2007. Long-term trends and regime shifts in sea surface temperature on the continental shelf of the northeast United States. *Continental Shelf Research*. 27(18): 2313-2328.
- Friedland, K., Leaf, R., Kane, J., Tommasi, D., Asch, R., Rebuck, N., Ji, R., Large, S., Stock, C., and Saba, V. 2015. Spring bloom dynamics and zooplankton biomass response on the US Northeast Continental Shelf. *Continental Shelf Research*. 102: 47-61.
- Friedland, K., McManus, C., Morse, R., and Link, J. 2019. Event scale and persistent drivers of fish and macroinvertebrate distributions on the Northeast US Shelf. *ICES Journal of Marine Science*. 76(5): 1316-1334.
- Friedland, K., Morse, R., Manning, J., Melrose, D., Miles, T., Goode, A., Brady, D., Kohut, J., and Powell, E. 2020. Trends and change points in surface and bottom thermal environments of the US Northeast Continental Shelf Ecosystem. *Fisheries Oceanography*. 19 pages.
- Gabriel, W. L. and Mace, P. M. 1999. A Review of Biological Reference Points in the Context of the Precautionary Approach. Proceedings, 5th NMFS NSAW. NOAA Technical Memo. NMFS-F/SPO-40. 13 pages.
- Gaillard, J., Hebblewhite, M., Loison, A., Fuller, M., Powell, R., Basille, M., Van Moorter, B. 2010. Habitat–performance relationships: finding the right metric at a given spatial scale. *Philosophical Transactions of the Royal Society B*. 365: 2255-2265.
- García, D. 2020. FLBEI fisheries management simulation model. Definition of new criteria and guidelines for efficient validation of the model using global sensitivity analysis. *Ph.D. diss.*, University of the Basque Country, Leioa, Spain.

- Gattuso, J.-P., Magnan, A. K., Bopp, L., Cheung, W. W. L., Duarte, C. M., Hinkel, J., Mcleod, E., Micheli, F., Oschlies, A., Williamson, P., Billé, R., Chalastani, V. I., Gates, R. D., Irisson, J.-O., Middelburg, J. J., Pörtner, H.-O., and Rau, G. H. 2018. Ocean Solutions to Address Climate Change and Its Effects on Marine Ecosystems. *Frontiers in Marine Science*. 5:337. <https://doi.org/10.3389/fmars.2018.00337>
- Glenn, R. and Pugh, T. 2006. Epizootic Shell Disease in American Lobster (*Homarus Americanus*) in Massachusetts Coastal Waters: Interactions of Temperature, Maturity, and Intermolt Duration. *Journal of Crustacean Biology*. 26(4): 639-645.
- Goode A., Brady D., Steneck R., and Wahle R. 2019. The brighter side of climate change: how local oceanography amplified a lobster boom in the Gulf of Maine. *Global Change Biology*, 25: 3906–3917.
- Green, B. S., Gardner, C., Hochmuth, J. D., and Linnane, A. 2014. Environmental effects on fished lobsters and crabs. *Reviews in Fish Biology and Fisheries*, 24(2), 613–638. <https://doi.org/10.1007/s11160-014-9350-1>
- Haltuch, M., Punt, A., and Dorn, M. 2009. Evaluating the estimation of fishery management reference points in a variable environment. *Fisheries Research*. 100(1): 42-56.
- Haltuch, M. A., Brooks, E. N., Brodziak, J., Devine, J. A., Johnson, K. F., Klibansky, N., Nash, R. D. M., Payne, M. R., Shertzer, K. W., Subbey, S., and Wells, B. K. 2019. Unraveling the recruitment problem: A review of environmentally-informed forecasting and management strategy evaluation. *Fisheries Research* 217: 198-216.
- Hampton, J., Bigelow, K., and LaBelle, M. 1998. Effect of longline fishing depth, water temperature and dissolved oxygen on bigeye tuna (*Thunnus obesus*) abundance indices. *Oceanics Fisheries Programme*. 16 pages.
- Hanson, J.M. 2009. Predator-prey interactions of American lobster (*Homarus americanus*) in the southern Gulf of St. Lawrence, Canada. *New Zealand Journal of Marine and Freshwater Research*. 43: 69-88.
- Harris, B. and Stokesbury, K. 2006. Shell growth of sea scallops (*Placopecten magellanicus*) in the southern and northern Great South Channel, USA. *ICES Journal of Marine Science*. 63: 811-821.
- Hart, D. 2010. Forecasting methodology (SAMS model). 50th SAW Assessment Report (Appendix B12). Pages 699-701.
- Hart, D. and Chute, T. 2004. Sea scallop, *Placopecten magellanicus*, life history and habitat characteristics. NOAA Technical Memorandum NMFS-NE-189. 32 pages.
- Hart, D. and Chute, T. 2009a. Estimating von Bertalanffy growth parameters from growth increment data using a linear mixed-effects model, with an application to the sea scallop *Placopecten magellanicus*. *ICES Journal of Marine Science*. 66: 2165-2175.
- Hart, D. and Chute, T. 2009b. Verification of Atlantic sea scallop (*Placopecten magellanicus*) shell growth rings by tracking cohorts in fishery closed areas. *Canadian Journal of Fisheries and Aquatic Sciences*. 66: 751-758.

- Hayhoe, K., Edmonds, J., Kopp, R., LeGrande, A., Sanderson, B., Wehner, M., and Wuebbles, D. 2017. Climate models, scenarios, and projections. *In* Climate Science Special Report: Fourth National Climate Assessment, Volume I [Wuebbles, D.J., D.W. Fahey, K.A. Hibbard, D.J. Dokken, B.C. Stewart, and T.K. Maycock (eds.)]. U.S. Global Change Research Program, Washington, DC, USA. pages 133-160.
- Hazen, E., Jorgensen, S., Rykaczewski, R., Bograd, S., Foley, D., Jonsen, I., Shaffer, S. et al. 2012. Predicted habitat shifts of Pacific top predators in a changing climate. *Nature Climate Change*, 3: 234–238.
- Heikkinen, R., Luoto, M., Araujo, M., Virkkala, R., Thuiller, W., and Sykes, M. Methods and uncertainties in bioclimatic envelope modelling under climate change. *Progress in Physical Geography*. 30(6): 751-777.
- Hilborn, R. and Walters, C. J. 1992. *Quantitative Fisheries Stock Assessment- Choice, Dynamics and Uncertainty*. Springer Science & Business Media, Dordrecht. 570 pages.
- Hilborn, R. 2001. The state of the art in stock assessment: where we are and where we are going. *Scientia Marina*. 67(S1):15-20. <https://doi.org/10.3989/scimar.2003.67s115>
- Hill, J. K., Thomas, C. D., Fox, R., Telfer, M. G., Willis, S. G., Asher, J., and Huntley, B. 2002. Responses of butterflies to twentieth century climate warming: implications for future ranges. *Proceedings of the Royal Society of London Series B Biological Sciences*. 269: 2163–2171.
- Hodgdon, C., Tanaka, K., Runnebaum, J., Cao, J., and Chen, Y. 2020. A framework to incorporate environmental effects into stock assessments informed by fishery-independent surveys: a case study with American lobster (*Homarus americanus*). *Canadian Journal of Fisheries and Aquatic Sciences* 77(10): 1700-1710.
- Hodgdon, C. T., Mazur, M. D., Friedland, K. D., Willse, N., and Chen, Y. 2021. Consequences of model assumptions when projecting habitat suitability: a caution of forecasting under uncertainties. *ICES Journal of Marine Science*. 78(6): 2092-2108.
- Hodgdon, C., Shank, B., and Chen, Y. *Submitted*. Developing a Framework to Estimate Dynamic Reference Points Using a Thermally Explicit Spawning Stock Biomass / Recruitment Relationship. *Canadian Journal of Fisheries and Aquatic Sciences*. [Submitted]
- Hollowed, A., Bond, N., Wilderbuer, T., Stockhausen, W., A'mar, T., Beamish, R., Overland, J., and Schirripa, M. 2009. A framework for modelling fish and shellfish responses to future climate change. *ICES Journal of Marine Science*. 66(7): 1584-1594.
- Holsman, K., Ianelli, J., Aydin, K., Punt, A., and Moffitt, E. 2016. A comparison of fisheries biological reference points estimated from temperature-specific multi-species and single-species climate-enhanced stock assessment models. *Deep Sea Research Part II: Topical Studies in Oceanography*. 134: 360-378.
- Holthuis, L.B. 1991. *FAO Species Catalogue. Volume 13, Marine Lobsters of the World*. FAO Fisheries Synopsis. 125(13): 292 pages.
- Howell, P. 2012. The Status of the Southern New England Lobster Stock. *Journal of Shellfish Research*. 31(2): 573-579.

- Huntley, B., Barnard, P., Altwegg, R., Chambers, L., Coetzee, B., Gibson, L., Hockey, P., Hole, D., Midgley, G., Underhill, L., and Willis, S. 2010. Beyond bioclimatic envelopes: dynamic species' range and abundance modelling in the context of climatic change. *Ecography*. 33(3): 621-626.
- Hurtado-Ferro, F., Szuwalski, C., Valero, J., Anderson, S., Cunningham, C., Johnson, K., Licandeo, R., McGilliard, C., Monnahan, C., Muradian, M., Ono, K., Vert-pre, K., Whitten, A., and Punt, A. 2014. Looking in the rear-view mirror: bias and retrospective patterns in integrated, age-structured stock assessment models. *ICES Journal of Marine Science*. 72(1): 99-110.
- James-Pirri, M.J. and Cobb, J.S. 2000. Influence of size and delayed settlement on the recapture rate of newly settled American lobsters *Homarus americanus*. *Marine Ecology Progress Series*. 208: 197-203.
- Intergovernmental Panel on Climate Change (IPCC). 2019. Technical Summary [H.-O. Pörtner, D.C. Roberts, V. Masson-Delmotte, P. Zhai, E. Poloczanska, K. Mintenbeck, M. Tignor, A. Alegría, M. Nicolai, A. Okem, J. Petzold, B. Rama, N.M. Weyer (eds.)]. In: IPCC Special Report on the Ocean and Cryosphere in a Changing Climate [H.- O. Pörtner, D.C. Roberts, V. Masson-Delmotte, P. Zhai, M. Tignor, E. Poloczanska, K. Mintenbeck, A. Alegría, M. Nicolai, A. Okem, J. Petzold, B. Rama, N.M. Weyer (eds.)]. In press.
- Jury, S., Kinnison, M., Howell, W., Watson, W. III. 1994. The behavior of lobsters in response to reduced salinity. *Journal of Experimental Marine Biology and Ecology*. 180: 23-27.
- Jury, S. and Watson, W. III. 2013. Seasonal and sexual differences in the thermal preferences and movements of American lobsters. *Canadian Journal of Fisheries and Aquatic Sciences*. 70(11):1650-1657.
- Kleisner K.M., Fogarty M.J., McGee S., Hare J.A., Moret S., Perretti, C.T., and Saba, V.S. 2017. Marine species distribution shifts on the US Northeast Continental Shelf under continued ocean warming. *Progress in Oceanography*. 153: 24-36.
- Kuparinen, A., Mäntyniemi, S., Hutchings, J., and Kuikkab, S. 2012. Increasing biological realism of fisheries stock assessment: towards hierarchical Bayesian methods. *Environmental Reviews*. 20(2): 135-151.
- Kuriyama, P. T., Ono, K., Hurtado-Ferro, F., Hicks, A. C., Taylor, I. G., Licandeo, R. R., Johnson, K. F., Anderson, S. C., Monnahan, C. C., Rudd, M. B., Stawitz, C. C., and Valero, J. L. 2016. An empirical weight-at-age approach reduces estimation bias compared to modeling parametric growth in integrated, statistical stock assessment models when growth is time varying. *Fisheries Research*. 180:119-127. <https://doi.org/10.1016/j.fishres.2015.09.007>
- Lawler, J., Shafer, S., White, D., Kareiva, P., Maurer, E., Blaustein, A., and Bartlein, P. 2009. Projected climate-induced faunal change in the Western Hemisphere. *Ecology*. 90(3): 588-597.
- Lawton, P. and Lavalli, K. 1995. Postlarval, Juvenile, Adolescent, and Adult Ecology. *Biology of the Lobster Homarus americanus*. 42 pages.

- Le Bris, A., Pershing, A. J., Gaudette, J., Pugh, T. L., and Reardon, K. M. 2017. Multi-scale quantification of the effects of temperature on size at maturity in the American lobster (*Homarus americanus*). *Fisheries Research*. 186:397–406. <https://doi.org/10.1016/j.fishres.2016.09.008>
- Le Bris, A., Mills, K. E., Wahle, R. A., Chen, Y., Alexander, M. A., Allyn, A. J., Schuetz, J. G., Scott, J. D., and Pershing, A. J. 2018. Climate vulnerability and resilience in the most valuable North American fishery. *Proceedings of the National Academy of Sciences*. 115(8):1831–1836. <https://doi.org/10.1073/pnas.1711122115>
- Lehuta, S., Mahévas, S., Petitgas, P., and Pelletier, D. 2010. Combining sensitivity and uncertainty analysis to evaluate the impact of management measures with ISIS-fish: marine protected areas for the bay of biscay anchovy (*Engraulis encrasicolus*) fishery. *ICES Journal of Marine Science*. 67(5):1063-1075.
- Li, B., Tanaka, K., Chen, Y., Brady, D., and Thomas, A. 2017. Assessing the quality of bottom water temperatures from the Finite-Volume Community Ocean Model (FVCOM) in the Northwest Atlantic Shelf region. *Journal of Marine Systems*. 173: 21-30.
- Little, S. A. and Watson, W. H. 2003. Size at maturity of female American lobsters from an estuarine and coastal population. *Journal of Shellfish Research*. 22(3):857–863.
- Little, S. A., and Watson, W. H. 2005. Differences in the size at maturity of female American lobsters, *Homarus americanus*, captured throughout the range of the offshore fishery. *Journal of Crustacean Biology*. 25(4):585–592. <https://doi.org/10.1651/C-2552.1>
- Lorenzen, K. 2016. Toward a new paradigm for growth modeling in fisheries stock assessments: Embracing plasticity and its consequences. *Fisheries Research*. 180:4–22.
- Luoto, M., Pöyry, J., Heikkinen, R., and Saarinen, K. 2005. Uncertainty of bioclimate envelope models based on the geographical distribution of species. *Global Ecology and Biogeography*. 14(6): 575-584.
- MacDonald, B. and Thompson, R. 1985a. Influence of temperature and food availability on the ecological energetics of the giant scallop *Placopecten magellanicus* I: growth rates of shell and somatic tissue. *Marine Ecology Progress Series*. 25: 279-294.
- MacDonald, B. and Thompson, R. 1985b. Influence of temperature and food availability on the ecological energetics of the giant scallop *Placopecten magellanicus* II: reproductive output and total production. *Marine Ecology Progress Series*. 25: 295-303.
- MacDonald, B., Thompson, R., and Bayne, B. 1987. Influence of temperature and food availability on the ecological energetics of the giant scallop *Placopecten magellanicus* IV: reproductive effort, value and cost. *Oecologia*. 72: 550-556.
- Mace, P. M. 1994. Relationships between Common Biological Reference Points Used as Thresholds and Targets of Fisheries Management Strategies. *Canadian Journal of Fisheries and Aquatic Sciences*. 51: 110-122.
- MacLeod, C. 2010. Habitat representativeness score (HRS): a novel concept for objectively assessing the suitability of survey coverage for modelling the distribution of marine

- species. *Journal of the Marine Biological Association of the United Kingdom*. 90(7): 1269-1277.
- Madeira, D., Narciso, L., Cabral, H. N., and Vinagre, C. (2012). Thermal tolerance and potential impacts of climate change on coastal and estuarine organisms. *Journal of Sea Research*, 70, 32–41. <https://doi.org/10.1016/j.seares.2012.03.002>
- Maine Department of Marine Resources (MEDMR). 2016. Historical Maine Fisheries Landings Data [online]. Maine Department of Marine Resources. Available from <https://bit.ly/2rV0yzz>
- Maine Department of Marine Resources (MEDMR). 2006-2012. Ventless Trap Survey. Raw data.
- Maine Department of Marine Resources (MEDMR) and the New Hampshire Fish and Game Department (NHFGD). 2000-2016. Inshore Bottom Trawl Survey. Raw data.
- Mäki-Petäys, A., Muotka, T., Huusko, A., Tikkanen, P., and Kreivi, P. 1997. Seasonal changes in habitat use and preference by juvenile brown trout, *Salmo trutta*, in a northern boreal river. *Canadian Journal of Fisheries and Aquatic Sciences*. 54(3): 520-530.
- Mann, R. and Rudders, D. 2019. Age structure and growth rate in the sea scallop *Placopecten magellanicus*. Virginia Institute of Marine Science, College of William and Mary.
- Mantyka-pringle, C., Martin, T., and Rhodes, J. 2011. Interactions between climate and habitat loss effects on biodiversity: a systematic review and meta-analysis. *Global Change Biology*, 18: 1239–1252.
- Marin, F. and Luquet, G. 2004. Molluscan Shell Proteins. *Comptes Rendus Palevol*. 3(6-7): 469-492.
- Martínez-Rincón, R., Ortega-García, S., and Vaca-Rodríguez, J. 2012. Comparative performance of generalized additive models and boosted regression trees for statistical modeling of incidental catch of wahoo (*Acanthocybium solandri*) in the Mexican tuna purse-seine fishery. *Ecological Modelling*. 233: 20-25.
- Massachusetts Department of Marine Fisheries (MADMF). 1984-2016. Bottom Trawl Survey. Raw data.
- Maunder, M., Sibert, J., Fonteneau, A., Kleiber, P., and Harley, S. 2006. Interpreting catch per unit effort data to assess the status of individual stocks and communities. *ICES Journal of Marine Science*. 63(8): 1373-1385.
- Maunder, M. N., and Punt, A. E. 2013. A review of integrated analysis in fisheries stock assessment. *Fisheries Research*. 142:61–74. <https://doi.org/10.1016/j.fishres.2012.07.025>
- Maunder, M. and Piner, K. 2015. Contemporary fisheries stock assessment: many issues still remain. *ICES Journal of Marine Science*. 72(1): 7-18.
- May, R. 2004. Uses and Abuses of Mathematics in Biology. *Science*. 303(5659): 790-793.

- Mazur, M., Li, B., Chang, J., and Chen, Y. 2018. Using an individual-based model to simulate the Gulf of Maine American lobster (*Homarus americanus*) fishery and evaluate the robustness of current management regulations. *Canadian Journal of Fisheries and Aquatic Sciences*. 76(10):1709-1718. <http://dx.doi.org.wv-o-ursus-proxy02.ursus.maine.edu/10.1139/cjfas-2018-0122>
- Mazur, M. 2020. The Past, Present and Future of Conservation in the Maine Lobster Fishery. *Electronic Theses and Dissertations. PhD diss.* 3209. 170 pages.
- Mazur, M., Friedland, K., McManus, C., and Goode, A. 2020. Dynamic changes in American lobster suitable habitat distribution on the Northeast U.S. Shelf linked to oceanographic conditions. *Fisheries Oceanography*. 29(4): 349-365.
- Mbogga, M., Wang, X., and Hamann, A. 2010. Bioclimate envelope model predictions for natural resource management: dealing with uncertainty. *Journal of Applied Ecology*. 47(4): 731-740.
- McCay, D., Gibson, M., and Cobb, J.S. 2003. Scaling restoration of American lobsters: combined demographic and discounting model for an exploited species. *Marine Ecology Progress Series*. 264: 177-196.
- McLeese, D. and Wilder, D. 1958. The activity and catchability of the lobster (*Homarus americanus*) in relation to temperature. *Canadian Journal of Fisheries and Aquatic Sciences*. 15(6): 1345-1354.
- McMahon T. 1983. *Habitat Suitability Index Models: Coho Salmon*. FWS/OBW-82/10.49. U.S. Fish and Wildlife Service. Ft. Collins, USA. 40 pages.
- McMahan, M. D., Sherwood, G. D., and Grabowski, J. H. 2020. Geographic Variation in Life-History Traits of Black Sea Bass (*Centropristis striata*) During a Rapid Range Expansion. *Frontiers in Marine Science*. 7: 567758.
- Miller, T. J., O'Brien, L., and Fratantoni, P. S. 2018. Temporal and environmental variation in growth and maturity and effects on management reference points of Georges Bank Atlantic cod. *Canadian Journal of Fisheries and Aquatic Sciences*. 75(12):2159-2171. <https://doi.org/10.1139/cjfas-2017-0124>
- Mills, K., Pershing, A., Brown, C., Chen, Y., Chiang, F., Holland, D., Lehuta, S., Nye, J., Sun, J., Thomas, A., and Wahle, R. 2013. Fisheries Management in a Changing Climate: Lessons from the 2012 Ocean Heat Wave in the Northwest Atlantic. *Oceanography*. 26(2): 191-195.
- Mohn, R. 1999. The retrospective problem in sequential population analysis: An investigation using cod fishery and simulated data. *ICES Journal of Marine Science*. 56: 473-488.
- Mountain, D. 2012. Labrador slope water entering the Gulf of Maine—response to the North Atlantic Oscillation. *Continental Shelf Research*. 47: 150-155.
- Mountain, D. and Manning, J. 1994. Seasonal and interannual variability in the properties of the surface waters of the Gulf of Maine. *Continental Shelf Research*. 14(13-14): 1555-1581.

- Myers, R. A. 1998. When do environment-recruitment correlations work? *Reviews in Fish Biology and Fisheries*. 8: 285-305.
- National Marine Fisheries Service (NMFS). 2018. Fisheries of the United States, 2017 [online]. US Department of Commerce, National Marine Fisheries Service, NOAA Current Fishery Statistics No. 2017. Available from <https://bit.ly/34yyjDI>
- National Marine Fisheries Service (NMFS). 2020. Fisheries of the United States, 2018. U.S. Department of Commerce, NOAA Current Fishery Statistics No. 2018 Available at: <https://www.fisheries.noaa.gov/national/commercial-fishing/fisheries-united-states-2018>
- New England Fishery Management Council (NEFSC) Scientific and Statistical Committee (SSC). 2021. Terms of Reference – Overfishing levels (OFLs) and acceptable biological catch (ABC) recommendations for Atlantic sea scallops for fishing year 2022 and 2023 (default). *Memorandum*. 4 pages.
- New Jersey Department of Environmental Protection (NJDEP). 1988-2016. Trawl Survey. Raw Data.
- Northeast Fisheries Science Center. 1996. Report of the 22nd Northeast Regional Stock Assessment Workshop (22nd SAW): Stock Assessment Review Committee (SARC) consensus summary of assessments. Northeast Fisheries Science Center Ref. Doc. 96-13; 242 pages.
- Northeast Fisheries Science Center (NEFSC). 1984-2016. Bottom Trawl Survey. Raw data.
- Northeast Fisheries Science Center (NEFSC). 2006. National Oceanic and Atmospheric Administration (NOAA) Statistical Areas. Shapefile.
- Northeast Fisheries Science Center (NEFSC). 2018. 65th Northeast Regional Stock Assessment Workshop (65th SAW) Assessment Summary Report. US Department Commerce, Northeast Fisheries Science Center Reference Document. 18-08; 38 pages. Available from: <http://www.nefsc.noaa.gov/publications/>
- O'Brien, R. 2007. A Caution Regarding Rules of Thumb for Variance Inflation Factors. *Quality and Quantity*. 41(5): 673-690.
- O'Leary, C. A., Thorson, J. T., Miller, T. J., and Nye, J. A. 2020. Comparison of multiple approaches to calculate time-varying biological reference points in climate-linked population-dynamics models. *ICES Journal of Marine Science*. 77(3): 930-941.
- Perry A., Low P., Ellis J., and Reynolds J. 2005. Climate change and distribution shifts in marine fishes. *Science*, 308: 1912–1915.
- Pershing, A., Alexander, M., Hernandez, C., Kerr, L., Le Bris, A., Mills, K., Nye, J., Record, N., Scannell, H., Scott, J., Sherwood, G., and Thomas, A. 2015. Slow adaptation in the face of rapid warming leads to collapse of the Gulf of Maine cod fishery. *Science*. 350(6262): 809-812.
- Peterson, A. and Nakazawa, Y. 2008. Environmental data sets matter in ecological niche modelling: an example with *Solenopsis invicta* and *Solenopsis richteri*. *Global Ecology and Biogeography*. 17(1): 135-144.

- Petrie, B. and Drinkwater, K. 1993. Temperature and salinity variability on the Scotian Shelf and in the Gulf of Maine 1945–1990. *Journal of Geophysical Research: Oceans*. 98(11): 20079–20089.
- Pilditch, C. and Grant, J. 1999. Effect of temperature fluctuations and food supply on the growth and metabolism of juvenile sea scallops (*Placopecten magellanicus*). *Marine Biology*. 134(2): 235–248.
- Plagányi, É.E., Haywood, M.D.E., Gorton, R.J., Siple, M.C., and Deng, R.A. 2019. Management implications of modelling fisheries recruitment. *Fisheries Research* 217: 169–184.
- Planque, B. and Frédou, T. 1999. Temperature and the recruitment of Atlantic cod (*Gadus morhua*). *Canadian Journal of Fisheries and Aquatic Sciences*. 56: 2069–2077.
- Pratchett, M., Beruman, M., Marnane, M., Eagle, J., and Pratchett, D. 2008. Habitat associations of juvenile versus adult butterflyfishes. *Coral Reefs*. 27: 541–551.
- Punt, A. E. 2003. The performance of a size-structured stock assessment method in the face of spatial heterogeneity in growth. *Fisheries Research*. 65(1–3):391–409.
- Punt, A. E., Huang, T., and Maunder, M. N. 2013. Review of integrated size-structured models for stock assessment of hard-to-age crustacean and mollusc species. *ICES Journal of Marine Science*. 70(1):16–33. <https://doi.org/10.1093/icesjms/fss185>
- Punt, A. E., A'mar, T., Bond, N. A., Butterworth, D. S., de Moor, C. L., De Oliveira, J. A. A., Haltuch, M. A., Hollowed, A. B., and Szuwalski, C. 2014. Fisheries management under climate and environmental uncertainty: control rules and performance simulation. *ICES Journal of Marine Science*. 71(8):2208–2220. <https://doi.org/10.1093/icesjms/fst057>
- Reynolds, R. W., Smith, T. M., Liu, C., Chelton, D. B., Casey, K. S., and Schlabach, M. G. 2007. Daily high-resolution-blended analyses for sea surface temperature. *Journal of Climate*. 20: 5473–5496.
- Rheuban, J., Doney, S., Cooley, S., and Hart, D. 2018. Projected impacts of future climate change, ocean acidification, and management on the US Atlantic sea scallop (*Placopecten magellanicus*) fishery. *PLoS ONE*. 13(9).
- Rhode Island Department of Environmental Management (RIDEM). 1981–2016. Coastal Trawl Survey. Raw Data.
- Richards, L. and Schnute, J. 1986. An experimental and statistical approach to the question: is CPUE an index of abundance? *Canadian Journal of Fisheries and Aquatic Sciences*. 43: 1214–1227.
- Ricker, W. E. 1954. Stock and recruitment. *Journal of the Fisheries Research Board of Canada*. 11: 559–623.
- Roberts, C. 2007. *The Unnatural History of the Sea* (Book). Island Press. 456 pages.
- Rogers, L., Griffin, R., Young, T., Fuller, E., St. Martin, K., and Pinsky, M. 2019. Shifting habitats expose fishing communities to risk under climate change. *Nature Climate Change*, 9: 512–516.

- Roloff, G. and Kernohan, B. 1999. Evaluating Reliability of Habitat Suitability Index Models. *Wildlife Society Bulletin*. 27(4): 973-985.
- Rosenberg, A. A., and Restrepo, V. R. 1994. Uncertainty and Risk Evaluation in Stock Assessment Advice for U.S. Marine Fisheries. *Canadian Journal of Fisheries and Aquatic Sciences*. 51(12), 2715-2720. <https://doi-org.wv-o-ursus-proxy02.ursus.maine.edu/10.1139/f94-271>
- Saba, V., Griffies, S., Anderson, W., Winton, M., Alexander, M., Delworth, T., Hare, J., Harrison, M., Rosati, A., Vecchi, G., and Zhang, R. 2016. Enhanced warming of the Northwest Atlantic Ocean under climate change. *Journal of Geophysical Research: Oceans*. 121: 118-132.
- Saliccioli, J. D., Crutain, Y., Komorowski, M., and Marshall, D. C. 2016. Sensitivity Analysis and Model Validation. *In: Secondary Analysis of Electronic Health Records*. Springer, Cham. https://doi.org/10.1007/978-3-319-43742-2_17
- Saltelli, A., Aleksankina, K., Becker, W., Fennell, P., Ferretti, F., Holst, N., Li, S., and Wu, Q. 2019. Why so many published sensitivity analyses are false: A systematic review of sensitivity analysis practices. *Environmental Modelling and Software*. 114:29-39. <https://doi.org/10.1016/j.envsoft.2019.01.012>
- Schick, D. F. and Feindel, S. C. 2005. Maine Scallop Fishery: Monitoring and Enhancement. Final Report to the Northeast Consortium. 73 pages.
- Schuetz J., Mills K., Allyn A., Stamieszkin K., Bris A., and Pershing A. 2019. Complex patterns of temperature sensitivity, not ecological traits, dictate diverse species responses to climate change. *Ecography*, 42: 111–124.
- Shelton, A., Thorson, J., Ward, E., and Feist, B. 2014. Spatial semiparametric models improve estimates of species abundance and distribution. *Canadian Journal of Fisheries and Aquatic Sciences*. 71(11): 1655-1666.
- Sissenwine, M. P. and Shepard, J. G. 1987. An Alternative Perspective on Recruitment Overfishing and Biological Reference Points. *Canadian Journal of Fisheries and Aquatic Sciences*. 44: 913-918.
- Skern-Mauritzen, M., Ottersen, G., Handegard, N., Huse, G., Dingsør, G., Stenseth, N., and Kjesbu, O. 2016. Ecosystem processes are rarely included in tactical fisheries management. *Fish and Fisheries*. 17(1): 165-175.
- Slezak F. D., Suárez, C., Cecchi, G. A., Marshall, G., and Stolovitzky, G. 2010. When the Optimal Is Not the Best: Parameter Estimation in Complex Biological Models. *PLoS ONE*. 5(10):e13283. <https://doi.org/10.1371/journal.pone.0013283>
- Spees, J., Chang, S., Snyder, M., and Chang, E. 2002. Thermal acclimation and stress in the American lobster, *Homarus americanus*: equivalent temperature shifts elicit unique gene expression patterns for molecular chaperones and polyubiquitin. *Cell Stress and Chaperones*. 7(1): 97-106.

- Stanley, R. R. E., DiBacco, C., Lowen, B., Beiko, R. G., Jeffery, N. W., Van Wyngaarden, M., Bentzen, P., Brickman, D., Benestan, L., Bernatchez, L., Johnson, C., Snelgrove, P. V. R., Wang, Z., Wringe, B. F., and Bradbury, I. R.. 2018. A climate-associated multispecies cryptic cline in the northwest Atlantic. *Science Advances*. 4(3): 7 pages.
- Staples, K., Chen, Y., Townsend, D., and Brady, D. 2019. Spatiotemporal variability in the phenology of the initial intra-annual molt of American lobster (*Homarus americanus* Milne Edwards, 1837) and its relationship with bottom temperatures in a changing Gulf of Maine. *Fisheries Oceanography*, 28: 468–485.
- Stebbing, A., Turk, S., Wheeler, A., and Clarke, K. 2002. Immigration of southern fish species to south-west England linked to warming of the North Atlantic (1960–2001). *Journal of the Marine Biological Association of the United Kingdom*. 82(2): 177-180.
- Stewart, P. and Arnold, S. 1994. Environmental requirements of the sea scallop (*Placopecten magellanicus*) in eastern Canada and its response to human impacts. *Canadian Technical Report of Fisheries and Aquatic Sciences*. 2005:1-36.
- Stoner, A. W. 2004. Effects of environmental variables on fish feeding ecology: implications for the performance of baited fishing gear and stock assessment. *Journal of Fish Biology*. 65(6): 1445-1471.
- Subbey, S., Devine, J. A., Schaarschmidt, U., and Nash, R. D. M. 2014. Modelling and forecasting stock–recruitment: current and future perspectives. *ICES Journal of Marine Science*. 71(8): 2307–2322.
- Tanaka, K. and Chen, Y. 2015. Spatiotemporal variability of suitable habitat for American lobster (*Homarus americanus*) in Long Island Sound. *Journal of Shellfish Research*. 34: 531-543.
- Tanaka, K. and Chen, Y. 2016. Modeling spatiotemporal variability of the bioclimate envelope of *Homarus americanus* in the coastal waters of Maine and New Hampshire. *Fisheries Research*. 177: 137-152.
- Tanaka, K., Chang, J., Xue, Y., Li, Z., Jacobson, L., and Chen, Y. 2018. Mesoscale climatic impacts on the distribution of *Homarus americanus* in the US inshore Gulf of Maine. *Canadian Journal of Fisheries and Aquatic Sciences*. 18 pages.
- Tanaka K., Cao J., Shank B., Truesdell S., Mazur M., Xu L., and Chen Y. 2019. A model-based approach to incorporate environmental variability into assessment of a commercial fishery: a case study with the American lobster fishery in the Gulf of Maine and Georges Bank. *ICES Journal of Marine Science*. 76: 884–896.
- Tang, Q. 1985. Modification of the Ricker stock recruitment model to account for environmentally induced variation in recruitment with particular reference to the blue crab fishery in Chesapeake Bay. *Fisheries Research*. 3: 13-21.
- Thorson, J. T., Shelton, A. O., Ward, E. J., and Skaug, H. J. 2015. Geostatistical delta generalized linear mixed models improve precision for estimated abundance indices for West Coast groundfishes. *ICES Journal of Marine Science*. 72(5): 1297–1310.

- Thorson, J. T., and Barnett, L. A. K. 2017. Comparing estimates of abundance trends and distribution shifts using single- and multispecies models of fishes and biogenic habitat. *ICES Journal of Marine Science*. 74(5): 1311-1321.
- Thorson, J. 2019. Guidance for decisions using the Vector Autoregressive Spatio-Temporal (VAST) package in stock, ecosystem, habitat and climate assessments. *Fisheries Research*. 210: 143-161.
- Thouzeau, G., Robert, G., and Smith, S. 1991. Spatial variability in distribution and growth of juvenile and adult sea scallops *Placopecten magellanicus* (Gmelin) on eastern Georges Bank (Northwest Atlantic). *Marine Ecology Progress Series*. 74: 205-218.
- Tommasi, D., Stock, C. A., Pegion, K., Vecchi, G. A., Methot, R. D., Alexander, M. A., Checkley, D. M. Jr. 2017. Improved management of small pelagic fisheries through seasonal climate prediction. *Ecological Applications* 27: 378-388.
- Townsend, D., McGillicuddy, D. Jr, Thomas, M., and Rebeck, N. 2014. Nutrients and water masses in the Gulf of Maine - Georges Bank region: Variability and importance to blooms of the toxic dinoflagellate *Alexandrium fundyense*. *Deep-Sea Research Part II Topical Studies in Oceanography*. 103: 238-263.
- Tremblay, M. and Smith, S. 2002. Lobster (*Homarus americanus*) catchability in different habitats in late spring and early fall. *Marine and Freshwater Research*. 52(8): 1321-1331.
- Truesdell, S. 2014. Distribution, Population Dynamics and Stock Assessment for the Atlantic Sea Scallop (*Placopecten magellanicus*) in the Northeast US. *PhD diss.* University of Maine, Orono, Maine.
- Uzmann, J., Cooper, R., and Pecci, K. 1977. Migration and dispersion of tagged American lobsters, *Homarus americanus*, on the southern New England continental shelf. U.S. Department of Commerce NOAA Technical Report, National Marine Fisheries Service (NMFS). SSRF 705.
- Van Toor, M., Jaberg, C., and Safi, K. 2011. Integrating sex-specific habitat use for conservation using habitat suitability models. *Animal Conservation*. 14(5): 512-520.
- Vert-pre, K., Amoroso, R., Jensen, O., and Hilborn, R. 2013. Frequency and intensity of productivity regime shifts in marine fish stocks. *Proceedings of the National Academy of Sciences (PNAS)*. 110(5): 1779-1784.
- Virginia Institute of Marine Science. 2007-2016. Northeast Area Monitoring and Assessment Program. Raw Data.
- Waddy, S. L. and Aiken, D. E. 1991. Egg production in the American lobster, *Homarus americanus*. In *Crustacean Egg Production*. CRC Press. 24 pages.
- Wahle, R. A. and Steneck, R. S. 1991. Recruitment habitats and nursery grounds of the American lobster *Homarus americanus*: a demographic bottleneck? *Marine Ecology Progress Series* 69: 231-243.

- Wahle, R., Tully, O., and O'Donovan, V. 1996. Lipofuscin as an indicator of age in crustaceans: analysis of the pigment in the American lobster *Homarus americanus*. *Marine Ecology Progress Series*. 138: 117-123.
- Wahle, R. A. 2003. Revealing stock–recruitment relationships in lobsters and crabs: is experimental ecology the key? *Fisheries Research*. 65: 3–32.
- Wahle, R. A., and Fogarty, M. J. 2006. Growth and Development: Understanding and modelling growth variability in lobsters. *In Lobsters: Biology, Management Aquaculture and Fisheries*. Edited by Philips, B.F. Wiley-Blackwell, West Sussex, UK. pp 1-44.
- Wahle, R. A., Cobb, J. S., Incze, L., Lawton, P., Gibson, M., Glenn, R., Wilson, C., and Tremblay, J. 2010. The American lobster settlement index at 20 years: looking back - looking ahead. *Journal of the Marine Biological Association of India*. 52(2): 180-188.
- Wagner, M., Campbell, R., Boudreau, C., and Durbin, E. 2001. Nucleic acids and growth of *Calinus finmarchicus* in the laboratory under different food and temperature conditions. *Marine Ecology Progress Series*. 221: 185-197.
- Walters, C. 1998. Designing fisheries management systems that do not depend upon accurate stock assessment. In: Pitcher, T. J., Pauly D., and Hart P. J. B. *Reinventing Fisheries Management*. Fish & Fisheries Series. 23. Springer, Dordrecht.
- Wanamaker Jr, A., Kreutz, K., Schöne, B., Pettigrew, N., Borns, H., Introne, D., Belknap, D., Maasch, K., and Feindel, S. 2007. Coupled North Atlantic slope water forcing on Gulf of Maine temperatures over the past millennium. *Climate Dynamics*. 31(2-3): 183-194.
- Watling, J., Brandt, L., Mazzotti, F., and Romanach, S. 2013. *Use and Interpretation of Climate Envelope Models: A Practical Guide*. University of Florida, Gainesville, FL. 43 pages.
- Weiss, M., Curran, P., Peterson, B., and Gobler, C. 2007. The influence of plankton composition and water quality on hard clam (*Mercenaria mercenaria* L.) populations across Long Island's south shore lagoon estuaries (New York, USA). *Journal of Experimental Marine Biology and Ecology*. 345: 12-25.
- Wiens, J., Stralberg, D., Jongsomjit, D., Howell, C., and Snyder, M. 2009. Niches, models, and climate change: Assessing the assumptions and uncertainties. *PNAS*. 106(S2): 19729-19736.
- Wilberg, M., Thorson, J., Linton, B., and Berkson, J. 2009. Incorporating time-varying catchability into assessment models. *Reviews in Fisheries Science*. 18(1): 7-24.
- Xu, H., Miller, T. J., Hameed, S., Alade, L. A., and Nye, J. A. 2017. Evaluating the utility of the Gulf Stream Index for predicting recruitment of Southern New England-Mid Atlantic yellowtail flounder. *Fisheries Oceanography* 27: 85-95.
- Xue, H., Incze, L., Xu, D., Wolff, N., and Pettigrew, N. 2008. Connectivity of lobster populations in the coastal Gulf of Maine: Part I: Circulation and larval transport potential. *Ecological modelling*. 210(1-2): 193-211.
- Xue, Y., Guan, L., Tanaka, K., Li, Z., Chen, Y., and Ren, Y. 2017. Evaluating effects of rescaling and weighting data on habitat suitability modeling. *Fisheries Research*. 188: 84-94.

- Yu, H., Jiao, Y., and Carstensen, L. 2013. Performance comparison between spatial interpolation and GLM/GAM in estimating relative abundance indices through a simulation study. *Fisheries Research*. 147: 186-195.
- Zhang, Y., Chen, Y, and Chang, Y. 2011. Estimating biological reference points using individual-based per-recruit models for the Gulf of Maine American lobster, *Homarus americanus*, fishery. *Fisheries Research*. 108(2-3):385-392. <https://doi.org/10.1016/j.fishres.2011.01.014>
- Zhao, X., Ding, P., and Pang, J. 2019. Implications of ocean bottom temperatures on the catchability of American lobster. *E3S Web of Conferences*. Vol 79. 4 pages.
- Zuur, A. F., Leno, E. N., Walker, N., Saveliev, A. A., and Smith, G. M. 2009. *Mixed Effects Models and Extensions in Ecology with R*. Springer-Verlag New York. 574 pages.

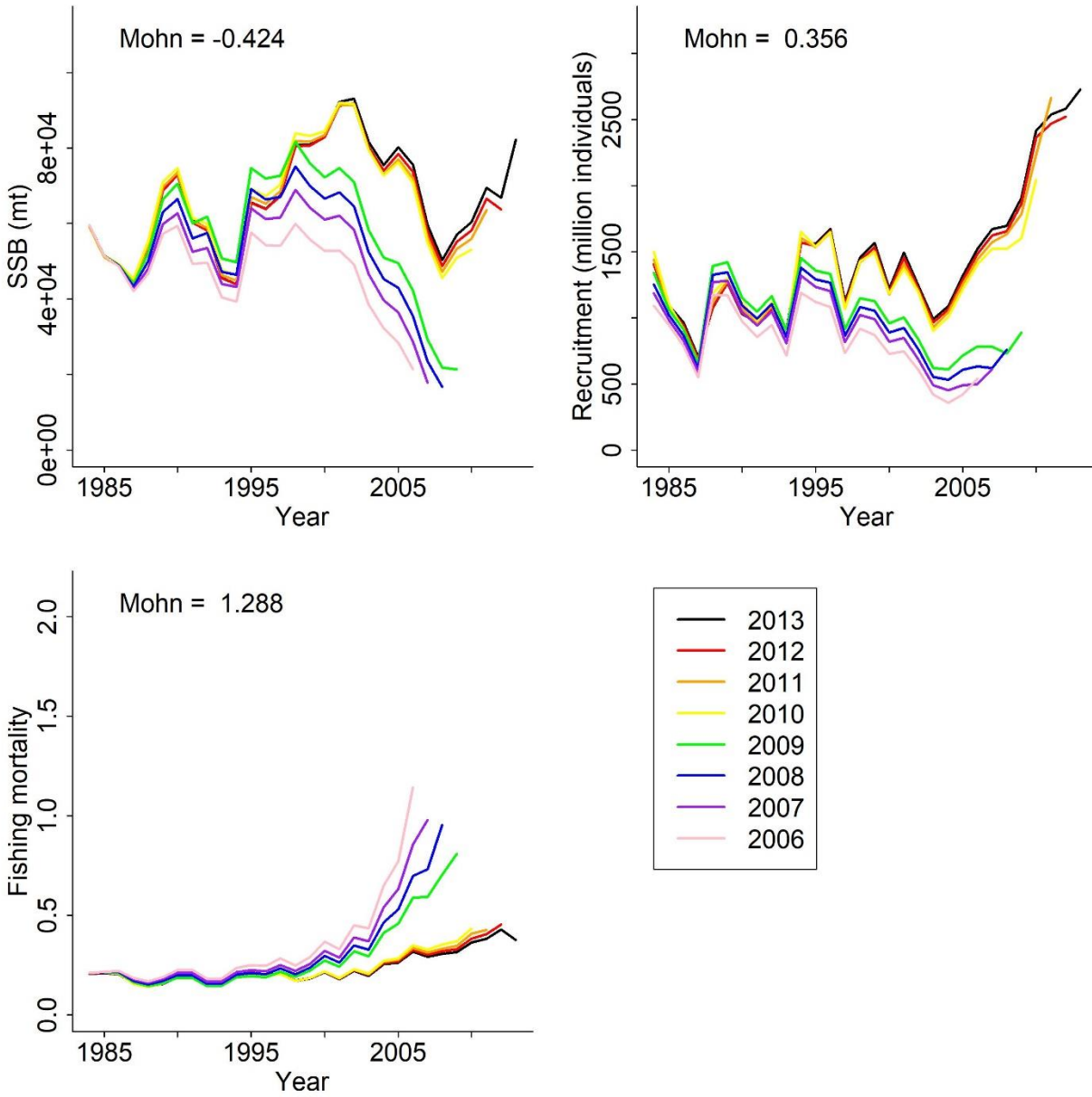


Figure S3.1. Retrospective patterns of spawning stock biomass (SSB) in metric tons (mt), recruitment in millions of individuals, and fishing mortality for UMM Scenario 1 (the base case). Mohn's rho values (Mohn) are displayed for each parameter and were calculated from seven-year peels.

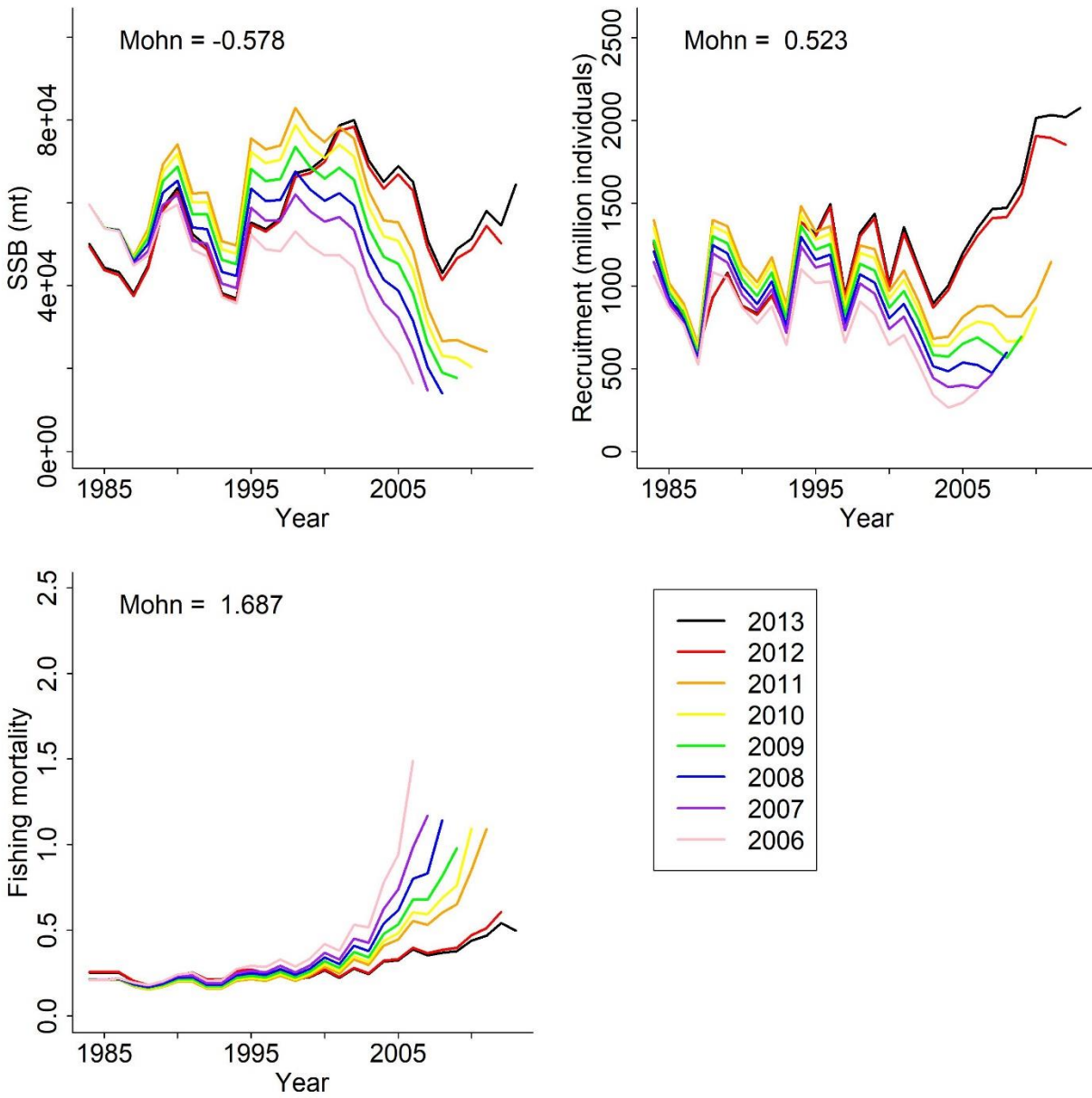


Figure S3.2. Retrospective patterns of spawning stock biomass (SSB) in metric tons (mt), recruitment in millions of individuals, and fishing mortality for UMM Scenario 2. Mohn's rho values (Mohn) are displayed for each parameter and were calculated from seven-year peels.

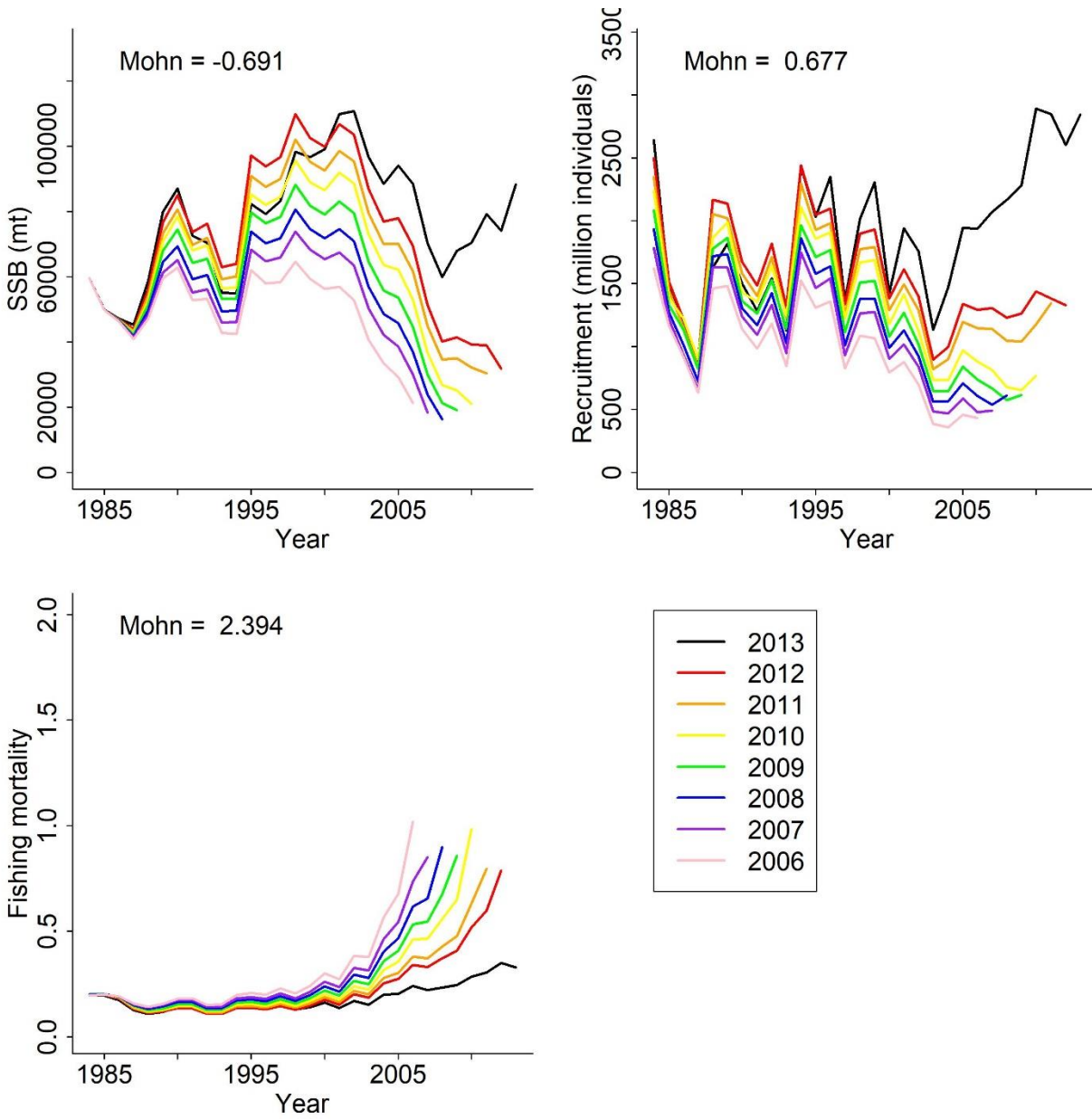


Figure S3.3. Retrospective patterns of spawning stock biomass (SSB) in metric tons (mt), recruitment in millions of individuals, and fishing mortality for UMM Scenario 3. Mohn's rho values (Mohn) are displayed for each parameter and were calculated from seven-year peels.

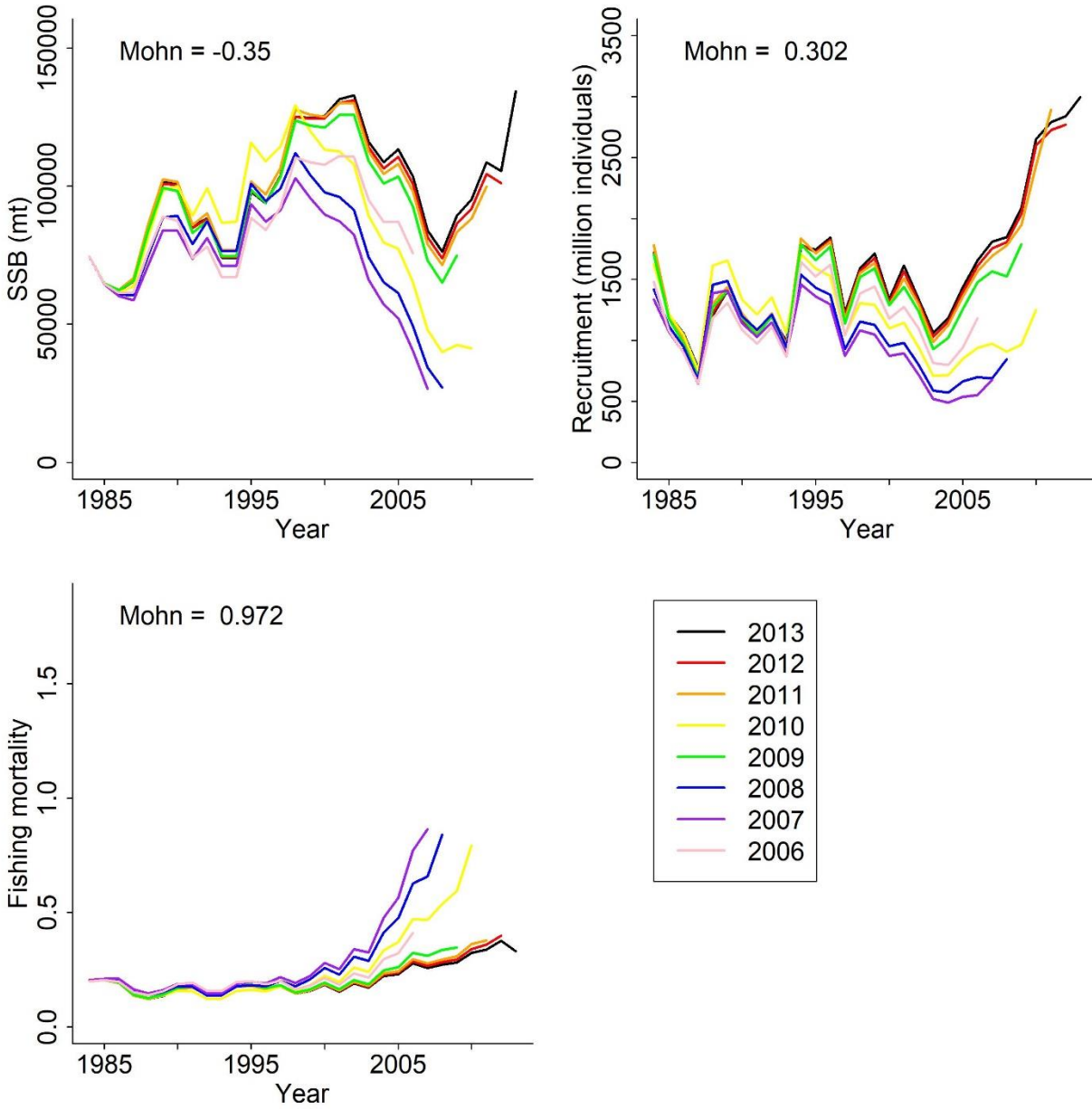


Figure S3.4. Retrospective patterns of spawning stock biomass (SSB) in metric tons (mt), recruitment in millions of individuals, and fishing mortality for UMM Scenario 4. Mohn's rho values (Mohn) are displayed for each parameter and were calculated from seven-year peels.

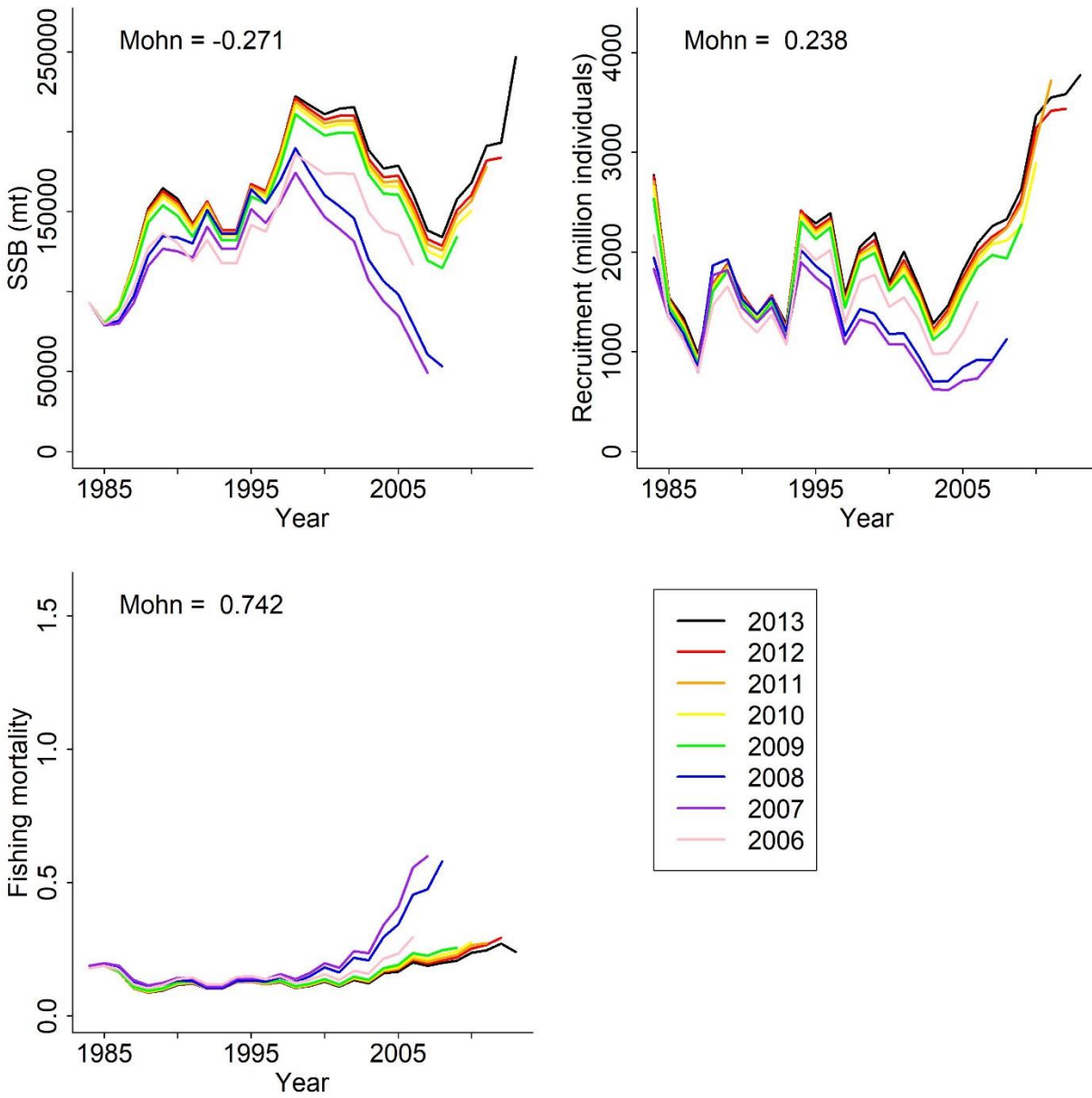


Figure S3.5. Retrospective patterns of spawning stock biomass (SSB) in metric tons (mt), recruitment in millions of individuals, and fishing mortality for UMM Scenario 5. Mohn's rho values (Mohn) are displayed for each parameter and were calculated from seven-year peels.

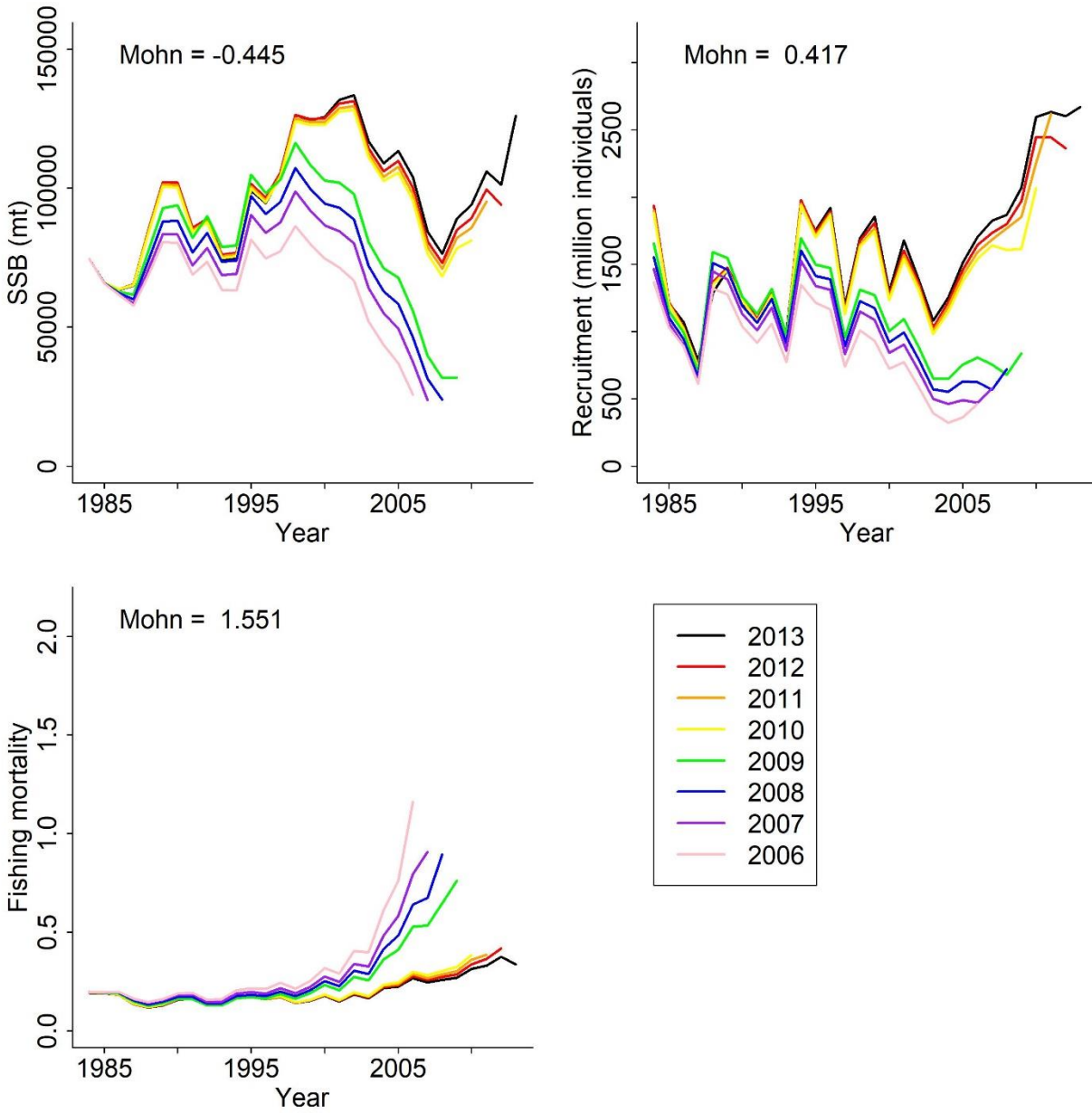


Figure S3.6. Retrospective patterns of spawning stock biomass (SSB) in metric tons (mt), recruitment in millions of individuals, and fishing mortality for UMM Scenario 6. Mohn's rho values (Mohn) are displayed for each parameter and were calculated from seven-year peels.

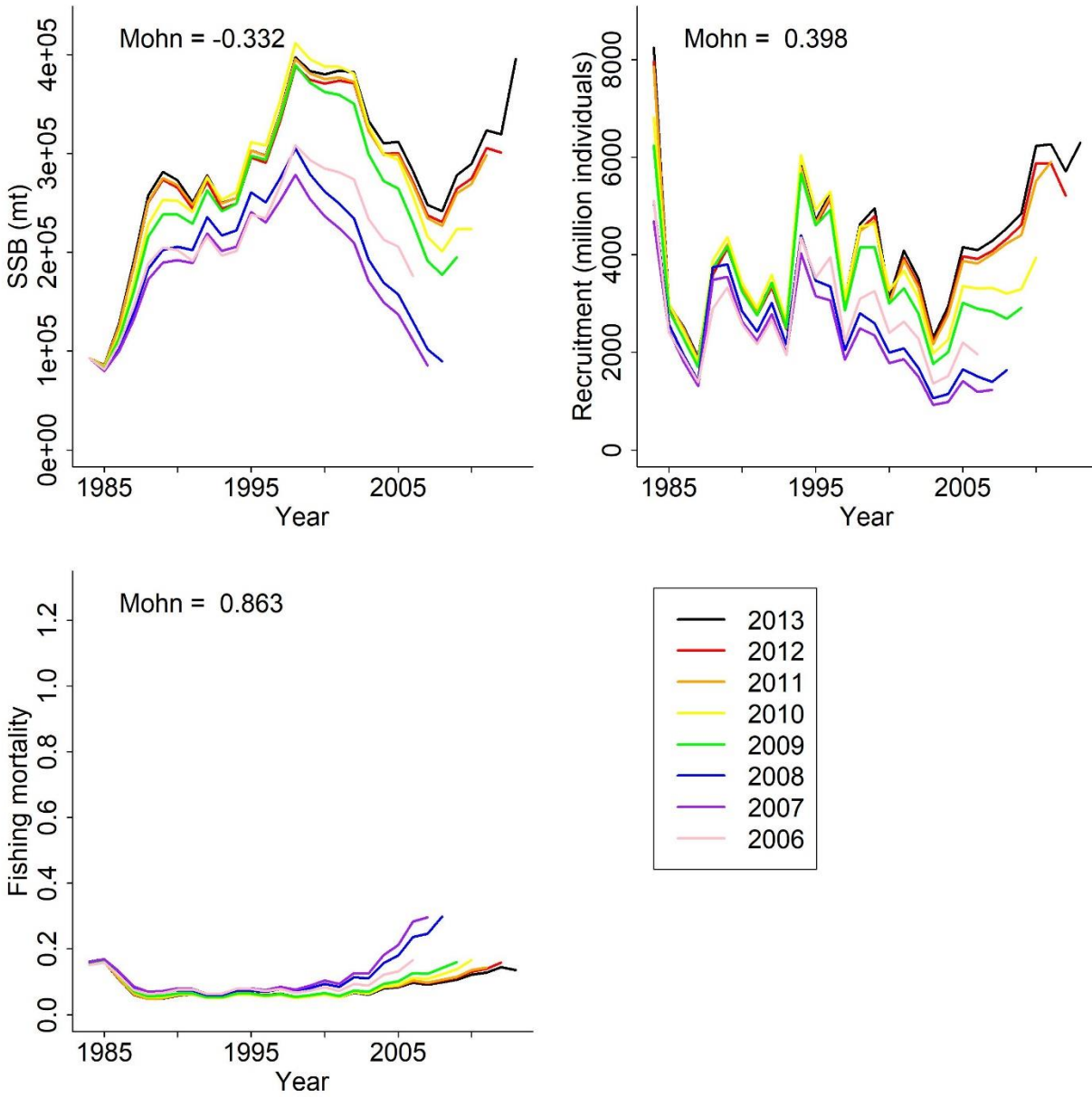


Figure S3.7. Retrospective patterns of spawning stock biomass (SSB) in metric tons (mt), recruitment in millions of individuals, and fishing mortality for UMM Scenario 7. Mohn's rho values (Mohn) are displayed for each parameter and were calculated from seven-year peels.

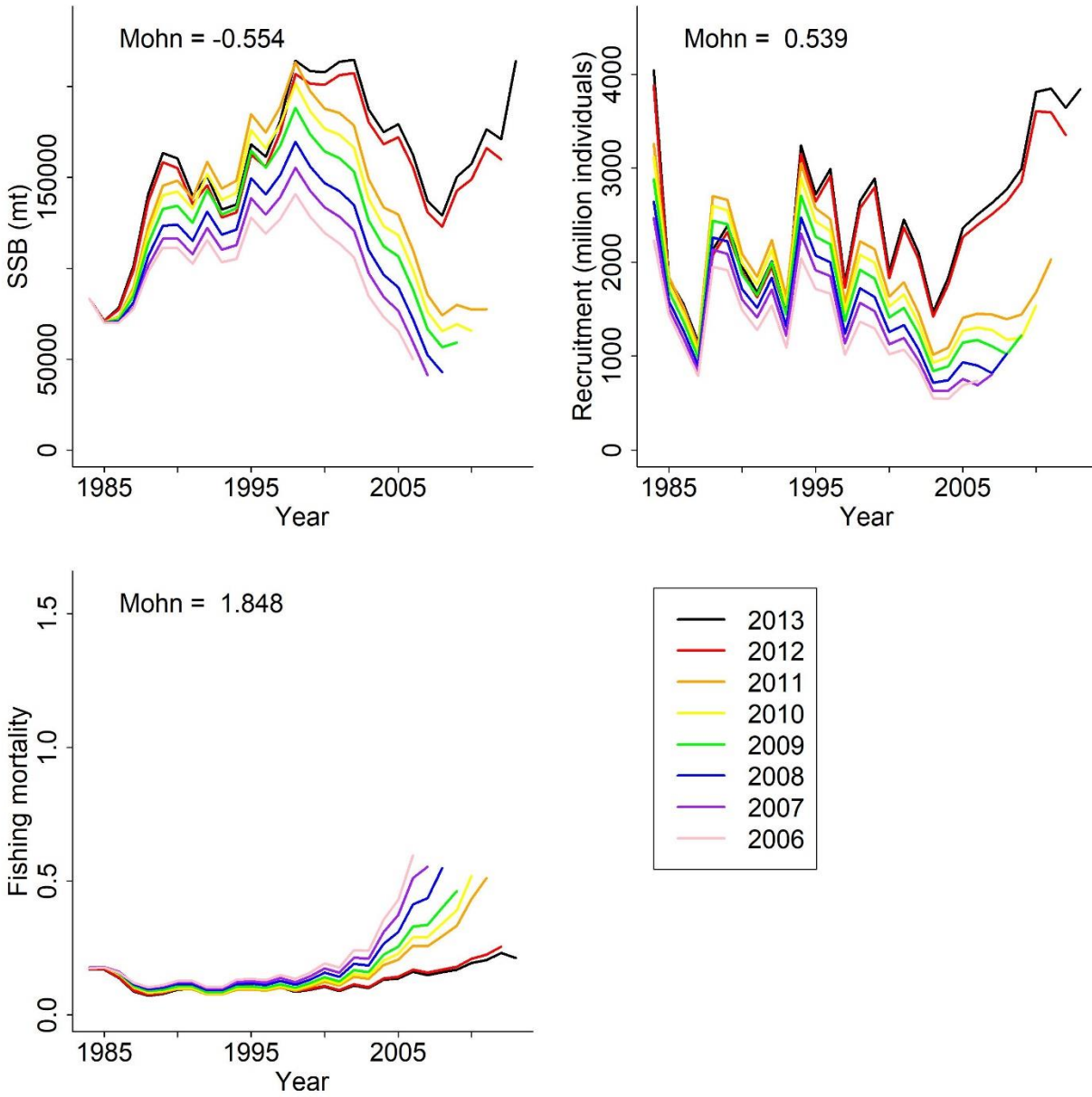


Figure S3.8. Retrospective patterns of spawning stock biomass (SSB) in metric tons (mt), recruitment in millions of individuals, and fishing mortality for the sensitivity analysis of growth and SAM. Mohn's rho values (Mohn) are displayed for each parameter and were calculated from seven-year peels. These plots represent a growth shift of 1.5 and a SAM of 82.41 mm.

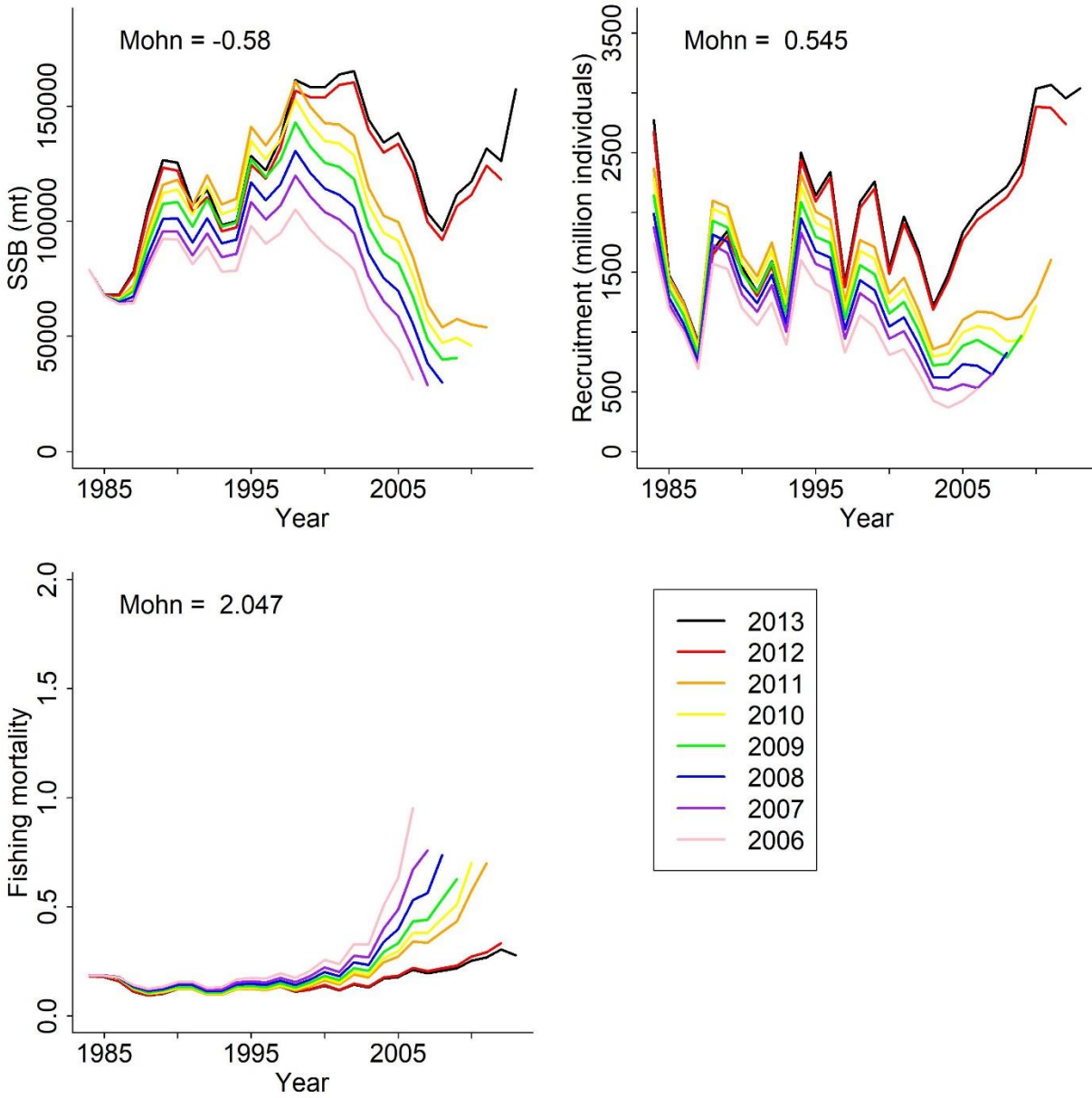


Figure S3.9. Retrospective patterns of spawning stock biomass (SSB) in metric tons (mt), recruitment in millions of individuals, and fishing mortality for the sensitivity analysis of growth and SAM. Mohn's rho values (Mohn) are displayed for each parameter and were calculated from seven-year peels. These plots represent a growth shift of 1.25 and a SAM of 83.81 mm.

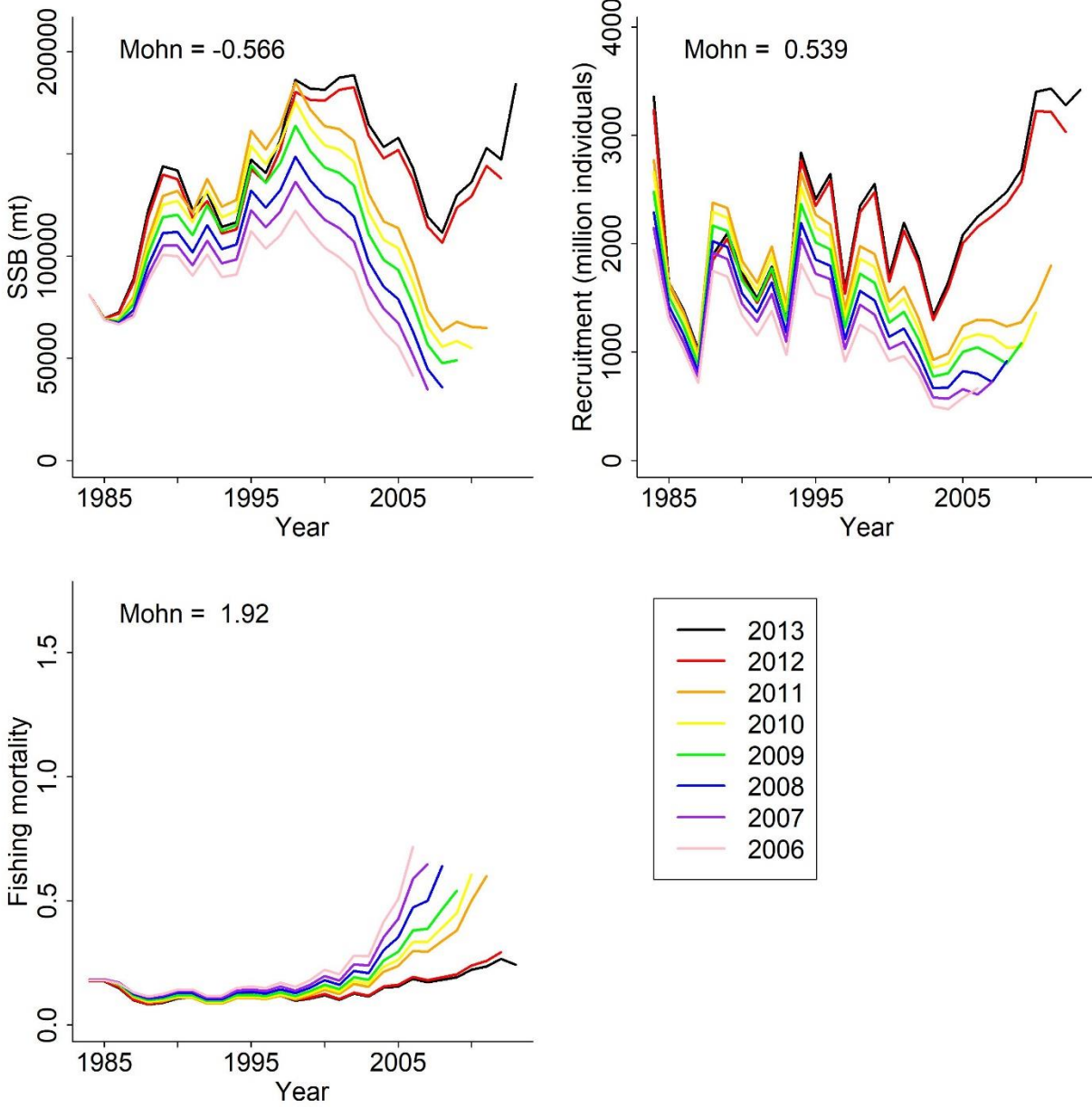


Figure S3.10. Retrospective patterns of spawning stock biomass (SSB) in metric tons (mt), recruitment in millions of individuals, and fishing mortality for the sensitivity analysis of growth and SAM. Mohn's rho values (Mohn) are displayed for each parameter and were calculated from seven-year peels. These plots represent a growth shift of 1.375 and a SAM of 83.11 mm.

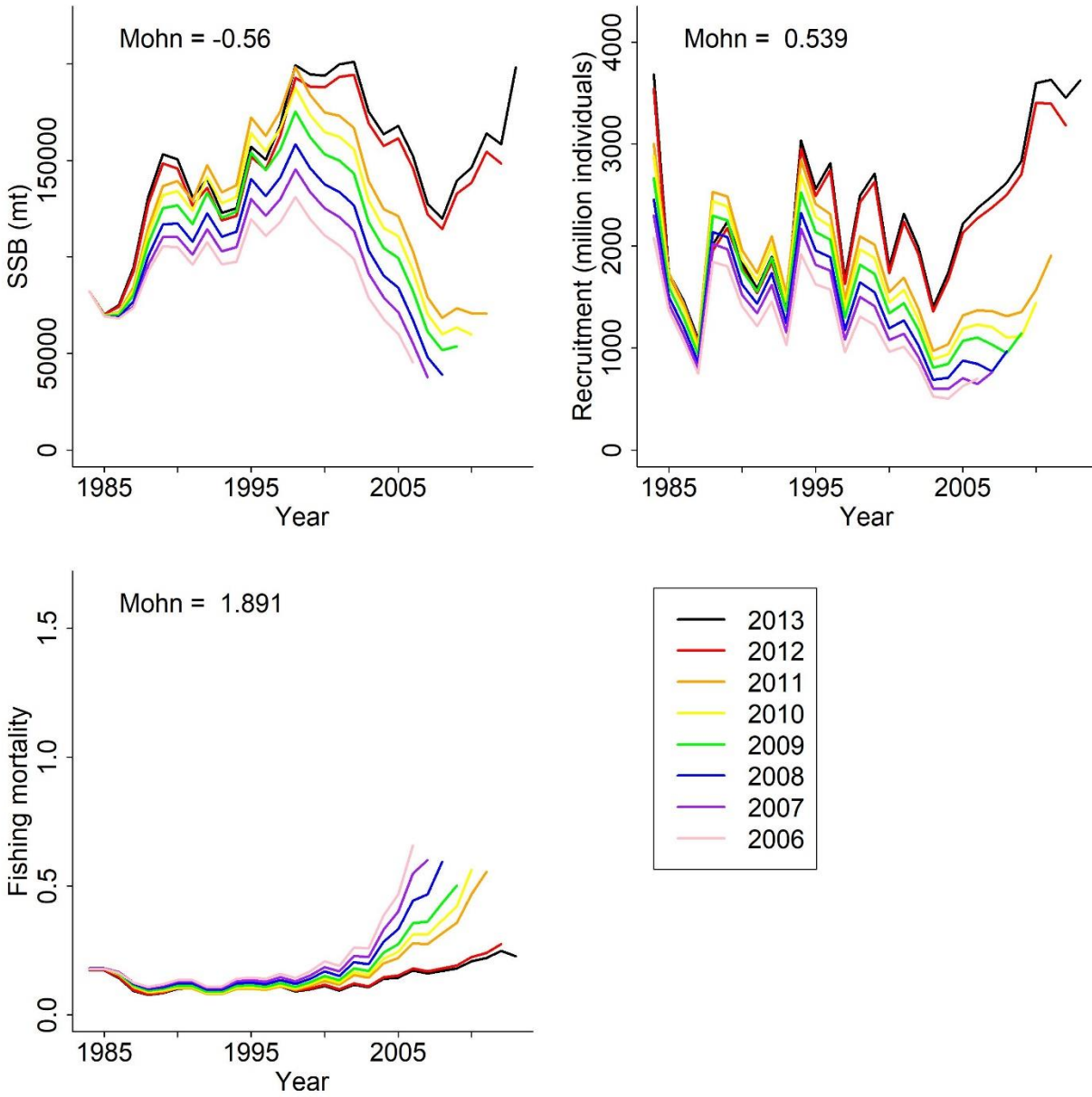


Figure S3.11. Retrospective patterns of spawning stock biomass (SSB) in metric tons (mt), recruitment in millions of individuals, and fishing mortality for the sensitivity analysis of growth and SAM. Mohn's rho values (Mohn) are displayed for each parameter and were calculated from seven-year peels. These plots represent a growth shift of 1.4375 and a SAM of 82.76 mm.

APPENDIX B

SUPPLEMENTARY MATERIAL FOR CHAPTER 4

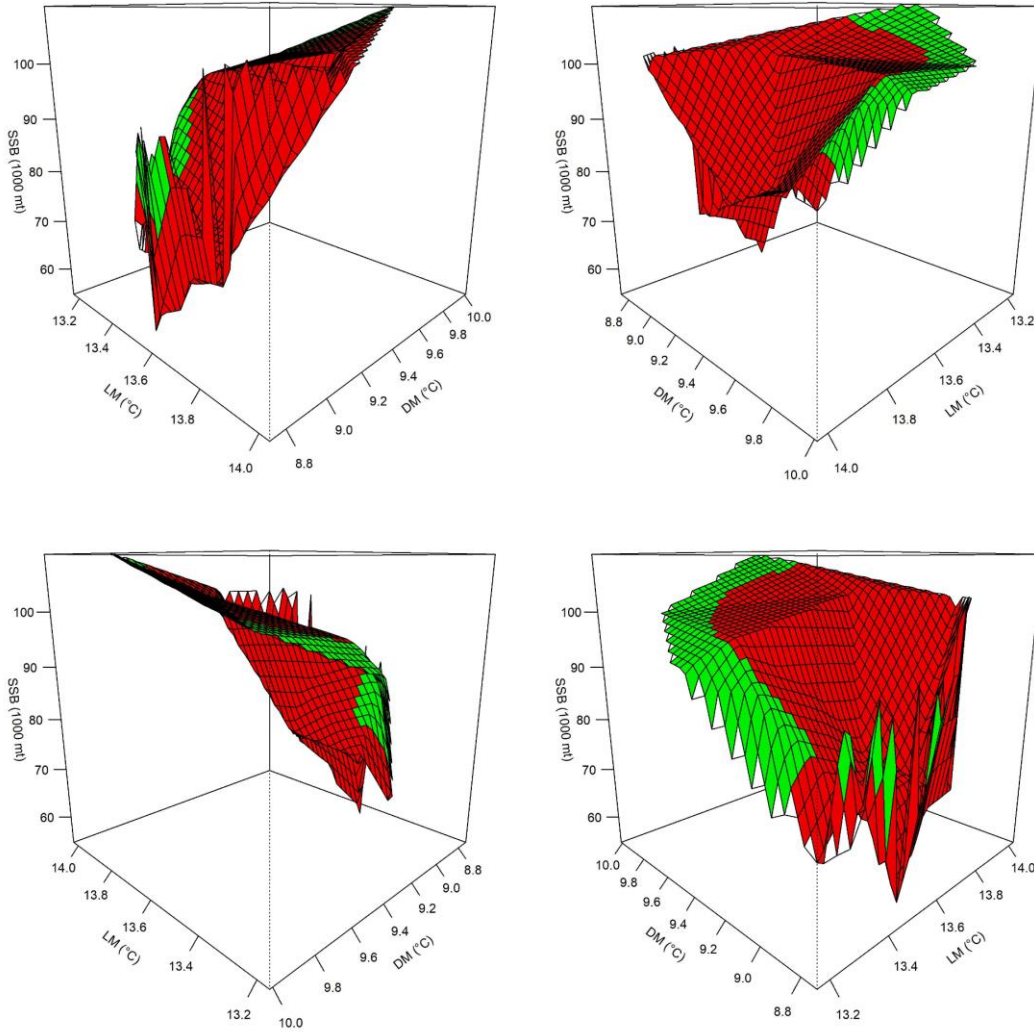


Figure S4.1. Surface plots of the combined effects of spawning stock biomass (SSB), LM, and DM on recruitment (R). Red represents areas where the combined effects from SSB, LM, and DM yield R values lower than the reference point (75th percentile of R 1984-2013; calculated as 557 million individuals) and green represents areas where the combined effects from SSB, LM, and DM yield R values higher than the reference point. The top-right plot represents a 90 degree clockwise rotation from the top-left plot. The bottom-left plot represents a 180 degree clockwise rotation from the top-left plot. The bottom-right plot represents a 270 degree clockwise rotation from the top-left plot. All plots generated in R (version 3.5.3) with package “akima” by interpolating observed values of variables.

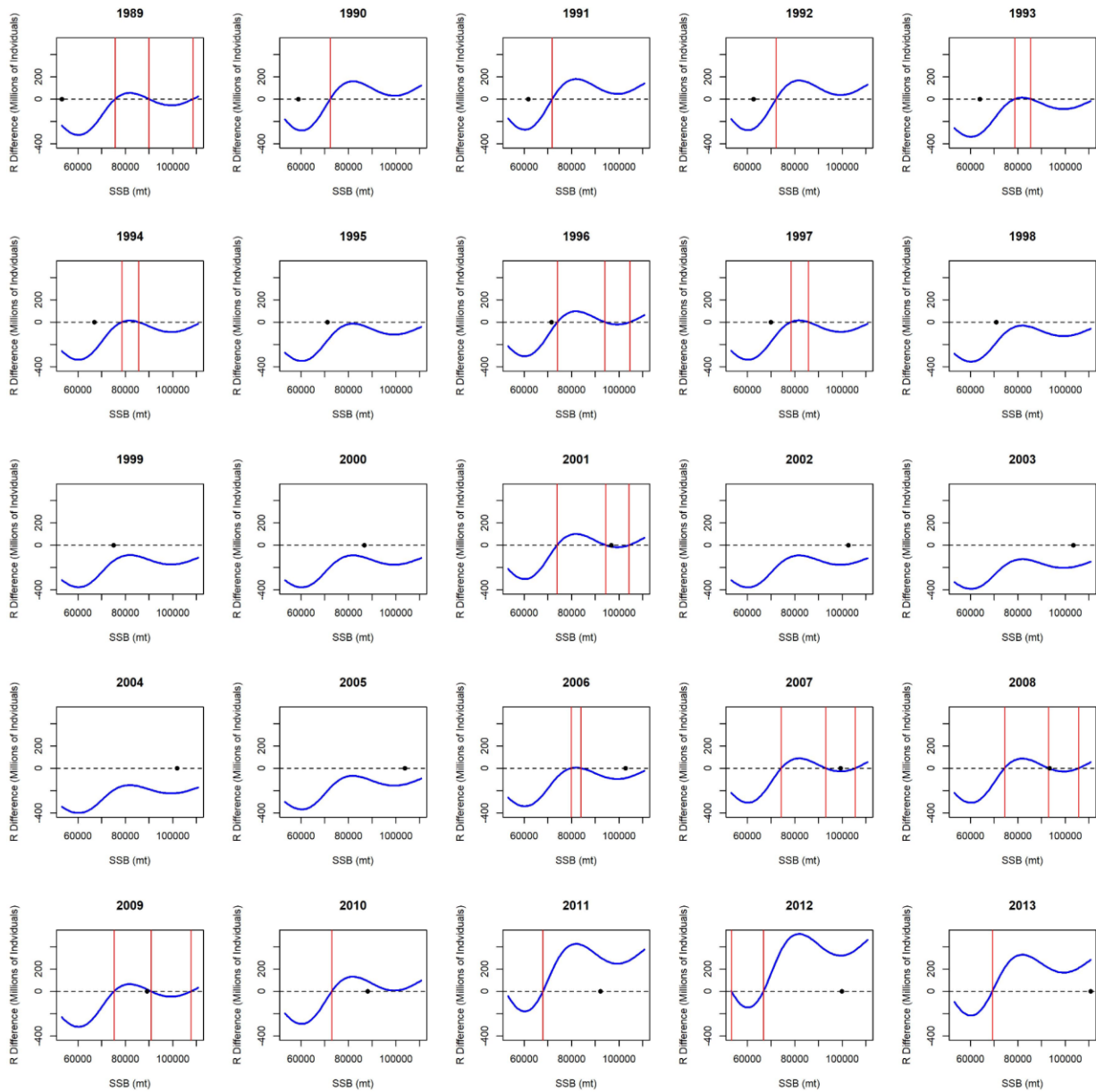


Figure S4.2. Hindcasts 1989-2013 of acceptable ranges of spawning stock biomass (SSB) in mt of years “X-5” through “X-3” that yield the desired recruitment (R) levels of the given year. R difference represents the difference between the calculated recruitment at a given value of SSB at the associated LM and DM and the chosen R-based reference point; in this case, the 75th percentile of R 1984-2013. Locations where the blue line is above the dotted R difference = 0 line represent acceptable SSB ranges. Red lines represent where the blue line crosses the R difference = 0 line. Black dots represent the average SSB years “X-5” to “X-3”. As a testament to the reliability of the SSB/R relationship and the dynamic BRP calculator, each year’s observed SSB (black dot) matches whether or not recruitment was above the 75th percentile that year.

APPENDIX C

SUPPLEMENTARY MATERIAL FOR CHAPTER 5

The two linear predictors used in the delta-GLMM:

$$\begin{aligned}
 p_1(i) = & \beta_1(t_i) + \sum_{f=1}^{n_{\omega 1}} L_{\omega 1}(f) \omega_1(s_i, f) + \sum_{f=1}^{n_{\varepsilon 1}} L_{\varepsilon 1}(f) \varepsilon_1(s_i, f, t_i) \\
 & + \sum_{p=1}^{n_p} \gamma_1(t_i, p) X(s_i, t_i, p) + \sum_{k=1}^{n_k} \lambda_1(k) Q(i, k)
 \end{aligned} \tag{S5.1}$$

$$\begin{aligned}
 p_2(i) = & \beta_2(t_i) + \sum_{f=1}^{n_{\omega 2}} L_{\omega 2}(f) \omega_2(s_i, f) + \sum_{f=1}^{n_{\varepsilon 2}} L_{\varepsilon 2}(f) \varepsilon_2(s_i, f, t_i) \\
 & + \sum_{p=1}^{n_p} \gamma_2(t_i, p) X(s_i, t_i, p) + \sum_{k=1}^{n_k} \lambda_2(k) Q(i, k)
 \end{aligned} \tag{S5.2}$$

where a list of parameters can be found in Table A1. From these predictors, encounter probability $r_1(i)$ and positive catch rates $r_2(i)$ can be estimated as:

$$r_1(i) = \text{logit}^{-1}(p_1(i)) \tag{S5.3}$$

$$r_2(i) = \alpha_i \times \exp(p_1(i)) \tag{S5.4}$$

where again a list of parameters can be found in Table A1. For more information, see Thorson et al. (2015) and Thorson (2019).

Table S5.1. A description of the parameters used in equations S5.1 through S5.4. Parameter definitions are from Thorson et al. 2019. For more information, see Thorson et al. (2015) and Thorson (2019).

Parameter	Description
$p_1(i)$	First linear predictor for observation i
$p_2(i)$	Second linear predictor for observation i
$r_1(i)$	Encounter probability for observation i
$r_2(i)$	Positive catch rate for observation i
$\beta_1(t_i)$	Intercept for first linear predictor in time interval t
$\beta_2(t_i)$	Intercept for second linear predictor in time interval t
$L_{\omega_1}(f)$	Loadings matrix for spatial covariation for first linear predictor for factor f
$L_{\omega_2}(f)$	Loadings matrix for spatial covariation for second linear predictor for factor f
$L_{\varepsilon_1}(f)$	Loadings matrix for spatio-temporal covariation for first linear predictor for factor f
$L_{\varepsilon_2}(f)$	Loadings matrix for spatio-temporal covariation for second linear predictor for factor f
$\gamma_1(t_i, p)$	Impact of habitat covariate p on first linear predictor in year t
$\gamma_2(t_i, p)$	Impact of habitat covariate p on second linear predictor in year t
$\lambda_1(k)$	Impact of catchability covariate k on first linear predictor
$\lambda_2(k)$	Impact of catchability covariate k on second linear predictor
$\omega_1(s_i, f)$	Spatial factors for first linear predictor for knot s and factor f
$\omega_2(s_i, f)$	Spatial factors for second linear predictor for knot s and factor f
$\varepsilon_1(s_i, f, t_i)$	Spatio-temporal factors for first linear predictor for knot s , factor f , and year t
$\varepsilon_2(s_i, f, t_i)$	Spatio-temporal factors for second linear predictor for knot s , factor f , and year t

Table S5.1 Continued.

$n_{\omega 1}$	Number of spatial factors for first linear predictor
$n_{\omega 2}$	Number of spatial factors for second linear predictor
$n_{\varepsilon 1}$	Number of spatio-temporal factors for first linear predictor
$n_{\varepsilon 2}$	Number of spatio-temporal factors for second linear predictor
$X(s_i, t_i, p)$	Covariate value for habitat covariate p in knot s and year t
$Q(i, k)$	Covariate value for catchability covariate k for observation i
n_p	Number of habitat covariates
n_k	Number of catchability covariates
f	Factor number
p	Habitat covariate number
k	Catchability covariate number
t_i	Time interval number (year) associated with observation i
s_i	Spatial location number (knot) associated with observation i
i	Observation number (survey instance)
α_i	Area covered for observation i (effort offset)

Thorson, J.T., Shelton, A.O., Ward, E.J., and Skaug, H.J. 2015. Geostatistical delta generalized linear mixed models improve precision for estimated abundance indices for West Coast groundfishes. *ICES Journal of Marine Science*. 72(5): 1297–1310.

Thorson, J. 2019. Guidance for decisions using the Vector Autoregressive Spatio-Temporal (VAST) package in stock, ecosystem, habitat and climate assessments. *Fisheries Research*. 210: 143-161.

APPENDIX D

SUPPLEMENTARY MATERIAL FOR CHAPTER 6

Table S6.1. Settings and data used in the lobster stock assessment model. Data and settings are identical to those used in Hodgdon et al. (2020). MEDMR: Maine Department of Marine Resources; NHFGD: New Hampshire Fish and Game Department; MADMF: Massachusetts Division of Marine Fisheries; NEFSC: New England Fisheries Science Center; mm: millimeter.

Years	1984 through 2013
Seasons	4 (Each 3 month time blocks)
Number of sexes	1 (Averaged across male and female)
Size range	53 mm to 223 mm carapace length
Size bins	5 mm (For a total of 34 bins)
Initial conditions	First year size composition assumed from survey data
Recruitment size	53 mm to 73 mm
SSB/R relationship	None
Growth	Prespecified seasonal growth transition matrices averaged across both sexes
Number of commercial fleets	1
Commercial fleet selectivity at size	Double logistic averaged across both sexes
Survey data	<p>MEDMR Ventless Trap Survey 2006-2012</p> <p>Spring MEDMR/NHFGD Inshore Bottom Trawl Survey 2001-2013</p> <p>Fall MEDMR/NHFGD Inshore Bottom Trawl Survey 2000-2013</p> <p>Spring MADMF Bottom Trawl Survey 1984-2013</p> <p>Fall MADMF Bottom Trawl Survey 1984-2013</p> <p>Spring NEFSC Bottom Trawl Survey 1984-2013</p> <p>Fall NEFSC Bottom Trawl Survey 1984-2013</p>

Table S6.1 Continued.

Survey selectivity at size	Double logistic averaged across both sexes
Fishing mortality rate	Instantaneous rates averaged across both sexes
Natural mortality rate	0.15 year ⁻¹ across all size groups, seasons, and sexes

Hodgdon, C., Tanaka, K., Runnebaum, J., Cao, J., and Chen, Y. 2020. A framework to incorporate environmental effects into stock assessments informed by fishery-independent surveys: a case study with American lobster (*Homarus americanus*). *Canadian Journal of Fisheries and Aquatic Sciences*. 77(10): 1700-1710.

APPENDIX E

SUPPLEMENTARY MATERIAL FOR CHAPTER 7

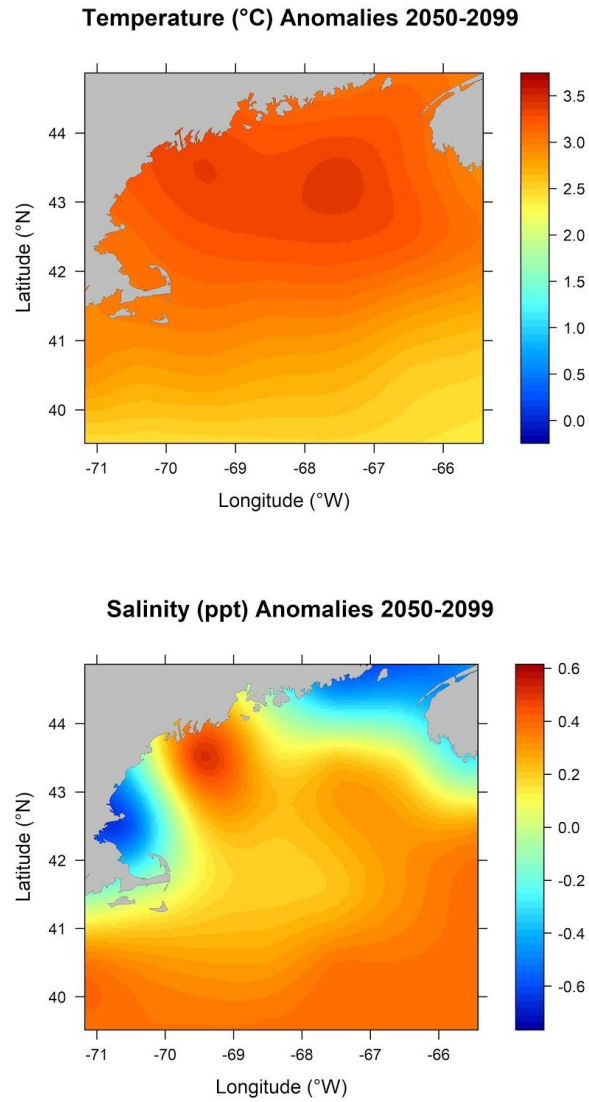


Figure S7.1. Interpolated anomalies from CMIP5 of bottom temperature in degrees Celsius (top) and salinity in parts per thousand (bottom) for RCP scenario 8.5 out to the reference periods 2006-2055 (right) and 2050-2099 (left). Data downscaled from NOAA's Climate Change Web Portal (available from <https://psl.noaa.gov/ipcc/ocn/>).

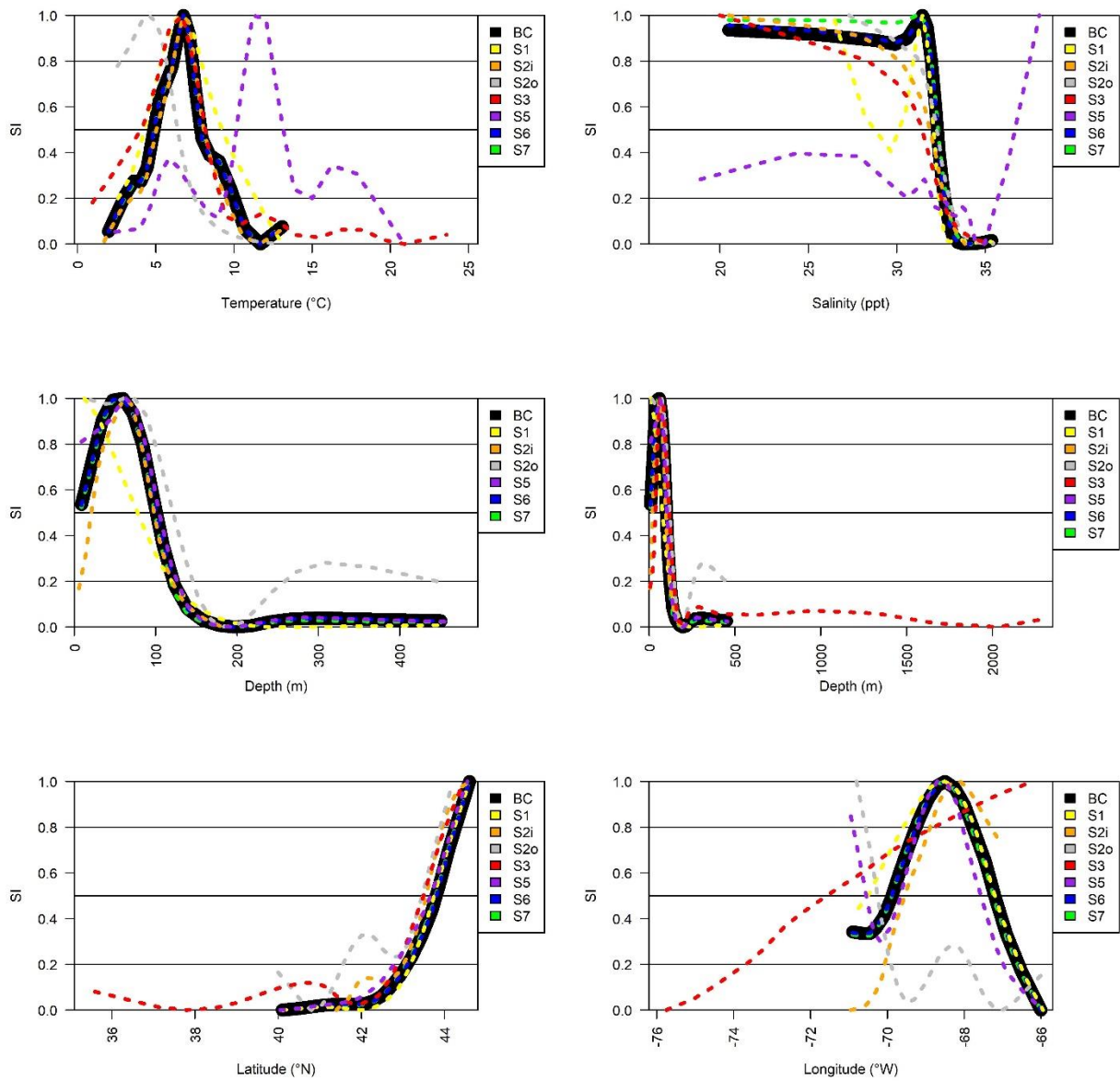


Figure S7.2 SIs for the base case and each scenario of bottom temperature in degrees Celsius (top left), bottom salinity in parts per thousand (top right), depth in meters with scenario 3 included (right) and without (left), latitude (bottom left), and longitude (bottom right) to male adult lobsters in the spring. Note that scenario 4 SI curves are not presented as they are identical to the base case; only missing the temperature component. The base case is denoted as “BC”, and scenarios are listed as scenario 1 (S1), scenario 2 for inshore indices (S2i), scenario 2 for offshore indices (S2o), scenario 3 (S3), scenario 5 (S5), scenario 6 (S6), and scenario 7 (S7). Also marked are SIs of 0.2, 0.5, and 0.8, representing values that are “Fair”, “Good”, and “Excellent”, respectively.

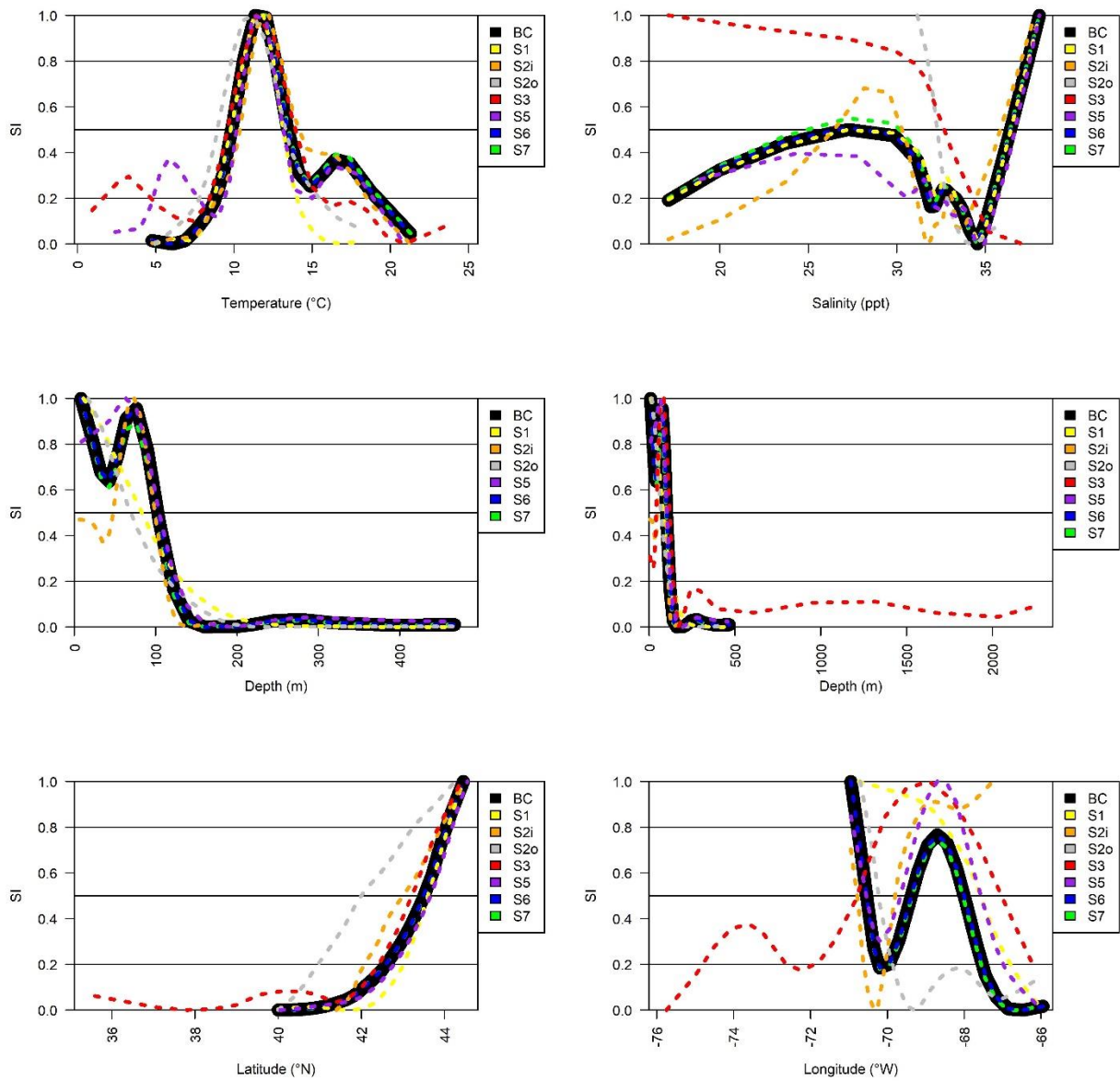


Figure S7.3. SIs for the base case and each scenario of bottom temperature in degrees Celsius (top left), bottom salinity in parts per thousand (top right), depth in meters with scenario 3 included (right) and without (left), latitude (bottom left), and longitude (bottom right) to male adult lobsters in the fall. Note that scenario 4 SI curves are not presented as they are identical to the base case; only missing the temperature component. The base case is denoted as “BC”, and scenarios are listed as scenario 1 (S1), scenario 2 for inshore indices (S2i), scenario 2 for offshore indices (S2o), scenario 3 (S3), scenario 5 (S5), scenario 6 (S6), and scenario 7 (S7). Also marked are SIs of 0.2, 0.5, and 0.8, representing values that are “Fair”, “Good”, and “Excellent”, respectively.

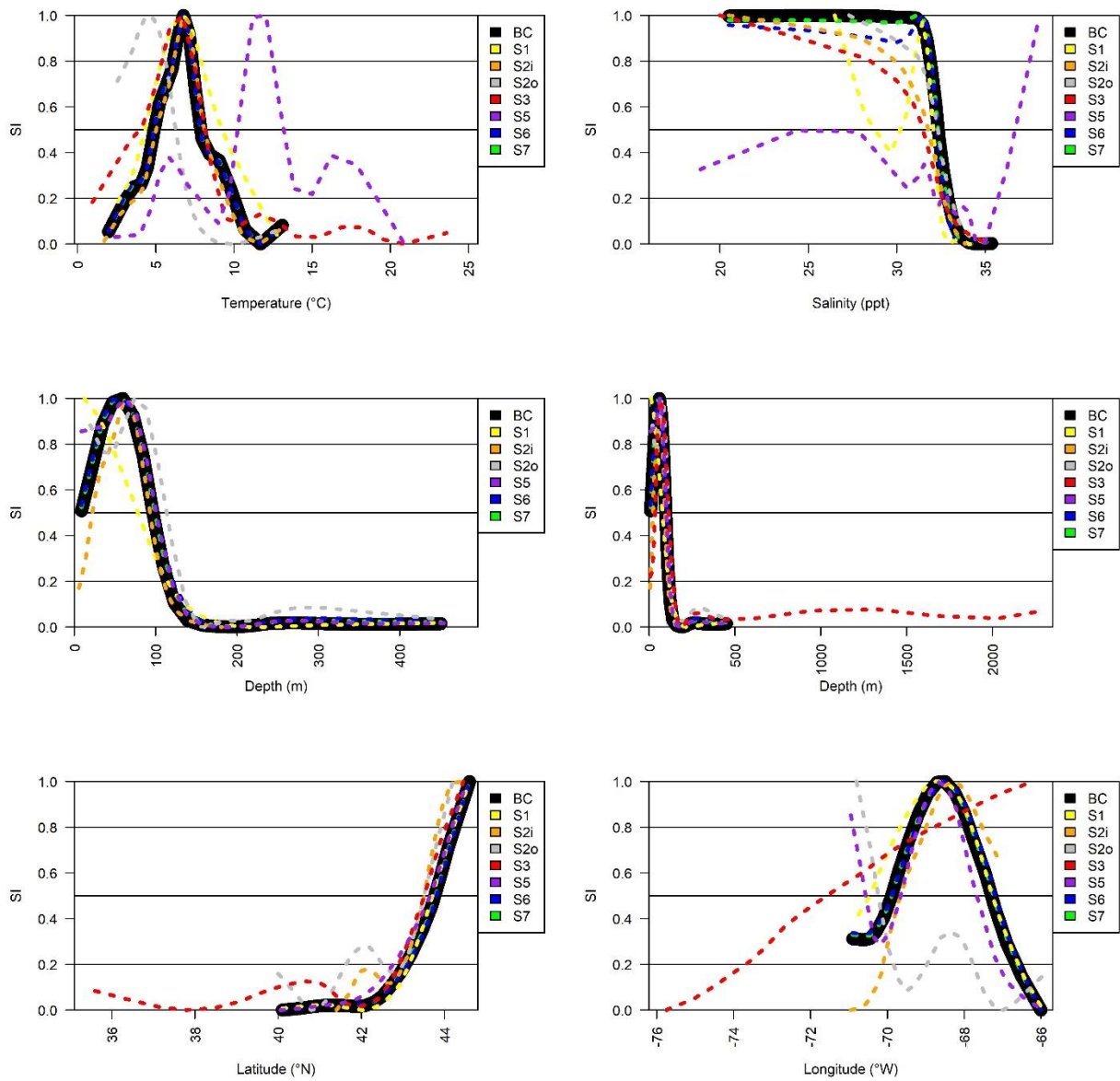


Figure S7.4. SIs for the base case and each scenario of bottom temperature in degrees Celsius (top left), bottom salinity in parts per thousand (top right), depth in meters with scenario 3 included (right) and without (left), latitude (bottom left), and longitude (bottom right) to male juvenile lobsters in the spring. Note that scenario 4 SI curves are not presented as they are identical to the base case; only missing the temperature component. The base case is denoted as “BC”, and scenarios are listed as scenario 1 (S1), scenario 2 for inshore indices (S2i), scenario 2 for offshore indices (S2o), scenario 3 (S3), scenario 5 (S5), scenario 6 (S6), and scenario 7 (S7). Also marked are SIs of 0.2, 0.5, and 0.8, representing values that are “Fair”, “Good”, and “Excellent”, respectively.

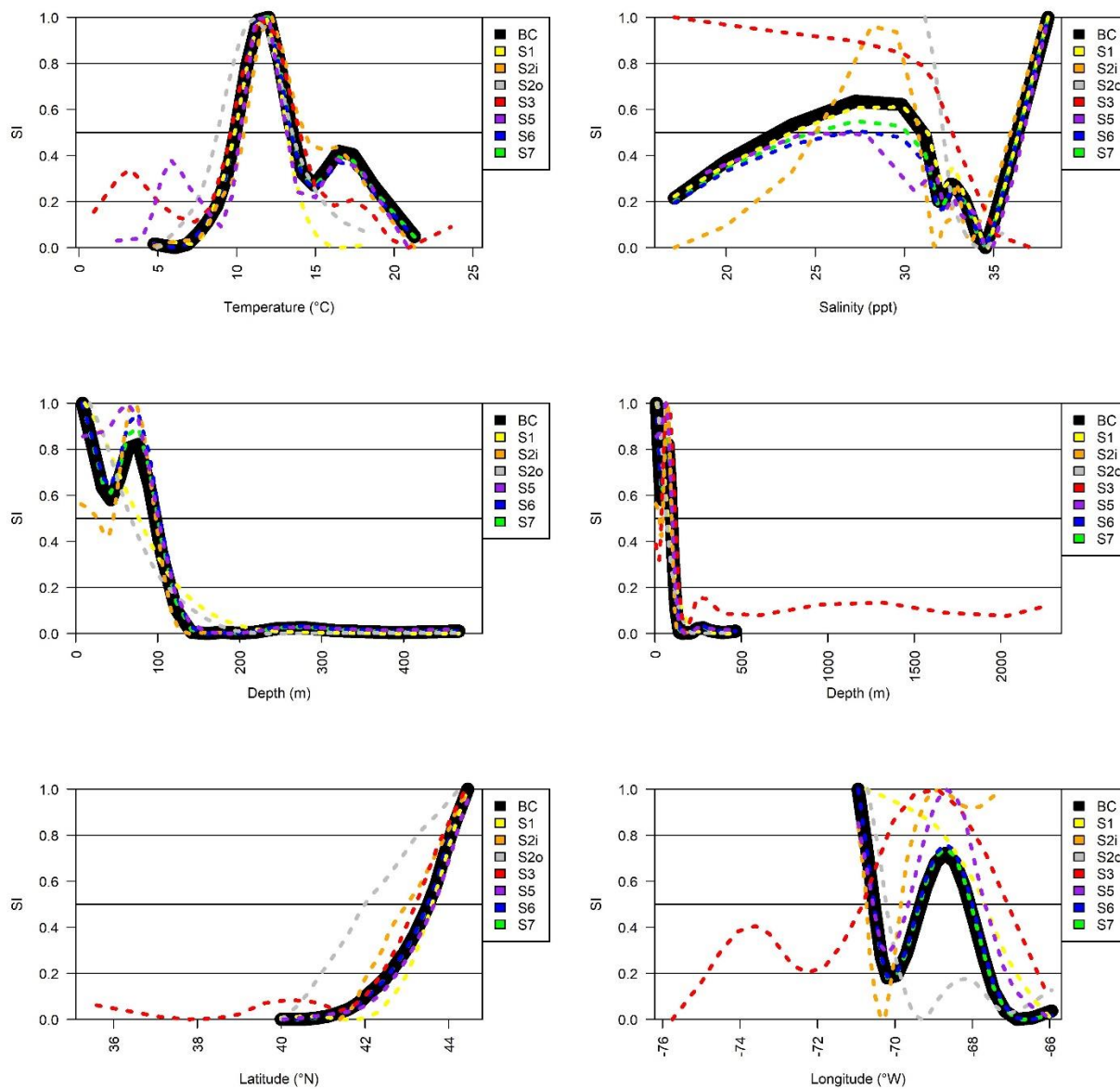


Figure S7.5. SIs for the base case and each scenario of bottom temperature in degrees Celsius (top left), bottom salinity in parts per thousand (top right), depth in meters with scenario 3 included (right) and without (left), latitude (bottom left), and longitude (bottom right) to male juvenile lobsters in the fall. Note that scenario 4 SI curves are not presented as they are identical to the base case; only missing the temperature component. The base case is denoted as “BC”, and scenarios are listed as scenario 1 (S1), scenario 2 for inshore indices (S2i), scenario 2 for offshore indices (S2o), scenario 3 (S3), scenario 5 (S5), scenario 6 (S6), and scenario 7 (S7). Also marked are SIs of 0.2, 0.5, and 0.8, representing values that are “Fair”, “Good”, and “Excellent”, respectively.

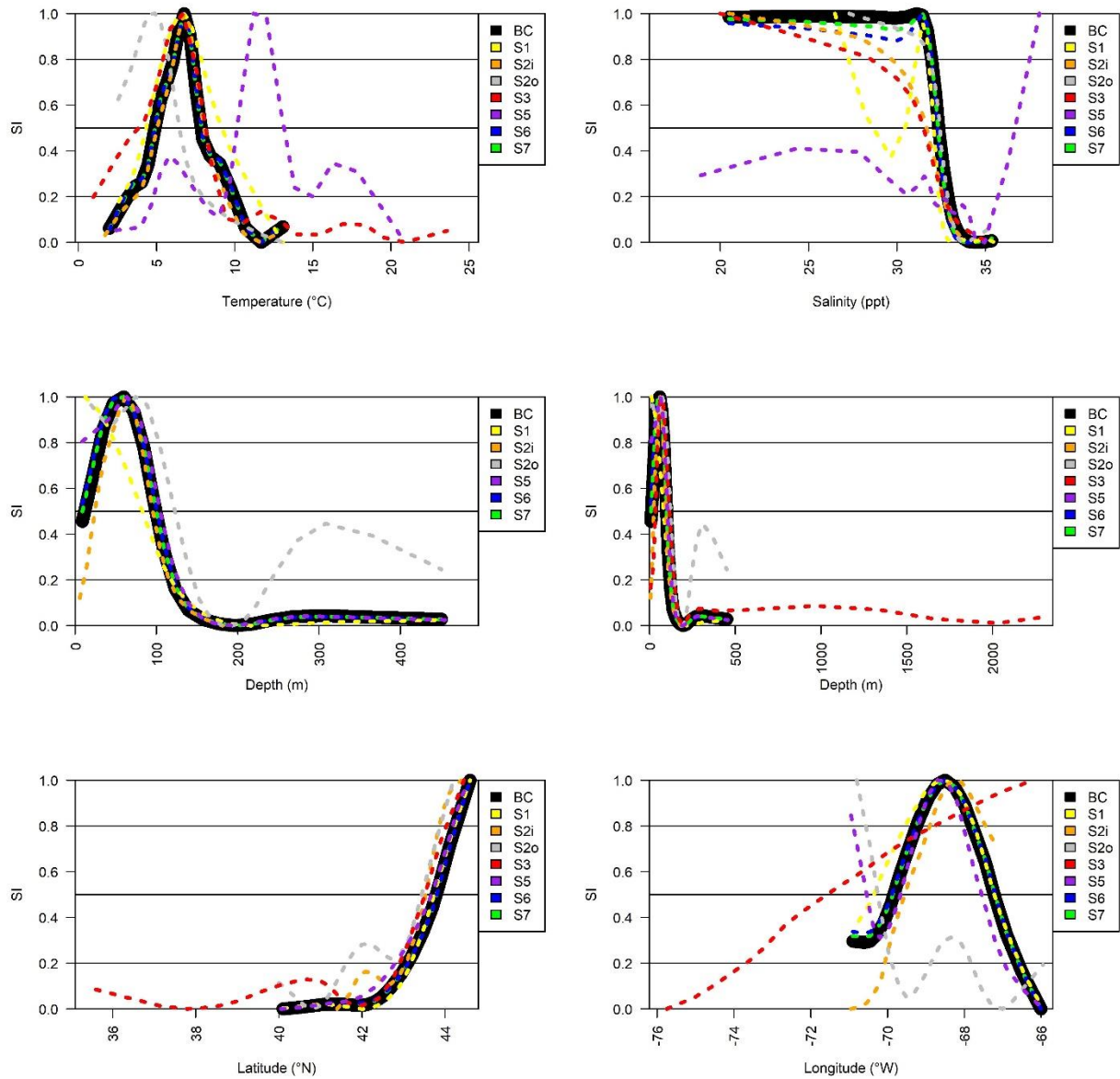


Figure S7.6. SIs for the base case and each scenario of bottom temperature in degrees Celsius (top left), bottom salinity in parts per thousand (top right), depth in meters with scenario 3 included (right) and without (left), latitude (bottom left), and longitude (bottom right) to female juvenile lobsters in the spring. Note that scenario 4 SI curves are not presented as they are identical to the base case; only missing the temperature component. The base case is denoted as “BC”, and scenarios are listed as scenario 1 (S1), scenario 2 for inshore indices (S2i), scenario 2 for offshore indices (S2o), scenario 3 (S3), scenario 5 (S5), scenario 6 (S6), and scenario 7 (S7). Also marked are SIs of 0.2, 0.5, and 0.8, representing values that are “Fair”, “Good”, and “Excellent”, respectively.

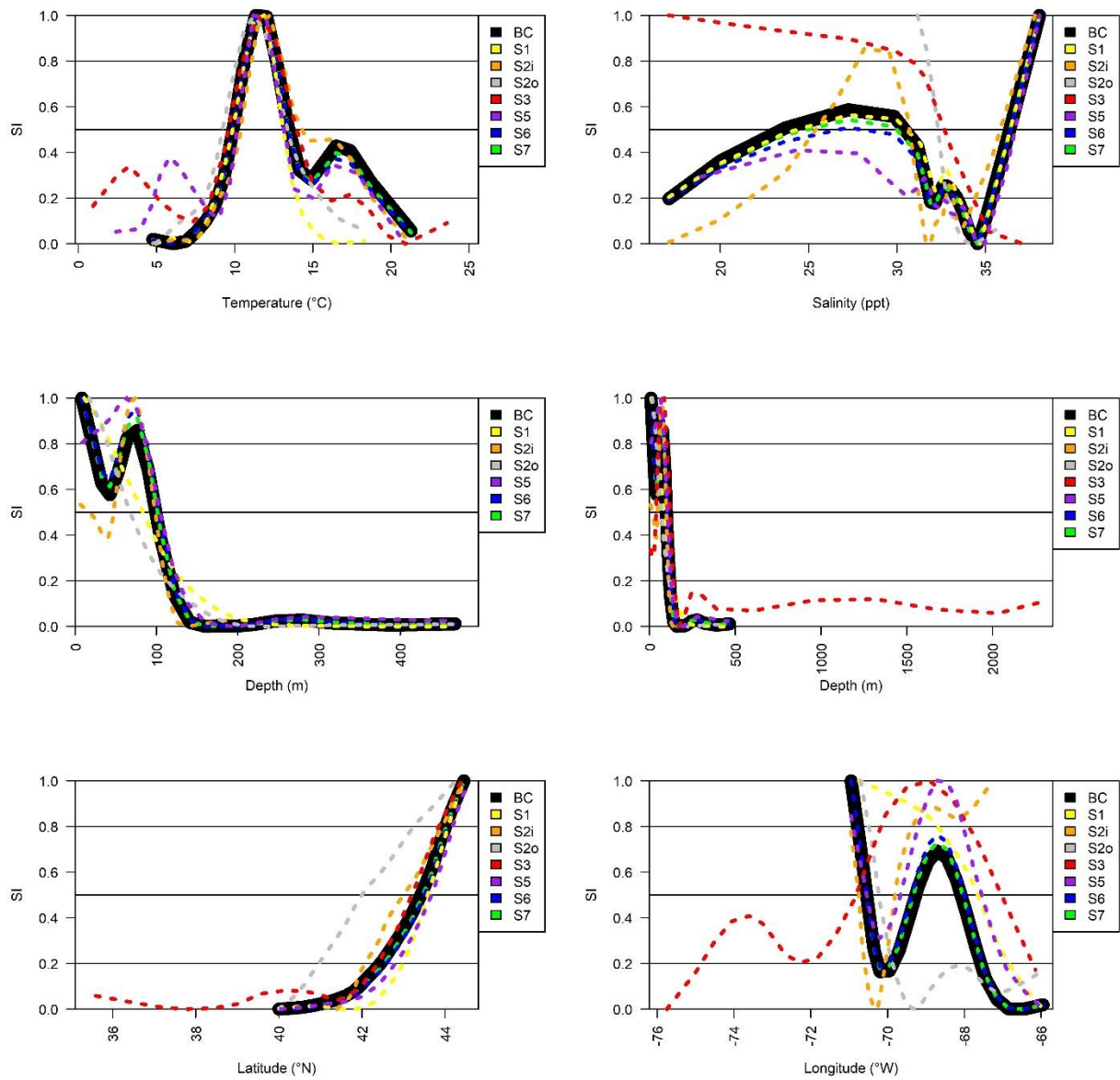


Figure S7.7. SIs for the base case and each scenario of bottom temperature in degrees Celsius (top left), bottom salinity in parts per thousand (top right), depth in meters with scenario 3 included (right) and without (left), latitude (bottom left), and longitude (bottom right) to female juvenile lobsters in the fall. Note that scenario 4 SI curves are not presented as they are identical to the base case; only missing the temperature component. The base case is denoted as “BC”, and scenarios are listed as scenario 1 (S1), scenario 2 for inshore indices (S2i), scenario 2 for offshore indices (S2o), scenario 3 (S3), scenario 5 (S5), scenario 6 (S6), and scenario 7 (S7). Also marked are SIs of 0.2, 0.5, and 0.8, representing values that are “Fair”, “Good”, and “Excellent”, respectively.

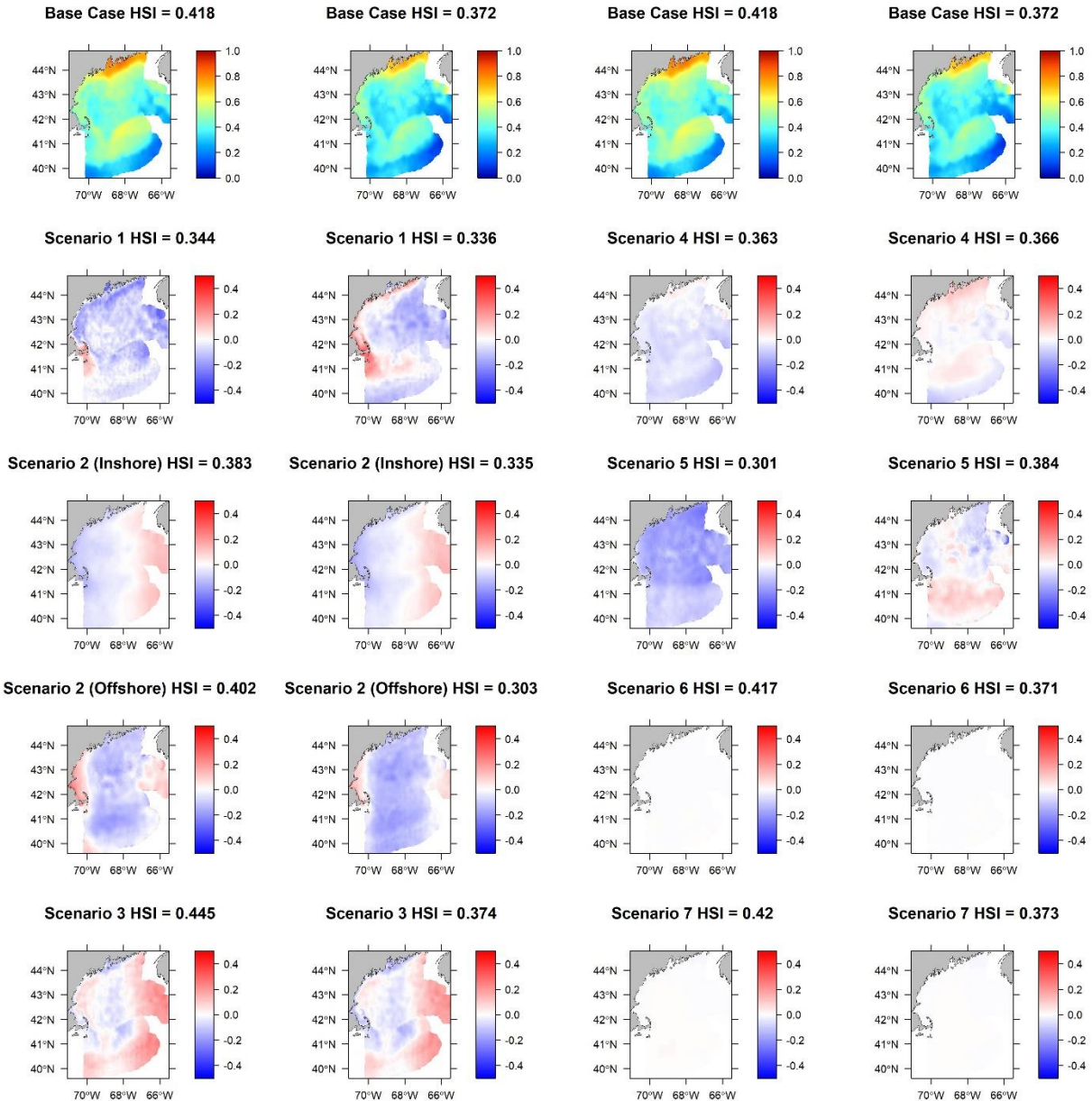


Figure S7.8. Spatial HSI from the base case (Row 1) for the historical period (Columns 1 and 3) and the future period (Columns 2 and 4) as well as spatial differences for each of the seven scenarios (Rows 2 through 5) to their respective base case maps in row 1 (Note that the base case maps in columns 1 and 3 are the same and those in columns 2 and 4 are the same). Blue represents areas in a given scenario that were predicted to have a lower HSI than the base case did. Red represents areas in a given scenario that were predicted to have a higher HSI than the base case did. The darker the respective shade, the greater the difference from the base case. Above each map is the scenario name and the average spatial HSI for that period and scenario. Results are for spring male adults. Note scenario 5 is combined seasons, scenario 6 is combined sexes, and scenario 7 is combined life stages.

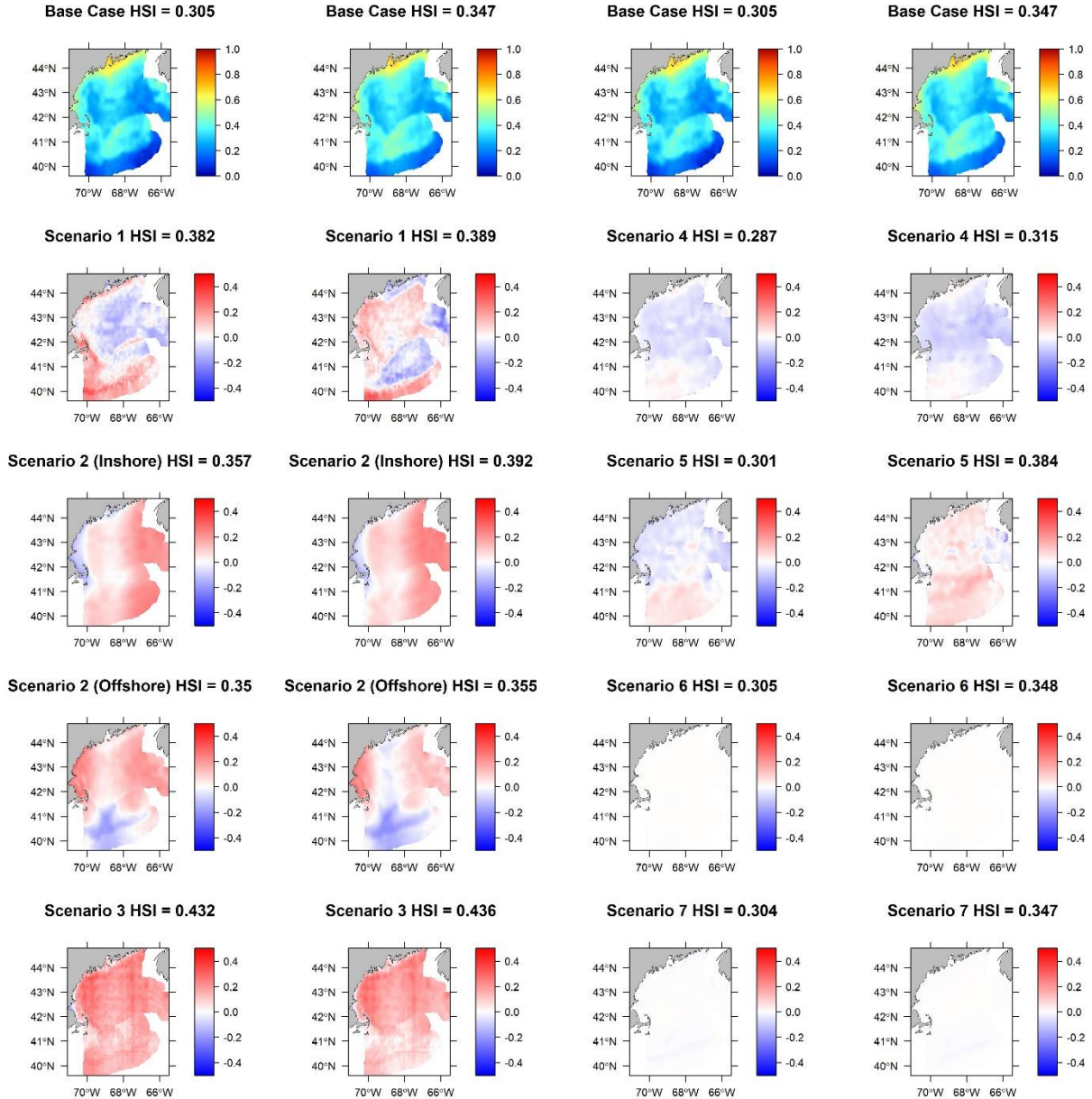


Figure S7.9. Spatial HSI from the base case (Row 1) for the historical period (Columns 1 and 3) and the future period (Columns 2 and 4) as well as spatial differences for each of the seven scenarios (Rows 2 through 5) to their respective base case maps in row 1 (Note that the base case maps in columns 1 and 3 are the same and those in columns 2 and 4 are the same). Blue represents areas in a given scenario that were predicted to have a lower HSI than the base case did. Red represents areas in a given scenario that were predicted to have a higher HSI than the base case did. The darker the respective shade, the greater the difference from the base case. Above each map is the scenario name and the average spatial HSI for that period and scenario. Results are for fall male adults. Note scenario 5 is combined seasons, scenario 6 is combined sexes, and scenario 7 is combined life stages.

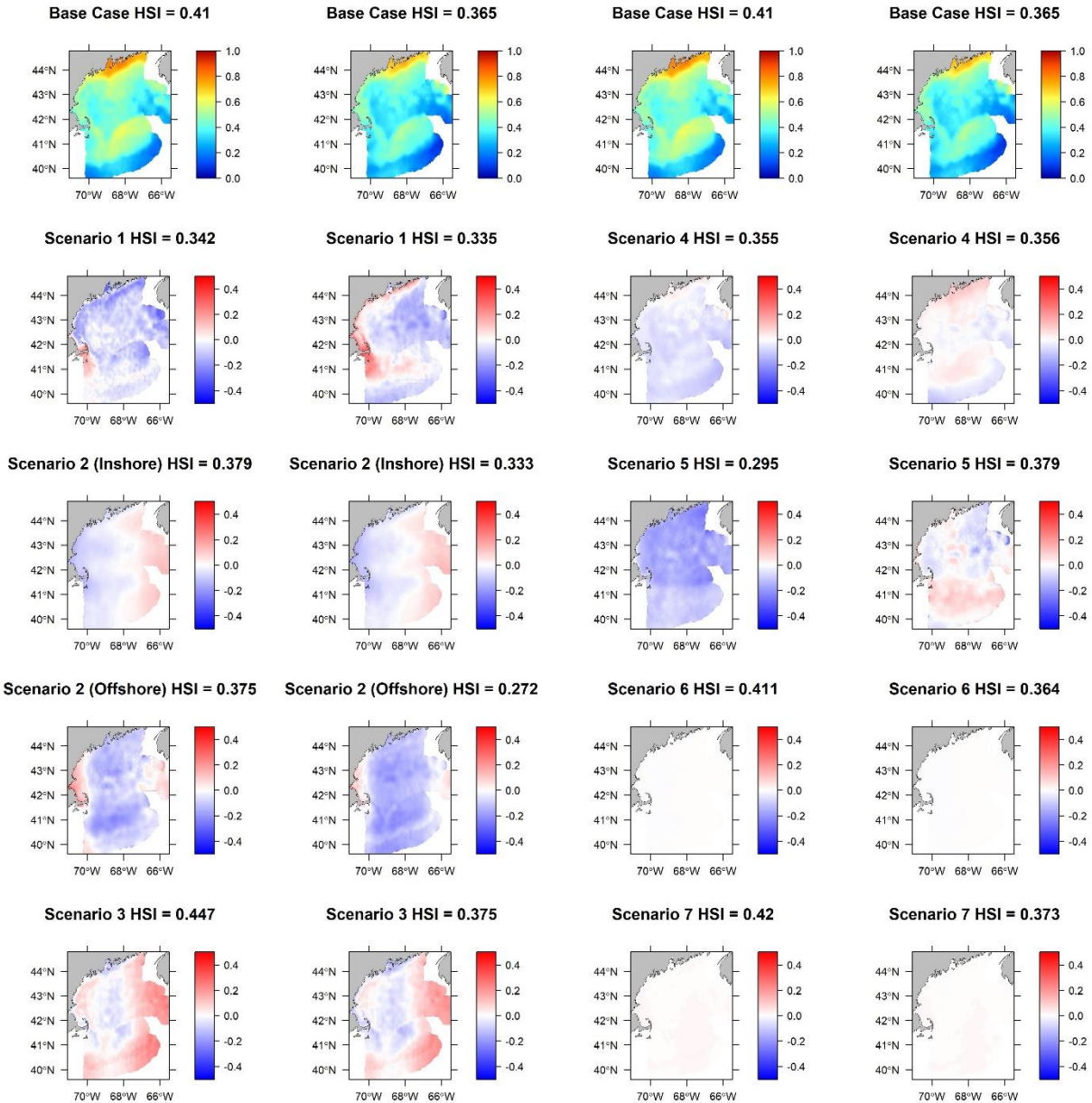


Figure S7.10. Spatial HSI from the base case (Row 1) for the historical period (Columns 1 and 3) and the future period (Columns 2 and 4) as well as spatial differences for each of the seven scenarios (Rows 2 through 5) to their respective base case maps in row 1 (Note that the base case maps in columns 1 and 3 are the same and those in columns 2 and 4 are the same). Blue represents areas in a given scenario that were predicted to have a lower HSI than the base case did. Red represents areas in a given scenario that were predicted to have a higher HSI than the base case did. The darker the respective shade, the greater the difference from the base case. Above each map is the scenario name and the average spatial HSI for that period and scenario. Results are for spring male juveniles. Note scenario 5 is combined seasons, scenario 6 is combined sexes, and scenario 7 is combined life stages.

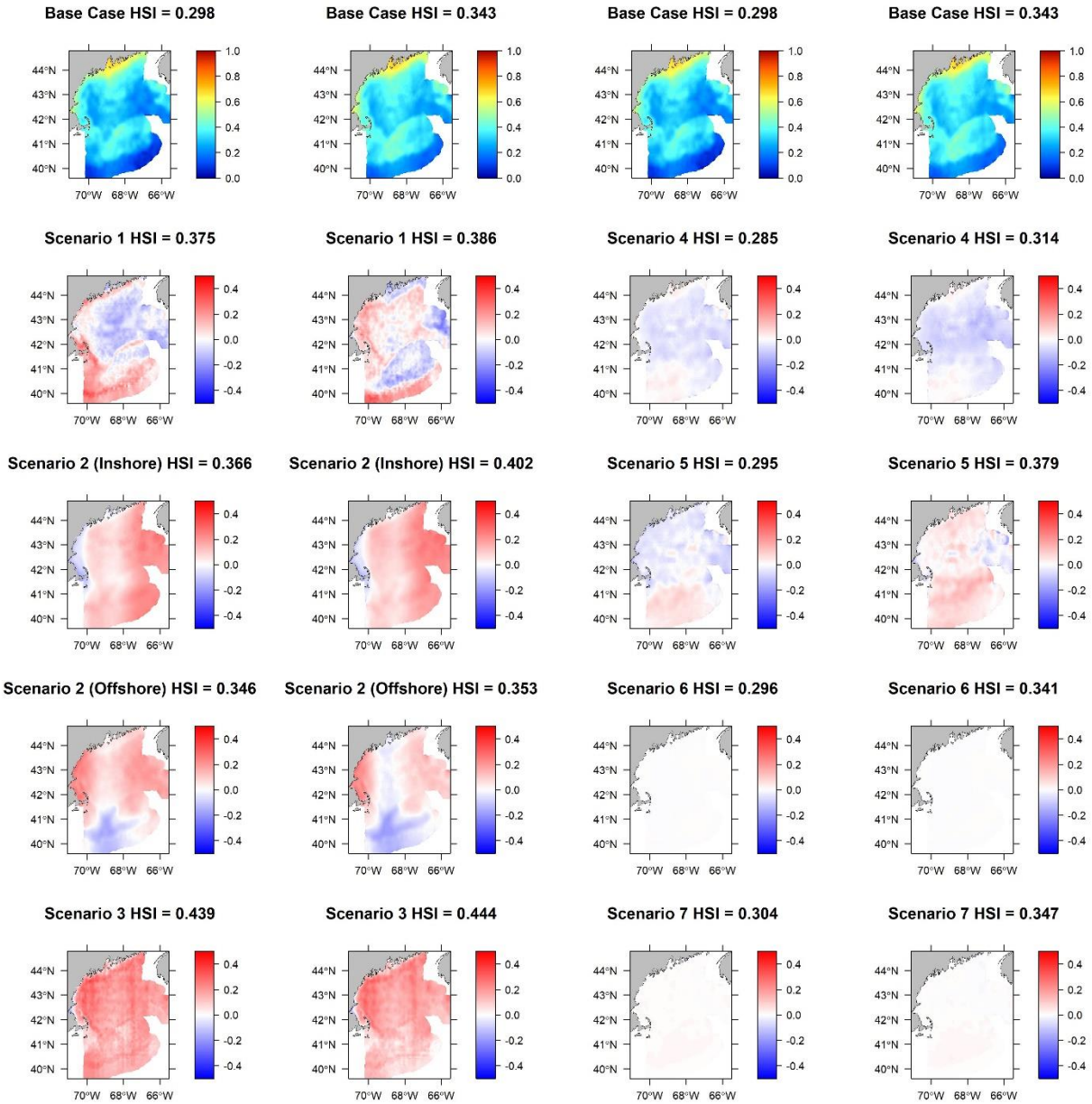


Figure S7.11. Spatial HSI from the base case (Row 1) for the historical period (Columns 1 and 3) and the future period (Columns 2 and 4) as well as spatial differences for each of the seven scenarios (Rows 2 through 5) to their respective base case maps in row 1 (Note that the base case maps in columns 1 and 3 are the same and those in columns 2 and 4 are the same). Blue represents areas in a given scenario that were predicted to have a lower HSI than the base case did. Red represents areas in a given scenario that were predicted to have a higher HSI than the base case did. The darker the respective shade, the greater the difference from the base case. Above each map is the scenario name and the average spatial HSI for that period and scenario. Results are for fall male juveniles. Note scenario 5 is combined seasons, scenario 6 is combined sexes, and scenario 7 is combined life stages.

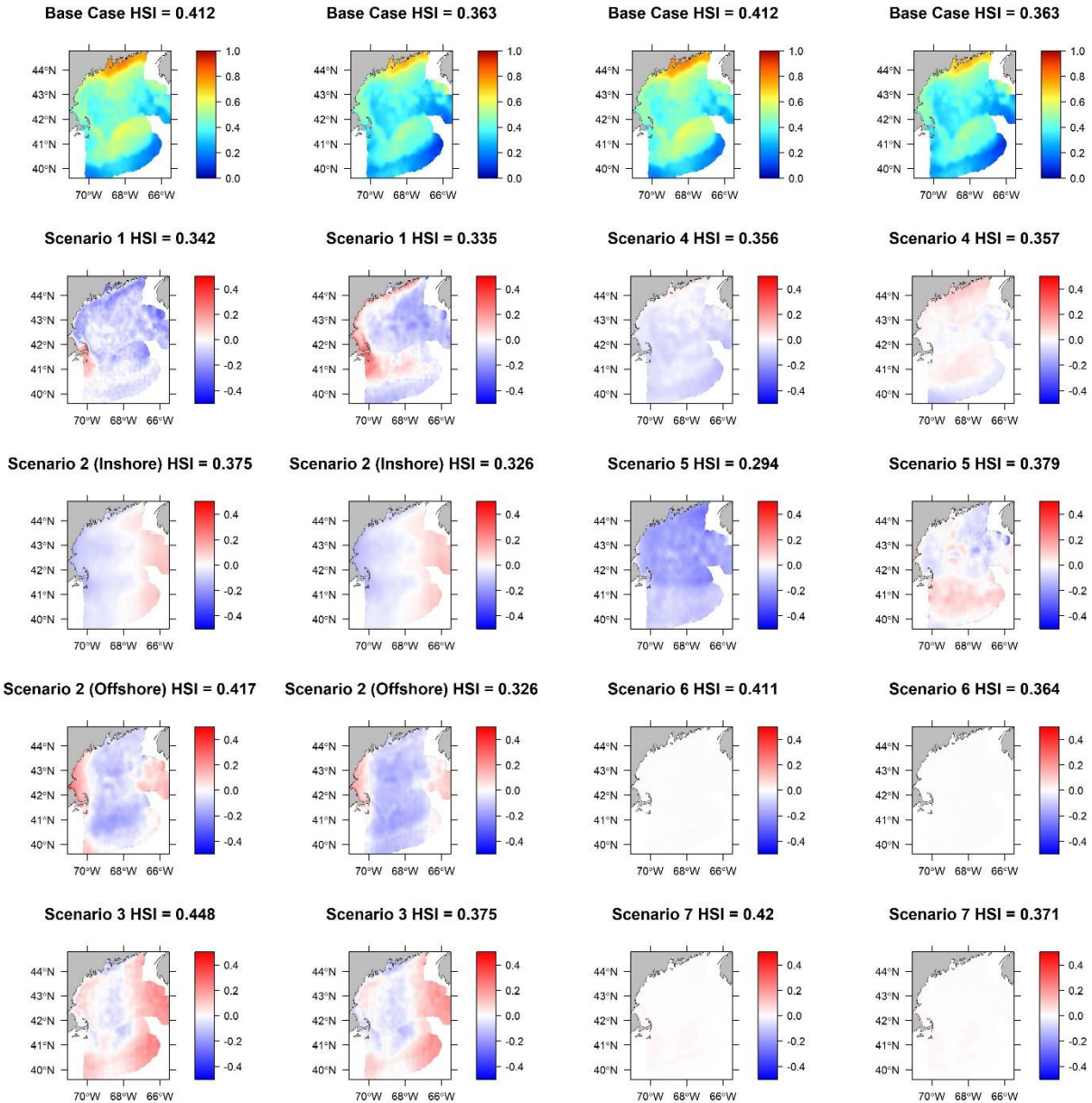


Figure S7.12. Spatial HSI from the base case (Row 1) for the historical period (Columns 1 and 3) and the future period (Columns 2 and 4) as well as spatial differences for each of the seven scenarios (Rows 2 through 5) to their respective base case maps in row 1 (Note that the base case maps in columns 1 and 3 are the same and those in columns 2 and 4 are the same). Blue represents areas in a given scenario that were predicted to have a lower HSI than the base case did. Red represents areas in a given scenario that were predicted to have a higher HSI than the base case did. The darker the respective shade, the greater the difference from the base case. Above each map is the scenario name and the average spatial HSI for that period and scenario. Results are for spring female juveniles. Note scenario 5 is combined seasons, scenario 6 is combined sexes, and scenario 7 is combined life stages.

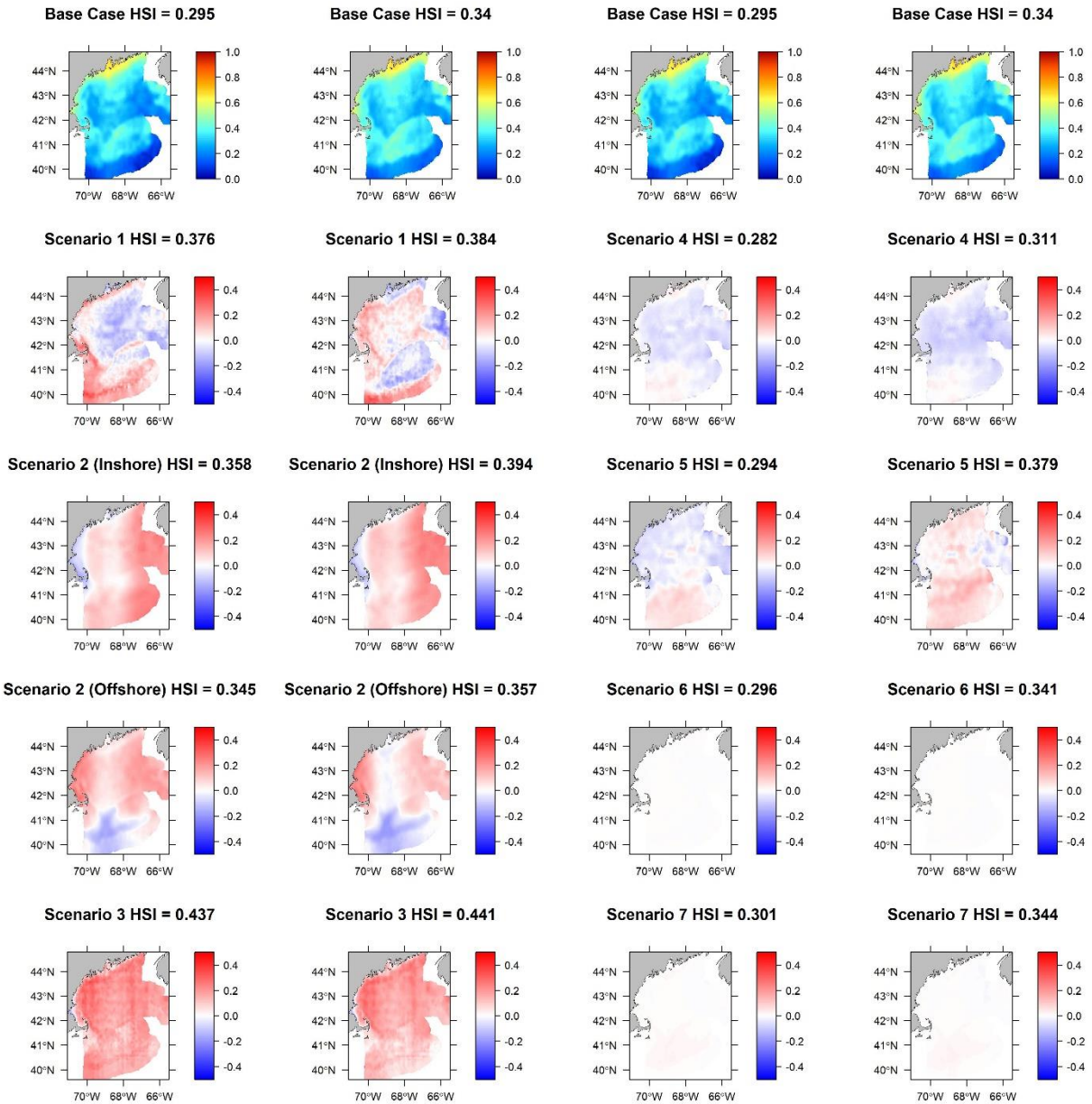


Figure S7.13. Spatial HSI from the base case (Row 1) for the historical period (Columns 1 and 3) and the future period (Columns 2 and 4) as well as spatial differences for each of the seven scenarios (Rows 2 through 5) to their respective base case maps in row 1 (Note that the base case maps in columns 1 and 3 are the same and those in columns 2 and 4 are the same). Blue represents areas in a given scenario that were predicted to have a lower HSI than the base case did. Red represents areas in a given scenario that were predicted to have a higher HSI than the base case did. The darker the respective shade, the greater the difference from the base case. Above each map is the scenario name and the average spatial HSI for that period and scenario. Results are for fall female juveniles. Note scenario 5 is combined seasons, scenario 6 is combined sexes, and scenario 7 is combined life stages.

As of April 2022,

Chapter 2 has been published as:

Hodgdon, C.T., Torre, M., & Chen, Y. 2020. Spatiotemporal variability in Atlantic sea scallop (*Placopecten magellanicus*) growth in the Northern Gulf of Maine. *Journal of Northwest Atlantic Fishery Science*. 51: 15-31. 10.2960/J.v51.m729

Chapter 3 has been submitted as:

Hodgdon, C.T., Khalsa, N., & Chen, Y. *Submitted*. Implications of Climate Driven Changes on Growth and Size-at-Maturity for Gulf of Maine Lobster. *Fishery Bulletin*.

Chapter 4 has been submitted as:

Hodgdon, C.T., Shank, B., & Chen, Y. *Submitted*. Developing a Framework to Calculate Dynamic Reference Points using a Thermally Explicit Spawning Stock Biomass / Recruitment Relationship. *Canadian Journal of Fisheries and Aquatic Sciences*.

Chapter 5 has been published as:

Hodgdon, C.T., Tanaka, K., Cao, J., Runnebaum, J., & Chen, Y. 2020. A framework to incorporate environmental effects into stock assessments informed by fishery-independent surveys: a case study with American lobster (*Homarus americanus*). *Canadian Journal of Fisheries and Aquatic Sciences*. 77(10): 1700-1710. <https://doi.org/10.1139/cjfas-2020-0076>

Chapter 6 has been submitted as:

Hodgdon, C.T. & Chen, Y. *Submitted*. A Comparison of Stochastic and Thermally Explicit Recruitment Projections for Gulf of Maine American Lobster. *Marine Ecology Progress Series*.

Chapter 7 has been published as:

Hodgdon, C.T., Mazur, M., Friedland, K., Willse, N., & Chen, Y. 2021. Consequences of False Assumptions when Projecting Habitat Suitability: A Caution of Forecasting under Uncertainties. *ICES Journal of Marine Science*. 78(6): 2092-2101. <https://doi.org/10.1093/icesjms/fsab101>

BIOGRAPHY OF THE AUTHOR

Cameron Hodgdon was born in Damariscotta, Maine, USA in 1995 to Tyler Hodgdon of Boothbay, Maine and Tracy Northrup of Whitefield, Maine. He attended Lincoln Academy High School in Newcastle, Maine and graduated in 2013 where he then went on to receive two Bachelor of Science degrees in Marine Biology and Applied Mathematics from the University of New England in Biddeford, Maine. After successfully defending his undergraduate thesis under Dr. James Sulikowski and graduating summa cum laude from the University of New England in 2017, Cameron began a graduate position with Dr. Yong Chen at the University of Maine's School of Marine Sciences. He is currently a candidate for the Doctor of Philosophy degree in Marine Biology from the University of Maine in August 2022.